ABSTRACT

Title of Dissertation: PRODUCTIVITY AND LIGHT-DEPENDENT RESPIRATION OF PHYTOPLANKTON, INCLUDING THE DINOFLAGELLATE *Karenia brevis*: ENVIRONMENTAL EFFECT INTERACTIONS

Bruna Fernanda Sobrinho
Doctor of Philosophy, 2026

Dissertation directed by: Professor Patricia M. Glibert
Marine Estuarine Environmental Sciences

Climate change is altering coastal ecosystems through increasing temperatures, intensifying storm activity, and enhancing terrestrial inputs of nutrients and dissolved organic matter. These environmental changes are expected to influence the physiology and bloom dynamics of harmful algal species such as the dinoflagellate *Karenia brevis*, which forms nearly annual blooms on the West Florida Shelf (WFS). This dissertation investigated how interacting stressors influence phytoplankton metabolism, with particular emphasis on the primary production and respiration. First, long-term data from 1998 to 2020 were analyzed and the correlations between *K. brevis*, Peace River discharge, and the ENSO index suggested that freshwater inflow and large-scale climate oscillations play both direct and indirect roles in regulating bloom dynamics on the WFS. To better quantify primary production and respiration, methodological improvements were developed using the $H_2{}^{18}O$ technique using Membrane Inlet Mass Spectrometry (MIMS). This approach enables the simultaneous quantification of gross primary production (GPP), net primary production (NPP), and gross respiration (GR; light-

dependent respiration) in small-volume incubations, providing a rapid and cost-effective method. Using this approach, opportunistic post-hurricane field experiments and laboratory manipulations examined the combined effects of elevated temperature and humic acid enrichment on the metabolic rates of *K. brevis* and associated phytoplankton communities. Results showed that warming consistently reduced primary production while enhancing both dark and light-dependent respiration, often shifting the system toward heterotrophic conditions. Complementary laboratory experiments using Pulse-Amplitude Modulated (PAM) fluorometry demonstrated that photosynthetic performance of *K. brevis* responds to interactions between temperature and nutrient form. While elevated temperatures can affect photosynthetic efficiency, nutrient form and availability can modulate these responses. Together, these findings demonstrate that warming, nutrient inputs, and storm-driven terrestrial runoff interact to regulate *K. brevis* metabolism and bloom dynamics. Incorporating physiological rates, terrestrial inputs, and climate-scale variability into predictive models will be essential for improving forecasts of harmful algal blooms and ecosystem metabolic balance in a warming coastal ocean.

PRODUCTIVITY AND LIGHT-DEPENDENT RESPIRATION OF PHYTOPLANKTON, INCLUDING THE DINOFLAGELLATE *Karenia brevis*: ENVIRONMENTAL EFFECT INTERACTIONS

by

Bruna Fernanda Sobrinho

Dissertation submitted to the Faculty of the Graduate School of the
University of Maryland, College Park, in partial fulfillment
of the requirements for the degree of
Doctor of Philosophy
2026

Advisory Committee:
Professor Patricia M. Glibert, Chair
Dr. Cynthia Heil
Professor Greg Silsbe
Professor Ming Li
Professor Vyacheslav Lyubchich
Dean's Representative: Professor Sujay Kaushal

Dedication

Dedico esta dissertação aos meus pais e ao meu irmão, cujo amor e apoio me deram coragem para voar longe, com a certeza de que sempre tenho um lugar para voltar!
E a minha vó Maria, que partiu sem que eu pudesse me despedir!

I dedicate this dissertation to my parents and my brother, whose love and support gave me the courage to fly far, with the certainty that I will always have a place to return to!
And to my grandmother Maria, who passed away before I had the chance to say goodbye!

Acknowledgements

This PhD has been a long, challenging, and joyful journey, one that took me away from my home country, allowed me to build a new home abroad, opened unimaginable doors, and introduced me to incredible places and people. None of what I accomplished over these past years would have been possible without the support of many.

First, I would like to thank my advisor, Dr. Patricia Glibert, who not only opened the doors of her laboratory but also of her home. I am deeply grateful for her guidance, mentorship, patience, and for all the knowledge she shared with me. Thank you, Pat, especially for your care beyond academia, for the wine and the many trips we shared. It has truly been an honor to have been your (possibly) last student.

I would like to thank my committee members: Dr. Cynthia Heil, Dr. Greg Silsbe, Dr. Ming Li, and Dr. Vyacheslav Lyubchich, for their time and dedication. I appreciate all the discussions and suggestions that helped improve my work over the years. I also thank Professor Sujay Kaushal for his availability to serve as my Dean's Representative.

I am grateful to Dr. Todd Kana and everyone at Bay Instruments for their collaboration in improving methods and for developing such innovative devices that made this study possible. I especially thank Todd for his patience in sharing his knowledge, for his help, and for his great sense of humor.

To all the faculty, administration, maintenance staff, and students at the Horn Point Laboratory: I am truly thankful for all the direct and indirect support during my time on campus. I felt genuinely welcomed in this community, and I could not have chosen a better place for graduate school. I am especially grateful for the wonderful friends I made at HPL.

A special thank you to Living by Truth Ministry for becoming my family in Cambridge. Being part of this ministry transformed my sense of belonging here. I am especially grateful to Shay Sisco and her family for opening their home to me and becoming my family here, surrounding me with immeasurable love and support.

There is something bittersweet about building a life in another country, because part of me will always remain in Brazil. Being here was only possible because, every day, I received unconditional love and support through video calls and messages. My deepest gratitude goes to my parents and my brother, who have always been, and will always be, my foundation and safe place. I also thank the rest of my family. I am immensely grateful to my friends for being who they are in my life, for being present for decades and continuing to be part of my daily life despite the distance. They have always been my favorite companions and a constant reminder that life can be light and joyful.

I would also like to acknowledge my funding sources, which made this work and my participation in conferences possible: the Izaak Walton League of America Scholarship; the Graduate School Dean's Fellowship, University of Maryland; the Travel Award from NOAA National Centers for Coastal Ocean Science, National Office for Harmful Algal Blooms; the Mature Woman's Grant from the Easton Branch of the American Association of University Women; the Ryan Saba Memorial Student Fellowship from Horn Point Laboratory; and the Horn Point Graduate Assistantship (2021–2023). I also thank NOAA for grants NA19NOS4780183 and NA23NOS4780286 and NSF award 2309082 (to PMG) and the Horn Point Laboratory for financial support.

Finally, I thank God for being my everything.

Table of Contents

List of Tables

List of Figures

Chapter 1: Introduction

It is undeniable that climate change has been causing negative impacts on the ocean and, consequently, increasing Harmful Algae Blooms (HABs) and hypoxia around the globe (Gobler, 2020; Glibert and Li 2023; Brenckman et al., 2025). Understanding these impacts becomes more complicated when we consider the interactions between the multi-stressors associated with climate change (Glibert et al., 2021; 2022). The warming of ocean water is a global phenomenon. However, different regions respond differently. Studies have shown that the rate of warming in the Gulf of Mexico (GoM; Gulf of America) is higher than the global rate, 0.15˚C decade^{-1} and 0.11˚C decade$^{-1,}$ respectively, resulting in an average increase of 1˚C since 1970 (Glenn et al., 2015; Wang et al., 2023). The temperature increase can have many impacts on the GoM, including an intensification of up to 40% of the hurricane activity and frequency, especially between August and September (Saunders and Lea, 2008).

The greater frequency of storms and hurricanes is altering the supply of nutrients in coastal waters. During periods of high runoff and rainfall, allochthonous organic matter, primarily in the form of humic acids (HA), fulvic acids, and other dissolved organic acids, can dominate the dissolved organic matter (DOM) pool (Thurman, 1985; Moran and Hodson, 1990). The increase of DOM, a process known as brownification, can alter the optical conditions of the water by reducing light penetration; however, it can also influence primary production, including the prospect of bloom development (Blanchet et al., 2022, and references therein; Urrutia-Cordero et al., 2017). For example, humic acids have been shown to be utilized in the growth of some dinoflagellates, such as *Prorocentrum minimum*, *Karenia brevis*, and *Pyrodinium bahamense* (Granéli et al., 1999; Heil, 2005; See et al., 2006; Muni-Morgan et al., 2023).

Nevertheless, the influence of humic enrichment combined with increasing temperature on phytoplankton metabolism, including both primary production and respiration, remains poorly understood.

Recent studies have indicated that climate change has also been causing changes in the composition of benthic and planktonic communities (e.g., Glibert, 2020; Griffith and Gobler, 2020). The warming of the surface waters not only increases the stratification of the water column, which favors dinoflagellates, but also influences ocean deoxygenation since oxygen solubility decreases as the temperature increases, thus facilitating the development of hypoxic conditions (Weiss,1970; Alam, 2023). Under warmer and more stratified conditions, combined with increased inputs of inorganic and organic nutrients (e.g., humic acids), the abundance, frequency, and spatial distribution of HABs are expected to increase (Glibert et al., 2022). The decomposition of HAB biomass is known to contribute to the depletion of oxygen during the senescent phase of a bloom, potentially leading to hypoxic conditions. However, little is known about the extent to which the respiration of HABs themselves contributes to deoxygenation, or how these rates may vary in response to changing environmental factors. Although recent studies associating HABs with hypoxia, especially in the GoM during *Karenia brevis* blooms (e.g., Milbrandt et al., 2021), questions remain about how HAB respiration compares to microbial respiration during bloom decay, and how both processes may respond to warming conditions.

The state of Florida is known for the diversity and frequency of HABs, with more than 75 different HAB species identified in these fresh and marine waters (reviewed in Heil and Muni-Morgan, 2021). Among those, *K. brevis* (Hansen and Moestrup, 2000) is the most frequent and studied HAB species in the Western Florida Shelf (WFS), as its blooms occur almost annually and can last up to 30 months. This species can produce the neurotoxin brevetoxin that is

responsible for the death of many marine organisms during blooms. Moreover, the toxin can pose a risk to public health as it can cause respiratory irritation in humans (Heil and Muni-Morgan, 2021). Given the frequency of occurrence and the environmental, economic, and public health impacts that *K. brevis* blooms can cause, this species is of fundamental importance in the study of HABs. To date, many studies have investigated the initiation and development of *K. brevis* blooms in the GoM; however, critical questions remain about how global-scale phenomena, such as the El Niño–Southern Oscillation (ENSO), influence these blooms, either directly or indirectly. Thus, studies investigating long-term data including these variables are important to better understand the dynamics of these events.

Similarly, little is known about how environmental parameters, such as temperature, nutrients, and light, influence productivity and respiratory processes on WFS, especially during *K. brevis* blooms. Quantifying these rates under varying conditions is critical to understanding *K. brevis* physiological adaptations during blooms. Understanding the short-term changes of these rates under different conditions would provide valuable physiological evidence to understand how these blooms can develop and be maintained in extreme conditions, such as temperatures above the optimum for this species. Further, the integration of these data into mechanistic models will enhance our ability to predict *K. brevis* bloom dynamics on the WFS. The data obtained in this study will therefore contribute to improving the predictive power and ecological accuracy of such models.

Karenia brevis *blooms in Western Florida*

The dinoflagellate *K. brevis* is well known for its annual and, in some years, prolonged

blooms in the WFS (Heil and Muni-Morgan, 2021; Stumpf et al. 2022; Glibert et al., 2025). The initiation of these events is well documented in the literature (e.g., Steidinger, 2009; Vargo, 2009; Weisberg et al., 2019). These blooms usually initiate offshore, and evidence suggests that *K. brevis* co-occurs and benefits from populations of the cyanobacteria *Trichodesmium* (Walsh and Steidinger, 2001), as it provides not only a direct supply of newly fixed nitrogen but also releases NH_4^+ and dissolved organic nitrogen (Bronk and Glibert, 1994). Dissolved organic matter is also produced as *Trichodesmium* dies and decomposes (Walsh and Steidinger, 2001; Lenes and Heil, 2010).

Physical oceanography plays an important role in *K. brevis blooms*, both in the initiation phase related to the upwelling of new nutrients and in the transportation phase of the cells nearshore via wind-driven and upwelling-related transport (Steidinger, 1975; Weisberg et al, 2014; Liu et al., 2016; Weisberg et al., 2016; 2019). Hurricanes can also play an important role in *K. brevis* blooms. For instance, the unusually high hurricane activity in 2004 led to elevated runoff and submarine groundwater discharge along the west Florida coast, fueling the persistent bloom observed in 2005 (Hu et al., 2006). Similarly, the 2018 *K. brevis* bloom was linked to intense flooding and runoff following Hurricane Irma in 2017 (Fritz, 2018). ENSO oscillations are directly related to the frequency and intensity of hurricanes. The El Niño phase brings wet and cool weather, and a greater frequency of storms to South Florida, while La Niña brings dry and warm weather Periods of mild La Niña and ENSO transitions bring a higher frequency of hurricanes that directly impact Florida (Schmidt et al., 2001; Klotzbach, 2011). Thus, understanding how these global-scale phenomena, such as ENSO, influence directly and indirectly *K. brevis* blooms in Florida is fundamental to understanding, and even predicting, periods with a higher probability of blooms and their magnitude.

Once near shore, these blooms can persist for several months as the cells can benefit from a variety of sources to maintain their blooms (Heil et al., 2014). River discharge and its associated nutrients are important in sustaining *K. brevis* blooms (e.g., Dixon and Steidinger, 2004; Li et al., 2021; Glibert et al. 2025). Further, these organisms can utilize a variety of inorganic and organic nutrients from multiple sources, such as nutrients released by other phytoplankton and zooplankton, benthic nutrient fluxes, atmospheric deposition, and decaying organic matter from dead fish (Heil et al., 2014), and they are mixotrophic and benefit from the ingestion of prey (Glibert et al., 2009; Ahn et al., 2023, 2025). Despite the well-understood initiation of *K. brevis* blooms, many unanswered questions related to the physiology of the cells and how the blooms can be maintained for long periods remain. The long-term record of these blooms holds many clues as to relationships with changing environmental factors.

Karenia brevis *and temperature*

Usually, *K. brevis* blooms initiate in early fall (August- September) and terminate in early spring (February-April) as the cells are dispersed offshore (Heil et al., 2022). However, sometimes these blooms can persist during the summer, even with temperatures exceeding their optimum range of 22 to 28˚C (Vargo, 2009; Ahn and Glibert, 2021), showing that even temperatures above 30˚C are not inhibiting blooms. There is still much to be understood about how *K. brevis* can overcome thermal stress in some years and persist above its documented thermal optimum.

Generally, phytoplankton present a classical response to temperature changes. That is, as the temperature increases, so does their growth rate, reaching a maximum at the optimum

temperature. Then, as the temperature continues to increase, the growth rate presents an abrupt decline (Eppley, 1972). However, not only do the growth rates increase with temperature, but likewise respiration. The response of both photosynthesis and respiration to changes in temperature is regulated by the enzymes involved in carbon fixation, electron transport, and different respiratory mechanisms (Raven and Geider, 1988). Respiration is more temperature-dependent than photosynthesis, and warming can have a significant impact on the metabolic balance of the oceans by increasing the rates of community respiration over the rates of gross primary production (Barton et al., 2020, and references therein). Consequently, hypoxia zones, such as in the GoM, will likely become more frequent in the future ocean, as warming waters increase not only the respiration rates but also influence ocean deoxygenation rates, facilitating the development of hypoxic conditions. Despite a recent study associating *K. brevis* bloom with hypoxia in the GoM (e.g., Milbrandt et al., 2021*;* Turley et al., 2022), many questions remain. To what extent does respiration by *K. brevis* contribute to oxygen depletion in bloom conditions? How do rates of respiration by *K. brevis* compare with heterotrophic respiration under the same environmental conditions? How will environmental factors, such as increasing temperature and/or the addition of nutrients from regular river flow and/or during tropical storms and hurricanes, influence productivity and respiratory rates?

Karenia brevis *and light*

Phytoplankton respond to light in the classically defined hyperbola, the Photosynthesis-Irradiance curve (PI curve, also referred to as a PE curve; Platt and Jassby, 1976). This relationship can be determined using different proxies such as O_2 evolution, CO_2 assimilation,

and Electron Transport Rates (ETR). Generally, the curves exhibit a predictable pattern. At the lowest light intensity, photosynthesis rates are a linear function of light. As irradiance levels increase, the rates become increasingly non-linear and rise to a saturation level, which can remain unchanged or can present photoinhibition depending upon both the irradiance and the duration of exposure (Sakshaug et al., 1997; Behrenfield et al., 2004; Glibert, 2024).

A basic, and classical, assumption is that respiration is independent of the light level with constant rates, as determined by parallel measurements made in the dark (Jassby and Platt, 1976). However, these rates are not constant and can, in fact, be light-dependent. These light-dependent respiration processes, such as cyclic electron flow, Mehler reaction, and photorespiration, help to regulate cellular redox by dissipating excess energy, preventing photoinhibition caused by excess of light or downstream metabolic limitation (Kana 1990; Kramer and Evans, 2011, and references therein). These pathways operate on a rapid timescale and have impacts on the net efficiency of photosynthetic processes since the more energy is dissipated, the lower the net production rates (Halsey and Jones, 2015). Therefore, it is crucial to understand how these processes respond not only to light variance but also to temperature and nutrient additions; thus, the establishment of the respiration-light relationships (RI or RE curves), similar to PE curves, and how such relationships may change as other environmental factors change, is an important step. Only a few studies have investigated respiration rates associated with a *K. brevis* (e.g., Hitchcock et al., 2010), but only so-called dark respiration, highlighting the necessity of studies investigating other respiratory processes. The improvement of the ^{18}O methodology described in this dissertation (Chapter 3) allows such measurements to be done in a rapid and more accessible way.

The influence of light on respiration rates is still not well studied. High rates of photorespiration have been measured associated with some dinoflagellates (e.g., Hochachka and Teal, 1964; Burris, 1977; Prézelin et al., 1977; Heil, 2005; Schaeffer et al., 2007; Schmoker et al., 2011; López-Sandoval et al., 2014; Hansen et al., 2016; Bercel and Kranz, 2019), but there are no measurements comparing photorespiration (or other respiratory pathways) under varying temperature or other environmental changes, especially in *K. brevis*. These rates have important implications for oxygen consumption and for net productivity in blooms, but especially in high biomass blooms that have been associated with oxygen depletion and hypoxia. Further, experiments testing how primary production and respiration rates vary under the interaction of multiple environmental factors (e.g., temperature, nutrients, and light) are essential to better understand the physiology of *K. brevis*. Research focusing on the physiology of these organisms is crucial to understanding the initiation, maintenance, and termination of blooms, as well as to improving prediction models.

Primary production terminology and methods

Photosynthesis can be determined as the amount of oxygen produced by PSII or the CO_2 fixed in the Calvin Cycle. These rates can be measured as Gross Primary Production (GPP), which is the total rate of O_2 or CO_2, or Net Primary Production (NPP), the rate of CO_2 or O_2 produced, accounting for all the autotrophic respiratory costs (Sakshaug et al., 1997). Traditionally, respiration is assumed to be constant, and it is usually measured in the dark; however, these rates can be light-dependent, as previously mentioned.

One of the common methods that estimates NPP and community respiration is from changes in dissolved O_2 concentration in light and dark incubations, so-called the light-dark bottle method. Then, GPP is calculated by adding NPP and respiration. Another commonly used method consists of measuring the rate of incorporation of radioactive isotope ^{14}C or, alternatively, the stable isotope ^{13}C (Falkowski and Raven, 2013; Glibert et al., 2019). With the latter method, bicarbonate labeled with ^{13}C ($H_{13}CO_3$) is added to the sample and changes in the ^{13}C:^{12}C ratio are measured using a mass spectrometer. Both C-based methods require a relatively large volume of water and can be expensive in terms of isotopes (Miller and Wheeler, 2012). Another method using isotopes consists of adding water labeled with ^{18}O and then measuring the evolution of oxygen with an isotope ratio mass spectrometer (Bender et al., 1987). Even though this technique provides relatively precise GPP measurements, it is not widely used as the methodology is complicated (Falkowski and Raven, 2013).

The ^{18}O method has been improved, and a modified Membrane Inlet Mass Spectrometry (MIMS) dissolved gas analyzer can be used to measure the enriched samples, which is less expensive than a regular mass spectrometer (Kana et al., 2006). The main advantage of this improved method is that it is considerably cheaper, the sample manipulation is easier, and only a small volume of sample is needed (~3 mL sample) with low isotope enrichment (1% of volume). Also, the analysis in the instrument is rapid, as samples can be analyzed in less than 5 minutes (Ferrón et al., 2016). As part of this dissertation, methodological improvements were developed for the use of MIMS to quantify primary production (GPP and NPP) and gross respiration using the $H_2{}^{18}O$ method (Chapter 3). These developments now allow for the measurement of these rates under a range of environmental conditions, including light, temperature, and nutrient availability, thereby advancing our understanding of phytoplankton physiology.

Hypothesis and Objectives

The overarching hypothesis of this dissertation is that climate change conditions will alter habitat suitability for *Karenia brevis* in multiple ways. Warmer waters, such as expected during summer, may be stressful for *K. brevis*, and photosynthesis rates may be decreased. However, the increase in temperature will increase respiration rates. Increasing runoff during tropical storms and hurricanes will also increase primary production and respiration rates, as it increases the amount of nutrients and organic matter. The interaction of nutrient availability and changing temperatures will alter the thermal niche of both photosynthesis and respiration, perhaps creating conditions allowing *K. brevis* to survive warmer waters.

The specific hypotheses include:

I. Interannual variation in *K. brevis* is at least in part a function of climatic variations, including ENSO and storm frequency.

II. *Karenia brevis* may be able to survive above its thermal optimum under conditions in which a secondary stress, i.e., nutrient limitation, is alleviated. However, different nutrient types (inorganic or organic compounds like humic acids) may influence the temperature response differently due to different physiology associated with metabolizing different nutrient forms.

III. Under conditions of high temperature, rates of light-dependent respiration will increase relative to photosynthesis, and light-dependent photosynthesis will also have high rates of photoinhibition and regulated and non-regulated photochemical quenching.

IV. Respiration rates may increase with temperature more than photosynthesis rates.

To address these hypotheses:

i. The relationship between blooms of *K. brevis* and environmental conditions on the WFS was investigated by performing a time-series analysis with available long-term data from 1998 to 2020 (*Chapter 2*).

ii. Methodological improvements were developed for the use of MIMS to quantify primary production (GPP and NPP) and gross respiration using the $H_2{}^{18}O$ method (*Chapter 3*).

iii. Post-hurricane field observations and laboratory experiments were used to examine how elevated temperature and humic acid enrichment influence primary production and respiration rates of natural phytoplankton communities containing *K. brevis* (*Chapter 4*).

iv. Primary production and light-dependent respiration rates, as well as Photosynthesis-Irradiance responses and Respiration-Irradiance responses of natural communities with *K. brevis* were determined from different ambient conditions and when exposed to different temperature and nutrient enrichments (*Chapter 5*).

v. Photosynthesis- Irradiance responses of cultured *K. brevis* were investigated under different temperatures (24, 27, 30˚C) and different nutrient forms (NO_3^-, NH_4^+, HA) and amounts in short term exposures (*Chapter 6*).

The main chapters of the dissertation consist of the following manuscripts:

1. Sobrinho, B. F.; Glibert, P. M; Lyubchich, V.; Heil, C. A.; Li, M. Time series analysis of the *Karenia brevis* blooms on the West Florida Shelf: relationships with El Niño – Southern Oscillation (ENSO) and its rate of change (2022). 19th International Conference on Harmful Algae Proceedings. doi.org/10.5281/zenodo.7036227 (*Chapter 2*).

2. Sobrinho, B.F.; Vidyarathna, N.; Kana, T. M.; Glibert, P. M. Improved primary production and gross respiration measurements using the $H_2{}^{18}O$ technique with Membrane Inlet Mass Spectrometry and introduction of a small volume–uniform irradiance incubation chamber. *Submitted to Journal of Phycology* (*Chapter 3*).
3. Sobrinho, B.F; Muni-Morgan, A.; Heil, C.; Glibert, P. M. Productivity, respiration, and dissolved organic matter degradation and effects of temperature in waters of southwest Florida following high riverine runoff: Implications for hypoxia and harmful algae. *Submitted to Frontiers in Marine Science* (*Chapter 4*)
4. Sobrinho, B.F.; Pinheiro-Silva, L.; Glibert, P. M. Influence of warming and nitrogen enrichment on photosynthesis and respiration rates during *Karenia brevis blooms. For submission to Environmental Research Letters* (*Chapter 5*).
5. Sobrinho, B.F.; Pinheiro-Silva, L.; Glibert, P. M. Interactive effects of temperature, nitrogen form, and humic substances on photosynthetic performance of the toxigenic dinoflagellate, *Karenia brevis. Submitted to Harmful Algae* (*Chapter 6*).

References

Ahn, S. H., & Glibert, P. M. (2021). Shining light on photosynthesis in the harmful dinoflagellate *Karenia mikimotoi* – Responses to short-term changes in temperature, nitrogen form, and availability. Phycology, 2(1), 30–44. https://doi.org/10.3390/phycology2010002

Ahn, S. H., Glibert, P. M., & Heil, C. A. (2023). In hot water: Interactions of temperature, nitrogen form and availability and photosynthetic and nitrogen uptake responses in natural *Karenia brevis* populations. Harmful Algae, 129, 102519. https://doi.org/10.1016/j.hal.2023.102519

Ahn, S. H., Mayali, X., Weber, P. K., & Glibert, P. M. (2025). Impact of nutritional history, prey quality, and quantity on grazing and photophysiological responses in the mixoplanktonic dinoflagellate *Karenia brevis*. Limnology and Oceanography. https://doi.org/10.1002/lno.70158

Alam, M. A. (2023). Climate change and its impact on depletion of oxygen levels on coastal waters and shallow seas. In N. Jayaraju, G. Sreenivasulu, M. Madakka, & M. Manjulatha (Eds.), Coasts, Estuaries and Lakes. Springer, Cham. https://doi.org/10.1007/978-3-031-21644-2_20

Barton, S., Jenkins, J., Buckling, A., Schaum, C. E., Smirnoff, N., Raven, J. A., & Yvon-Durocher, G. (2020). Evolutionary temperature compensation of carbon fixation in marine phytoplankton. Ecology Letters, 23(4), 722–733. https://doi.org/10.1111/ele.13469

Bender, M., Grande, K., Johnson, K., Marra, J., Williams, P. J. L., Sieburth, J., & Heinemann, K. (1987). A comparison of four methods for determining planktonic community production. Limnology and Oceanography, 32(5), 1085–1098. https://doi.org/10.4319/lo.1987.32.5.1085

Bercel, T. L., & Kranz, S. A. (2019). Insights into carbon acquisition and photosynthesis in *Karenia brevis* under a range of CO_2 concentrations. Progress in Oceanography, 172, 65–76. https://doi.org/10.1016/j.pocean.2019.01.011

Behrenfeld, M. J., Prasil, O., Babin, M., & Bruyant, F. (2004). In search of a physiological basis for covariations in light-limited and light-saturated photosynthesis. Journal of Phycology, 40(1), 4–25. https://doi.org/10.1046/j.1529-8817.2004.03083.x

Blanchet, C. C., Arzel, C., Davranche, A., Kahilainen, K. K., Secondi, J., Taipale, S., Lindberg, H., Loehr, J., Manninen-Johansen, S., Sundell, J., Maanan, M., & Nummi, P. (2022). Ecology and extent of freshwater browning – What we know and what should be studied next in the context of global change. Science of the Total Environment, 812, 152420. https://doi.org/10.1016/j.scitotenv.2021.152420

Brenckman, C. M., Parameswarappa Jayalakshmamma, M., Pennock, W. H., Ashraf, F., & Borgaonkar, A. D. (2025). A review of harmful algal blooms: Causes, effects, monitoring, and prevention methods. Water, 17(13), 1980. https://doi.org/10.3390/w17131980

Bronk, D. A., Glibert, P. M., & Ward, B. B. (1994). Nitrogen uptake, dissolved organic nitrogen release, and new production. Science, 265(5180), 1843–1846. https://doi.org/10.1126/science.265.5180.1843

Burris, J. E. (1977). Photosynthesis, photorespiration, and dark respiration in eight species of algae. Marine Biology, 39, 371–379. https://doi.org/10.1007/BF00391940

Dixon, L. K., & Steidinger, K. A. (2004). Correlation of *Karenia brevis* presence in the eastern Gulf of Mexico with rainfall and riverine flow. Marine Ecology Progress Series, 636, 29–32.

Eppley, R. W. (1972). Temperature and phytoplankton growth in the sea. Fishery Bulletin, 70(4), 1063–1085.

Falkowski, P. G., & Raven, J. A. (2013). Aquatic photosynthesis. Princeton University Press.

Ferrón, S., del Valle, D. A., Björkman, K. M., Quay, P. D., Church, M. J., & Karl, D. M. (2016). Application of membrane inlet mass spectrometry to measure aquatic gross primary production by the 18O in vitro method. Limnology and Oceanography: Methods, 14(9), 610–622. https://doi.org/10.1002/lom3.10116

Fritz, A. (2018). How climate change is making "red tide" algal blooms worse. The Washington Post. https://www.washingtonpost.com/news/capital-weather-gang/wp/2018/08/14/how-climate-change-is-making-red-tide-algal-blooms-even-worse/Accessed on November 10, 2025.

Glenn, E., Comarazamy, D., González, J. E., & Smith, T. (2015). Detection of recent regional sea surface temperature warming in the Caribbean and surrounding region. Geophysical Research Letters, 42(16), 6785–6792. https://doi.org/10.1002/2015GL065002

Glibert, P. M. (2020). Harmful algae at the complex nexus of eutrophication and climate change. Harmful Algae, 91, 101583. https://doi.org/10.1016/j.hal.2019.03.001

Glibert, P. M. (2024). Phytoplankton whispering: An introduction to the physiology and ecology of microalgae. Springer Nature. Cham, Switzerland, 758 pp.

Glibert, P.M., A.H.W. Beusen, A.F. Bouwman, J.M. Burkholder, K.J. Flynn, C.A. Heil, M. Li, C.-H. Lin, C.J. Madden, A. Mitra, W. Nardin, G. Silsbe, Y. Song and F. Zhang. (2021). Multifacteted climate change and nutrient effects on harmful algae require multifaceted models. In: L.M. Botana, M. C. Louzao and. N. Vilariño. Climate change and marine and freshwater toxins, 2nd edition. De Gruyter GmbH, Berlin. pp. 473-518.

Glibert, P. M., Burkholder, J. A. M., Kana, T. M., Alexander, J., Skelton, H., & Shilling, C. (2009). Grazing by *Karenia brevis* on *Synechococcus* enhances its growth rate and may help to sustain blooms. Aquatic Microbial Ecology, 55(1), 17–30. https://doi.org/10.3354/ame01279

Glibert, P. M., Cai, W.-J., Hall, E. R., Li, M., Main, K. L., Rose, K. A., Testa, J. M., & Vidyarathna, N. K. (2022). Stressing over the complexities of multiple stressors in marine and estuarine systems. Ocean-Land-Atmosphere Research, 2022, 9787258. https://doi.org/10.34133/2022/9787258

Glibert, P. M., Heil, C. A., & Li, M. (2025). More sustained, more severe blooms and shifting monthly patterns of the toxigenic dinoflagellate *Karenia brevis* on the West Florida Shelf. Harmful Algae, 139, 102967. https://doi.org/10.1016/j.hal.2025.102967

Glibert, P.M. and M. Li. 2023. Warming, wheezing, blooming waters: hypoxia and harmful algae. In: D. Baird (ed), Treatise on estuarine and coastal science, 2nd edition. Elsevier, pp. 401-444. https://doi.org/10.1016/b978-0-323-90798-9.00066-4

Glibert, P. M., Middelburg, J. J., McClelland, J. W., & Jake Vander Zanden, M. (2019). Stable isotope tracers: Enriching our perspectives and questions on sources, fates, rates, and pathways of major elements in aquatic systems. Limnology and Oceanography, 64(3), 950–981. https://doi.org/10.1002/lno.11087

Gobler, C. J. (2020). Climate change and harmful algal blooms: Insights and perspective. Harmful Algae, 91, 101731. https://doi.org/10.1016/j.hal.2019.101731

Granéli, E., Carlsson, P., & Legrand, C. (1999). The role of C, N and P in dissolved and particulate organic matter as a nutrient source for phytoplankton growth, including toxic species. Aquatic Ecology, 33(1), 17–27. https://doi.org/10.1023/A:1009925515059

Griffith, A. W., & Gobler, C. J. (2020). Harmful algal blooms: A climate change co-stressor in marine and freshwater ecosystems. Harmful Algae, 91, 101590. https://doi.org/10.1016/j.hal.2019.03.008

Halsey, K. H., & Jones, B. M. (2015). Phytoplankton strategies for photosynthetic energy allocation. Annual Review of Marine Science, 7, 265–297. https://doi.org/10.1146/annurev-marine-010814-015813

Hansen, G., Moestrup, Ø., & Roberts, K. R. (2000). Light and electron microscopical observations on the type species of *Gymnodinium, G. fuscum* (Dinophyceae). Phycologia, 39(5), 365–376. https://doi.org/10.2216/i0031-8884-39-5-365.1

Hansen, P. J., Ojamäe, K., Berge, T., Trampe, E. C., Nielsen, L. T., Lips, I., & Kühl, M. (2016). Photoregulation in a kleptochloroplastidic dinoflagellate, *Dinophysis acuta*. Frontiers in Microbiology, 7, 785. https://doi.org/10.3389/fmicb.2016.00785

Heil, C. A. (2005). Influence of humic, fulvic and hydrophilic acids on the growth, photosynthesis and respiration of the dinoflagellate *Prorocentrum minimum* (Pavillard) Schiller. Harmful Algae, 4(3), 603–618. https://doi.org/10.1016/j.hal.2004.08.010

Heil, C. A., & Muni-Morgan, A. L. (2021). Florida's harmful algal bloom (HAB) problem: Escalating risks to human, environmental and economic health with climate change. Frontiers in Ecology and Evolution, 9, 646080. https://doi.org/10.3389/fevo.2021.646080

Heil, C. A., Dixon, L. K., Hall, E., Garrett, M., Lenes, J. M., O'Neil, J. M., Walsh, B. M., Bronk, D. A., Killberg-Thoreson, L., & Weisberg, R. H. (2014). Blooms of *Karenia brevis* on the West Florida Shelf: Nutrient sources and potential management strategies based on a multi-year regional study. Harmful Algae, 38, 127–140. https://doi.org/10.1016/j.hal.2014.07.016

Hitchcock, G. L., Kirkpatrick, G., Minnett, P., & Palubok, V. (2010). Net community production and dark community respiration in a *Karenia brevis* (Davis) bloom in West Florida coastal waters, USA. Harmful Algae, 9(4), 351–358. https://doi.org/10.1016/j.hal.2010.01.002

Hochachka, P. W., & Teal, J. M. (1964). Respiratory metabolism in a marine dinoflagellate. The Biological Bulletin, 126(2), 274–281. https://doi.org/10.2307/1539525

Hu, C., Muller-Karger, F. E., & Swarzenski, P. W. (2006). Hurricanes, submarine groundwater discharge, and Florida's red tides. Geophysical Research Letters, 33(11), L11601. https://doi.org/10.1029/2005GL025449

Kana, T. M. (1990). Light-dependent oxygen cycling measured by an oxygen-18 isotope dilution technique. Marine Ecology Progress Series, 64, 293-300. https://doi.org/10.3354/meps064293

Kana, T. M., Cornwell, J. C., & Zhong, L. (2006). Determination of denitrification in the Chesapeake Bay from measurements of N_2 accumulation in bottom water. Estuaries and Coasts, 29, 222-231. https://doi.org/10.1007/BF02781991

Klotzbach, P. J. (2011). El Niño–Southern Oscillation's impact on Atlantic basin hurricanes and U.S. landfalls. Journal of Climate, 24(4), 1252–1263. https://doi.org/10.1175/2010JCLI3799.1

Kramer, D. M., & Evans, J. R. (2011). The importance of energy balance in improving photosynthetic productivity. Plant Physiology, 155(1), 70–78. https://doi.org/10.1104/pp.110.166652

Li, M. F., Glibert, P. M., & Lyubchich, V. (2021). Machine learning classification algorithms for predicting *Karenia brevis* blooms on the West Florida Shelf. Journal of Marine Science and Engineering, 9(9), 999. https://doi.org/10.3390/jmse9090999

Lenes, J. M., & Heil, C. A. (2010). A historical analysis of the potential nutrient supply from the N_2-fixing marine cyanobacterium *Trichodesmium* spp. to *Karenia brevis* blooms in the eastern Gulf of Mexico. Journal of Plankton Research, 32(10), 1421–1431. https://doi.org/10.1093/plankt/fbq061

Liu, Y., Weisberg, R. H., Lenes, J. M., Zheng, L., Hubbard, K., & Walsh, J. J. (2016). Offshore forcing on the "pressure point" of the West Florida Shelf: Anomalous upwelling and its influence on harmful algal blooms. Journal of Geophysical Research: Oceans, 121, 10.1002/2016JC011938.

López-Sandoval, D. C., Rodríguez-Ramos, T., Cermeño, P., Sobrino, C., & Marañón, E. (2014). Photosynthesis and respiration in marine phytoplankton: Relationship with cell size, taxonomic affiliation, and growth phase. Journal of Experimental Marine Biology and Ecology, 457, 151–159. https://doi.org/10.1016/j.jembe.2014.04.013

Milbrandt, E. C., Martignette, A. J., Thompson, M. A., Bartleson, R. D., Phlips, E. J., Badylak, S., & Nelson, N. G. (2021). Geospatial distribution of hypoxia associated with a *Karenia*

brevis bloom. Estuarine, Coastal and Shelf Science, 259, 107446. https://doi.org/10.1016/j.ecss.2021.107446

Miller, C. B., & Wheeler, P. A. (2012). Biological oceanography. John Wiley & Sons.

Moran, M. A., & Hodson, R. E. (1994). Dissolved humic substances of vascular plant origin in a coastal marine environment. Limnology and Oceanography, 39(4), 762–771. https://doi.org/10.4319/lo.1994.39.4.0762

Muni-Morgan, A., Lusk, M. G., Heil, C., Goeckner, A. H., Chen, H., McKenna, A. M., & Holland, P. S. (2023). Molecular characterization of dissolved organic matter in urban stormwater pond and municipal wastewater discharges transformed by the Florida red tide dinoflagellate *Karenia brevis*. Science of the Total Environment, 904, 166291. https://doi.org/10.1016/j.scitotenv.2023.166291

Platt, T., & Jassby, A. D. (1976). The relationship between photosynthesis and light for natural assemblages of coastal marine phytoplankton. Journal of Phycology, 12(4), 421–430. https://doi.org/10.1111/j.1529-8817.1976.tb02866.x

Prézelin, B. B., Meeson, B. W., & Sweeney, B. M. (1977). Characterization of photosynthetic rhythms in marine dinoflagellates: I. Pigmentation, photosynthetic capacity and respiration. Plant Physiology, 60(3), 384–387. https://doi.org/10.1104/pp.60.3.384

Sakshaug, E., Bricaud, A., Dandonneau, Y., Falkowski, P. G., Kiefer, D. A., Legendre, L., Takahashi, M. (1997). Parameters of photosynthesis: Definitions, theory and interpretation of results. Journal of Plankton Research, 19(11), 1637–1670. https://doi.org/10.1093/plankt/19.11.1637

Saunders, M. A., & Lea, A. S. (2008). Large contribution of sea surface warming to recent increase in Atlantic hurricane activity. Nature, 451(7178), 557–560. https://doi.org/10.1038/nature06422

Schaeffer, B. A., Kamykowski, D., McKay, L., Sinclair, G., & Milligan, E. J. (2007). A comparison of photoresponse among ten different *Karenia brevis* (Dinophyceae) isolates. Journal of Phycology, 43(4), 702–714. https://doi.org/10.1111/j.1529-8817.2007.00377.x

Schmoker, C., Thor, P., Hernández-León, S., & Hansen, B. W. (2011). Feeding, growth and metabolism of the marine heterotrophic dinoflagellate *Gyrodinium dominans*. Aquatic Microbial Ecology, 65(1), 65–73. https://doi.org/10.3354/ame01533

Schmidt, N., Lipp, E. K., Rose, J. B., & Luther, M. E. (2001). ENSO influences on seasonal rainfall and river discharge in Florida. Journal of Climate, 14(4), 615–628. https://doi.org/10.1175/1520-0442(2001)014<0615:EIOSRA>2.0.CO;2

See, J. H., Bronk, D. A., & Lewitus, A. J. (2006). Uptake of *Spartina*-derived humic nitrogen by estuarine phytoplankton in nonaxenic and axenic culture. Limnology and Oceanography, 51(5), 2290–2299. https://doi.org/10.4319/lo.2006.51.5.2290

Steidinger, K. A. (1975). Implications of dinoflagellate life cycles on initiation of *Gymnodinium breve* red tides. Environmental Letters, 9(2), 129–139. https://doi.org/10.1080/00139307509435842

Steidinger, K. A. (2009). Historical perspective on *Karenia brevis* red tide research in the Gulf of Mexico. Harmful Algae, 8(4), 549–561. https://doi.org/10.1016/j.hal.2008.11.009

Thurman, E. M. (1985). Transport, origin and source of dissolved organic carbon. In Organic Geochemistry of Natural Waters (pp. 67-85). Dordrecht: Springer Netherlands. https://doi.org/10.1007/978-94-009-5095-5_3

Turley, B. D., Karnauskas, M., Campbell, M. D., Hanisko, D. S., & Kelble, C. R. (2022). Relationships between blooms of *Karenia brevis* and hypoxia across the West Florida Shelf. Harmful Algae, 114, 102223. https://doi.org/10.1016/j.hal.2022.102223

Urrutia-Cordero, P., Ekvall, M. K., Ratcovich, J., Soares, M., Wilken, S., Zhang, H., & Hansson, L. A. (2017). Phytoplankton diversity loss along a gradient of future warming and brownification in freshwater mesocosms. Freshwater Biology, 62(11), 1869–1878. https://doi.org/10.1111/fwb.13027

Vargo, G. A. (2009). A brief summary of the physiology and ecology of *Karenia brevis* Davis (G. Hansen and Moestrup comb. nov.) red tides on the West Florida Shelf and of hypotheses posed for their initiation, growth, maintenance, and termination. Harmful Algae, 8(4), 573–584. https://doi.org/10.1016/j.hal.2008.11.002

Walsh, J. J., & Steidinger, K. A. (2001). Saharan dust and Florida red tides: The cyanophyte connection. Journal of Geophysical Research: Oceans, 106(C6), 11597–11612. https://doi.org/10.1029/1999JC000123

Wang, Z., Boyer, T., Reagan, J., & Hogan, P. (2023). Upper-oceanic warming in the Gulf of Mexico between 1950 and 2020. Journal of Climate, 36(8), 2721–2734. https://doi.org/10.1175/JCLI-D-22-0409.1

Weisberg, R. H., Liu, Y., Lembke, C., Hu, C., Hubbard, K., & Garrett, M. (2019). The coastal ocean circulation influence on the 2018 West Florida Shelf *K. brevis* red tide bloom. Journal of Geophysical Research: Oceans, 124(4), 2501–2512. https://doi.org/10.1029/2018JC014887

Weisberg, R. H., Zheng, L., Liu, Y., Corcoran, A. A., Lembke, C., Hu, C., Lenes, J. M., & Walsh, J. J. (2016). *Karenia brevis* blooms on the West Florida Shelf: A comparative study of the robust 2012 bloom and the nearly null 2013 event. Continental Shelf Research, 120, 106–121. https://doi.org/10.1016/j.csr.2016.03.011

Weisberg, R. H., Zheng, L., Liu, Y., Lembke, C., Lenes, J. M., & Walsh, J. J. (2014). Why no red tide was observed on the West Florida Continental Shelf in 2010. Harmful Algae, 38, 119–126. https://doi.org/10.1016/j.hal.2014.04.010

Weiss, R. F. (1970). The solubility of nitrogen, oxygen and argon in water and seawater. Deep-Sea Research and Oceanographic Abstracts, 17(4), 721–735. https://doi.org/10.1016/0011-7471(70)90037-9

Chapter 2: Time series analysis of the *Karenia brevis* blooms on the West Florida Shelf: relationships with El Niño – Southern Oscillation (ENSO) and its rate of change[1]

Abstract

Blooms of the toxigenic dinoflagellate *Karenia brevis* occur regularly in the Gulf of Mexico, especially along the coast of western Florida, USA. Here, time-series data from 1998 to 2020 were used to examine relationships between *K. brevis* abundance and the El Niño – Southern Oscillation (ENSO) and its rate of change, as well as temperature, precipitation, river flow, and salinity. This time series includes periods of substantial blooms (~ 1.4×10^6 cells L^{-1}) and times characterized by background cell concentrations (~1.0×10^3 cells L^{-1}). El Niño brings wet and cool weather to South Florida, including a greater frequency of storms, while La Niña brings dry and warm weather. However, mild La Niña and periods of ENSO transitions bring a higher frequency of hurricanes that directly impact Florida. Excluding the large bloom of 2020–2021 (not included herein), the highest *K. brevis* abundances observed were associated with blooms in 2004–2005 and 2017–2018, both of which occurred when hurricanes followed drought periods. High correspondences between cell concentrations, Peace River discharge and ENSO index indicated that freshwater flow, and climate oscillations may play important roles–both direct and indirect–on *K. brevis* blooms on the West Florida Shelf. These time-series analyses will help to inform new models of bloom formation and termination in western Florida waters and may help to guide nutrient reduction targets from river discharge.

[1] **Sobrinho, B. F**., Glibert, P. M., Lyubchich, V., Heil, C. A., & Li, M. (2022). Time series analysis of *Karenia brevis* blooms on the West Florida Shelf: Relationships with El Niño–Southern Oscillation (ENSO) and its rate of change. In C. J. Band-Schmidt & C. F. Rodríguez-Gómez (Eds.), Proceedings of the 19th International Conference on Harmful Algae (pp. 365). International Society for the Study of Harmful Algal Blooms. La Paz, Mexico.

Introduction

Blooms of the toxigenic dinoflagellate *Karenia brevis* occur annually in the eastern Gulf of Mexico (Steidinger, 2009). Bloom duration can vary from months to years, and blooms can extend up to 1000 kilometers along the coastline. Blooms initiate offshore (20–65 km) and the transportation of the cells nearshore occurs via the bottom Ekman layer driven by wind-driven and upwelling-related transport (Steidinger, 1975; Weisberg et al., 2016). Both physical drivers and nutrient supply are important to the initiation, development, and maintenance of *K. brevis* blooms (reviewed in Heil and Muni-Morgan, 2021; Li et al., 2021).

Oscillations of El Niño and La Niña, the El Niño - Southern Oscillation (ENSO), affect southwest Florida in complex ways. El Niño brings wet and cool weather to South Florida, including a greater frequency of storms, while La Niña brings dry and warm weather. However, both mild La Niña periods and transitions in ENSO periods may bring a higher frequency of hurricanes, which increase both freshwater flows and associated nutrient delivery to coasts. This study investigated the relationship between environmental conditions (temperature, salinity, river discharge and the ENSO) and the *K. brevis* concentration along the southwestern coast of Florida, using available long-term data.

Materials and Methods

Overview of Florida HAB database

Geo-referenced *K. brevis* surface cell concentration data (cells L^{-1}) with associated temperature (˚C), and salinity data for southwest Florida from 1998 to 2020 were obtained by

request from the Florida Fish and Wildlife Research Institute (FWRI). This *K. brevis* cell concentration database (the Florida HAB Historical Database) contains data collected by state and county agencies, private research institutions and university researchers and represents samples collected during research, routine monitoring, and event response sampling of suspected or confirmed *K. brevis* events. This analysis is limited to data post-1998 when routine sampling intensified, but the database contains records dating back to 1953. This analysis also does not include the large bloom that began in late 2020.

Monthly ENSO status was derived from the US National Oceanic and Atmospheric Administration (NOAA; https://ggweather.com/enso/oni.htm). These data are reported as running 3-month averages. Precipitation (mm) data and the discharge of the Peace and Caloosahatchee Rivers (cubic feet s^{-1}) data were from the United States Geological Survey (sites USGS 2296750 and USGS 2292000, respectively; https://waterdata.usgs.gov/nwis). The Peace River is one of the largest rivers in Florida with a natural flow. The Caloosahatchee River is significantly larger; however, its flow is actively managed and thus does not necessarily parallel precipitation trends.

Statistical analysis

Monthly *K. brevis* cell concentration averages were calculated for the whole southwest Florida to compare all variables during the study period of 22 years. To determine relationships, correlations were estimated using Pearson's correlations between these monthly averaged *K. brevis* (log-transformed) abundances and environmental variables were calculated. As there is a possibility of a lag response in *K. brevis* concentration in relation to environmental conditions

(Dixon and Steidinger, 2004), cross-correlation analysis with lags 0–12 months was performed. Multi-co-linearity was assessed before estimating a model with a combination of predictors. A generalized additive mixed model (GAMM) representing the relationship between Peace River discharge and environmental parameters (ENSO index and precipitation) was also developed. In both approaches, normality, variance homogeneity, and uncorrelatedness of model residuals were assessed using residual time series and Q–Q plots, Shapiro–Wilk normality tests, and plots of the autocorrelation function. As the residuals of the models presented non-normal distribution, the sieve bootstrap approach was used to obtain sample distributions of the model coefficients and assess their statistical significance. All analyses were performed using R language (R Core Team, 2021).

Results and Discussion

Blooms of *K. brevis* typically originate in late summer, following the wet season (e.g., Lenes and Heil, 2010). However, annual variations in bloom duration and intensity are large. In years of substantial La Niña, when dry conditions develop, blooms are typically short lived, as exemplified by the 2000 bloom (Figure 2.1a). The spring accumulations of *K. brevis* during 2000 represented the prolonged bloom that was initiated the previous year. In contrast, during El Niño years (e.g., 2015), blooms may be sustained at high cell abundances for a longer period throughout the fall months, following the more significant flows of the summer wet season (Figure 2. 1b). The annual timing of blooms implies that nutrients delivered during the summer wet season help to sustain nearshore blooms into the fall months and may help to regulate the magnitude of blooms that develop.

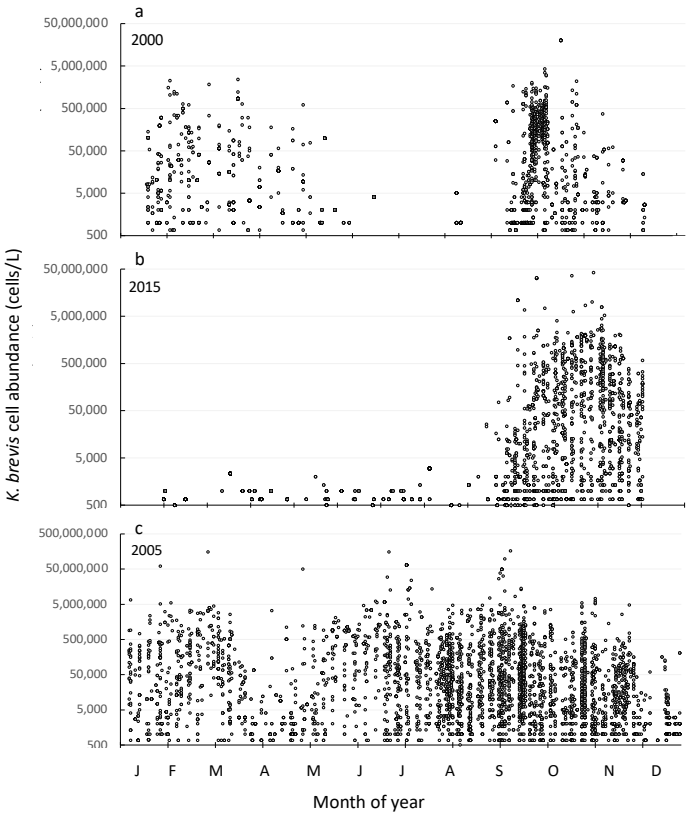

Figure 2.1 Examples of the variation in annual *K. brevis* bloom intensity and timing. The year 2000 was a year of La Niña, 2015 was a year of substantial El Niño, and 2005 was a year of transition from El Niño to La Niña. Note difference in scales between years.

Extreme bloom conditions are witnessed only occasionally, as exemplified in 2005, when high cell abundances were observed throughout the year (Figure 2.1c), including throughout the summer months. That blooms can be sustained throughout the summer months, at least during some years, implies that higher summer temperatures are not an obstacle to sustaining blooms. While summer temperatures may exceed the temperature optimum for growth (Steidinger, 2009; Vargo, 2009), they are not necessarily inhibiting for growth, especially if sufficient nutrients are available. In 2005, when the bloom was sustained through the summer months, flow from the Caloosahatchee River was three times its long-term average during the months of April and May, thus potentially delivering above average nutrient loads early in that year.

Positive significant correlations between Peace River discharge, ENSO, and *K. brevis* were observed with zero lag (Table 2.1). Dixon and Steidinger (2004) observed a similar relationship between *K. brevis* concentration and Peace River flows for the 1953-1998 period. Moreover, the GAMM indicated a statistically significant relationship between the Peace River discharge and ENSO at both lag 0 and 1 month. Although cross-correlation analysis showed a lag response of 2 months between ENSO and *K. brevis*, it was not statistically significant in the model. Also, significant negative relationships were observed between precipitation, salinity, temperature, and *K. brevis* (Table 2.1). No significant relationships were observed with flow from the Caloosahatchee River, as was observed by Dixon and Steidinger (2004) for 1953-1998. While overall flows from the Caloosahatchee River are higher than those of the Peace River, flows are more irregular, as they are actively managed to avoid inland flooding, which leads to a lack of long-term correlations across years.

Table 2.1 Statistically significant cross-correlation between time series of log-transformed *K. brevis* and the environmental variables with lags ranging from 0 to 12 months. P-values are in parentheses.

Variables	**Lag**	**Correlation (p-value)**
ENSO	0	0.15 (0.01)
Pease River discharge	0	0.14 (0.01)
Precipitation	0	-0.13 (0.02)
Salinity	0	-0.13 (0.03)
Temperature	0	-0.15 (0.01)

Blooms in 2000, 2010 and 2020, were associated with intensive La Niña conditions (ENSO<1), while bloom years such as 2015 had intensive El Niño conditions (ENSO>1). More common, however, are bloom years that are neutral with respect to La Niña or El Niño (i.e. mild

ENSO conditions). Intensive La Niña years bring drought and few hurricanes, but milder La Niña conditions and ENSO transition periods can yield hurricanes that directly impact the Florida coast (Figure 2.2). Excluding the large bloom that is currently ongoing (2020–2021), the highest annual abundances of *K. brevis* observed in this study were during the 2004–2005 and 2017–2018 blooms, which occurred when hurricane events followed drought periods (Figure 2.2). When combining these data, the periods of largest blooms occurred during transition periods in the ENSO index (Figure 2.2).

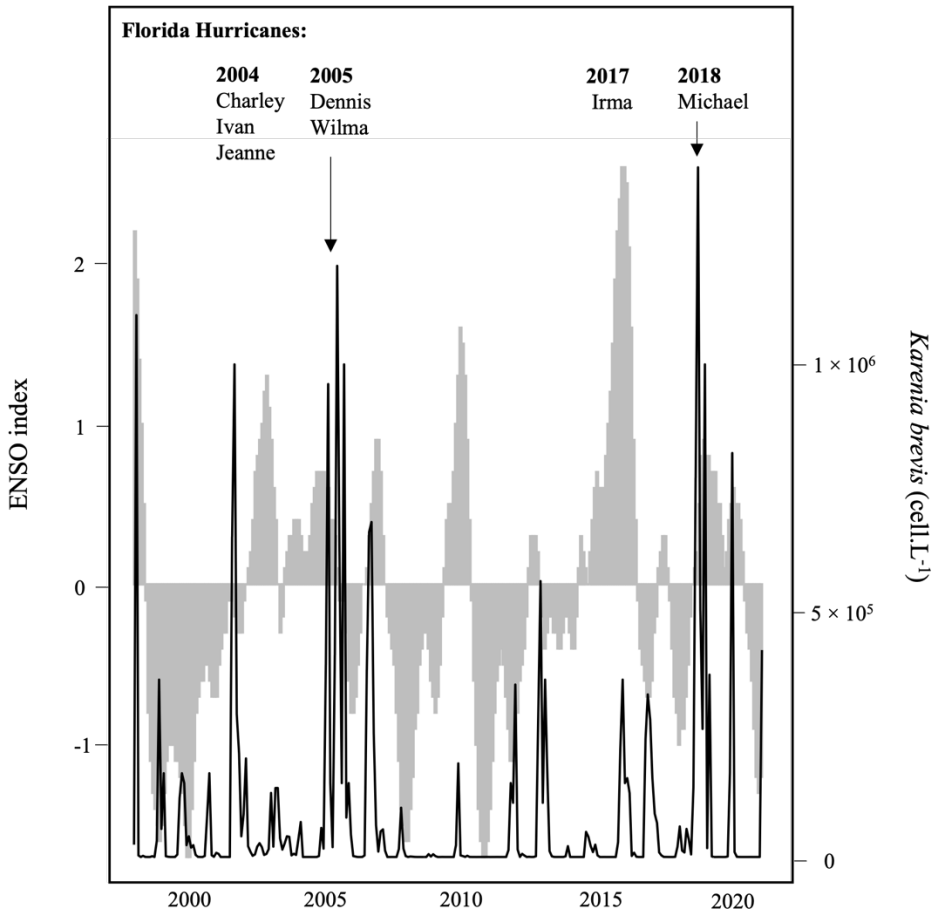

Figure 2.2 ENSO index and *K. brevis* abundance (cells L^{-1}) between the years 1998 and 2020.

Nutrient loads were not directly addressed herein, however Li et al. (2021) demonstrated that the probability of *K. brevis* increased with increasing river flows across all discharge levels, suggesting that the composition of nutrients discharged by different rivers impacts localized coastal *K. brevis* blooms. Medina et al. (2020) observed NO_{3+2} levels at lock S79 upriver of the Caloosahatchee River mouth were related to localized *K. brevis* concentrations at the river mouth from 2012-2018, although it was unclear if this effect was the result of river or estuarine nutrient sources. Effects of nutrient loads on HABs associated with hurricanes and ENSO have also been documented for Lake Okeechobee, the Indian River Lagoon and Florida Bay (Phlips et al., 2020; Glibert et al., 2023). A study using a three-dimensional ocean-biogeochemical model has also identified ENSO as the main driver of the variability of plankton biomass in the northern Gulf of Mexico during winter and spring (Gomez et al., 2019).

In sum, as the river drainages impacting the West Florida Shelf are large, changes in precipitation can translate to large changes in discharges and associated nutrients. Changes in discharge arising from ENSO oscillations as well as active management have the potential to affect *K. brevis* bloom timing, duration, and intensity through changes in nutrient delivery and salinity and temperature. These relationships may also help to inform potential nutrient reduction strategies to mitigate blooms.

References

Dixon, L. K., & Steidinger, K. A. (2004). Correlation of *Karenia brevis* presence in the eastern Gulf of Mexico with rainfall and riverine flow. *Marine Ecology Progress Series*, 636, 29–32.

Glibert, P. M., Heil, C. A., Madden, C. J., & Kelly, S. P. (2023). Dissolved organic nutrients at the interface of fresh and marine waters: flow regime changes, biogeochemical cascades and picocyanobacterial blooms—the example of Florida Bay, USA. *Biogeochemistry*, 164(1), 229-255. https://doi.org/10.1007/s10533-021-00760-4

Gomez, F.A., Lee, SK., Hernandez, F.J. et al. ENSO-induced co-variability of salinity, plankton biomass and coastal currents in the northern Gulf of Mexico. (2019) *Sci Rep 9*, 178. https://doi.org/10.1038/s41598-018-36655-y

Heil, C. A., & Muni-Morgan, A. L. (2021). Florida's harmful algal bloom (HAB) problem: Escalating risks to human, environmental and economic health with climate change. *Frontiers in Ecology and Evolution*, 9, 646080. https://doi.org/10.3389/fevo.2021.646080

Lenes, J. M., & Heil, C. A. (2010). A historical analysis of the potential nutrient supply from the N_2-fixing marine cyanobacterium *Trichodesmium* spp. to *Karenia brevis* blooms in the eastern Gulf of Mexico. *Journal of Plankton Research*, 32(10), 1421–1431. https://doi.org/10.1093/plankt/fbq061

Li, M. F., Glibert, P. M., & Lyubchich, V. (2021). Machine learning classification algorithms for predicting *Karenia brevis* blooms on the West Florida Shelf. *Journal of Marine Science and Engineering*, 9(9), 999. https://doi.org/10.3390/jmse9090999

Medina, M., Huffaker, R., Jawitz, J. W., & Muñoz-Carpena, R. (2020). Seasonal dynamics of terrestrially sourced nitrogen influenced *Karenia brevis* blooms off Florida's southern Gulf Coast. *Harmful Algae*, 98, 101900. https://doi.org/10.1016/j.hal.2020.101900

Phlips, E. J., Badylak, S., Nelson, N. G., & Havens, K. E. (2020). Hurricanes, El Niño and harmful algal blooms in two sub-tropical Florida estuaries: Direct and indirect impacts. *Scientific Reports*, 10(1), 1910. https://doi.org/10.1038/s41598-020-58771-4

R Core Team. A Language and Environment for Statistical Computing. (2021). Available online: https://www.R-project.org/

Steidinger, K. A. (1975). Implications of dinoflagellate life cycles on initiation of *Gymnodinium breve* red tides. *Environmental Letters*, 9(2), 129–139. https://doi.org/10.1080/00139307509435842

Steidinger, K. A. (2009). Historical perspective on *Karenia brevis* red tide research in the Gulf of Mexico. *Harmful Algae,* 8(4), 549–561. https://doi.org/10.1016/j.hal.2008.11.009

Vargo, G. A. (2009). A brief summary of the physiology and ecology of *Karenia brevis* Davis (G. Hansen and Moestrup comb. nov.) red tides on the West Florida Shelf and of hypotheses posed for their initiation, growth, maintenance, and termination. *Harmful Algae*, 8(4), 573–584. https://doi.org/10.1016/j.hal.2008.11.002

Weisberg, R. H., Zheng, L., Liu, Y., Corcoran, A. A., Lembke, C., Hu, C., Lenes, J. M., & Walsh, J. J. (2016). *Karenia brevis* blooms on the West Florida Shelf: A comparative study of the robust 2012 bloom and the nearly null 2013 event. *Continental Shelf Research*, 120, 106–121. https://doi.org/10.1016/j.csr.2016.03.011

Chapter 3: Improved primary production and gross respiration measurements using the $H_2{}^{18}O$ technique with Membrane Inlet Mass Spectrometry and introduction of a small volume–uniform irradiance incubation chamber[2]

Abstract

A significant improvement in the $H_2{}^{18}O$ technique for phytoplankton gross primary productivity (GPP), net primary productivity (NPP), and gross respiration (GR) is described that reduces cost, labor, and time over the traditional isotope ratio mass spectrometer (IRMS) method. Membrane Inlet Mass Spectrometry (MIMS) was optimized to measure small (3 mL) samples with low isotope enrichment (1% ^{18}O) and at high analytical precision (~1 per mil). A Photosynthetron was used to measure up to 10-point light curves of GPP, NPP, and GR using 50 mL of sample water with an isotope cost of <$15 per experiment. A new incubation device is described, a Coronatron, that allows up to 12 samples with nutrient manipulation under uniform irradiance. Example light curves from highly contrasting natural water samples are presented that show elevated GPP relative to NPP and substantial light-stimulated GR, and example nutrient manipulation curves are presented showing GPP, NPP and GR as a function of changes in ambient nitrate concentrations and different temperatures under constant light.

[2] **Sobrinho, B. F.**; Vidyarathna, N; Kana, T. M.; Glibert, P. M. Improved primary production and gross respiration measurements using the $H_2{}^{18}O$ technique with Membrane Inlet Mass Spectrometry and introduction of a small volume–uniform irradiance incubation chamber. *Submitted to Journal of Phycology*

Introduction

Phytoplankton are responsible for a significant portion of oxygen (O_2) production through photosynthetic processes. Accurate determinations of O_2 evolution (Gross Primary Production, GPP, and Net Primary Production, NPP) and uptake processes (Respiration, R) across different aquatic environments, from highly productive areas to low-productivity zones, are of great importance and relevance. It is close to 100 years since Gaarder and Gran (1927) introduced the popular 'light bottle-dark bottle' technique. This technique made it possible to directly measure both NPP and R rates in paired light and dark incubations and to use that information to derive GPP by adding back R to the NPP result. Insofar as the processes measured in dark incubations are reflective of community respiration (CR), they encompass the consumption of O_2 by all organisms in the water (i.e., bacteria, autotrophs, heterotrophs, zooplankton, etc.). Thus, the potential for CR to impact the GPP measurement is high. In addition, the light bottle-dark bottle technique assumes that CR is unaffected by light whether by material cycling in the light or by physiological processes.

In the 1950s, photosynthesis researchers discovered light stimulation of O_2 consumption in isolated chloroplasts and microalgae (Mehler and Brown,1952; reviewed by Glibert 2024). This process is not captured in traditional dark bottle (i.e. CR) measurements. In experiments by Mehler and Brown (1952), the O_2 stable isotope, $^{18}O_2$, was used to distinguish O_2 consumption from O_2 production reactions in photosynthetic systems. Photosynthetic O_2 production is derived from two water molecules that have an ^{16}O abundance of 99.8% and therefore photosynthetic production is very close to 100% mass $^{32}O_2$. The measurement of O_2 consumption was accomplished using isotope dilution, that is, by artificially enriching the sample with labeled O_2 (either as mass 34 or 36), which is unaffected by photosynthesis, and measuring the rate of

change of the labeled O_2 concentration due to consumption (respiration) reactions. Such experiments measured the true rate of gross O_2 production and gross O_2 consumption occurring simultaneously. These early physiology studies established the existence of a photosynthetic O_2 cycle involving O_2 evolution at photosystem II and O_2 reduction downstream (acceptor side) of photosystem I and a light dependency on O_2 uptake. The eponymous Mehler reaction (a part of the "water-water cycle"), which is observed to varying extents in most photosynthetic organisms, has been interpreted as a mechanism to dissipate energy and/or a mechanism to adjust the ATP/NADPH ratio according to demand as the Mehler reaction can drive non-cyclic photophosphorylation (Makino et al., 2002; Kramer and Evans, 2010). There are additional O_2 consumption reactions that are influenced directly by light, including chlororespiration and photorespiration, and indirectly by light including normal mitochondrial and alternative respiration. There is a near absence of information on these light-dependent processes in natural phytoplankton systems. Herein, we term Gross Respiration (GR) as the total O_2 uptake, including light-dependent and light-independent processes.

To obtain values of GR, some researchers have added ^{18}O-labeled water and measured the evolution of O_2 with an Isotope Ratio Mass Spectrometer (IRMS) in natural environments (e.g., Bender et al., 1987). With this approach, GPP is derived from the increase in isotope enrichment of O_2, NPP is determined by the change in total O_2 using high precision O_2/Ar measurements, and GR is determined from GPP–NPP. On the one hand, the method is highly sensitive for GPP measurements as the production of new mass 34 from photosynthesis is measured against trace levels of background mass 34 oxygen (i.e. ~0.4% of total O_2). On the other hand, NPP is a less sensitive measurement because the change in O_2 concentration, which can be very small, is measured against a relatively high concentration of mass 32 O_2 in the

sample. Even though this technique can provide GPP measurements for oligotrophic waters, it is not widely used as the instrumentation required is expensive and the methodology complicated (Falkowski and Raven, 2013).

In 1963, Hoch and Kok (1963) described a new analytical method, Membrane Inlet Mass Spectrometry (MIMS), which soon became the preferred method for photosynthetic O_2 cycling investigations of algae and chloroplasts in the laboratory owing to its rapid response time and relatively easy construction. However, while suitable for laboratory cultures, this technique lacked the precision to measure the low O_2 fluxes in natural phytoplankton samples. For ecological measurements of GPP and GR, an incubation technique was required. Kana (1992) used isotope dilution methodology in which a water sample was enriched with $^{18}O_2$ and the change in isotope enrichment and net change in O_2 was measured by a quadrupole mass spectrometer and Winkler titrations, respectively (Figure 3.1). This method was subsequently improved using MIMS for determinations of both isotope ratios and O_2 concentration changes (Suggett et al. 2009).

While the $H_2{}^{18}O$ technique continues to be used in several oceanographic laboratories with access to an isotope ratio mass spectrometer (IRMS), a degree of simplification was introduced by Ferrón et al (2016) by using MIMS for the measurement of isotope ratios and net O_2 changes ($\Delta O_2/Ar$). MIMS instruments are typically constructed with less expensive mass spectrometers (approx. factor of 3-5 relative to IRMS) and provide rapid and direct analysis of raw water samples. Ferrón et al (2016) demonstrated that despite the lower precision of MIMS compared to IRMS, the resulting GPP and NPP rates measured on oligotrophic (<1 μmol O_2 L^{-1} d^{-1}) ocean samples were comparable.

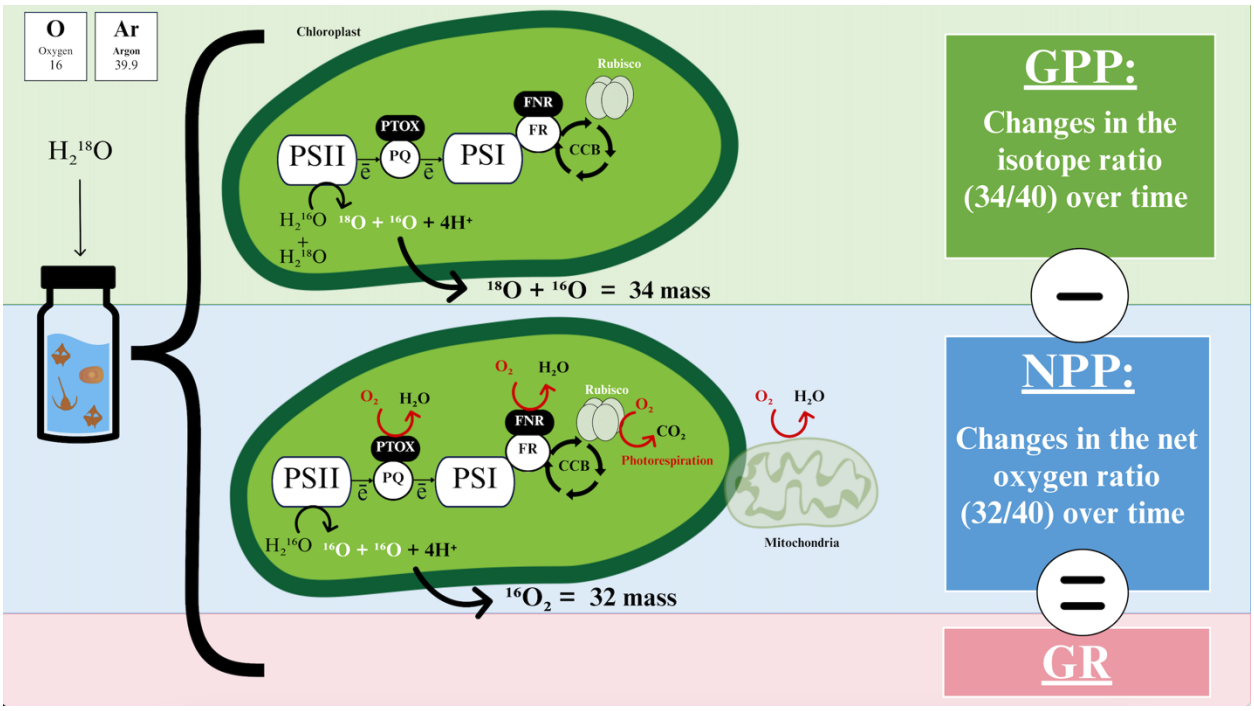

Figure 3.1 Schematic of the estimation of Gross Primary Production (GPP), Net Primary Production (NPP), and Gross Respiration (GR) from a single incubation vial using the $H_2{}^{18}O$ technique with Membrane Inlet Mass Spectrometry (MIMS). During photosynthesis, cells use both natural water, containing predominantly (99.8%) ^{16}O, and isotope-enriched water with ^{18}O added to the incubation. The incorporation of both ^{16}O and ^{18}O results in the production of O_2 with mass 34, which allows GPP to be estimated based on its change over time. Rates of NPP are calculated from the net O_2 signal (mass 32) over time, reflecting the balance of O_2-producing and O_2-consuming processes. GR is determined as the difference between GPP and NPP, tracing the consumption of the labeled ^{18}O to specifically identify light-dependent respiration. Although MIMS can quantify individual gas species with linear calibration curves, improved precision is achieved by using gas ratio measurements. Biologically inert argon (Ar) is used as a reference gas, and the mass ratios 32/40 and 34/40 are used to calculate the primary production and GR rates. The phytoplankton symbols are from the Integration and Application Network (IAN), University of Maryland Center for Environmental Science.

Motivated by the success of Ferrón et al (2016) with MIMS, we sought to reduce the cost and improve the flexibility of incubation protocols to provide methods for physiological experiments on natural water samples. Such experiments would allow a direct test of ideas and understanding derived from laboratory experiments on algal cultures. We describe a method that uses lower sample volumes and hence lower isotope costs, that can be scaled to greater sample numbers. MIMS was optimized to measure small (3 mL) samples with low isotope enrichment

(1% ^{18}O) and at high analytical precision (~1 per mil). A new incubation device is also described that allows small volume incubations under constant and uniform irradiance for investigating effects of nutrients and/or other chemical or temperature manipulations.

Materials and Methods

Membrane Inlet Mass Spectrometry

The $H_2{}^{18}O$ technique requires high precision measurement of $^{32}O_2$ and $^{34}O_2$. Whereas MIMS can quantitate individual gas species and generally exhibits linear calibration curves, improved precision is obtained using gas ratio measurements. In the present case, biologically inert Argon (Ar; mass 40) was used as a reference gas and mass ratios 32/40 and 34/40 were measured.

Instrument performance

Calibration curves for quadrupole mass spectrometers (QMS) are influenced by vacuum pressure relationships and instrument parameterization, typically with respect to ion source settings and gas injection rates. The performance of the QMS was evaluated using an open leak device calibrated at three pressures (CLO-5-3P-Air, Vacuum Technology, Inc, Oak Ridge, TN). An open leak simulates the behavior of a membrane inlet in that gas entering the QMS is proportional to the varying concentration of dissolved gas behind the membrane. The calibrated leak was attached to a hand pump (0-700 kPa; MagnumPro, East Hills Instruments, Westbury, NY) with digital pressure gauge (Accu Cal Plus, 3D Instruments, Anaheim, CA) which delivered air to the QMS in the range of approx. 1×10^{-5} to 2×10^{-4} mbar-L s^{-1} and resulted in QMS

pressures in the range of approx. 1×10^{-7} mbar to 2×10^{-6} mbar. The QMS had a gas-tight ion source so the pressure inside the ion source was higher than the chamber gauge pressure.

The calibrated leak allowed the identification of the pressure region and ion source parameters that yielded linear and proportional relationships with ion currents and constancy of gas ratio data. The onset of curvature in the pressure-ion current relationship was observed at approx. 5×10^{-7} mbar QMS pressure, and the membrane inlet was configured to yield QMS pressure $<5\times10^{-7}$. Generally, linear relationships were observed between pressure and ion currents, but the degree of proportionality (slope and intercept) was influenced by ion source parameters. For single point calibrations used during sample analyses, proportionality is required and calibration curves should extrapolate through the origin. The QMS was tuned so that intercepts were $<\pm1\%$ of typical sample values.

Incubation devices

Experiments were conducted in two types of incubations devices. The first is a "Photosynthetron" (MacIntyre et al., 1996). The vial holder is an aluminum block with 24 through holes and an internal channel for thermostated water for temperature control. The block accommodated two sets of duplicate dark conditions and two sets of 10 light intensities each ranging from limited to saturated intensities (up to ~1000 μmol photons m^{-2} s^{-1}) (Figure 3.2a). The device was made to accommodate 3 mL screw-capped vials (12.5 mm diameter; Labco Exetainer). Irradiance levels for individual vials were set using neutral density filters printed from gray scale images on transparent film and positioned below each vial. Irradiances were calibrated using an H. Walz ULM-500 meter and US-SQS/L spherical sensor positioned inside a Exetainer vial filled with water.

The second device, herein termed a “Coronatron” (based on its resemblance to a corona virus once vials are inserted; Figure 3.2b), is a spherical incubator (integrating sphere) with 12 placeholders for the same type of 3 mL vials, with each vial receiving the same irradiance from an internal light source. The Coronatron allows sample manipulations of nutrients or other amendments under identical irradiances. The incubator operated at ambient temperature facilitated by an internal fan. The incubator was typically used inside small thermostated incubators (Vevor 25L) to maintain temperatures different from room temperature. Uniformity of irradiance across all vials was within a few percent. The internal white (4000K) light sources were Xicado “Artist Series” LED modules (p/n XIM09953513A3A) with adjustable output. Irradiance was measured similarly to the Photosynthetrons.

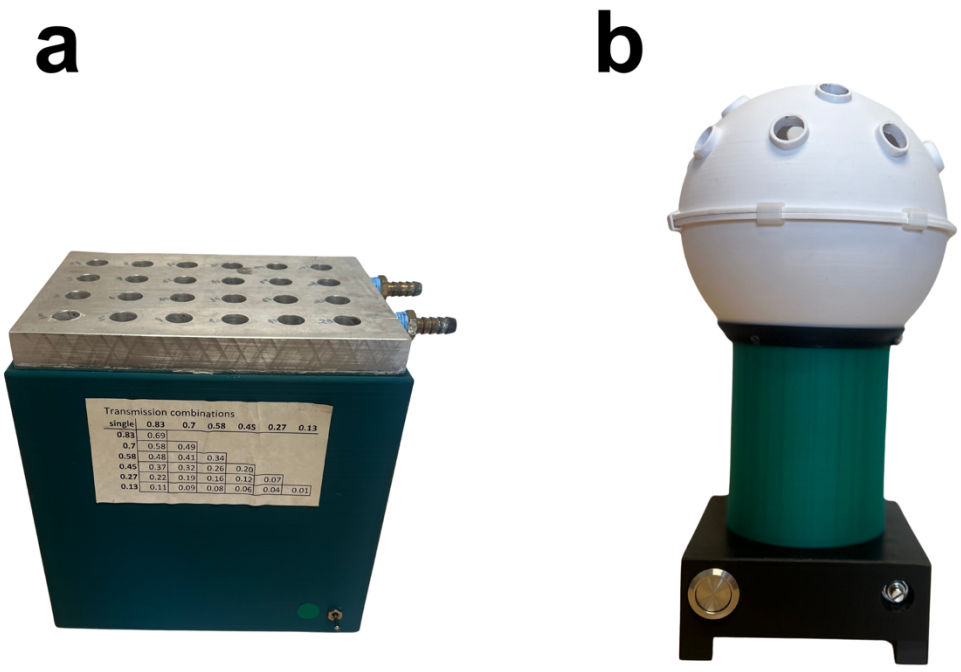

Figure 3.2 (a) Photosynthetron and (b) Coronatron.

Experiments on natural samples spanning a gradient of conditions

The evaluation experiments described herein were conducted across a range of aquatic environments with various concentrations of chlorophyll-*a*, temperatures and salinity (Table 3.1). Environmental water was initially screened through 100-micron nylon mesh and then returned within 30 minutes to the laboratory for processing. Two types of experiments are illustrated here to demonstrate the application of the technique using Photosynthetrons, to measure the effect of irradiance, and in Coronatrons, to measure the effect of nutrient and temperature manipulations.

For measurements of GPP and GR as a function of irradiance, surface waters were collected from three contrasting sites: the Choptank River, Maryland, USA, Charlotte Harbor, Florida, USA., and Lake Sarasota, Florida (Table 3.1). For comparison, experiments were also conducted using a culture of *Karenia brevis* during exponential growth. For measurements of GPP and GR as a function of varying nutrient content at constant irradiance, surface water samples were collected from New Pass, Sarasota, Florida, and incubated at different temperatures by placing the Coronatrons in thermostated incubators (Table 3.1).

Once in the laboratory, water samples were enriched using >98% enrichment $H_2{}^{18}O$ at 1% volume/volume and carefully dispensed into 3 mL screw-capped vials with Viton septa containing glass beads. The septa were punched from 3 mm Viton duro 60 sheet material. Stock Exetainer septa (chlorobutyl rubber) cannot be used due to a pronounced photochemical reaction with O_2. The vials were filled using a repeater pipette and capped with no headspace to avoid air contamination. Triplicate samples were immediately fixed with saturated mercuric chloride ($HgCl_2$, ~0.1% v/v), representing a time zero value. The remaining vials were incubated in the custom-made Photosynthetrons or Coronatrons to determine relationships as a function of light

or nutrient addition. For the Coronatron experiments, the incubation devices were placed in small, portable temperature control incubators to further evaluate temperature effects. The incubation time varied according to the biomass of each sampling station, ranging from 4 to 10 hours. After the incubation, samples were fixed with $HgCl_2$ and stored at room temperature in jars filled with water (to minimize air contamination) until MIMS analysis, which occurred within about 7 days.

Table 3.1 Sample collection site for experiments with its specific chlorophyll-*a* concentrations ($\mu g\ L^{-1}$), temperature (˚C) and salinity.

Sample	**Chl-*a* ($\mu g\ L^{-1}$)**	**Temperature (˚C)**	**Salinity**	**Experiment**
Charlotte Harbor, FL USA	2.22	25	31	PE curves
Choptank River, MD, USA	5.04	21	15	PE curves
Choptank River, MD, USA	9.91	24	15	Sample storage
Karenia brevis culture	156	25	30	PE curves
Microcystis sp. bloom – Lake Sarasota, FL, USA	262	25	NA	PE curves
New Pass, Sarasota, FL, USA	2.20	20	NA	Nutrient and temperature manipulation

Water samples were filtered through GF/F filters and stored frozen until further analysis. Chlorophyll-*a* (Chl-*a*) was analyzed using high performance liquid chromatography (HPLC, Agilent HPL) at the Horn Point Analytical Services Laboratory according to Van Heukelum and Thomas (2001).

Sample storage experiment

To evaluate the efficacy of sample preservation and storage, an experiment was conducted using water samples collected from the Choptank River (Table 3.1). Samples were prepared following the procedure described previously, and triplicate samples were incubated in the Coronatrons for six hours under constant light and at ambient temperature. After incubation, the samples were stored submerged in water-filled jars at room temperature for a period of 30 days. Measurements were performed after 1 day, 7 days, and 30 days of storage to assess potential losses of the 32/40 and 34/40 mass signals in preserved samples over time.

Rate determination

The mass-to-charge ratios (m/z) of the relative abundance of dissolved ^{16}O:^{16}O (mass 32), ^{18}O:^{16}O (mass 34) and Ar (mass 40) in the samples were measured by MIMS and recorded using instrumentation software Quickdata (Bay Instruments LLC).

Rates of GPP were calculated based on the change in the mass 34 isotope concentration of dissolved O_2 over the incubation time (Equation 1).

$$GPP = \left(\frac{\left(\Delta[\frac{34}{40}] \times [Ar] \right)}{2 * ({}^{18}O(H_2O) + 0.002) * t} \right) \qquad \textit{(Equation 1)}$$

where $\Delta 34/40$, represents the change in the isotope to Ar ratio over time, [Ar] is the solubility of Argon at the incubation temperature, $^{18}O(H_2{}^{18}O)$ is the isotope ratio of the incubation water, which is calculated based on the amount of $^{18}O(H_2{}^{18}O)$ added in the total volume of the incubation flask and the percent enrichment (98-99%) of stock ^{18}O water; 0.002 represents the

natural abundance of ^{18}O; and *t* represents the incubation time. This equation provides ^{18}O-GPP in μM O_2 h^{-1}. Though the IRMS method typically uses $\delta^{18}O$ for GPP measurements, we chose to use Ar as a reference to avoid the changes in the O_2 (mass 32) concentration in high activity samples which can affect the concentration of the reference gas (mass 32).

Rates of NPP were determined from the net change in O_2/Ar (mass 32/40) ratio (Equation 2).

$$NPP = \frac{\Delta 32/40 \times [Ar]}{t} \qquad \textit{(Equation 2)}$$

where $\Delta 32/40$, represents the change in the O_2/Ar over time, [Ar] is the solubility (μM) of Ar at the incubation temperature, and *t* represents the incubation time. This equation provides NPP in μM O_2 h^{-1}. Then, gross O_2 uptake (GR) was determined from the difference between GPP and NPP. Finally, GPP, NPP, and GR ratios obtained were normalized to the Chl-*a* concentration of each sample, providing μmol O_2 (μg Chl-*a*)$^{-1}$ h^{-1}.

Lastly, the overall sampling precision was assessed by calculating the percent coefficient of variation (% CV) of the 34/32 signals among replicate T_0 (n = 29) and T_f (T-final, n = 31) samples.

Limitations of the method: sample preparation

The accuracy of this method is influenced more by sample preparation and handling technique than by analytical measurements by MIMS. From filling the pipette to dispensing the samples into vials, it is crucial to minimize exposure to air and ensure there are no air bubbles and headspace in the pipette. The sample water cannot be assumed to be in equilibrium with air.

Additionally, it is important to homogenize the pipette prior to and during dispensing samples into the vials, as certain algae can settle quickly. When filling the vials, the pipette should be gently lifted to avoid the formation of air bubbles, and it is essential to leave a meniscus before sealing each vial. These precautions significantly enhance the accuracy and precision of the results.

Photosynthesis-irradiance and nutrient-response curve fitting

Initially, the ggplot2 package in R was used to generate scatter plots with smoothing lines using the locally estimated scatterplot smoothing (LOESS) for the visualization of the rates measured (GPP, NPP, and GR) and light (PAR). LOESS is a nonparametric method that uses local regression to fit a smooth curve; however, no assumptions are made about the underlying structure of the data.

Several photosynthesis-irradiance (PE or PI) models have been described in the literature that could be applied to the dataset. However, this study does not aim to evaluate or compare these models, as this analysis is beyond the scope of this paper. For illustrative purposes, the Jassby and Platt (1976) model was selected, and its fitting was conducted using the R package 'phytotools' (Silsbe and Malkin, 2015). Relationships of GR vs E (GR vs irradiance) vary in their shape and no one single curve-fit model is appropriate for all relationships (Kana, 1993; Lewitus and Kana 1995). In some cases, saturating curve-fits, such as Jassby and Platt (1976) appear appropriate (see below).

Results

Primary production and gross respiration as a function of light (PE curves)

The example data presented here range from natural seawater with low Chl-*a* concentrations (e.g., 2.22 µg L^{-1}) to samples collected during a thick lake bloom (e.g., 262 µg L^{-1}) and batch cultures of dinoflagellates with enriched seawater medium (156 µg L^{-1}). The heterogeneity of the samples used here demonstrates the efficiency of this technique in quantifying primary production and respiration rates across a wide variety of aquatic ecosystems.

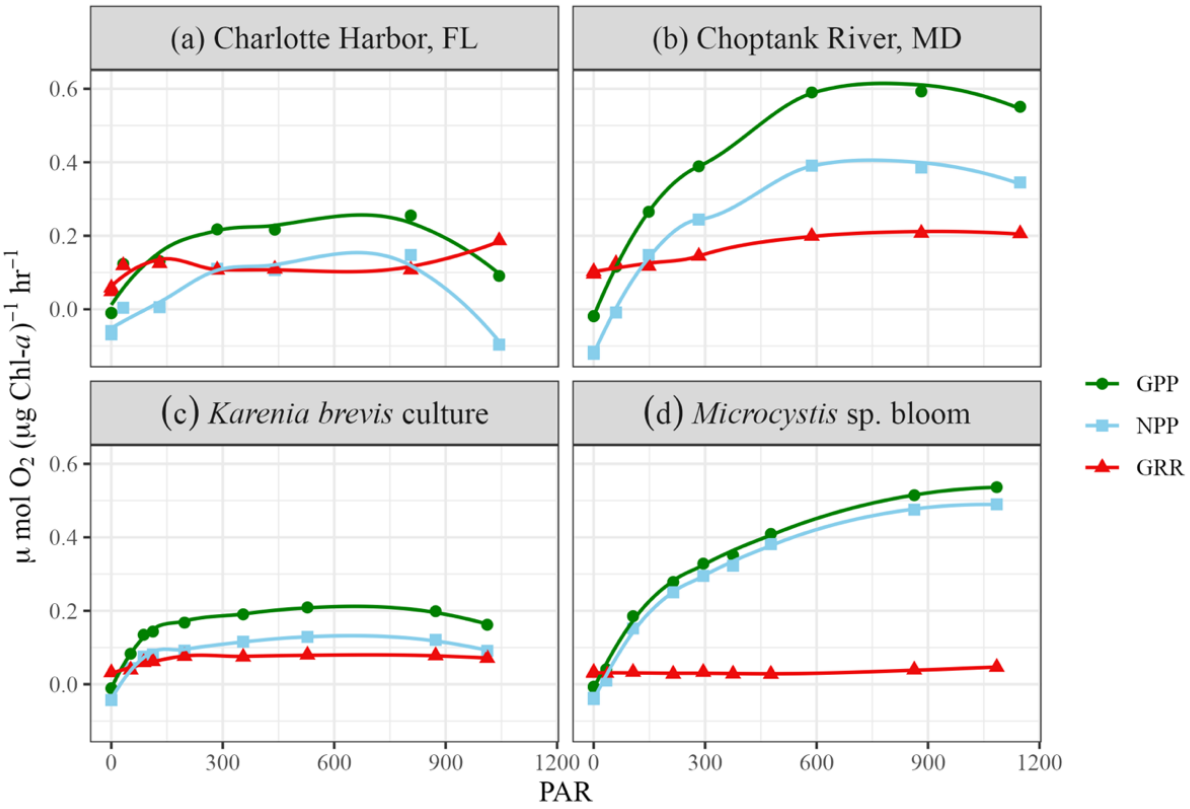

Figure 3.3 Rates of Gross Primary Production (GPP), Net Primary Production (NPP), and Gross Respiration (GR) (µmol O_2 (µg Chl-*a*)$^{-1}$ h^{-1}) as a function of light (PAR, µmol photons m^{-2} s^{-1}). Panels represent measurements from (a) Charlotte Harbor, FL, USA; (b) Choptank River, MD, USA; (c) *Karenia brevis* culture; and (d) *Microcystis* sp. bloom – Lake Sarasota, FL, USA.

Generally, the PE curves exhibited the classic hyperbolic response to light (Figure 3.3), where both GPP and NPP rates increased with light intensity until reaching the saturation irradiance (E_k), ranging from 40 to 423 µmol photons m^{-2} s^{-1}, depending on the sample (Table 3.2). At the highest light intensities (~1000 µmol photons m^{-2} s^{-1}), photoinhibition was observed, except for *Microcystis* sp. Light-dependent rates of R (GR) differed according to the community composition (Figure 3.3). For example, GR not only increased with light but also accounted for up to 47% of GPP in the *Karenia brevis* cultures. In contrast, during the *Microcystis* sp. bloom, GR remained low across all light intensities, with no substantial light-dependency observed, a characteristic more typical of cyanobacteria.

Table 3.2 Parameters derived from the Jassby and Platt (1976) model fitting the relationship between oxygen production (GPP and NPP) and uptake rates (GR) (µmol O_2 (µg Chl-*a*) $^{-1}$ h^{-1}) and irradiance (PAR, µmol photons m^{-2} s^{-1}). α^B is the initial slope of the PE curve (µmol O_2 (µg Chl-*a)* $^{-1}$ h^{-1}) [µmol photons m^{-2} s^{-1}]$^{-1}$), E_k is the light saturation coefficient (µmol photons m^{-2} s^{-1}), and P_{max} is the maximum oxygen production rate (µmol O_2 (µg Chl-*a*) $^{-1}$ h^{-1}).

		α^B	E_k	P_{max}
Charlotte Harbor, FL	GPP	0.005	40.0	0.18
	NPP	0.000	177.1	0.06
	GR	0.006	19.6	0.12
Choptank River, MD	GPP	0.002	318.1	0.58
	NPP	0.001	384.3	0.38
	GR	0.002	90.5	0.18
Karenia brevis culture	GPP	0.002	107.1	0.18
	NPP	0.001	122.7	0.11
	GR	0.001	89.4	0.07
Microcystis sp. bloom	GPP	0.001	404.1	0.52
	NPP	0.001	423.0	0.48
	GR	0.001	39.4	0.03

Primary production and gross respiration as a function of nutrients and temperature

Samples were enriched with different concentrations of nitrate (NO_3^-), with the control receiving no addition, and experimental enrichments of 1 µM, 5 µM, and 10 µM. Incubations were performed at different temperatures, including ambient temperature (20˚C), 24˚C, and 28˚C, under constant light conditions using the Coronatrons (~120 µmol photons m^{-2} s^{-1}) (Figure 3.4).

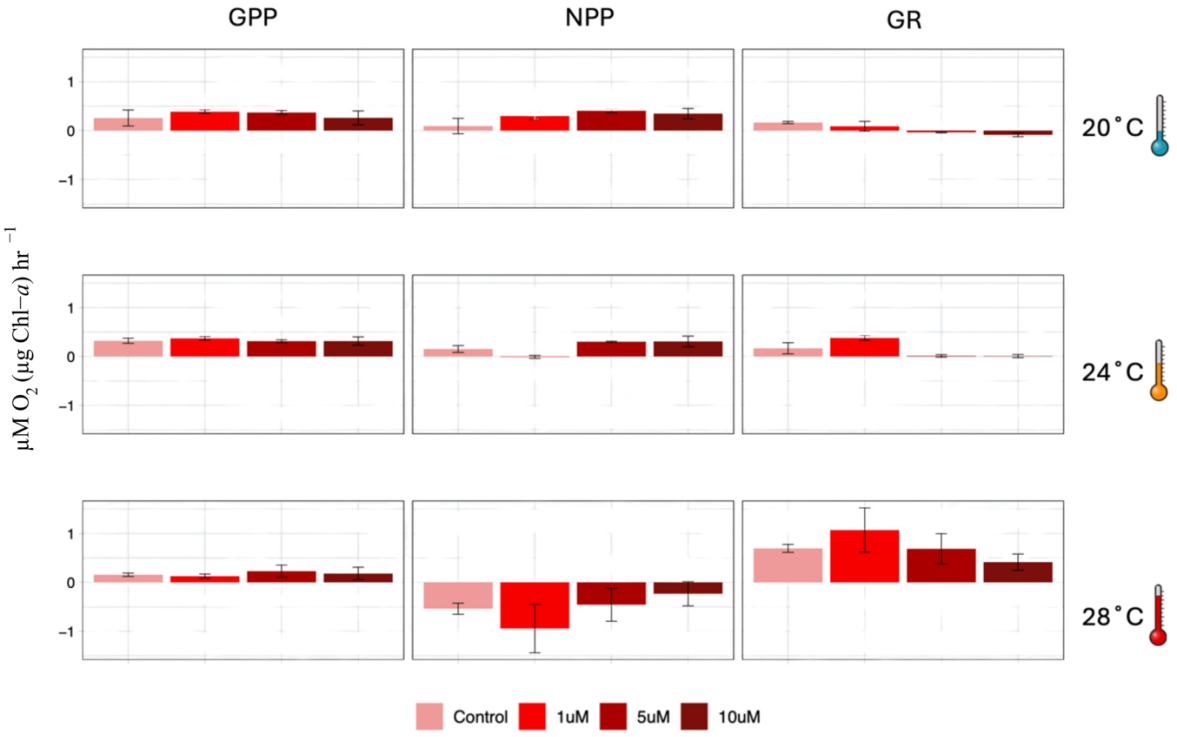

Figure 3.4 Average rates of Gross Primary Production (GPP), Net Primary Production (NPP), and Gross Respiration (GR) (µmol O_2 (µg Chl-*a*)$^{-1}$ h^{-1}) with standard deviations (n=3) under different temperatures (20 ˚C, 24 ˚C, and 28 ˚C) and nitrate enrichment levels (control, 1 µM, 5 µM, and 10 µM).

Both primary production (GPP and NPP) and gross respiration (GR) rates exhibited variations according to the combination of treatments (Figure 3.4). GPP rates showed a slight

increase with NO_3^- addition, whereas the lowest GPP values were observed at the highest temperature tested (28˚C). Similarly, NPP presented higher rates under nutrient-enriched conditions, even though NPP became negative at 28˚C. In contrast, GR rates initially increased then decreased with NO_3^- enrichment, and were highest at 28˚C, where GR exceeded both GPP and NPP rates. Overall, these results suggest that while nutrient enrichment can stimulate primary production, elevated temperatures may diminish this effect due to increased GR rates.

Sample storage experiment

The results of the sample storage experiment for the O_2 ratios showed similar patterns over time (Figure 3.5). For the 32/40 measurements, mean values remained relatively stable between Day 1 and Day 7 (16.86 and 16.84, respectively), with a slight decrease by Day 30 (16.01), demonstrating a slight loss of O_2 relative to Ar after one month of storage. The 34/40 measurements showed a greater decline between Day 1 and Day 7 (from 0.086 to 0.076), reaching even lower values on Day 30 (0.067). The associated standard deviations for both ratios increased over time, indicating greater variability and potential degradation of sample integrity with longer storage. These results demonstrate that storage for up to 30 days led to a loss of stability for both 32/40 and 34/40 signals, with the latter being more affected. The greater loss of mass 34 O_2 compared to mass 32 O_2 is consistent with a small gas permeability of the Viton septa whereby the gas gradient with respect to air or overlying water is greatest for the enriched mass 34 isotope. This emphasizes the need to analyze preserved samples within a few days to minimize alterations in gas composition.

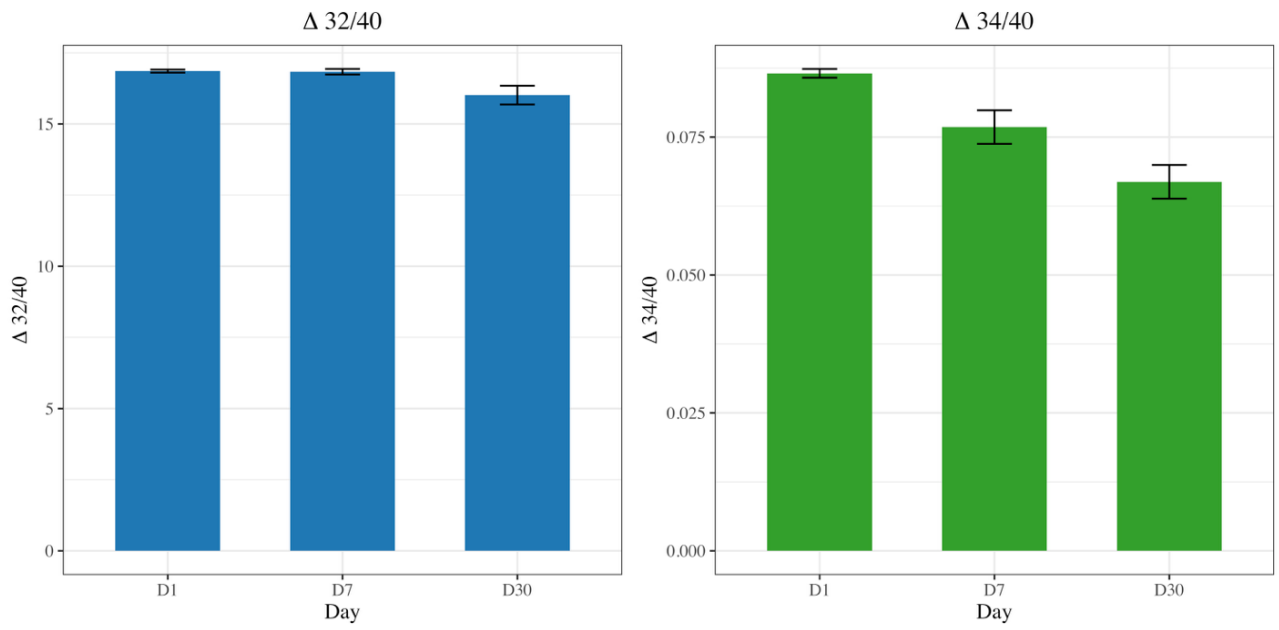

Figure 3.5 Mean values with standard deviation (n = 3) of the oxygen isotope ratios 32/40 (blue) and 34/40 (green) measured in preserved samples over a 30-day storage period.

Sampling precision

While the coefficient of variation (CV) of T_0 sample measurements reflects only the variability associated with sampling and handling, the CV of T_f samples also incorporates biological activity occurring during the incubation period (2 – 15 h) among replicates. The %CV of all T_0 samples and 23 of the T_f samples was below 0.10%. Only 6 T_f out of 31 samples exhibited slightly higher %CV values, ranging from 0.1–0.9%. Among all replicate measurements, only two samples exceeded a %CV of 0.9% (Table 3.3). These results indicate that overall sampling precision was high, with minimal variability among replicates even after incubation, confirming that this approach provides highly reproducible measurements.

Table 3.3 Summary of percent coefficient of variance (% CV) calculated for 34/32 signals of replicate (n=2 – 4) samples. Total of 60 data sets were assessed and grouped according to the range of % CV. Upper panel shows the summary of all the data and the lower panel shows the summery of T_f data.

	CV (%)			
	<0.05	0.05-0.10	0.10-0.90	>0.90
$^{18}O/^{16}O$				
Number of data sets (n = 2 – 4)	14	38	6	2
% of total	23.3	63.3	10.0	3.3
Mean (± SD)	0.036 ±0.017%	0.092 ±0.024%	0.026 ±0.51%	1.30 ±0.19%
Number of T_f data sets	7	16	6	2
% T_f data sets	50	42.1	100	100
Mean (± SD)- T_f data	0.037 ±0.025%	0.098 ±0.025%	0.026 ±0.51%	1.30 ±0.19%

Discussion

The original light bottle-dark bottle method utilized Winkler titrations for the determination of dissolved O_2 concentration. By measuring the change in O_2 concentration in separate illuminated and darkened bottles over time, the net O_2 production (NPP) and net O_2 community consumption (CR) of the plankton could be determined. As a central concept for understanding photosynthesis in nature, understanding the uncertainty–if not controversy–regarding the dark bottle measurement is important.

A basic assumption in the PE curve models used in aquatic sciences is that R is independent of the light level and with constant rates, as determined by parallel measurements made in the dark (Jassby and Platt, 1976). The measurement of GPP using non-isotopic O_2 methods depends on the assumption that R is unaffected by light. With such techniques, values of R (or CR) must be assumed to be equal to the dark O_2 flux, despite uncertainty over this

assumption. However, these rates are not constant and can be light-dependent and processes, such as cyclic electron flow, Mehler reaction, and photorespiration help to regulate cellular redox by dissipating excess energy preventing photoinhibition caused by excess of light or downstream metabolic limitation (Kana 1990; Lewitus and Kana 1995; Pringault et al., 2007; Kramer and Evans, 2011; Glibert 2024 and references therein). In this study, we have provided an improved approach to measure light-dependent O_2 cycling in a single, small volume sample suitable for measuring natural phytoplankton.

Within aquatic sciences, the early observations of photosynthetic O_2 cycling described in the physiological literature were not considered in the ecological determinations of GPP for a number of decades. The development of ^{18}O methods that were capable of measuring low biomass samples typical of natural waters only came in the 1980's and the emphasis in oceanography was on measuring 'true' GPP to assess ocean productivity and not the influence of light on R. Developing an understanding of the physiology of O_2 consumption processes in natural waters was hampered by the large expense and/or limited availability of instrumentation for conducting ^{18}O experiments.

A motivation for measuring GPP by ^{18}O methods is to provide an unambiguous measure of phytoplankton photosynthesis, unencumbered by assumptions of the contribution of light to O_2 uptake processes. In fact, GPP by ^{18}O methods is a direct measure of PSII activity, similar to measurements made by PSII variable fluorescence techniques (Suggett et al. 2009). As the origin of reductant via the PSII oxygen evolving complex, PSII activity provides the upper bound of photosynthetic reductant available to the cell and hence can legitimately be called gross photosynthetic activity.

Ambiguity comes in with the interpretation of GPP whereby PP (primary productivity) is not precisely defined. Commonly, GPP is considered to be the productivity of the phytoplankton with respect to cellular growth. Implicit in this is a relationship to biomass (or in aquatic sciences, its proxy chlorophyll). Values of GPP from ^{18}O experiments, however, represent the photosynthetic activity of reductant formation and it is the fate of this reductant that determines how close its measure is to GPP for biomass productivity. Whereas the majority of reductant normally flows to photosynthetic CO_2 reduction, variable fractions can flow to O_2, nitrogen (N), and other cellular reduction reactions at the expense of CO_2 assimilation and C-based productivity (Glibert et al., 2016). Though N reduction (and other reactions) is relatively constrained due to elemental stoichiometry (Lomas et al., 2021), O_2 reduction is highly variable and its rate can exceed 50% of O_2 evolution (Kana, 1993). Hence, GPP by the ^{18}O method can be significantly higher than GPP estimates using non-isotope O_2 methods. There is a great need for more measurements of gross O_2 cycling in phytoplankton systems to understand the variability and extent of photosynthetic oxygen reduction in nature.

Use of the $H_2{}^{18}O$ technique in natural phytoplankton research has heretofore largely been in the context of measuring GPP in ocean water masses through in situ or simulated in situ incubations. Extending this technique using Photosynthetrons and Coronatrons provides additional experimental capability to study physiological responses to environmental factors (e.g. light, temperature and nutrients). With further application, it will be possible to establish comparative systems and species data with regard to R-E (R-I) relationships similar to P-E (P-I) curves. The process of light-dependent R remains under-explored and there are no established models describing the relationship between R and light as the responses are distinct, and a single model would not be sufficient to capture them. For illustrative purposes, we selected the Jassby

and Platt (1976) model to fit our production and respiration data, as it was observed that some GR curves mimic the GPP and NPP curves. This is an interesting and significant observation in that it indicates a *fractional* diversion of photosynthetic reductant to O_2 that is dependent of light. This implies that there is a loss of photosynthetic efficiency of C reduction in those experiments.

Previous studies have demonstrated how the isotope technique using MIMS provides a precise, simple, and affordable method for measuring *in vitro* productivity in various aquatic ecosystems (e.g., Kana, 1990; Kana et al., 1994; Ferrón et al., 2016). The main advantage of the modified method described here is that is considerably cheaper, the sample manipulation is easier, and only a small volume of sample is needed (~3 mL sample) with low isotope enrichment (1% of volume), thereby providing greater flexibility for physiological research on natural phytoplankton. Also, the analysis in the instrument is rapid, as samples can be analyzed in less than 5 minutes (Kana et al., 1994; Ferrón et al., 2016). The improvements in the $H_2{}^{18}O$ technique, as well as the introduction of the new Coronatron incubation device described herein to complement the now-common use of Photosynthetron incubators, will enable more accurate quantification and understanding of phytoplankton productivity across various environmental gradients. These enhancements make the method more accessible by reducing costs, labor, and time compared to traditional methods used for measuring primary production. With those able to take MIMS to sea, the rapid processing of such samples makes modifications of experimental protocols not only possible, but finely tuned, as conditions change. The diversity of samples and conditions assessed in this study highlights the efficiency of this technique across a wide range of aquatic ecosystems, from highly productive environments to low-productivity, near oligotrophic areas.

There are improvements needed to handle low biomass samples with reliability. Reproducibility (or noise in the P-E curves) is largely attributed to the level of care in sample collection, preparation and handling. Concentration of O_2 in natural waters are typically in disequilibrium relative to solubility. Hence, the O_2 concentration of a collected water sample will change if exposed to air especially if the sample temperature changes. Thus, any sample being prepared for enrichment and dispensing to sample tubes must be well mixed and vials must be capped immediately. A dispensing apparatus that avoids plastics (which are gas permeable) and bubbles that can gently fill a vial may be advantageous.

Conclusion

This study advances the application of the $H_2{}^{18}O$ technique with MIMS techniques by demonstrating its efficacy in simultaneously quantifying GPP, NPP, and GR in natural phytoplankton communities using small-volume incubations (3 mL). With advanced incubation devices, including Coronatrons and Photosynthetrons, this method enhances the ability to investigate the physiological responses of phytoplankton to multiple environmental factors, such as light, temperature, and nutrients. Compared with traditional approaches, the technique described here offers a simpler, more cost-effective, and rapid alternative, thus enabling broader application. While methodological improvements are still needed for reliable measurements in low-biomass samples, the reproducibility and efficiency demonstrated across varied aquatic environments highlight the robustness of the approach. Collectively, these methodological improvements will contribute to a more accurate and comprehensive understanding of phytoplankton productivity and respiration, both dark and light, across different environments

providing new opportunities for comparative studies and model development in aquatic photosynthesis research.

References

Bender, M., Grande, K., Johnson, K., Marra, J., Williams, P. J. L., Sieburth, J., & Heinemann, K. (1987). A comparison of four methods for determining planktonic community production. *Limnology and Oceanography, 32*(5), 1085–1098. https://doi.org/10.4319/lo.1987.32.5.1085

Campbell, A. M., Fleisher, J., Sinigalliano, C., White, J. R., & Lopez, J. V. (2015). Dynamics of marine bacterial community diversity of the coastal waters of the reefs, inlets, and wastewater outfalls of southeast Florida. *MicrobiologyOpen, 4*(2), 1–19. https://doi.org/10.1002/mbo3.245

Ferrón, S., del Valle, D. A., Björkman, K. M., Quay, P. D., Church, M. J., & Karl, D. M. (2016). Application of membrane inlet mass spectrometry to measure aquatic gross primary production by the 18O in vitro method. *Limnology and Oceanography: Methods, 14*(9), 610–622. https://doi.org/10.1002/lom3.10116

Gaarder, T., & Gran, H. H. (1927). Investigations of the production of plankton in the Oslo Fjord. *ICES Journal of Marine Science.* https://doi.org/10.17895/ices.pub.19272251

Glibert, P. M., Wilkerson, F. P., Dugdale, R. C., Raven, J. A., Dupont, C. L., Leavitt, P. R., Parker, A. E., Burkholder, J. M., & Kana, T. M. (2016). Pluses and minuses of ammonium and nitrate uptake and assimilation by phytoplankton and implications for productivity and community composition, with emphasis on nitrogen-enriched conditions. *Limnology and Oceanography*, 61(1), 165–197. https://doi.org/10.1002/lno.10203

Glibert, P. M. (2024). *Phytoplankton whispering: An introduction to the physiology and ecology of microalgae.* Springer Nature. Cham, Switzerland. 753 pp.

Hoch, G., & Kok, B. (1963). A mass spectrometer inlet system for sampling gases dissolved in liquid phases. *Archives of Biochemistry and Biophysics, 101*(1), 160–170. https://doi.org/10.1016/0003-9861(63)90546-0

Jassby, A. D., & Platt, T. (1976). Mathematical formulation of the relationship between photosynthesis and light for phytoplankton. *Limnology and Oceanography, 21*(4), 540–547. https://doi.org/10.4319/lo.1976.21.4.0540

Kana, T. M. (1990). Light-dependent oxygen cycling measured by an oxygen-18 isotope dilution technique. *Marine Ecology Progress Series*, 64, 293-300. https://doi.org/10.3354/meps064293

Kana, T. M. (1992). Relationship between photosynthetic oxygen cycling and carbon assimilation in *Synechococcus*WH7803 (Cyanophyta). *Journal of Phycology, 28*(3), 304–308. https://doi.org/10.1111/j.0022-3646.1992.00304.x

Kana, T. M. (1993). Rapid oxygen cycling in *Trichodesmium thiebautii. Limnology and Oceanography, 38*(1), 18–24. https://doi.org/10.4319/lo.1993.38.1.0018

Kana, T. M., Darkangelo, C., Hunt, M. D., Oldham, J. B., Bennett, G. E., & Cornwell, J. C. (1994). Membrane inlet mass spectrometer for rapid high-precision determination of N_2, O_2, and Ar in environmental water samples. *Analytical Chemistry, 66*(23), 4166–4170. https://doi.org/10.1021/ac00095a009

Kramer, D. M., & Evans, J. R. (2011). The importance of energy balance in improving photosynthetic productivity. *Plant Physiology, 155*(1), 70–78. https://doi.org/10.1104/pp.110.166652

Lewitus, A. J., & Kana, T. M. (1995). Light respiration in six estuarine phytoplankton species: Contrasts under photoautotrophic and mixotrophic growth conditions. *Journal of Phycology, 31*(5), 754–761. https://doi.org/10.1111/j.0022-3646.1995.00754.x

Lomas, M. W., Baer, S. E., Mouginot, C., Terpis, K. X., Lomas, D. A., Altabet, M. A., & Martiny, A. C. (2021). Varying influence of phytoplankton biodiversity and stoichiometric plasticity on bulk particulate stoichiometry across ocean basins. *Communications Earth & Environment, 2*(1), 143. https://doi.org/10.1038/s43247-021-00212-9

MacIntyre, H. L., Geider, R. J., & McKay, R. M. (1996). Photosynthesis and regulation of Rubisco activity in net phytoplankton from Delaware Bay. *Journal of Phycology, 32*(5), 718–731. https://doi.org/10.1111/j.0022-3646.1996.00718.x

Makino, A., Miyake, C., & Yokota, A. (2002). Physiological functions of the water–water cycle (Mehler reaction) and the cyclic electron flow around PSI in rice leaves. *Plant and Cell Physiology, 43*(9), 1017–1026. https://doi.org/10.1093/pcp/pcf124

Mehler, A. H., & Brown, A. H. (1952). Studies on reactions of illuminated chloroplasts. III. Simultaneous photoproduction and consumption of oxygen studied with oxygen isotopes. *Archives of Biochemistry and Biophysics, 38*(1), 365–370. https://doi.org/10.1016/0003-9861(52)90042-8

Pringault, O., Tassas, V., & Rochelle-Newall, E. (2007). Consequences of respiration in the light on the determination of production in pelagic systems. *Biogeosciences, 4*(1), 105–114. https://doi.org/10.5194/bg-4-105-2007

Silsbe, G. M., & Malkin, S. Y. (2015). Package ‘phytotools’.

Suggett, D. J., MacIntyre, H. L., Kana, T. M., & Geider, R. J. (2009). Comparing electron transport with gas exchange: Parameterizing exchange rates between alternative photosynthetic currencies for eukaryotic phytoplankton. *Aquatic Microbial Ecology, 56*(2), 147–162. https://doi.org/10.3354/ame01303

Van Heukelem, L., & Thomas, C. S. (2001). Computer-assisted high-performance liquid chromatography method development with applications to the isolation and analysis of phytoplankton pigments. *Journal of Chromatography A, 910*(1), 31–49. https://doi.org/10.1016/S0378-4347(00)00603-4

Chapter 4: Temperature effects on productivity, respiration, and dissolved organic matter degradation in subtropical Florida waters following hurricane-driven riverine runoff and brownification[3]

Abstract

Increasing ocean water temperatures and storm-driven terrestrial inputs are gradually affecting subtropical coastal ecosystems. This study examined how elevated temperature and humic acid enrichment, both under post-hurricane (Debby, Milton and Helene) in situ conditions and controlled laboratory manipulations, influence metabolic rates of *Karenia brevis* and associated phytoplankton communities on the West Florida Shelf (WFS). We hypothesized that warming, combined with hurricane-driven humic inputs, would decrease primary production rates while stimulating respiration and dissolved organic matter (DOM) degradation, shifting metabolic balance toward net heterotrophy. Gross primary production (GPP), net primary production (NPP), gross respiration (GR; light-dependent processes), and dark respiration were quantified using Membrane Inlet Mass Spectrometry, and changes in the fluorescent DOM (FDOM) composition was performed using spectrofluorometric analysis. Across stations, increasing temperature consistently reduced GPP, shifted NPP toward negative values, and enhanced both dark and light-dependent respiration. In many experiments, GR exceeded NPP and occasionally GPP, highlighting the substantial and often under-quantified contribution of light-dependent respiration to total oxygen consumption. Both Hurricanes Helene and Milton delivered terrestrially derived, humic-rich FDOM. Increasing temperature was associated with enhanced

[3] **Sobrinho, B.F**; Muni-Morgan, A.; Heil, C.; Glibert, P.M. Temperature effects on productivity, respiration, and dissolved organic matter degradation in subtropical Florida waters following hurricane-driven riverine runoff and brownification. *Submitted to Frontiers in Microbiology*

biological production of labile, protein-like FDOM and concurrent shifts toward lower humification. Together, these responses increased oxygen demand while reducing oxygen solubility, conditions conducive to hypoxia. These findings demonstrate how warming and hurricane-driven brownification interact to amplify respiratory metabolism, highlighting the vulnerability of subtropical coastal systems to hypoxia development under future climate scenarios.

Introduction

Ocean and coastal systems are increasingly being affected by climate change and the multiple environmental stressors related to it. Warming and nutrient pollution are among the most important drivers reshaping aquatic environments. Estuaries and coastal zones respond rapidly to these pressures, and by integrating terrestrial and marine influence, act as sentinels of environmental changes (Cloern et al., 2016). At the same time, extreme weather events, including storms, heatwaves, and droughts, are also becoming more frequent and intense (Glibert & Li 2023). Understanding the complexities of these overlapping interactions remain a major challenge (Bijma et al., 2013; Glibert et al., 2022; Eddy et al., 2025; Guild et al., 2025). Relationships between temperature increase, nutrient enrichment, hypoxia and harmful algal blooms (HABs) have received considerable attention (e.g., Anderson et al., 2008; Hallegraeff, 2010; Martínez et al., 2017; Gobler et al., 2017; Glibert, 2019; Griffith & Gobler, 2020; Glibert et al., 2021). However, less understood are the effects of changing terrestrial dissolved organic matter (DOM) loads to coastal water due to changes in extreme weather events, riverine discharge, sea level rise and other factors, and how those loads are altering primary production

and respiration. This is especially true in subtropical waters where organic loads and brownification have been poorly studied.

The increasing frequency and intensity of storms, hurricanes, and high riverine runoff associated with climate change are altering the delivery of nutrients and organic matter to coastal waters. During periods of intense runoff, allochthonous organic matter, primarily in the form of terrestrially derived, colored humic and fulvic acids, can dominate the dissolved organic matter (DOM) pool (Thurman 1985; Moran & Hodson 1994). Storm-driven turbulence further mobilizes sediments and detritus from nearshore vegetation, enhancing the export of organic matter and nutrients to coastal zones (e.g., Miles et al., 2013; Bianucci et al., 2018; Chen et al., 2019). In urbanized watersheds engineered drainage networks, increased impervious surface area and wastewater effluent contribute additional loads of DOM including labile dissolved organic nitrogen (DON) that can stimulate HABs (Bronk et al., 2010; Kaushal & Belt, 2012). Although humic substances have traditionally been considered largely refractory (Opsahl and Benner, 1997; Benner, 2002; Coates et al., 2002), growing evidence shows that this pool, or a large fraction of this pool, can be biologically reactive, with implications for water quality, biogeochemical cycles, and the structure and functioning of planktonic communities (Stepanauskas et al., 2002; Wiegner et al., 2006; Boyer et al., 2006; See et al., 2006; Mendoza & Zika, 2014; Hounshell et al., 2022; Yin et al., 2025; Zhang et al., 2025).

A substantial fraction of DOM, up to 80% in freshwater, consists of dissolved humic substances, naturally colored, high-molecular-weight organic acids (Thurman, 1985). The enrichment of coastal waters with these materials, a process known as brownification, alters underwater light fields and can influence primary production and bloom dynamics (Urrutia-Cordero et al., 2017; Blanchet et al., 2022). In addition to their optical effects, humic substances

can play an important role as metal chelators (e.g., Musani et al., 1980) and can also serve as a nutrient source; much of the nitrogen (N) they contain is in the form of loosely bound ammonium (NH_4^+) that can be released through photooxidation or ion-exchange processes as riverine waters mix with higher-salinity coastal waters (Bushaw et al., 1996; Bushaw-Newton & Moran, 1999; Cochlan & Bronk, 2001; See et al., 2006). Brownification can reduce light penetration while simultaneously enhancing heat absorption, creating warmer and darker conditions that may selectively favor taxa adapted to such environments (Williamson et al., 2015; Pilla et al., 2018). Several dinoflagellates, including *Prorocentrum minimum*, *Karenia brevis*, and *Pyrodinium bahamense*, have been shown to use humic-derived substrates (Granéli et al., 1999; Heil et al., 2005; See et al., 2006; Muni-Morgan et al., 2023; Zhang et al., 2025). However, the influence of humic enrichment combined with increasing temperature on phytoplankton metabolism, including both primary production and respiration, remains poorly understood especially in subtropical waters.

Warming and organic matter enrichment can enhance oxygen consumption in coastal waters (Breitburg et al., 2018). At the same time, oxygen solubility decreases with increasing temperature and with the input of fresh waters (Schmidtko et al., 2017). Warmer conditions also promote higher water column stability and stratification, isolating water masses rich in organic matter and restricting vertical mixing (e.g., Lønborg et al., 2020; Goñi et al., 2021). Together, these processes stimulate respiration processes, which rise with temperatures (Wikner et al., 2023), and contribute to the expansion and intensification of hypoxia regionally and globally (Weiss,1970; Diaz & Rosenberg, 2008; Grégoire et al., 2021; Alam, 2023). Respiration has also been shown to increase with DOM loading (Pace et al. 2021). However, there are still many questions regarding how these rates of respiration contribute to hypoxia and how these rates may

be influenced by different environmental factors. Importantly, with increased knowledge of the processes contributing to respiration, it is now clear that traditional methods of measuring respiration via changes in oxygen (i.e., "light bottle-dark bottle" techniques, Gaarder & Gran, 1927) are insufficient to fully characterize those rates, as they only measure dark respiration. Phytoplankton also respire in the light, through processes such as cyclic electron flow, the Mehler reaction, and photorespiration, which regulate cellular redox by dissipating excess energy, preventing photoinhibition caused by excess of light or downstream metabolic limitation (Kana 1990; Lewitus & Kana 1995, Kramer & Evans, 2011, Glibert 2024 and references therein). However, the contribution of light-dependent respiration to the total community respiration remains under quantified, especially under conditions of elevated DOM. Therefore, to fully constrain how DOM impacts respiration, it is necessary to measure these rates, not just those measured in the dark.

The Gulf of Mexico (GoM; Gulf of America) provides an ideal setting to investigate the impacts of multiple environmental stressors related to climate change, including the increasing organic loads associated with hurricanes. The northern GoM is characterized by one of the largest regions of human-induced hypoxia in the world, and the largest along the U.S. coastline (Rabalais & Turner, 2019; Pontius & McIntosh, 2024). Surface water temperatures in the GoM have increased at nearly twice the rate observed in the global ocean surface (Wang et al., 2023). Due to its location near the warm waters of the North Atlantic, including the Caribbean Sea, Florida experiences more hurricanes than any other U.S. state (Malmstadt et al., 2009, 2010; Gilliam, 2021). Notably, in 2023, Florida experienced Hurricane Idalia (August 30, 2023) and in 2024 Florida was impacted by three major hurricanes: Debby (August 3, 2024), Helene (September 26, 2024), and Milton (October 9, 2024).

Hurricanes Idalia (Category 4) and Debby (Category 1) generated extreme rainfall across Florida's west coast (National Weather Service, 2024), resulting in intense river flow and flooding, considerably enhancing freshwater discharge to coastal waters and the export of terrestrially derived sediments and organic matter to the coastal ocean. In contrast, Helene (Category 4) was primarily a storm-surge–dominated event, producing less rainfall but generated record-high surge levels along Florida's west coast due to strong onshore winds. This led to major coastal flooding and sand deposition (Florida State University Climate Center, 2024). Hurricane Milton (Category 5) combined extreme storm surge with heavy rainfall, resulting in a mixed forcing regime in which both surge-driven coastal erosion and rainfall-enhanced river discharge contributed to sediment resuspension and organic matter export to the coastal ocean (National Hurricane Center, 2024). Such extreme events can–and did–intensely alter the typical distribution of DOM on the West Florida Shelf (WFS) (e.g., Conmy et al., 2009; Mendoza & Zika, 2014).

A unique feature of the eastern GoM that can also contribute to local anoxia/hypoxia is the annual blooms of the toxic dinoflagellate *K. bre*vis. These blooms can be sustained by hurricanes and tropical storms by delivering large pulses of nutrients and organic matter, sometimes comparable to the entire annual nutrient load to the region (Hu et al., 2006; Fritz, 2018; Chen & Li, 2025). Studies have reported the presence of hypoxia during intense *K. brevis* blooms (Smith, 1975; Heyl et al., 1978; Milbrandt et al., 2021; Turley et al., 2022). Recently it has been hypothesized that hypoxia occurring in parallel to a *K. brevis* red tide event is more likely to occur with warmer ocean temperatures and increased fluxes of organic nutrients, especially after hurricanes (Milbrandt et al. 2021; Figure 4.1). Moreover, respiration rates by dinoflagellates are inherently high. However, it remains unclear how the respiration rates of *K.*

brevis and its associated phytoplankton community compare to those of microbial communities during organic matter decomposition.

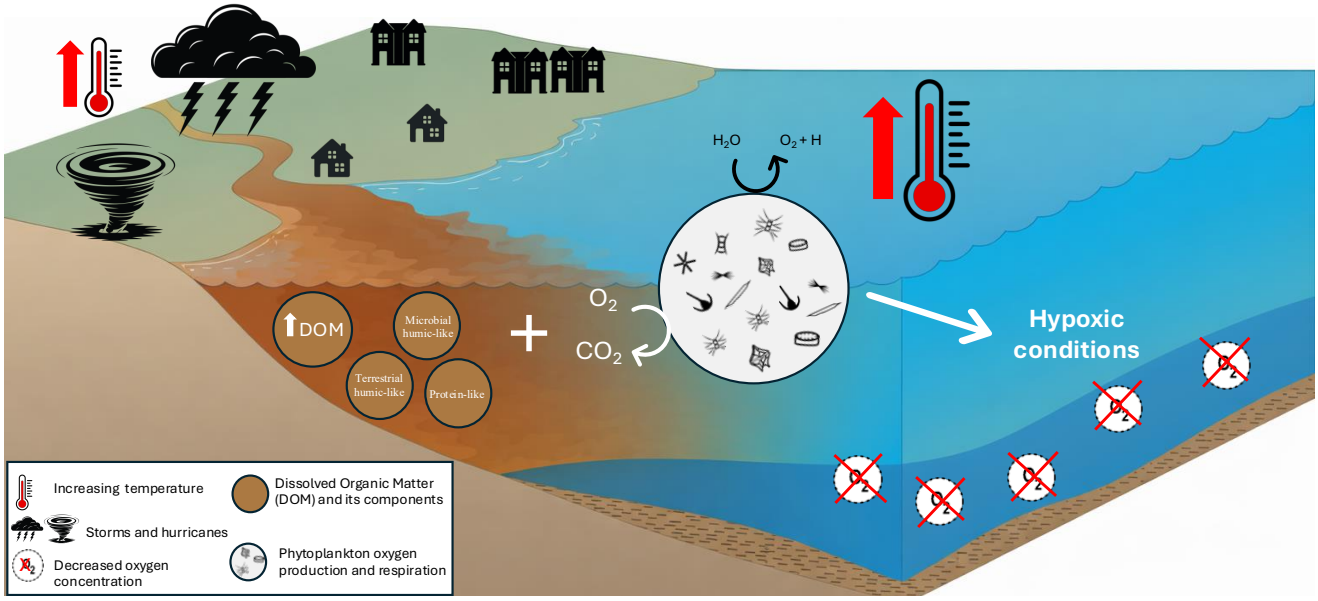

Figure 4.1 Conceptual figure illustrating the combined effects of warming and intensifying hurricanes on coastal biogeochemistry and oxygen dynamics in a subtropical system such as the Gulf of Mexico Rising temperatures increase the frequency and intensity of tropical storms and hurricanes, enhancing rainfall, river discharge, and terrestrial runoff. These processes deliver elevated loads of dissolved organic matter (DOM) to coastal waters, including terrestrial humic-like, microbial humic-like, and protein-like components. Simultaneously, warming of surface water increases water-column stratification, reducing vertical mixing and oxygen ventilation of deeper waters, while higher temperatures decrease oxygen solubility. Under warmer conditions and increased DOM availability, respiratory processes are favored, while primary production is reduced, shifting the system toward net heterotrophy. The combined effects of enhanced respiration, reduced oxygen, and lower oxygen solubility promote oxygen depletion and increase the likelihood of hypoxic conditions. Icons were adapted from the Integration and Application Network (IAN), University of Maryland Center for Environmental Science (UMCES) and Adobe Illustrator. The brownish water effect was added using AI-assisted editing.

This study examined how increased temperature and humic acid enrichment, both under *in situ* post-hurricane conditions and through controlled laboratory manipulations, affect the metabolic rates of *K. brevis* and the associated phytoplankton community on the WFS. We

hypothesized that increasing temperature, combined with hurricane-driven inputs of humic acids, will reduce primary production while stimulating respiration processes and DOM degradation. Together, these processes will shift metabolic balance toward greater net heterotrophy, thereby increasing the likelihood of hypoxia development in WFS waters. To assess these effects, gross primary production (GPP), net primary production (NPP), gross respiration (i.e., the sum of light-dependent metabolic processes, GR), and dark respiration rates of dissolved oxygen were measured. Changes in the chemical character of fluorescent DOM (FDOM) as a function as temperature were also measured. These findings provide new insight into how climate-related stressors may interact to influence the balance between autotrophic and heterotrophic processes in coastal phytoplankton communities with important links to, and implications for, the development of hypoxia conditions.

Materials and Methods

Overview and sampling

All water samples used in experiments were collected from rivers discharging onto the WFS, or from coastal WFS waters in August and September 2023 (5 days before and 7 days after Hurricane Idalia) and between August and November 2024 after hurricanes Debby (August 8, 5 days post storm), Helene (October 1, 6 days post storm), and Milton (November 20 – 23, 6 weeks post storm; Figure 4.2). Sampling efforts in August 2023 and also following hurricanes Debby and Helene were conducted on a single day, whereas sampling after hurricane Milton extended across three days.

Pre and post Hurricane Idalia sampling involved collections of ambient nutrient conditions, and measurements of the light dependency of GR in Charlotte Harbor. The pre-hurricane measurements also serve as a comparative non-impacted summer condition, against which the rate measurements following Hurricane Debbie can be compared.

Different types of experiments or measurements were undertaken for all post hurricane sampling in 2024, depending on date of sampling (Table 1). The first involved comparisons of varying concentrations of humic-rich waters derived from different sites sampled in the days to weeks following hurricanes Debby to assess the effects on primary production and respiration in water with varying levels of natural organic loads. The second involved artificial manipulation of humic loads and their effects on primary production and respiration. For the second type of experiment, water samples from nearshore (New Pass and Siesta Key) were collected and subsequently inoculated with addition of humic material previously extracted from water collected from the humic-rich Shark River Slough in southwest Florida (details below). Respiration rates were measured across ambient and manipulated temperatures (+ 3–5˚C) in the dark to reflect community respiration and in the light to reflect light-dependent respiration (i.e., GR). The third set of measurements, in a subset of samples, involved characterizing the FDOM transformation in the temperature-manipulated incubations (Table 4.1).

Table 4. 1 Summary of sampling efforts following Hurricanes Idalia, Debby, Helene, and Milton, including the stations where water was collected and the experiments conducted for each event. Site locations are shown in Figure 2.

Hurricane	**Station sites**	**Experiments**
Idalia (Category 4; landfall at Big Bend, Florida)	Charlotte Harbor (CH)	• Pre hurricane rates of light dependent Gross Respiration
Debby (Category 1; landfall at Steinhatchee, Florida)	Tampa Bay (TB), Siesta Key (SK), Caloosahatchee River (CR) and Charlotte Harbor (CH)	• Primary Production and Gross Respiration Rates vs. temperature • Dark and light Respiration Rates
Helene (Category 4; landfall near Perry, Florida)	New Pass (NP) and Siesta Key (SK)	• Primary Production and Gross Respiration Rates vs. temperature • FDOM transformation vs. temperature • Dark and Light Respiration Rates
Milton (Category 5; landfall near Siesta Key, Florida)	New Pass (NP) and Siesta Key (SK)	• Primary Production and Gross Respiration Rates + humic acid enrichment vs. temperature • FDOM transformation + humic acid enrichment vs. temperature • Dark and Light Respiration Rates • Dark Respiration vs. temperature

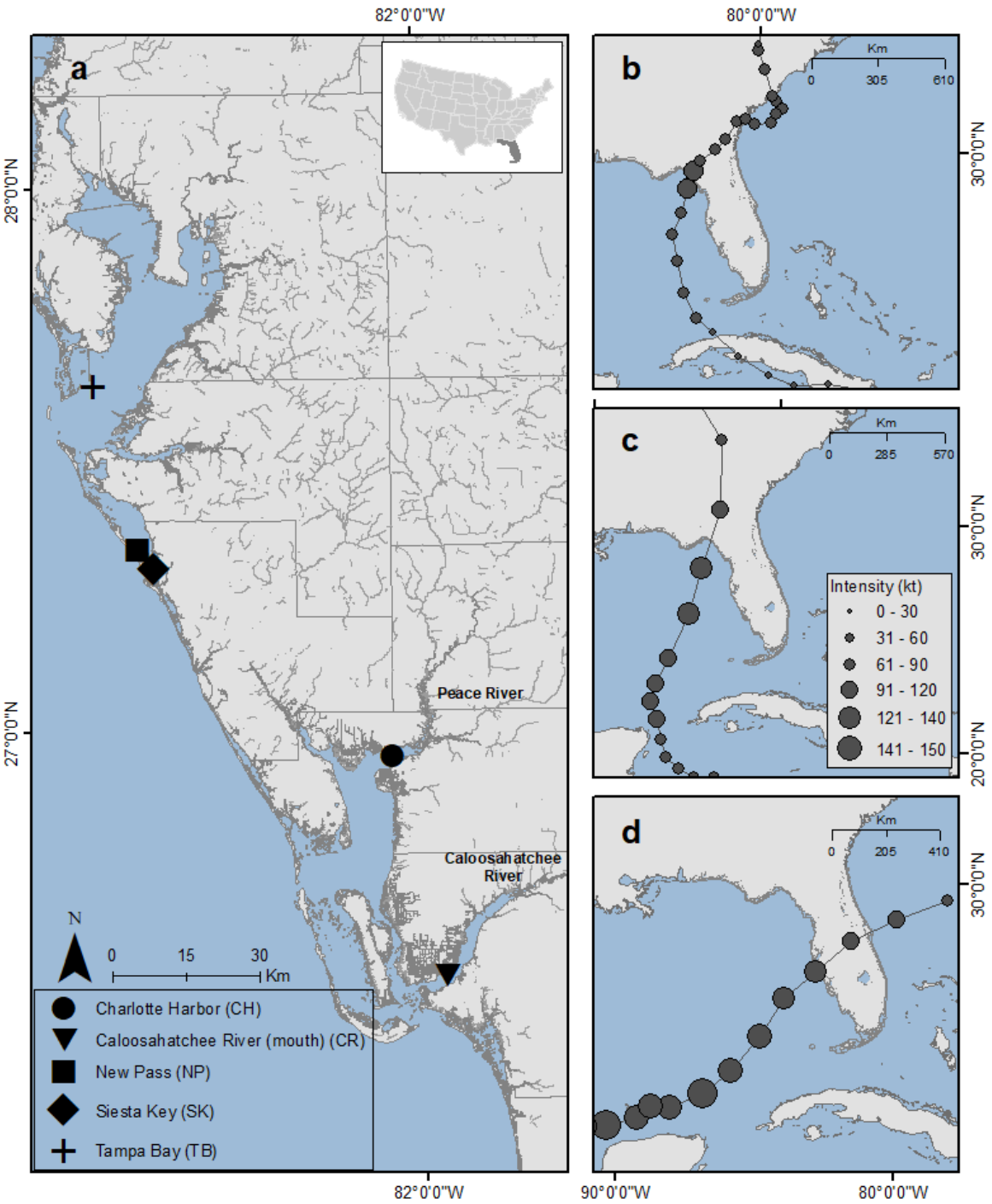

Figure 4.2 (a) Map of sampling sites on the West Florida Shelf: Charlotte Harbor (CH), Caloosahatchee River (mouth; CR), New Pass (NP), Siesta Key (SK) and Tampa Bay (TB). Tracks of Hurricane Debbie (b), Helene (c) and Milton (d) along the West Florida coast. Hurricane intensity (expressed in knots, kt) data were obtained from the RAMMB Tropical Cyclone Realtime database hosted by the Cooperative Institute for Research in the Atmosphere (CIRA), Colorado State University.

Ambient parameters, nutrients, and chlorophyll-a analyses

In the field, water was collected with a Niskin bottle lowered to ~5 cm below the water surface then transferred to a clean (10% HCl, followed by three deionized water rinses) 10 L Nalgene carboy. Measurements of temperature and salinity were taken of each sample on site using a ProQuatro or a YSI ProSolo. Samples were returned to the laboratory within 2 hours of sampling and immediately filtered through precombusted GF/F filters (450ºC, 2 hr). Given that sampling was performed opportunistically and largely in response to the occurrence of hurricanes, the collection of environmental data was not always uniform across experiments, and some parameters were unavailable for certain sampling days.

For samples pre and post Idalia and post Helene, determinations of NO_{3+2} (hereafter termed NO_3), PO_4, NH_4 and Chlorophyll-*a* (Chl-*a*) are available. Filtrates and filters were stored frozen. All nutrient analyses were carried out at the Mote Marine Laboratory using a continuous segmented flow analyzer (Auto-analyzer 3 SEAL) according to Dixon et al. (2014). Concentrations of Chl-*a* were analyzed using high-performance liquid chromatography (HPLC, Agilent HPL) at the Horn Point Analytical Services Laboratory according to Van Heukelum and Thomas (2001). In addition, for these same samples, concentrations of dissolved organic carbon (DOC) and colored dissolved organic matter (CDOM) were also measured, using an excitation wavelength of 280 nm. Cell abundance and classification were performed on raw water samples preserved with Lugol's solution (5%) in a Sedgewick-Rafter chamber (1 mL) using a Zeiss Axio Vert.A1 inverted microscope.

Humic acid extraction

All humic material used in enrichment studies was originally collected and isolated from the Shark River Slough, Florida, several years prior to this study, and stored frozen until analysis. The water samples for humic extractions were collected in precleaned carboys (10% HCl followed by three deionized water rinses). Water was returned to the lab and filtered through precombusted GF/F filters within 6 hours of collection and stored at 4˚C in darkness until further extraction. Humic acids were extracted according to a modification of the method of Leenheer (1981) using XAD-8 resin (Sigma Chemical) and Duolite A-7 anion exchange resin, as previously described in Heil (2005). The XAD-8 resin was cleaned (sequential 100% washes of diethyl ether, acetonitrile, methanol, and ether), slurried with distilled water, and packed into glass columns. The columns were subsequently cleaned and prepared as per Heil (2005). Just before extraction, the filtered water sample was acidified to pH 2.0 with 6.0 N HCl. Then, approximately 40 liters of the sample was passed through the XAD-8 column, which was subsequently rinsed with 100 mL of distilled water, followed by elution with 0.1 N NaOH. The resulting eluant was acidified with 6.0N HCl (Liao et al. 1982, Bowles et al. 1989), then centrifuged (3000 g, 20 min). The resulting pellet, representing the humic material, was washed with distilled water, recentrifuged, and dissolved in 0.1 N NaOH, passed through a cation exchange column, reacidified, and recentrifuged again. The dried humic fraction was dissolved in 50 mL of milli-Q water to make a humic stock solution with a concentration of 1 mg L^{-1} then filtered (0.2 μm Nuclepore filter) and stored in darkness at 4˚C.

Primary production and respiration rates measurements

All water collected was initially screened at the time of sample collection through a 100-micron nylon mesh to separate the smaller fractions of phytoplankton from zooplankton. After return to the laboratory, portions of the screened water samples (30 – 60 mL) were enriched with ~1% of $H_2{}^{18}O$ (Marshall Isotopes Ltd.) and dispensed without headspace into 12-15, 3 mL screw-capped vials sealed with Viton septa. To assess light-dependent gross respiration (GR) in the pre-Idalia experiments, vials were incubated in Photosynthetrons (MacIntyre et al., 1996) with light ranging from 0 to 800 μmole photons m^{-2} sec^{-2}. For all samples conducted in 2024, constant light (~130 μmol photons m^{-2} s^{-1}) was provided to all vials in custom made incubation devices, hereafter called "Coronatrons" (Bay Instruments LLC; Sobrinho et al. in review). Then, the Coronatrons were placed in three different constant temperature incubators for up to 8 hours (Figure 4.3).

Depending on sample or experiment, vials represented single, replicate or triplicate treatments. Rates of GR coincident with rates of gross primary production (GPP), net primary production (NPP) were calculated for all treatments. The constant temperature treatments included near-ambient temperature, ambient temperature +3˚C, and ambient temperature +6–8˚C. Before incubation of all experiments, triplicate vials were immediately fixed with mercuric chloride ($HgCl_2$, ~1% v/v), representing a time zero value. At the end of the incubation period, samples were removed from the Coronatrons, fixed with $HgCl_2$ (~1% v/v), placed completely underwater in jars at room temperature until analysis (within days) to minimize air contamination. Subsequent analysis was performed by Membrane Inlet Mass Spectrometry (MIMS) (Bay Instruments LLC, Easton, Maryland) (Sobrinho et al. in review). Rates of GPP,

NPP, and GR were calculated as described below and normalized by the Chl-*a* concentration of each sample.

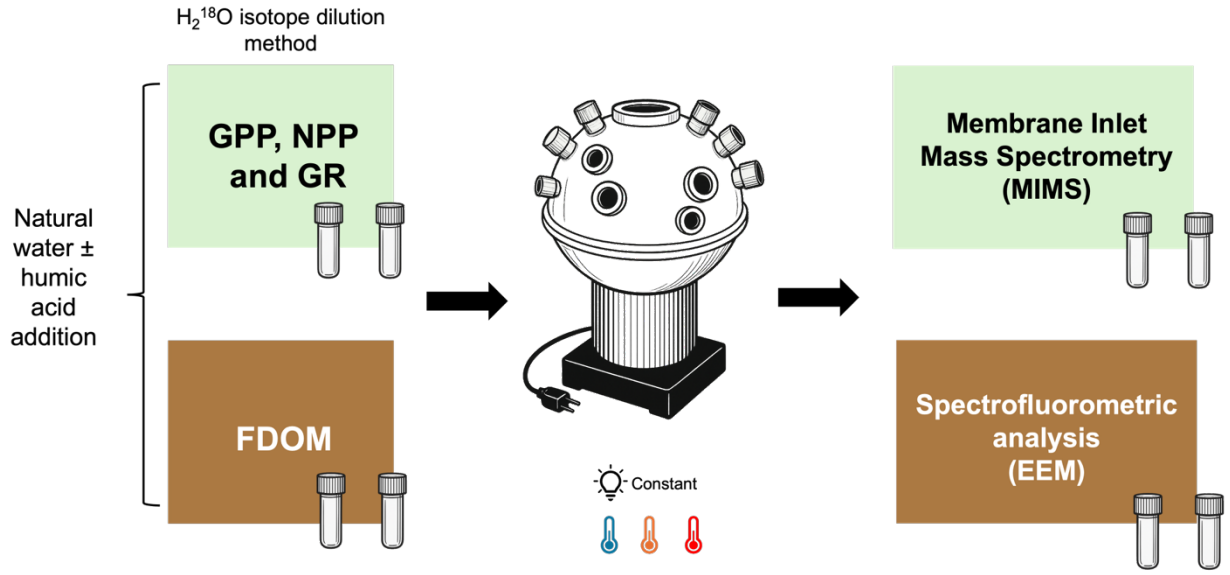

Figure 4.3 Schematic overview of the incubation setup used to quantify primary production (GPP, NPP) and Gross respiration (GR), as well as changes in dissolved organic matter (FDOM) composition. Water samples were dispensed into 3-mL gas-tight vials and incubated for up to 8 hours in custom-built incubators ("Coronatrons"), each maintained at constant light and at three temperature treatments (ambient, ambient + 3°C, and ambient + 6 – 8˚C). At the end of the incubation, vials enriched with ~1% $H_2{}^{18}O$ were fixed and analyzed by Membrane Inlet Mass Spectrometry (MIMS) to quantify metabolic rates. For select sites/dates, approximately 1 mL from each vial was transferred into an acid washed (10% HCl) and baked (232˚C, 2 h) scintillation vial and placed in the refrigerator (4˚C) in the dark for fluorescence excitation-emission matrix-parallel factor (EEM-PARAFAC) analysis of FDOM. ChatGPT was used to generate the Coronatrons icon.

An additional experiment was conducted post-Hurricane Milton, involving enrichment of samples with 6 mg L^{-1} of the previously extracted humic acids prior to enrichment with ~1% of $H_2{}^{18}O$. The amount of humic acid enrichment was based on prior measurements of colored DOM (CDOM) from samples from Charlotte Harbor (May and August 2023; E. Hall, unpublished data), which ranged from 1.3 to 12.9 mg l^{-1}.

To measure dark respiration (i.e., Community Respiration, CR) as a function of water temperature, water samples with no isotope added were carefully dispensed in 7mL vials and placed in a custom-made temperature control block with cool water circulating at one end and warm water at another, yielding a gradient of five values ranging from -5˚C to +5˚C relative to ambient temperature. After incubation (6–8 hours), vials were stored in water filled jars as described above and subsequently analyzed by MIMS as described below (Sobrinho et al. in review).

In parallel with the measurements of GPP, NPP and GR in the Coronatron incubations for samples collected following Hurricanes Debby and Helene, a replicate set of vials with no isotope enrichments was incubated in the Coronatrons for subsequent analysis of FDOM. After incubation, vials were frozen for subsequent spectrofluorimetric analysis at the University of South Florida (Horiba Aqualog, Horiba Instruments Inc.) as described in detail below.

Calculations and statistical analyses

To determine the rates of GPP, NPP, and GR, the mass-to-charge ratios (m/z) of the relative abundance of dissolved ^{16}O:^{16}O (mass 32), ^{18}O:^{18}O (mass 34), and Ar (mass 40) in the samples were measured by MIMS (Sobrinho et al. in review). Data analysis was by the software Quickdata (Bay Instruments LLC) according to Kana (1990), Kana et al. (1994), and Ferrón et al. (2016). Rates of GPP were calculated based on the change in the isotope ratio of dissolved O_2 over the incubation time (mass 34/40) (Equation 1).

$$GPP = \left(\frac{\left(\Delta[\frac{34}{40}] \times [Ar] \right)}{2 * ({}^{18}O(H_2O) + 0.002) * t} \right) \qquad \textit{(Equation 1)}$$

where $\Delta 34/40$, represents the change in the isotope to Ar ratio over time, [Ar] is the solubility of Argon at the incubation temperature, $^{18}O(H_2{}^{18}O)$ is the isotope ratio of the incubation water, which is calculated based on the amount of $^{18}O(H_2{}^{18}O)$ added in the total volume of the incubation flask and the percent enrichment (98-99%) of stock ^{18}O water; 0.002 represents the natural abundance of ^{18}O; and *t* represents the incubation time. This equation provides ^{18}O-GPP in μmol O_2 h^{-1}.

Rates of NPP were determined from the net change in O_2/Ar (mass 32/40) (Equation 2).

$$NPP = \frac{\Delta 32/40 \times [Ar]}{t} \qquad \textit{(Equation 2)}$$

where $\Delta 32/40$ represents the change in the O_2/Ar over time, [Ar] is the solubility of Ar at a certain temperature, and *t* represents the incubation time. This equation provides ^{18}O-NPP in μmol O_2 h^{-1}. Dark respiration rates were estimated from the NPP rates. Then, gross O_2 uptake (GR) was determined from the difference between GPP and NPP. Finally, GPP, NPP, and GR ratios obtained were normalized by the Chl-*a* concentration of each sample, providing μmol O_2 (μg Chl-*a*) $^{-1}$ h^{-1}.

To test the relationship between dark respiration and temperatures, linear models were used. The normality of data was checked with the Shapiro-Wilks test, and the homogeneity of variance was assessed. All statistical analyses were performed using the R language (R Core Team, 2021).

Dissolved organic matter analysis

For samples collected at the NP and SK sites after Hurricanes Helene and Milton, the effects of temperature on the composition of fluorescent DOM (FDOM) were determined using (fluorescence excitation-emission matrix-parallel factor analysis (EEM-PARAFAC; Xu et al. 2021). This is a nondestructive technique that detects fluorophores at low concentrations in a three-dimensional landscape. This landscape, or EEM, is then mathematically deconvoluted via PARAFAC to identify fluorescent compounds such as humic acids and protein-like compounds (Muni-Morgan et al., 2024). Various indices, including the biological index (BIX) and humification index (HIX) were calculated using the EEM absorbance and fluorescence spectra to resolve the degradation state, origin, and reactivity of DOM using the staRdom package in 'Rstudio' (version 4.2.2). The BIX is calculated using the ratio of fluorescence intensity of emissions 380/430 nm, obtained at an excitation wavelength of 310 nm (Huguet et al., 2009). Values greater than 1 are indicative of recent autochthonous production. The HIX is calculated by dividing the sum of emission intensities in the 435–480 nm region by the sum of total fluorescence intensities between the 300–345 nm and 435–480 nm regions, where the value of 1 is the highest degree of humification (Ohno, 2002). High values of HIX are associated with DOM that is higher in molecular weight, more aromatic, and of terrestrial origin.

Scans of EEM were performed on all samples (n=60) using a Horiba Aqualog (Horiba Instruments Inc). Prior to analysis, all samples were brought to a final volume of 3 mL using Milli-Q water and stabilized to room temperature prior to fluorescence analysis. Samples were analyzed in an acid-soaked (10% HCl; 24 h) 1 cm quartz cuvette, which was rinsed 20 times with Milli-Q water before being scanned. Before sample analysis, validation checks for water Raman

peak signal-to-noise and emission calibration were performed, as well as standardization of fluorescence intensity in quinine sulfate units (QSU) using a 1 ppm standard of quinine sulfate solution scanned at an excitation wavelength of 347.5 nm. Excitation wavelengths were measured from 239 to 800 nm (3 nm increments), and emission wavelengths were measured from 248 to 827 nm (5 nm increments).

Fluorescence EEM spectral correction was performed through subtraction of a sample blank of Milli-Q water to remove Raman scatter. The EEMs were corrected for inner filter effect (IFE), 1st and 2nd order Rayleigh scattering and normalized to the Raman peak of the Milli-Q water (Aqualog Software v 3.6) to enable a direct comparison of relative fluorescence between all sample EEMs. A single PARAFAC model was created in PLS Toolbox v 9.2 (Eigenvector Research Inc., Manson, WA, USA) in MATLAB (R2023a) to determine the underlying fluorophores in all samples using methods outlined in Stedmon and Bro (2008). The resultant model explained 99.1% of the data, which was validated using split half analysis (86.1), the core consistency diagnostic (61), and visual examination of residuals. The PARAFAC model was exported to the online spectral database OpenFluor to match underlying components to the existing literature using a Tucker congruence of 0.95 on the uploaded emission and excitation spectra (Murphy et al., 2014). The FDOM peaks were further compared visually to the commonly described Coble peaks (Coble 1996).

The PARAFAC model components were identified as terrestrial humic-like (C1), microbial humic-like (C2), and protein-like (C3). The C1 component has two excitation maxima at <250 and 370 nm, and one emission maximum at 480 nm. It is defined by Coble (1996) as humic-like peak C which is ubiquitous and has been observed in both terrestrial and marine DOM with minor differences in peak positions (Coble, 1996; Stedmon & Markager, 2005). This

component is indicative of allochthonous, or terrestrially derived humics. The C2 component matches the spectral characteristics of Coble peak M and is considered microbially produced or autochthonous humics of recent biological origin (Coble 1996). It has two excitation maxima at <250 and 300 nm, and one emission maximum at 400 nm. Lastly, the C3 component is defined as Coble peak T, resembling the spectra of tryptophan (Coble 2006). It has an excitation/emission maximum at 270/310 nm. Protein-like DOM is considered highly labile and can originate via biological production or cell lysis. Tryptophan is also used a marker for anthropogenic DOM originating from wastewater (Harris et al., 2024).

Results

Pre and Post Hurricane Idalia

Ambient conditions post Hurricane Idalia substantially altered the environmental conditions of Charlotte Harbor (CH). While temperatures were nearly the same (29.6˚C pre and 28.8ºC post), salinity declined from 23.7 to 16.0. Nitrogen loading substantially increased with NH_4 increasing from 1.63 to 3.41 μM and NO_3 increasing from <0.07 to 2.56 μM (Supplementary Table 4.1). Concentrations of DOC increased from 686 to 1080 μM and CDOM increased from 39.5 to 88.5 m^{-1} (Supplementary Table 4.1). Rates of light dependent GR averaged 0.13 μM O_2 (μg chl a^{-1} hr^{-1}) (Supplementary Figure 4.1).

Post-Hurricane Debby

Ambient conditions and phytoplankton community

The ambient temperature was similar at all stations (28˚C) in August 2024. Concentrations of Chl-*a* were 1.84 µg L^{-1} at Tampa Bay (TB), 3.59 µg L^{-1} at Siesta Key (SK), 2.32 µg L^{-1} at Caloosahatchee River (CR), and 4.31 µg L^{-1} at Charlotte Harbor (CH). Phytoplankton community composition varied considerably among stations (Supplementary Table 4.2). Station TB showed the highest cell densities in comparison with other sites, with cell concentrations dominated by diatoms (~1.28 cells × 10^7 L^{-1}), with smaller contributions from "other" taxa (~2.4 × 10^5 cells × L^{-1}). At SK, total biomass was considerably lower, cyanobacteria (~9.6 × 10^5 cells L^{-1}) were the main group, followed by diatoms (~6.6 × 10^5 cells L^{-1}), suggesting freshwater inputs. Station CR exhibited the lowest overall abundances, with < 2 × 10^5 cells L^{-1}, with diatoms dominating abundance. At CH, cell densities increased again relative to CR, with cyanobacteria (~6.6 × 10^5 cells L^{-1}) and diatoms (~2.2 × 10^5 cells L^{-1}) forming most of the community. *Karenia brevis* was not detected at any station.

Primary production and respiration rates

Following Hurricane Debby in August 2024, excessive rainfall caused widespread wastewater spills and organic matter inputs, generating a pronounced gradient of water colors across the sampling stations (Figure 4.4). Elevated concentrations of CDOM were evident in the more inner-shelf sites, particularly the Caloosahatchee River and Charlotte Harbor (Figure 4.4).

Figure 4.4 (A) Satellite image showing sediment plumes and stormwater runoff along southwest Florida following Hurricane Ian. Image acquired by the U.S. Geological Survey (Landsat 7) on October 2, 2022 (public domain; available at https://www.usgs.gov/media/images/landsat-7-captures-hurricane-ian-aftermath-sanibel-island). (B)Visual gradient of water color across stations sampled from north to south: Tampa Bay (TB), New Pass (NP), Siesta Key (SK), Caloosahatchee River mouth (CR), Charlotte Harbor (CH), and the upper Caloosahatchee River (S79). The darkest waters (CH, CR, and especially S79) represent the most inland stations, where terrestrial influence and organic matter inputs are strongest.

Across all stations, rates of GPP consistently declined with increasing experimental temperatures. At 28˚C, GPP ranged from 0.31–1.16 µmol O_2 (µg Chl-*a*)$^{-1}$ h^{-1}, but decreased to 0.21 – 0.79 at 33˚C. This represents reductions of up to 32% in GPP rates from 28˚C to 33˚C (Figure 4.5).

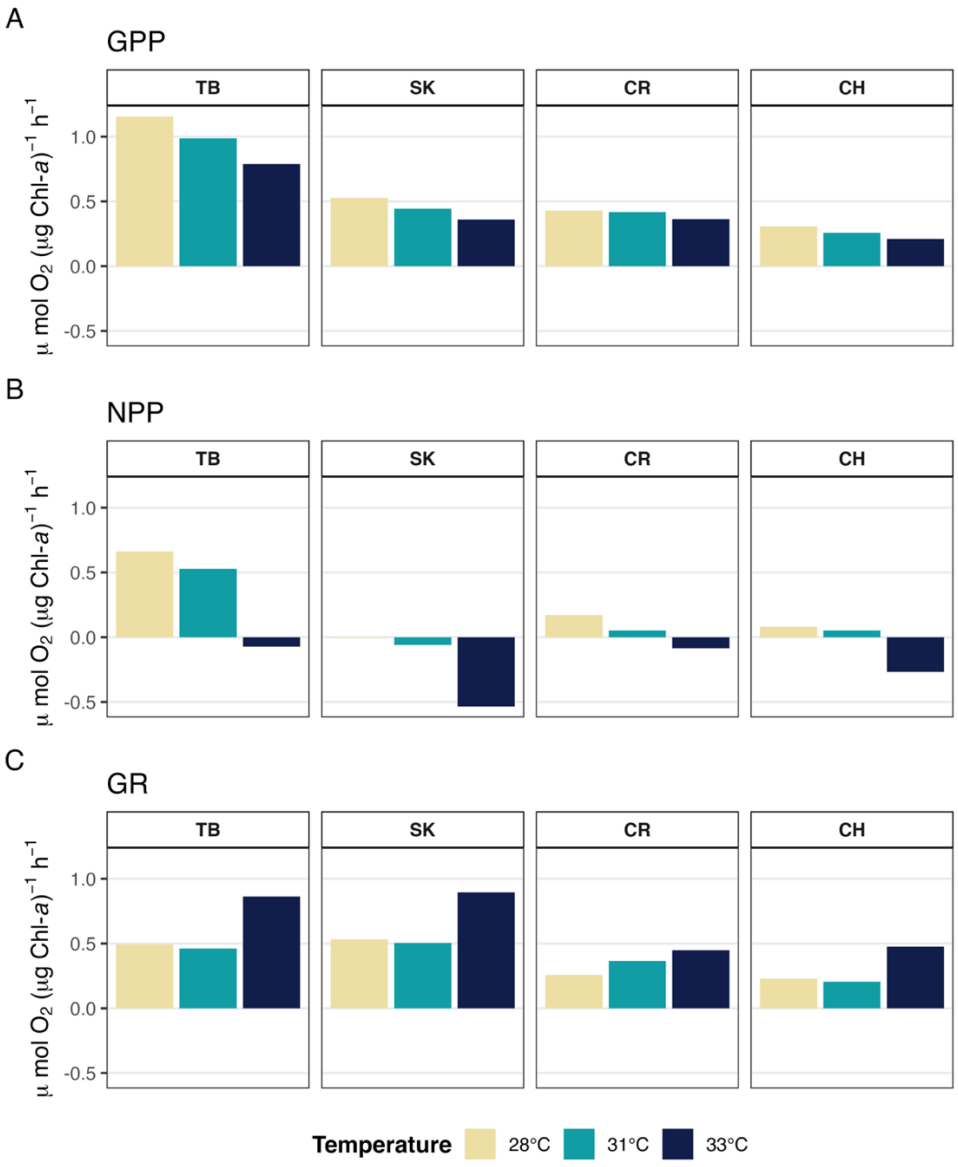

Figure 4.5 Gross primary production (GPP; panel A), net primary production (NPP; panel B), and gross respiration (GR; panel C) (µmol O_2 (µg Chl-*a*)$^{-1}$ h^{-1}) measured under three temperature treatments (28˚C, 31˚C and 33˚C) across four stations: Tampa Bay (TB), Siesta Key (SK), Caloosahatchee River mouth (CR) and Charlotte Harbor (CH).

Declines were generally stronger in the more 'colored' stations (CR and CH), where baseline GPP was already lower, and the effects of warming were more pronounced. Rates of NPP showed a similar negative response to temperature. At 28˚C, NPP ranged from -0.006 to 0.663 µmol O_2 (µg Chl-*a*)$^{-1}$ h-1, but decreased to values between -0.536 and -0.073 µmol O_2 (µg Chl-*a*)$^{-1}$ h^{-1}at 33˚C. At 33˚C, all stations exhibited negative NPP, indicating that respiration exceeded photosynthesis at elevated temperatures. Rates of GR increased noticeably with warming, from 0.23 – 0.53 µmol O_2 (µg Chl-*a*)$^{-1}$ h^{-1} at 28˚C to 0.45 – 0.90 µmol O_2 (µg Chl-*a*)$^{-1}$ h^{-1} at 33˚C, representing increases of up to 109% in GR rates. The largest temperature-driven stimulation of GR occurred in the colored-water stations (CR and CH) (Figure 4.5).

Dark vs. light respiration rates

At ambient temperature (28˚C), light-dependent rates of GR and dark respiration exhibited distinct patterns across stations (Figure 4.6). In TB, light respiration was over an order of magnitude higher than dark respiration, 0. 492 and 0.040 µmol O_2 (µg Chl-*a*)$^{-1}$ h^{-1}, respectively. A similar pattern occurred in SK, where light respiration (0.533) exceeded dark respiration (0.344) by 55%, indicating strong light-driven respiration in these clearer coastal waters. In contrast, the more colored waters, CR and CH, exhibited the opposite pattern: dark respiration rates were equal to or slightly higher than rates of light respiration.

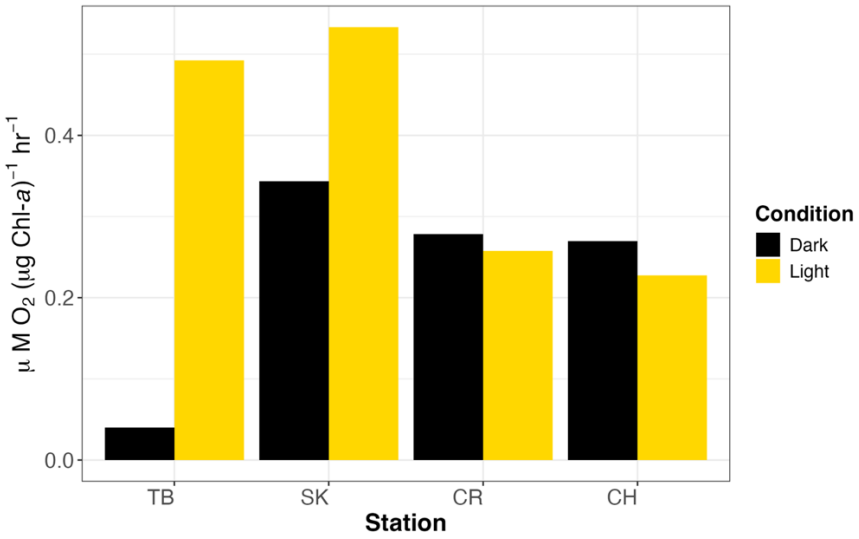

Figure 4.6 Dark respiration and light-dependent respiration (GR) measured at ambient temperature (28˚C) across four stations: Tampa Bay (TB), Siesta Key (SK), Caloosahatchee River mouth (CR), and Charlotte Harbor (CH).

Post Hurricane Helene

Ambient conditions and phytoplankton community

In October 2024, temperatures were similar among stations (28˚C), and Chl-*a* concentrations were 10.09 and 8.55 at NP and SK, respectively. Phytoplankton community composition differed among stations (Supplementary Table 2). No *K. brevis* was detected at either NP or SK. At NP, total cell abundance was primarily dominated by diatoms (4.60×10^5 cells $\times$ L^{-1}), with smaller contributions from dinoflagellates (4×10^4 cells $\times$ L^{-1}) and other taxa ($\sim 3 \times 10^4$ cells $\times$ L^{-1}). Cyanobacteria were not detected at this station. In contrast, SK exhibited higher total cell densities, largely dominated by cyanobacteria ($\sim 1.13 \times 10^7$ cells $\times$ L^{-1}). Microscopic examination revealed that many of these cells consisted of small coccoid forms embedded in mucilaginous aggregates, which did not appear physiologically healthy. These cells were identified as *Microcystis* sp. colonies, most likely transported via runoff from Phillippi

Creek which discharges near the Siesta Key station during rainfall events. *Microcystis* can persist in salt waters for approximately 3 – 4 days before cellular disintegration. Although the cells observed at SK were likely non-viable, their morphology remained identifiable. Diatoms (~5.40 $\times 10^5$ cells $\times L^{-1}$), dinoflagellates (~8×10^4 cells $\times L^{-1}$), and other taxa (~1.10×10^5 cells $\times L^{-1}$) contributed comparatively less to total abundance. The dominance of cyanobacteria at SK suggests stronger freshwater or nutrient-enriched influences relative to NP.

Primary production and respiration rates

At both NP and SK, temperature had similar effects on GPP, NPP, and GR (Figure 4.7). Rates of GPP were similar among temperatures, varying from 0.05 to 0.07 μmol O_2 (μg Chl-*a*)$^{-1}$ h^{-1} at NP, while SK presented higher GPP rates (0.10 – 0.11 μmol O_2 (μg Chl-*a*)$^{-1}$ h^{-1}) (Figure 4.7A). Rates of NPP presented a negative relationship with temperature, shifting from slightly positive values at 28˚C (0.03 μmol O_2 (μg Chl-*a*)$^{-1}$ h^{-1} at NP and 0.01 μmol O_2 (μg Chl-*a*)$^{-1}$ h^{-1} and SK), to increasingly negative values at higher temperatures, -0.007 μmol O_2 (μg Chl-*a*)$^{-1}$ h^{-1}at NP and -0.03 μmol O_2 (μg Chl-*a*)$^{-1}$ h^{-1} at SK (Figure 4.7B). In contrast, rates of GR increased consistently with temperature, with the highest GR rates observed at 32˚C, reaching 0.17 μmol O_2 (μg Chl-*a*)$^{-1}$ h^{-1} at SK (Figure 4.7C).

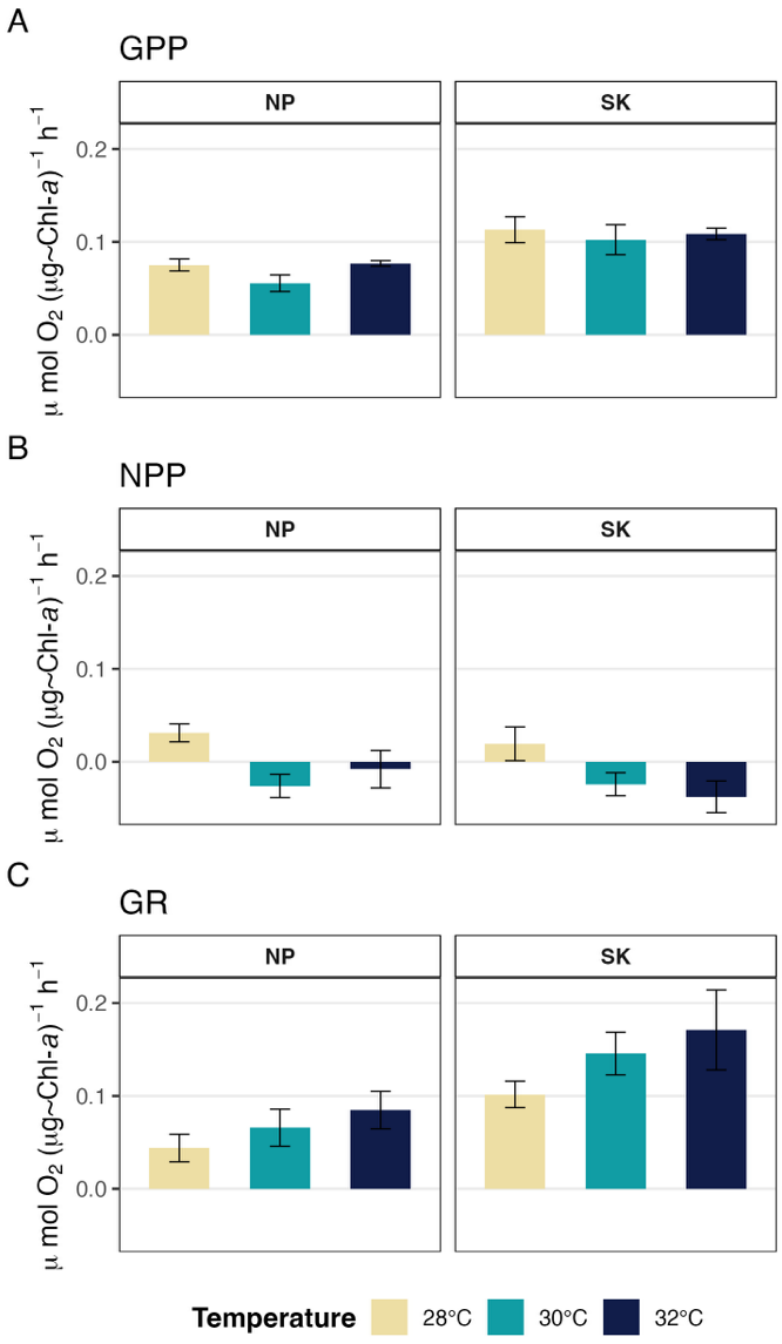

Figure 4.7 Gross primary production (GPP, A), net primary production (NPP, B), and gross respiration (GR; C) (µmol O_2 (µg Chl-*a*)$^{-1}$ h^{-1}) measured under three temperature treatments (28˚C, 30˚C, and 32˚C) across two stations: New Pass (NP) and Siesta Key (SK). Ambient temperature was 28˚C.

FDOM transformations

For sites NP and SK, warming resulted in shifts in relative fluorescence of all FDOM components (Figure 4.8). Mean initial BIX values at T0 were lower at site SK (0.79) vs NP (0.91) (Table 4.2), suggesting a smaller contribution of recently produced, microbially derived FDOM at SK relative to NP. Values of FDOM reflected more humified organic matter at site SK with mean initial HIX values of 0.81 at T0 vs. 0.61 at the NP site. Consistent reductions in component C1 (Terrestrial humic-like) were observed at all temperatures at both sites SK and NP. Increases in C2 (Microbial humic-like) were only observed in NP samples vs SK. Increases in C3 (Protein-like) were consistent with increasing temperature for NP and especially SK, along with increases in BIX. Conversely, the FDOM pool became less humified with increasing temperature as indicated by decreasing HIX values with increasing temperature at both sites.

Table 4. 2 Mean biological index (BIX) and humification index (HIX) values ± standard error of the mean at sites Siesta Key (SK) and New Pass (NP) across temperature treatments following Hurricane Helene.

Treatment	**Site**	**BIX**	**HIX**	**n**
T0	SK	0.79 ± 0.01	0.81 ± 0.01	3
28˚C	SK	0.80 ± 0.02	0.79 ± 0.01	3
30˚C	SK	0.78 ± 0.01	0.76 ± 0.03	3
32˚C	SK	0.86 ± 0.01	0.73 ± 0.04	3
T0	NP	0.91 ± 0.03	0.63 ± 0.03	3
28˚C	NP	0.92 ± 0.02	0.61 ± 0.03	3
30˚C	NP	0.94 ± 0.01	0.60 ± 0.04	3
32˚C	NP	1.00 ± 0.05	0.61 ± 0.05	3

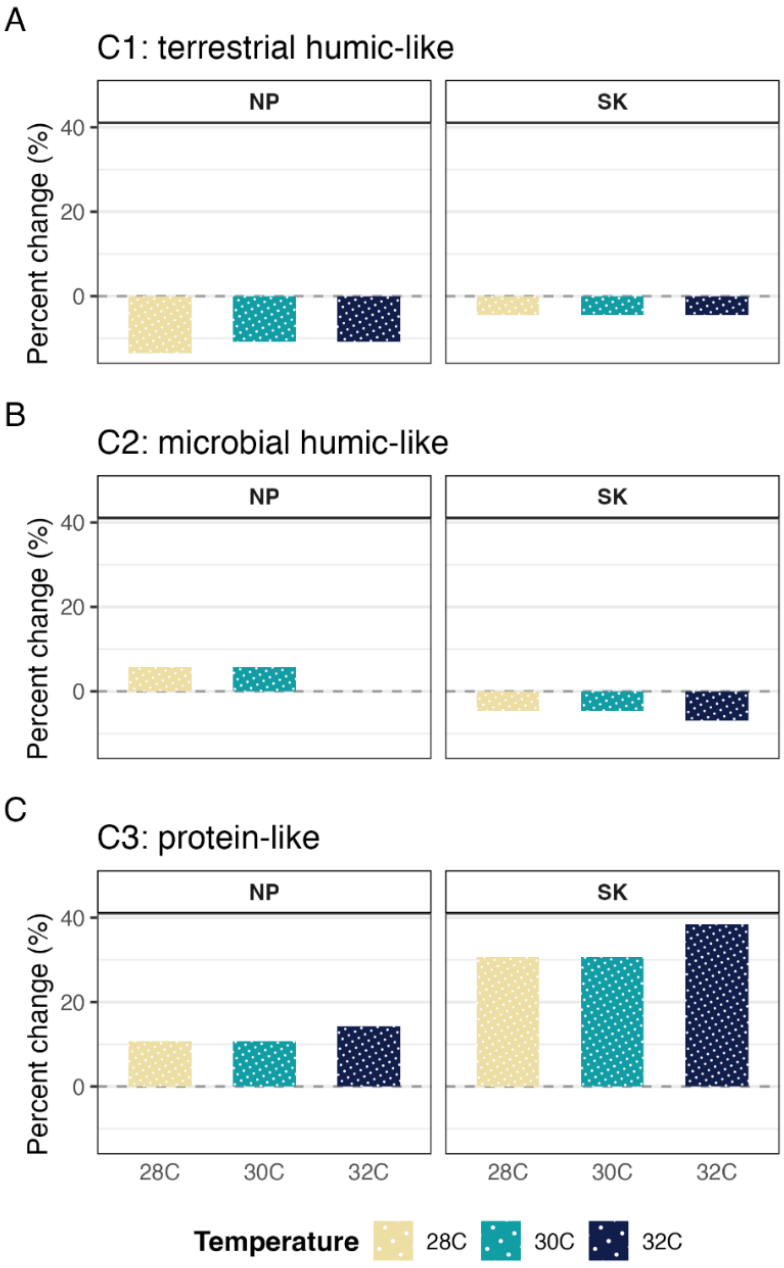

Figure 4.8 Percent change in each FDOM component (C1= terrestrial humic-like (panel A), C2 = microbial humic-like (panel B), C3 = protein-like (panel C)) generated by the PARAFAC model. Calculations are based on changes in relative fluorescence at T0 for each site (New Pass = NP; Siesta Key = SK) and temperature (28˚C, 30˚C, and 32˚C). Ambient temperature was 28˚C.

Dark vs. light respiration rates

In the post Helene samples, rates of dark and light respiration showed similar patterns between stations (Figure 4.9). Dark respiration exceeded light respiration at both sites, especially at SK, where respiration rates were consistently high.

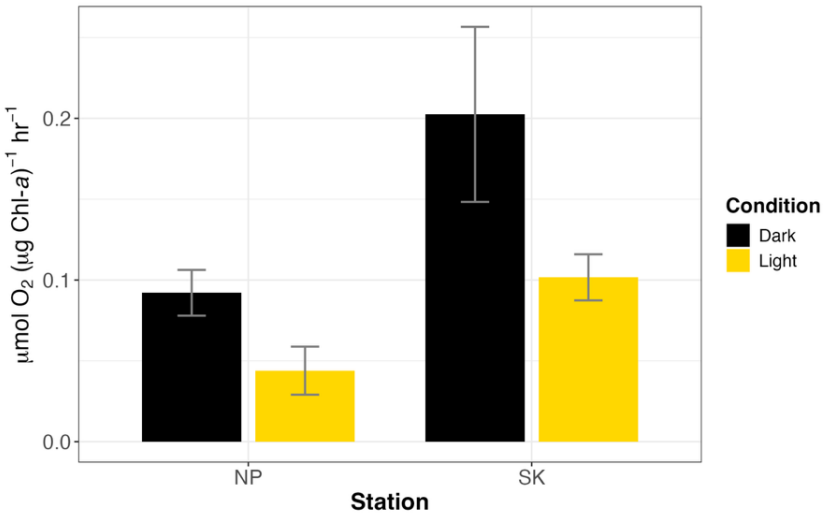

Figure 4.9 Mean (n = 3) dark community respiration and light-dependent respiration rates with standard deviation measured at ambient temperature (28˚C) across two stations: New Pass (NP) and Siesta Key (SK).

Post Hurricane Milton

Ambient conditions and dominant phytoplankton community

Environmental conditions during the three sampling days post Hurricane Milton showed relatively similar water temperatures (19 – 23˚C) and moderate salinity at both NP and SK (31 – 33). Nutrient concentrations at NP and SK were low overall, with NH_4^+ (3.7 – 3.9 µM) being the

dominant inorganic nitrogen form, while NO_3^- + NO_2^- and PO_4^{-3} remained below 1 µM at both sites (Supplementary Table 4.1).

Phytoplankton community composition was similar with varied abundance among days and stations (Supplementary Table 4.2). Day 1 showed the highest biomass at SK, dominated by diatoms (~ 4×10^6 cells L^{-1}), with *Skeletonema costatum* representing 80% of the community composition, while NP had lower abundances (8×10^5 cells L^{-1}) but a proportionally higher contribution of *K. brevis* (~ 4×10^5 cells L^{-1}). At site NP on day 2 there was a strong decline in total cells, with diatoms remaining dominant, but by Day 3, abundances increased (~3.6×10^6 cells L^{-1}), returning to levels similar to Day 1 and still dominated by diatoms, with *K. brevis* contributing moderately across all days (6×10^4 cells L^{-1} and 4×10^5 cells L^{-1}).

Primary production and respiration rates

On day 1 of experiments after Hurricane Milton, primary production and respiration responses showed similar patterns across stations and treatments (Figure 4.10). Rates of NP, GPP remained positive at 24˚C (0.14) and 27˚C (0.09), but declined to 0.01 µmol O_2 (µg Chl-*a*)$^{-1}$ h^{-1} at 30˚C. Rates of NPP decreased from 0.05 µmol O_2 (µg Chl-*a*)$^{-1}$ h^{-1} at 24˚C to -0.45 at 30˚C. Rates of GR increased modestly with temperature, rising from 0.09 (24˚C) to 0.46 µmol O_2 (µg Chl-*a*)$^{-1}$ h^{-1} at 30˚C.

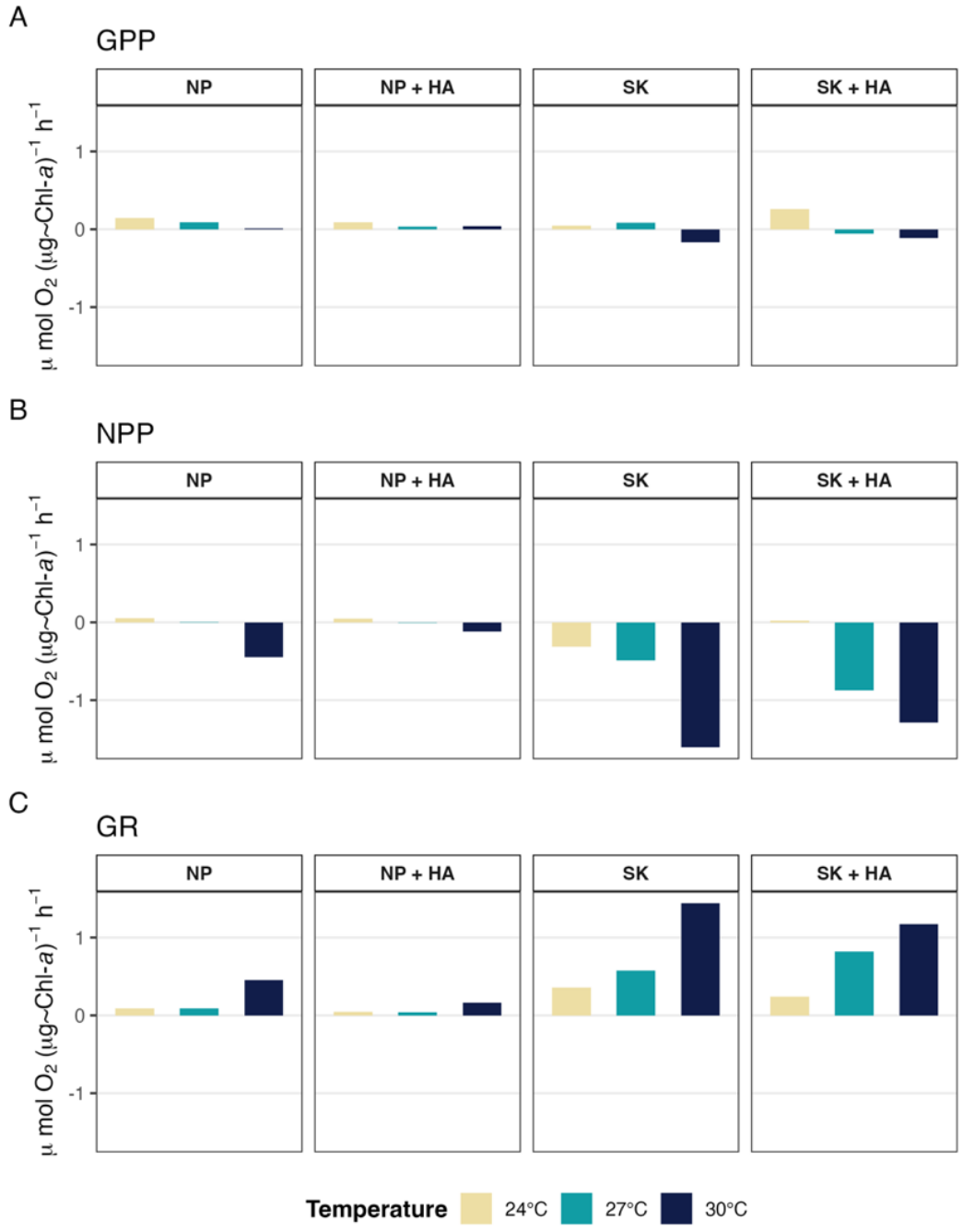

Figure 4.10 Gross primary production (GPP) (A), net primary production (NPP) (B), and gross respiration (GR) (C) at New Pass (NP) and Siesta Key (SK) with and without humic acid (HA) enrichment across three temperature treatments (24˚C, 27˚C, 30˚C) following Hurricane Milton.

The experiments with added humic acids to the NP samples showed some influence on the rates when compared to no addition: GPP ranged narrowly from 0.04 to –0.12, NPP remained

low but positive (0.03–0.09), and GR increased slightly with temperature (0.05 to 0.16) (Figure 4.10). Station SK exhibited stronger temperature sensitivity in comparison with NP (Figure 4.10)**.** Rates of GPP were slightly positive at lower temperatures (0.05–0.08**)** but became negative at 30˚C (-0.17). Rates of NPP declined from -0.31 at 24˚C to -1.61 µmol O_2 (µg Chl-*a*)$^{-1}$ h^{-1} at 30˚C. Rates of GR increased sharply with temperature, from 0.36 (24˚C) to 1.44 µmol O_2 (µg Chl-*a*)$^{-1}$ h^{-1} at 30˚C. Similar to the pattern observed at NP, the addition of humic acids at SK resulted in a slight increase in both GPP and NPP, accompanied by a small reduction in GR when compared to the control. GPP rate was 0.26 µmol O_2 (µg Chl-*a*)$^{-1}$ h^{-1} at 24˚C and declined to -0.11 at 30˚C. Rates of NPP increased from 0.02 to -1.29 µmol O_2 (µg Chl-*a*)$^{-1}$ h^{-1} at 30˚C, while GR increased substantially, reaching 1.17 µmol O_2 (µg Chl-*a*)$^{-1}$ h^{-1} at 30˚C.

FDOM transformations

The relative contributions of the FDOM components for sites NP and SK were sensitive to temperature changes across all treatments, but a more stable DOM pool was observed with treatments amended with humic acids vs unamended (Figure 4.11). Values of BIX at NP (0.98) were higher than those at SK (0.89) at T0 (Table 4.3), consistent with the previous experiment post Helene. However, BIX was higher at both NP and SK post Milton vs. post Helene. In general, C1 (Terrestrial humic-like) and C2 (Microbial humic-like) were more stable than C3 (Protein-like) in which a greater percent change in relative contribution was observed (Figure 4.11). The percentage of C1 declined with increasing temperature at NP and SK but increased with the additions of HA. Additions of HA increased the humification of the FDOM pool as indicated by greater HIX values at T0 in the HA amended vs. unamended treatments (Table 4.3). Contributions of C2 remained relatively stable at 24˚C across all treatments but generally

decreased with increasing temperature. Reductions in HIX with increasing temperature were observed in the unamended treatments except for NP at 30 ˚C. Conversely, HIX values increased with the HA amended treatments but did not show a consistent trend with increasing temperature.

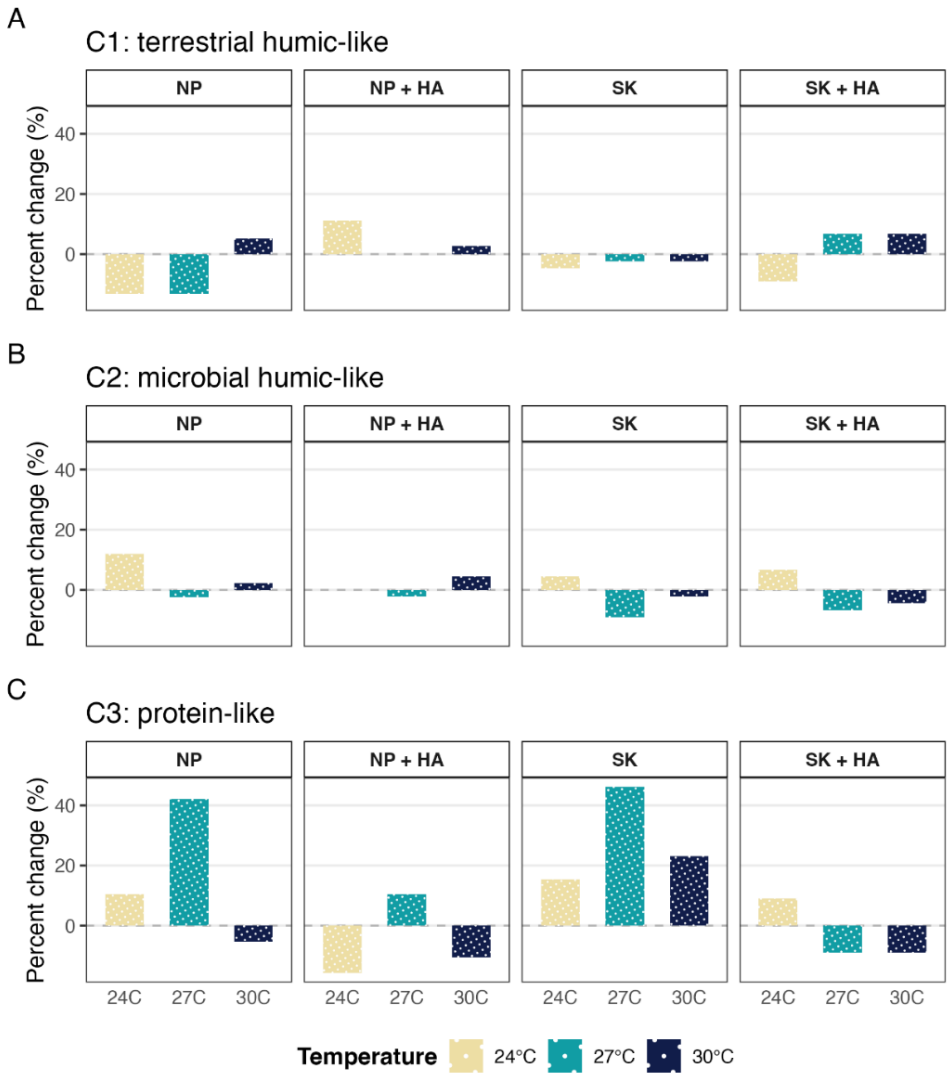

Figure 4.11 Percent change in each FDOM component (C1= terrestrial humic-like, C2 = microbial humic-like, C3 = protein-like) generated by the PARAFAC model. Calculations are based on changes in relative fluorescence at T0 for each site (New Pass = NP; Siesta Key = SK) and temperature (24˚C, 27˚C, 30˚C). Treatments that received additions of humic acid are denoted "+ HA".

Table 4. 3 Mean biological index (BIX) and humification index (HIX) values at sites New Pass (NP) and Siesta Key (SK) with and without humic acid (HA) enrichment across temperature treatments following Hurricane Milton. For samples greater than n=1, the standard error of the mean is expressed.

Treatment	Site	BIX	HIX	n
T0	SK	0.89 ± 0.02	0.77 ± 0.00	3
24˚C	SK	0.90	0.76	1
27˚C	SK	0.88	0.73	1
30˚C	SK	0.85	0.76	1
T0	NP	0.94 ± 0.01	0.70 ± 0.02	3
24˚C	NP	0.98	0.67	1
27˚C	NP	1.00	0.64	1
30˚C	NP	0.88	0.74	1
T0	SK + HA	0.83 ±0.03	0.80 ± 0.02	3
24˚C	SK + HA	0.80	0.77	1
27˚C	SK + HA	0.87	0.82	1
30˚C	SK + HA	0.87	0.83	1
T0	NP + HA	0.92 ± 0	0.72 ± 0.02	3
24˚C	NP + HA	0.86	0.74	1
27˚C	NP + HA	0.94	0.69	1
30˚C	NP + HA	0.93	0.73	1

Dark respiration vs. temperature

The response of dark respiration to increasing temperature at station NP exhibited a strong and highly significant linear relationship at both Day 2 and Day 3 (p-values = <0.001) (Supplementary Figure 4.2). Respiration rates increased from approximately 0.20 and 0.01 µmol O_2 (µg Chl-*a*)$^{-1}$ h^{-1} at 24˚C to nearly 0.55 µmol and 0.59 O_2 (µg Chl-*a*)$^{-1}$ h^{-1} at 32˚C during Day 2 and Day 3, respectively, representing more than a tenfold increase over the experimental temperature range.

Dark vs. light respiration rates

Dark and light respiration rates showed similar patterns between incubation days and light conditions (Figure 4.12), the mean respiration rates were higher under dark conditions than under light conditions, with both treatments showing relatively large variability among replicates.

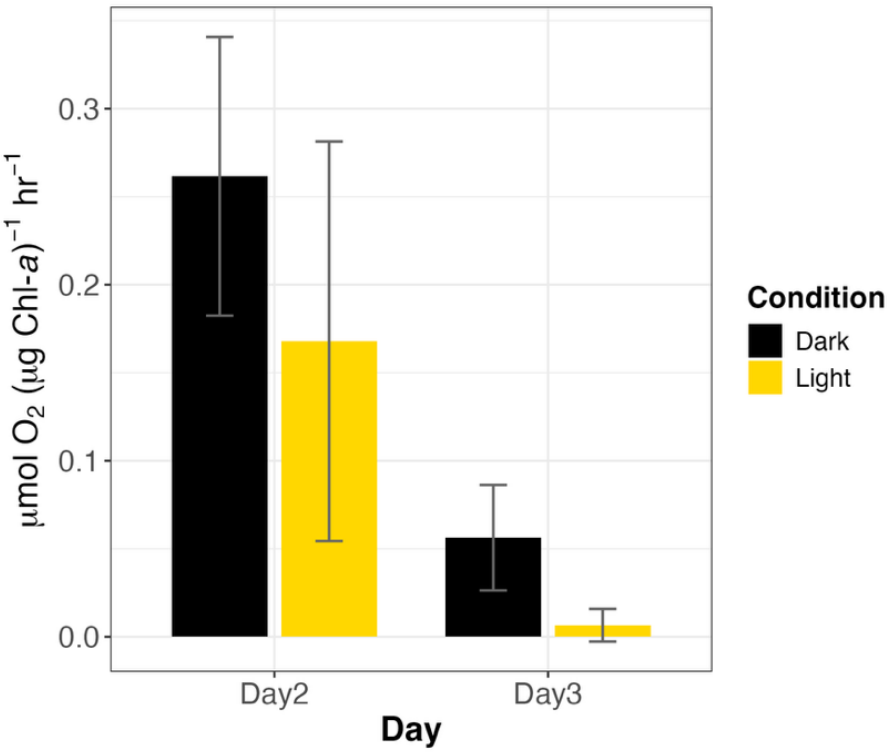

Figure 4.12 Mean dark community respiration and light-dependent respiration rates with standard deviation measured at ambient temperature (23 – 24 ˚C) in New Pass at Day 2 and Day 3.

Discussion

This study was conducted to assess the impacts of DOM on rates of productivity and respiration and involved opportunistic sampling following a series of hurricanes that impacted

the southwest Florida coastal region in 2024. The results of this study highlighted the substantial contribution of light-dependent processes to total respiration, a process that is often under-quantified and the importance of brownification and respiration in otherwise typically oligotrophic waters. Importantly, the patterns observed here have direct implications for hypoxia development on the WFS. Warmer waters, combined with elevated DOM inputs following hurricanes, enhanced respiration rates, both dark and light-dependent respiration, and accelerated DOM degradation. These processes collectively increase oxygen demand while simultaneously reducing oxygen solubility, conditions that favor hypoxic conditions.

In the oligotrophic subtropical waters of the WFS, it has previously been shown that daily GPP is often closely balanced by dark respiration, resulting in very low or near-zero NPP under non-bloom conditions (Hitchcock et al., 2000). Those experiments, conducted in Florida in 1996, involved depth-integrated daily primary production rated measured using the $H_2{}^{18}O$ method, while dark community respiration was measured through dark bottle-light bottle comparative incubations. In that study, dark CR consumed most of the GPP. Similar to some of the patterns observed in results reported herein, total daily light respiration rates exceeded dark respiration, highlighting the importance of light-dependent respiratory processes in regulating the metabolic balance of the system (Hitchcock et al., 2000). Overall, these results indicated that during this period the WFS functioned as a slightly heterotrophic system. Here, the effects of DOM discharges from hurricanes, and resulting brownification underscore that the WFS can, indeed, be a net heterotrophic system.

Primary production and respiration rates

The results of the several different kinds of experiments performed following the hurricane events of 2024 presented a consistent pattern: GPP declined substantially with warming, with even stronger reductions observed with temperature increases in the colored, DOM-rich waters after Hurricane Debby. The NPP rates also decreased with temperature, becoming predominantly negative above 30˚C. In the WFS, temperatures above 30˚C are commonly observed during summer in surface waters (Liu et al., 2006; Li et al., 2022; Nickerson et al., 2023; Sorinas et al., 2023). In contrast, GR increased sharply with warming, often exceeding both GPP and NPP. Rates of GR also increased with DOM loading when the pre-Idalia rates are compared to those measured post-Helene. It is well known that respiration is more temperature-dependent than photosynthesis, so that warming disproportionately accelerates respiratory losses relative to carbon fixation (Barton et al., 2020, and references therein). In this study, this was evident not only in the strong temperature dependence of dark respiration experiments, but also in the light-dependent respiration (i.e., GR) rates that were measured. Further, GR was comparable to, or even exceeded, dark respiration under ambient conditions in several cases, most notably at Tampa Bay (TB) after Hurricane Debby. These findings highlight that light-driven respiratory processes (e.g., Mehler reaction, cyclic electron flow, photorespiration) represent a substantial portion of oxygen consumption. Consequently, relying solely on traditional light–dark bottle methods may possibly underestimate respiration rates and overestimate NPP, particularly under conditions of warming and elevated DOM.

Consistent patterns have also been observed in other estuaries of Florida. Arriola et al. (2025) quantified ecosystem metabolism using dissolved oxygen measurements from *in situ*

probes in Tampa Bay and Biscayne Bay. They estimated vertically integrated GPP, NPP and ecosystem respiration (ER) using the oxygen mass-balance approach originally described by Odum (1956), where ER is derived from nighttime oxygen budgets assuming zero GPP, and GPP is calculated from daytime oxygen budgets assuming constant ER. Their results showed that daily GPP and ER were of similar magnitude, with NPP typically much smaller, indicating that these estuaries operate near metabolic balance with only minor shifts toward autotrophy or heterotrophy. In Tampa Bay, positive NPP was most often associated with periods of higher light availability, increased nutrient supply, and areas benefiting from seagrass recovery and water-quality improvements, while negative NPP occurred more frequently under conditions of elevated terrestrial organic-matter inputs or reduced light. Together, these findings demonstrate that subtropical coastal systems are highly sensitive to relatively small changes in temperature, salinity, light, and organic-matter loading, which can shift ecosystem metabolism toward autotrophy or heterotrophy.

Contrasting results were observed by Hitchcock et al. (2010), who investigated community metabolism during *K. brevis* blooms on the WFS. In that study, rates of daily gross primary production were estimated using the $H_2{}^{18}O$ method, while dark community respiration was determined from dark bottle incubations. The net community production was derived from the difference between gross production and respiration, and light-dependent respiration was calculated as the difference between gross production and net community production. A comparison of dark community respiration rates from 12- and 24-hour incubations showed that respiration during the photoperiod was approximately two-fold higher than at night. Accordingly, light respiration rates exceeded the maximum rates of dark respiration. Their results showed that, during periods of elevated biomass, respiration nearly balanced

phytoplankton production, although daytime oxygen production could still exceed respiratory demand. In the study herein, only one sample was collected during a *K. brevis* bloom (~400,000 cells L^{-1}at NP), and at this station, as well as across non-bloom stations, GR exceeded both GPP and NPP, particularly at 30˚C.

The trends observed in these experiments collectively demonstrate that an increase of only a few degrees in temperature can shift the system toward a more heterotrophic state, especially when combined with storm-driven inputs of organic matter. Considering that phytoplankton respiration frequently exceeded production in our experiments, these results indicate that warming and hurricane-enhanced DOM inputs may increase the development of hypoxia conditions on the WFS. Furthermore, studies have associated hypoxic conditions with *K. brevis* blooms in the WFS (Smith, 1975; Heyl et al., 1978; Milbrandt et al., 2021; Turley et al., 2022). Typically, *K. brevis* blooms initiate in early fall (August – September) and terminate in early spring (February – April) (Heil & Muni-Morgan., 2021). However, these blooms can occasionally overwinter and persist into the summer months, even when temperatures exceed their optimal growth range of 22 – 28˚C (e.g., Vargo, 2009; Ahn et al., 2023; Glibert et al., 2025), indicating that temperatures above 30˚C do not necessarily suppress their blooms. *Karenia brevis* can thermally acclimate, and its photosynthetic and nutritional responses depend not only on prior temperature exposure but also on the nitrogen form available (Ahn & Glibert, 2021; Ahn et al., 2023).

Hurricanes can further influence *K. brevis* bloom dynamics on the WFS: for example, runoff and submarine groundwater discharge were enhanced during the unusually active 2004 hurricane season along the WFS and were hypothesized to support the extensive *K. brevis* bloom during 2005 (Hu et al., 2006). Similarly, the 2018 bloom was associated with substantial

flooding and runoff following Hurricane Irma in 2017 (Fritz, 2018). Modeling work by Chen and Li (2025) showed that the strong winds and heavy rainfall associated with Hurricane Ian intensified runoff and stratification on the WFS, first triggering a brief diatom bloom that subsequently transitioned into a prolonged *K. brevis* bloom. Together, these examples highlight how hurricane-driven pulses of freshwater, nutrients, and organic matter can set the stage for large and persistent blooms in this region. These intense events are expected to become more common, as extreme weather is increasing in intensity and frequency under climate change (Glibert & Li, 2023), and Florida experiences major events roughly every two years (Malmstadt et al., 2010). Such storms can profoundly reshape nutrient delivery and hydrological conditions, often creating environments favorable for *K. brevis* blooms.

Warming and DOM enrichment both enhance oxygen consumption in coastal waters, and respiration is known to increase with elevated DOM loading (Pace et al., 2021). Consistent with this evidence, the experiments reported here following the 2024 hurricane events showed that GPP and NPP declined substantially with warming, and it was even more pronounced in the colored, DOM-rich waters after Hurricane Debby. In contrast, GR increases sharply with temperature, frequently exceeding both GPP and NPP. These findings highlight the complex interactions among oceanographic and meteorological processes that influence both hypoxia formation and *K. brevis* bloom dynamics on the WFS.

FDOM

Both hurricanes Helene and Milton delivered terrestrial humic FDOM that was degraded throughout both incubation experiments. The increases in temperature were associated with enhanced biological production of labile, protein-like FDOM and decreases in HIX. Together

these results suggest that increasing ocean water temperatures, particularly when coupled with storm-driven terrestrial inputs, can lead to a proportional shift from humified, or terrestrially dominated FDOM to an increasingly labile FDOM pool which can stimulate microbial respiration, thus increasing oxygen demand and contributing to the development of hypoxia.

Work by Mendoza and Zika (2014) found spatiotemporal variability of humic- and protein-like FDOM along transects beginning at the mouths of the Shark, Caloosahatchee, and Peace Rivers offshore onto the southwest Florida continental shelf. Results showed that increases in humic like fluorophores delivered via riverine flow, anthropogenic sources such as runoff, and wind driven sediment resuspension correspond with increases in protein-like DOM indicating increased biological production. In highly urbanized, HAB-prone systems such as Tampa Bay, the timing of these inputs is critical. For example, monthly and seasonal (wet vs. dry) monitoring of urban residential runoff and rainfall entering Tampa Bay revealed shifts in FDOM quality and reactivity. During the wet season, increases in labile FDOM (proteinaceous and microbially derived) were observed concomitant with increased fluxes of DOC and DON which can correspond with the timing of HABs in Tampa Bay waters (Muni-Morgan et al., 2024). The hurricane-driven humic pulses and subsequent production of protein-like FDOM observed in this study fit within a broader picture in which extreme rainfall and storm events define “windows” of enhanced DOM delivery that stimulates respiration and autochthonous production and amplify the effects of warming on oxygen demand.

As microbial and phytoplankton communities become more metabolically active under warming, greater releases of proteinaceous DOM likely reflect increased exudation, cell turnover, and cellular lysis, which can further reinforce bloom dynamics by fueling heterotrophic activity and nutrient recycling. At site NP values of BIX were consistently higher than at SK post

Hurricanes Helene and Milton. This indicates greater microbial activity at NP which could be a result of contributions of labile DOM from the surrounding watershed. For example, NP sits at the mouth of Sarasota Bay which received over 64 million liters of sewage post hurricane Debby (Farrow, 2024) which preceded Hurricanes Helene and Milton. Conversely, FDOM was more complex and humified at site SK and dominated by terrestrially derived material at T0 which could be due to rainfall generated runoff or riverine inputs. Such a role of precipitation and river discharge in structuring humic-like and protein-like FDOM on the southwest Florida shelf is consistent with the patterns described by Mendoza and Zika (2014). However, increases in relative proportion of protein-like C3 for SK samples more than doubled those in NP. These results suggest that humic compounds at SK stimulated microbial growth by providing nutrients and/or carbon leading to the production of protein-like DOM as a byproduct of metabolism and growth.

Post Hurricane Milton, substantial increases in C3 with increasing temperature were observed in the unamended treatments at NP and SK. For example, a percent change exceeding 40% at both NP and SK at 27˚C was observed, highlighting a potential "sweet spot" for DOM processing. This response was markedly lower in the humic acid amended treatments, suggesting that increased humic complexity may constrain autochthonous production of labile DOM, regardless of temperature. However, BIX values decreased at 30˚C in the unamended NP and SK treatments, suggesting a reduction in autochthonous DOM production potentially due to thermal stress or complete exhaustion of labile DOM compounds.

When comparing FDOM dynamics with respiration rates, a link between percent change in DOM and respiration rates was observed. Under stress conditions, an increase in protein-like FDOM is expected, which was evident in our results, especially at higher temperatures. Post-

Hurricane Helene, dark community respiration and GR rates were higher at SK compared to NP, consistent with the observed increase in the protein-like component (C3) at SK, particularly under elevated temperature conditions. Similarly, post-Hurricane Milton, respiration rates were also higher at SK than NP and increased with temperature. However, in contrast to Helene, the C3 component peaked at 27˚C at both stations (SK and NP), suggesting that the production of protein-like DOM exhibited distinct temperature optima depending on the post-hurricane context or its rapid decomposition at 30˚C.

Conclusion

All experiments exhibited temperature-driven declines in GPP, a shift toward negative NPP, and increased GR at higher temperatures, demonstrating that warming consistently suppresses photosynthesis while enhancing respiratory metabolism. In most experiments, rates of GR were higher than NPP, and sometimes higher than GPP emphasizing how respiration, including light-dependent respiratory processes, are stimulated with temperature increase. In subtropical coastal ecosystems, where elevated seawater temperatures often coincide with increased terrestrial organic matter inputs (e.g., humic substances), promoting brownification, these metabolic shifts may be further amplified, as shown in the comparison of GR rates post-Helene relative to pre-Idalia rates measured at the same station. Since these systems integrate both terrestrial and marine influence, they are uniquely vulnerable to the interaction of these multiple stressors. Therefore, studies that quantify how these rates change under different temperatures, and how the addition of HA may alter these rates, are essential for understanding the complexity of these processes and how climate change is and will continue to influence them.

Furthermore, measuring and incorporating these rates can help improve mechanistic models to better understand how the ocean will change in the future.

References

Ahn, S. H., & Glibert, P. M. (2021). Shining light on photosynthesis in the harmful dinoflagellate *Karenia mikimotoi* – Responses to short-term changes in temperature, nitrogen form, and availability. *Phycology*, 2(1), 30–44. https://doi.org/10.3390/phycology2010002

Ahn, S. H., Glibert, P. M., & Heil, C. A. (2023). In hot water: Interactions of temperature, nitrogen form and availability and photosynthetic and nitrogen uptake responses in natural *Karenia brevis* populations. *Harmful Algae*, 129, 102519. https://doi.org/10.1016/j.hal.2023.102519

Alam, M. A. (2023). Climate change and its impact on depletion of oxygen levels on coastal waters and shallow seas. In N. Jayaraju, G. Sreenivasulu, M. Madakka, & M. Manjulatha (Eds.), *Coasts, Estuaries and Lakes*. Springer. https://doi.org/10.1007/978-3-031-21644-2_20

Anderson, D. M., Burkholder, J. M., Cochlan, W. P., Glibert, P. M., Gobler, C. J., Heil, C. A., Kudela, R. M., Parsons, M. L., Rensel, J. E. J., Townsend, D. W., Trainer, V. L., & Vargo, G. A. (2008). Harmful algal blooms and eutrophication: Examining linkages from selected coastal regions of the United States. *Harmful Algae*, 8(1), 39–53. https://doi.org/10.1016/j.hal.2008.08.017

Arriola, J. M., Najjar, R. G., Briceño, H., Hu, C., Herrmann, M., & Beck, M. W. (2025). Ecosystem metabolic rates estimated from diel oxygen measurements in two subtropical estuaries. *Estuaries and Coasts*, 48(6), 155. https://doi.org/10.1007/s12237-025-01597-y

Barton, S., Jenkins, J., Buckling, A., Schaum, C. E., Smirnoff, N., Raven, J. A., & Yvon-Durocher, G. (2020). Evolutionary temperature compensation of carbon fixation in marine phytoplankton. *Ecology Letters*, 23(4), 722–733. https://doi.org/10.1111/ele.13469

Benner, R. (2002). Chemical composition and reactivity. In D. A. Hansell & C. A. Carlson (Eds.), *Biogeochemistry of marine dissolved organic matter* (pp. 59–90). Academic Press. https://doi.org/10.1016/B978-012323841-2/50005-1

Bianucci, L., Balaguru, K., Smith, R. W., Leung, L. R., & Moriarty, J. M. (2018). Contribution of hurricane-induced sediment resuspension to coastal oxygen dynamics. *Scientific Reports*, 8(1), 15740. https://doi.org/10.1038/s41598-018-33640-3

Bijma, J., Pörtner, H. O., Yesson, C., & Rogers, A. D. (2013). Climate change and the oceans–What does the future hold? *Marine Pollution Bulletin*, 74(2), 495-505. https://doi.org/10.1016/j.marpolbul.2013.07.022

Blanchet, C. C., Arzel, C., Davranche, A., Kahilainen, K. K., Secondi, J., Taipale, S., Lindberg, H., Loehr, J., Manninen-Johansen, S., Sundell, J., Maanan, M., & Nummi, P. (2022). Ecology and extent of freshwater browning – What we know and what should be studied next in the context of global change. *Science of the Total Environment*, 812, 152420. https://doi.org/10.1016/j.scitotenv.2021.152420

Boyer, J. N., Dailey, S. K., Gibson, P. J., Rogers, M. T., & Mir-Gonzalez, D. (2006). The role of dissolved organic matter bioavailability in promoting phytoplankton blooms in Florida Bay. *Hydrobiologia,* 569(1), 71–85. https://doi.org/10.1007/s10750-006-0123-2

Breitburg, D., Levin, L. A., Oschlies, A., Grégoire, M., Chavez, F. P., Conley, D. J., Garçon, V., Gilbert, D., Gutiérrez, D., Isensee, K., Jacinto, G. S., Limburg, K. E., Montes, I., Naqvi, S. W. A., Pitcher, G. C., Rabalais, N. N., Roman, M. R., Rose, K. A., Seibel, B. A., Telszewski, M., Yasuhara, M., & Zhang, J. (2018). Declining oxygen in the global ocean and coastal waters. *Science*, 359(6371), eaam7240. https://doi.org/10.1126/science.aam7240

Bronk, D. A., Roberts, Q. N., Sanderson, M. P., Canuel, E. A., Hatcher, P. G., Mesfioui, R., Filippino, K. C., Mulholland, M. R., & Love, N. G. (2010). Effluent organic nitrogen (EON): bioavailability and photochemical and salinity-mediated release. *Environmental Science & Technology*, 44(15), 5830-5835. https://doi.org/10.1021/es101115g

Bushaw, K. L., Zepp, R. G., Tarr, M. A., Schulz-Jander, D., Bourbonniere, R. A., Hodson, R. E., Miller, W. L., Bronk, D. A., & Moran, M. A. (1996). Photochemical release of biologically available nitrogen from aquatic dissolved organic matter. *Nature*, 381(6581), 404–407. https://doi.org/10.1038/381404a0

Bushaw-Newton, K. L., & Moran, M. A. (1999). Photochemical formation of biologically available nitrogen from dissolved humic substances in coastal marine systems. *Aquatic Microbial Ecology*, 18(3), 285-292. https://doi.org/10.3354/ame018285

Chen, Y., & Li, M. (2025). Impact of Hurricane Ian (2022) on a *Karenia brevis* bloom on the West Florida Shelf. *Geophysical Research Letters*, 52(6), e2024GL113500. https://doi.org/10.1029/2024GL113500

Chen, S., Lu, Y., Dash, P., Das, P., Li, J., Capps, K., Majidzadeh, H., & Elliott, M. (2019). Hurricane pulses: Small watershed exports of dissolved nutrients and organic matter during large storms in the Southeastern USA. *Science of the Total Environment*, 689, 232-244. https://doi.org/10.1016/j.scitotenv.2019.06.351

Cloern, J. E., Abreu, P. C., Carstensen, J., Chauvaud, L., Elmgren, R., Grall, J., Greening, H., Johansson, J. O. R., Kahru, M., Sherwood, E. T., Xu, J., & Yin, K. (2016). Human activities and climate variability drive fast-paced change across the world's estuarine–coastal ecosystems. *Global Change Biology*, 22(2), 513-529. https://doi.org/10.1111/gcb.13059

Coates, J. D., Cole, K. A., Chakraborty, R., O'Connor, S. M., & Achenbach, L. A. (2002). Diversity and ubiquity of bacteria capable of utilizing humic substances as electron donors for anaerobic respiration. *Applied and Environmental Microbiology*, 68(5), 2445-2452. https://doi.org/10.1128/AEM.68.5.2445-2452.2002

Coble, P. G. (1996). Characterization of marine and terrestrial DOM in seawater using excitation-emission matrix spectroscopy. *Marine Chemistry*, 51(4), 325-346. https://doi.org/10.1016/0304-4203(95)00062-3

Cochlan, W. P., & Bronk, D. A. (2001). Nitrogen uptake kinetics in the Ross Sea, Antarctica. *Deep Sea Research Part II: Topical Studies in Oceanography*, 48(19-20), 4127-4153. https://doi.org/10.1016/S0967-0645(01)00083-2

Conmy, R. N., Coble, P. G., Cannizzaro, J. P., & Heil, C. A. (2009). Influence of extreme storm events on West Florida Shelf CDOM distributions. *Journal of Geophysical Research*: *Biogeosciences*, 114(G4). https://doi.org/10.1029/2009JG000981

Diaz, R. J., & Rosenberg, R. (2008). Spreading dead zones and consequences for marine ecosystems. *Science*, 321(5891), 926-929. https://doi.org/10.1126/science.1156401

Dixon, L. K., Kirkpatrick, G. J., Hall, E. R., & Nissanka, A. (2014). Nitrogen, phosphorus and silica on the West Florida Shelf: Patterns and relationships with *Karenia* spp. occurrence. *Harmful Alga*e, 38, 8-19. https://doi.org/10.1016/j.hal.2014.07.001

Eddy, T. D., Heneghan, R. F., Bryndum- Buchholz, A., Fulton, E. A., Harrison, C. S., Tittensor, D. P., et al. (2025). Global and regional marine ecosystem models reveal key uncertainties in climate change projections. *Earth's Future*, 13, e2024EF005537. https://doi.org/10.1029/2024EF005537

Ferrón, S., del Valle, D. A., Björkman, K. M., Quay, P. D., Church, M. J., & Karl, D. M. (2016). Application of membrane inlet mass spectrometry to measure aquatic gross primary production by the 18O in vitro method. *Limnology and Oceanography*: *Methods*, 14(9), 610–622. https://doi.org/10.1002/lom3.10116

Florida State University Climate Center. (2024). Hurricane Helene summary report. https://climatecenter.fsu.edu/images/docs/Hurricane-Helene-Summary-Report.pdf. Accessed on February 21, 2026

Fritz, A. (2018). How climate change is making 'Red Tide' algal blooms worse. The Washington Post. https://www.washingtonpost.com/news/capital-weather-gang/wp/2018/08/14/how-climate-change-is-making-red-tide-algal-blooms-even-worse/. Accessed on February 21, 2026

Gaarder, T., & Gran, H. H. (1927). Investigations of the production of plankton in the Oslo Fjord. *ICES Journal of Marine Science*. https://doi.org/10.17895/ices.pub.19272251

Gilliam, F. S. (2021). Impacts of tropical cyclones on longleaf pine ecosystems of Florida: Tropical cyclogenesis, landfall frequencies, and climate change. *Frontiers in Ecology and Evolution*, 9, 595791. https://doi.org/10.3389/fevo.2021.595791

Glibert, P. M. (2019). Harmful algae at the complex nexus of eutrophication and climate change. *Harmful Algae*, 91, 101583. https://doi.org/10.1016/j.hal.2019.03.001

Glibert, P. M. (2024). *Phytoplankton whispering: An introduction to the physiology and ecology of microalgae*. Springer Nature. Cham, Switzerland. 753 pp.

Glibert, P. M., & Li, M. (2024). Warming, wheezing, blooming waters: Hypoxia and harmful algae. In D. Baird (Ed.), *Treatise on estuarine and coastal science* (2nd ed., pp. 401–444). Elsevier. https://doi.org/10.1016/B978-0-323-90798-9.00066-4

Glibert, P.M., Cai, W.-J., Hall, E.R., Li, M., Main, K.L., Rose, K.A., Testa, J.M., & Vidyarathna, N.K. (2022). Stressing over the complexities of multiple stressors in marine and estuarine systems. *Ocean–Land–Atmosphere Research*, 2022, 9787258. https://doi.org/10.34133/2022/9787258

Glibert, P. M., Beusen, A. H. W., Bouwman, A. F., Burkholder, J. M., Flynn, K. J., Heil, C. A., Li, M., Lin, C.-H., Madden, C. J., Mitra, A., Nardin, W., Silsbe, G., Song, Y., & Zhang, F. (2020). Multifaceted climatic change and nutrient effects on harmful algae require multifaceted models. In L. M. Botana, M. C. Louzao, & N. Vilariño (Eds.), *Climate change and marine and freshwater toxins* (2nd ed., pp. 473–518). De Gruyter. https://doi.org/10.1515/9783110625738-012

Glibert, P. M., Heil, C. A., & Li, M. (2025). More sustained, more severe blooms and shifting monthly patterns of the toxigenic dinoflagellate *Karenia brevis* on the West Florida Shelf. *Harmful Algae*, 139, 102967. https://doi.org/10.1016/j.hal.2025.102967

Gobler, C. J., Doherty, O. M., Hattenrath-Lehmann, T. K., Griffith, A. W., Kang, Y., & Litaker, R. W. (2017). Ocean warming since 1982 has expanded the niche of toxic algal blooms in the North Atlantic and North Pacific oceans. *Proceedings of the National Academy of Sciences,* 114(19), 201619575. https://doi.org/10.1073/pnas.1619575114

Goñi, M. A., Juranek, L. W., Sipler, R. E., & Welch, K. A. (2021). Particulate organic matter distributions in the water column of the Chukchi Sea during late summer. *Journal of Geophysical Research: Oceans*, 126(9), e2021JC017664. https://doi.org/10.1029/2021JC017664

Granéli, E., Carlsson, P., & Legrand, C. (1999). The role of C, N and P in dissolved and particulate organic matter as a nutrient source for phytoplankton growth, including toxic species. *Aquatic Ecology*, 33(1), 17–27. https://doi.org/10.1023/A:1009925515059

Griffith, A. W., & Gobler, C. J. (2020). Harmful algal blooms: A climate change co-stressor in marine and freshwater ecosystems. *Harmful Algae*, 91, 101590. https://doi.org/10.1016/j.hal.2019.03.008

Grégoire, M., Garçon, V., Garcia, H., Breitburg, D., Isensee, K., Oschlies, A., et al. (2021). A global ocean oxygen database and atlas for assessing and predicting deoxygenation and ocean health in the open and coastal ocean. *Frontiers in Marine Science*, 8, 724913. https://doi.org/10.3389/fmars.2021.724913

Guild, R., Wang, X., & Quijón, P. A. (2025). Climate change impacts on coastal ecosystems. *Environmental Research: Climate*, 3(4), 042006. https://doi.org/10.1088/2752-5295/ad9f90

Hallegraeff, G. M. (2010). Ocean climate change, phytoplankton community responses, and harmful algal blooms: A formidable predictive challenge. *Journal of Phycology*, 46(2), 220–235. https://doi.org/10.1111/j.1529-8817.2010.00815.x

Harris, N. A., Sorensen, J. P. R., Marchant, B., Old, G. H., Naden, P. S., Bowes, M. J., Scarlett, P. M., Nicholls, D. J. E., Armstrong, L. K., Wickham, H. D., Read, D. S., Lapworth, D., Bond, T., & Pond, K. (2024). Temporal drivers of tryptophan-like fluorescent dissolved organic matter along a river continuum. *Science of the Total Environment*, 928, 172285. https://doi.org/https://doi.org/10.1016/j.scitotenv.2024.172285

Heil, C. A. (2005). Influence of humic, fulvic and hydrophilic acids on the growth, photosynthesis and respiration of the dinoflagellate *Prorocentrum minimum* (Pavillard) Schiller. *Harmful Algae*, 4(3), 603–618. https://doi.org/10.1016/j.hal.2004.08.010

Heil, C. A., & Muni-Morgan, A. L. (2021). Florida's harmful algal bloom (HAB) problem: Escalating risks to human, environmental and economic health with climate change. *Frontiers in Ecology and Evolution*, 9, 646080. https://doi.org/10.3389/fevo.2021.646080

Heyl, M. G., Freeberg, L. R., & Dickinson, K. D. (1978). Dissolved oxygen during *Gymnodinium br*eve blooms along the Florida west coast, 1976–1978. *Journal of Environmental Science & Health Part A*, 13(10), 725-731. https://doi.org/10.1080/10934527809374851

Hitchcock, G. L., Vargo, G. A., & Dickson, M. L. (2000). Plankton community composition, production, and respiration in relation to dissolved inorganic carbon on the West Florida Shelf, April 1996. *Journal of Geophysical Research: Oceans*, 105(C3), 6579-6589. https://doi.org/10.1029/1998JC000293

Hitchcock, G. L., Kirkpatrick, G., Minnett, P., & Palubok, V. (2010). Net community production and dark community respiration in a *Karenia brevis* (Davis) bloom in West Florida coastal waters, USA. *Harmful algae*, 9(4), 351-358. https://doi.org/10.1016/j.hal.2010.01.002

Hounshell, A.G., Fegley, S.R., Hall, N.S. et al. (2022). Riverine discharge and phytoplankton biomass control dissolved and particulate organic matter dynamics over spatial and temporal scales in the Neuse River Estuary, North Carolina. *Estuaries and Coasts*, 45, 96–113. https://doi.org/10.1007/s12237-021-00955-w

Hu, C., Muller-Karger, F. E., & Swarzenski, P. W. (2006). Hurricanes, submarine groundwater discharge, and Florida's red tides. *Geophysical Research Letters*, 33(11), L11601. https://doi.org/10.1029/2005GL025449

Huguet, A., Vacher, L., Relexans, S., Saubusse, S., Froidefond, J. M., & Parlanti, E. (2009). Properties of fluorescent dissolved organic matter in the Gironde Estuary. *Organic Geochemistry*, 40(6), 706-719. https://doi.org/10.1016/j.orggeochem.2009.03.002

Kana, T. M. (1990). Light-dependent oxygen cycling measured by an oxygen-18 isotope dilution technique. *Marine Ecology Progress Series*, 64, 293-300. https://doi.org/10.3354/meps064293

Kana, T. M., Darkangelo, C., Hunt, M. D., Oldham, J. B., Bennett, G. E., & Cornwell, J. C. (1994). Membrane inlet mass spectrometer for rapid high-precision determination of N2, O2, and Ar in environmental water samples. *Analytical Chemistry*, 66(23), 4166–4170. https://doi.org/10.1021/ac00095a009

Kaushal, S. S., & Belt, K. T. (2012). The urban watershed continuum: evolving spatial and temporal dimensions. *Urban Ecosystems*, 15(2), 409-435. https://doi.org/10.1007/s11252-012-0226-7

Kramer, D. M., & Evans, J. R. (2011). The importance of energy balance in improving photosynthetic productivity. *Plant Physiology*, 155(1), 70– 78. https://doi.org/10.1104/pp.110.166652

Leenheer, J. A. (1981). Comprehensive approach to preparative isolation and fractionation of dissolved organic carbon from natural waters and wastewaters. *Environmental Science & Technology*, 15(5), 578-587. https://doi.org/10.1021/es00087a010

Lewitus, A. J., & Kana, T. M. (1995). Light respiration in six estuarine phytoplankton species: Contrasts under photoautotrophic and mixotrophic growth conditions. *Journal of Phycology*, 31(5), 754–761. https://doi.org/10.1111/j.0022-3646.1995.00754.x

Li, G., Wang, Z., & Wang, B. (2022). Multidecade trends of sea surface temperature, chlorophyll-*a* concentration, and ocean eddies in the Gulf of Mexico. *Remote Sensing*, 14(15), 3754. https://doi.org/10.3390/rs14153754

Liu, Y., Weisberg, R. H., & He, R. (2006). Sea surface temperature patterns on the West Florida Shelf using growing hierarchical self-organizing maps. *Journal of Atmospheric and Oceanic Technology*, 23(2), 325-338. https://doi.org/10.1175/JTECH1848.1

Lønborg, C., Carreira, C., Jickells, T., & Álvarez-Salgado, X. A. (2020). Impacts of global change on ocean dissolved organic carbon (DOC) cycling. *Frontiers in Marine Science*, 7, 466. https://doi.org/10.3389/fmars.2020.00466

MacIntyre, H. L., Geider, R. J., & McKay, R. M. (1996). Photosynthesis and regulation of Rubisco activity in net phytoplankton from Delaware Bay. *Journal of Phycology, 32*(5), 718–731. https://doi.org/10.1111/j.0022-3646.1996.00718.x

Malmstadt, J.C., Elsner, J.B., Jagger, T.H. (2010). Frequency and Intensity of Hurricanes Within Florida's Threat Zone. In: Elsner, J., Hodges, R., Malmstadt, J., Scheitlin, K. (eds) *Hurricanes and Climate Change*. Springer, Dordrecht. https://doi.org/10.1007/978-90-481-9510-7_11

Malmstadt, J., Scheitlin, K., & Elsner, J. (2009). Florida hurricanes and damage costs. *Southeastern Geographer*, 49, 108–131. https://doi.org/10.1353/sgo.0.0045

Martínez, A., Méndez, Si., Fabre, A., & Ortega, L. (2017). Intensificación de floraciones de dinoflagelados marinos en Uruguay. *INNOTEC*, 13(13), 19–25. https://doi.org/10.26461/13.02

Mendoza, W. G., & Zika, R. G. (2014). On the temporal variation of DOM fluorescence on the southwest Florida continental shelf. *Progress in Oceanography*, 120, 189-204. https://doi.org/10.1016/j.pocean.2013.08.010

Milbrandt, E. C., Martignette, A. J., Thompson, M. A., Bartleson, R. D., Phlips, E. J., Badylak, S., & Nelson, N. G. (2021). Geospatial distribution of hypoxia associated with a *Karenia brevis* bloom. *Estuarine, Coastal and Shelf Science*, 259, 107446. https://doi.org/10.1016/j.ecss.2021.107446

Miles, T., Glenn, S. M., & Schofield, O. (2013). Temporal and spatial variability in fall storm induced sediment resuspension on the Mid-Atlantic Bight. *Continental Shelf Research*, 63, S36-S49. https://doi.org/10.1016/j.csr.2012.08.006

Moran, M. A., & Hodson, R. E. (1994). Dissolved humic substances of vascular plant origin in a coastal marine environment. *Limnology and Oceanography*, 39(4), 762–771. https://doi.org/10.4319/lo.1994.39.4.0762

Muni-Morgan, A., Lusk, M. G., Heil, C., Goeckner, A. H., Chen, H., McKenna, A. M., & Holland, P. S. (2023). Molecular characterization of dissolved organic matter in urban stormwater pond and municipal wastewater discharges transformed by the Florida red

tide dinoflagellate *Karenia brevis*. *Science of the Total Environment*, 904, 166291. https://doi.org/10.1016/j.scitotenv.2023.166291

Muni-Morgan, A. L., Lusk, M. G., & Heil, C. A. (2024). *Karenia brevis* and *Pyrodinium bahamense* utilization of dissolved organic matter in urban stormwater runoff and rainfall entering Tampa Bay, Florida. *Water*, 16(10), 1448. https://doi.org/10.3390/w16101448

Murphy, K. R., Stedmon, C. A., Wenig, P., & Bro, R. (2014). OpenFluor–an online spectral library of auto-fluorescence by organic compounds in the environment. *Analytical Methods*, 6(3), 658-661. https://doi.org/10.1039/C3AY41935E

Musani, L., Valenta, P., Nürnberg, H. W., Konrad, Z., & Branica, M. (1980). On the chelation of toxic trace metals by humic acid of marine origin. *Estuarine and Coastal Marine Scienc*e, 11(6), 639-649. https://doi.org/10.1016/S0302-3524(80)80015-6

National Hurricane Center. (2024). *Tropical cyclone report: Hurricane Milton* (AL142024). National Oceanic and Atmospheric Administration. https://www.nhc.noaa.gov/data/tcr/AL142024_Milton.pdf. Accessed on February 21, 2026

National Weather Service. (2024). Post tropical cyclone report. National Oceanic and Atmospheric Administration. https://www.weather.gov/media/tbw/TropicalEventSummary/PSHTBW_2024AL04_Debby_Summary.pdf. Accessed on February 21, 2026

Nickerson, A. K., Weisberg, R. H., Zheng, L., & Liu, Y. (2023). Sea surface temperature trends for Tampa Bay, West Florida Shelf and the deep Gulf of Mexico. *Deep Sea Research Part II: Topical Studies in Oceanography*, 211, 105321. https://doi.org/10.1016/j.dsr2.2023.105321

Odum, H. T. (1956). Primary production in flowing waters. *Limnology and Oceanography*, 1(2), 102–117. https://doi.org/10.4319/lo.1956.1.2.0102

Ohno, T. (2002). Fluorescence inner-filtering correction for determining the humification index of dissolved organic matter. *Environmental Science & Technology*, 36(4), 742-746. https://doi.org/10.1021/es0155276

Opsahl, S., & Benner, R. Distribution and cycling of terrigenous dissolved organic matter in the ocean. *Nature*, 386, 480–482 (1997). https://doi.org/10.1038/386480a0

Pace, M. L., Buelo, C. D., & Carpenter, S. R. (2021). Phytoplankton biomass, dissolved organic matter, and temperature drive respiration in whole lake nutrient additions. *Limnology and Oceanography*, 66(6), 2174-2186. https://doi.org/10.1002/lno.11738

Pilla, R. M., Williamson, C. E., Zhang, J., Smyth, R. L., Lenters, J. D., Brentrup, J. A., Knoll, L. B., & Fisher, T. J. (2018). Browning-related decreases in water transparency lead to long-term increases in surface water temperature and thermal stratification in two small lakes. *Journal of Geophysical Research: Biogeosciences*, 123(5), 1651-1665. https://doi.org/10.1029/2017JG004321

Pontius, J., & McIntosh, A. (2024). Gulf of Mexico dead zone. In *Environmental Problem Solving in an Age of Climate Change: Volume One: Basic Tools and Techniques* (pp. 45-56). Cham: Springer International Publishing. https://doi.org/10.1007/978-3-031-48762-0_5

Rabalais, N. N., & Turner, R. E. (2019). Gulf of Mexico hypoxia: Past, present, and future. *Limnology and Oceanography Bulletin*, 28(4), 117-124. https://doi.org/10.1002/lob.10351

Schmidtko, S., Stramma, L., & Visbeck, M. (2017). Decline in global oceanic oxygen content during the past five decades. *Nature*, 542(7641), 335-339. https://doi.org/10.1038/nature21399

See, J. H., Bronk, D. A., & Lewitus, A. J. (2006). Uptake of Spartina-derived humic nitrogen by estuarine phytoplankton in nonaxenic and axenic culture. *Limnology and Oceanography*, 51(5), 2290-2299. https://doi.org/10.4319/lo.2006.51.5.2290

Smith, G. B. (1975). The 1971 red tide and its impact on certain reef communities in the mid-eastern Gulf of Mexico. *Environmental Letters*, 9(2), 141-152. https://doi.org/10.1080/00139307509435843

Sobrinho, B. F., Vidyarathna, N., Kana, T. M., & Glibert, P. M. (in review). Improved primary production and gross respiration measurements using the $H_2{}^{18}O$ technique with membrane inlet mass spectrometry and introduction of a small volume–uniform irradiance incubation chamber. *Manuscript submitted for publication*.

Sorinas, L., Weisberg, R. H., Liu, Y., & Law, J. (2023). Ocean-atmosphere heat exchange seasonal cycle on the West Florida Shelf derived from long term moored data. *Deep Sea Research Part II: Topical Studies in Oceanography*, 212, 105341. https://doi.org/10.1016/j.dsr2.2023.105341

Stedmon, C. A., & Bro, R. (2008). Characterizing dissolved organic matter fluorescence with parallel factor analysis: a tutorial. *Limnology and Oceanography: Methods,* 6(11), 572-579. https://doi.org/10.4319/lom.2008.6.572

Stedmon, C. A., & Markager, S. (2005). Resolving the variability in dissolved organic matter fluorescence in a temperate estuary and its catchment using PARAFAC analysis. *Limnology and Oceanography*, 50(2), 686-697. https://doi.org/10.4319/lo.2005.50.2.0686

Stepanauskas, R., Jørgensen, N. O., Eigaard, O. R., Žvikas, A., Tranvik, L. J., & Leonardson, L. (2002). Summer inputs of riverine nutrients to the Baltic Sea: Bioavailability and eutrophication relevance. *Ecological Monographs*, 72(4), 579-597. https://doi.org/10.1890/0012-9615(2002)072[0579:SIORNT]2.0.CO;2

Thurman, E. M. (1985). Transport, origin and source of dissolved organic carbon. In E. M. Thurman (Ed.), *Organic Geochemistry of Natural Waters* (pp. 67–85). Dordrecht: Springer Netherlands. https://doi.org/10.1007/978-94-009-5095-5_3

Turley, B. D., Karnauskas, M., Campbell, M. D., Hanisko, D. S., & Kelble, C. R. (2022). Relationships between blooms of *Karenia brevis* and hypoxia across the West Florida Shelf. *Harmful Algae*, 114, 102223. https://doi.org/10.1016/j.hal.2022.102223

Urrutia-Cordero, P., Ekvall, M. K., Ratcovich, J., Soares, M., Wilken, S., Zhang, H., & Hansson, L. A. (2017). Phytoplankton diversity loss along a gradient of future warming and brownification in freshwater mesocosms. *Freshwater Biology*, 62(11), 1869–1878. https://doi.org/10.1111/fwb.13027

Van Heukelem, L., & Thomas, C. S. (2001). Computer-assisted high-performance liquid chromatography method development with applications to the isolation and analysis of phytoplankton pigments. *Journal of Chromatography* A, 910(1), 31-49. https://doi.org/10.1016/S0378-4347(00)00603-4

Vargo, G. A. (2009). A brief summary of the physiology and ecology of *Karenia brevis* Davis (G. Hansen and Moestrup comb. nov.) red tides on the West Florida Shelf and of hypotheses posed for their initiation, growth, maintenance, and termination. *Harmful Algae*, 8(4), 573–584. https://doi.org/10.1016/j.hal.2008.11.002

Wang, Z., Boyer, T., Reagan, J., & Hogan, P. (2023). Upper-oceanic warming in the Gulf of Mexico between 1950 and 2020. *Journal of Climate*, 36(8), 2721–2734. https://doi.org/10.1175/JCLI-D-22-0409.1

Weiss, R. F. (1970). The solubility of nitrogen, oxygen and argon in water and seawater. *Deep-Sea Research and Oceanographic Abstracts*, 17(4), 721–735. https://doi.org/10.1016/0011-7471(70)90037-9

Wiegner, T. N., Seitzinger, S. P., Glibert, P. M., & Bronk, D. A. (2006). Bioavailability of dissolved organic nitrogen and carbon from nine rivers in the eastern United States. *Aquatic Microbial Ecology*, 43(3), 277-287. https://doi.org/10.3354/ame043277

Wikner, J., Vikström, K., & Verma, A. (2023). Regulation of marine plankton respiration: A test of models. *Frontiers in Marine Science*, 10, 1134699. https://doi.org/10.3389/fmars.2023.1134699

Williamson, C. E., Overholt, E. P., Pilla, R. M., Leach, T. H., Brentrup, J. A., Knoll, L. B., Mette, E. M., & Moeller, R. E. (2015). Ecological consequences of long-term browning in lakes. *Scientific Reports*, 5(1), 18666. https://doi.org/10.1038/srep18666

Yin, H., Huang, T., Wang, B., Zhang, Y., Hu, J., Zhu, L., & Chen, K. (2025). Dissolved organic matter sources in urban outfall water before and during rainfall, indicated via its fluorescence fingerprinting. *Applied Geochemistry*, 106447. https://doi.org/10.1016/j.apgeochem.2025.106447

Zhang, H., Zeng, C., Zhang, X., Wang, X., & Li, K. (2025). Differential responses and adaptive mechanisms of diatoms and dinoflagellates to changes in dissolved organic nitrogen components. *Harmful Algae*, 150, 103005. https://doi.org/10.1016/j.hal.2025.103005

Supplementary Table 4.1 Ambient environmental conditions measured during sampling periods before and after Hurricane Idalia, after Hurricane Helene, and after Hurricane Milton. Environmental parameters include water temperature (˚C), salinity, ammonium (NH_4^+, µM), nitrate (NO_3^-, µM), dissolved organic carbon (DOC, µM), chromophoric dissolved organic matter (CDOM, absorption at 280 nm), and chlorophyll-*a* (Chl-*a,* µg L^{-1}).

Sample time/condition	Station	Temperature (˚C)	Salinity	NH_4^+ µM	NO_3^- µM	DOC µM	CDOM @280 nm	Chl-*a* µg L^{-1}
Aug 23, 2023 Pre Idalia	Charlotte Harbor	29.6	23.7	1.63	<0.07	686	39.5	10.08
Sept 9. 2023 Post Idalia	Charlotte Harbor	28.8	16.0	3.41	2.56	1080	88.5	17.85
Oct. 2, 2024 Post Helene	Charlotte Harbor	29.6	5.7	4.83	14.9	1420	229.4	0.40
Nov 20, 2024 Post Milton	New Pass	22.7	33.0	3.75	0.19			4.75
Nov 20, 2024 Post Milton	Siesta Key	22.9	31.0	3.86	0.20			2.86

Supplementary Table 4.2 Phytoplankton community composition and abundance (cells L^{-1}) for samples collected post Hurricanes Debbie, Helene and Milton. "Total other" includes cryptomonads, raphidophytes, and other flagellates.

Sampling time	**Phytoplankton Groups**	**Tampa Bay (TB)**	**New Pass (NP)**	**Siesta Key (SK)**	**Caloosa-hatchee River (CR)**	**Charlotte Harbor (CH)**
Post Hurricane Debbie	*Karenia brevis*	0		0	0	0
	Dinoflagellates	8×10^4		4×10^4	3×10^4	0
	Diatoms	1.3×10^7		6.6×10^5	6×10^4	2.2×10^5
	Cyanobacteria	0		9.6×10^5	0	6.6×10^5
	Total other	2.4×10^5		6.6×10^5	1.8×10^5	2.4×10^5
Post Hurricane Helene	*Karenia brevis*		0	0		
	Dinoflagellates		4×10^4	8×10^4		
	Diatoms		4.6×10^5	5.4×10^5		
	Cyanobacteria		0	1.1×10^7		
	Total other		3×10^4	1.1×10^5		
Post Hurricane Milton (day 1)	*Karenia brevis*		4×10^5	6×10^4		
	Dinoflagellates		2×10^4	0		
	Diatoms		8×10^5	4×10^6		
	Cyanobacteria		0	7×10^5		
	Total other		4×10^4	4×10^4		

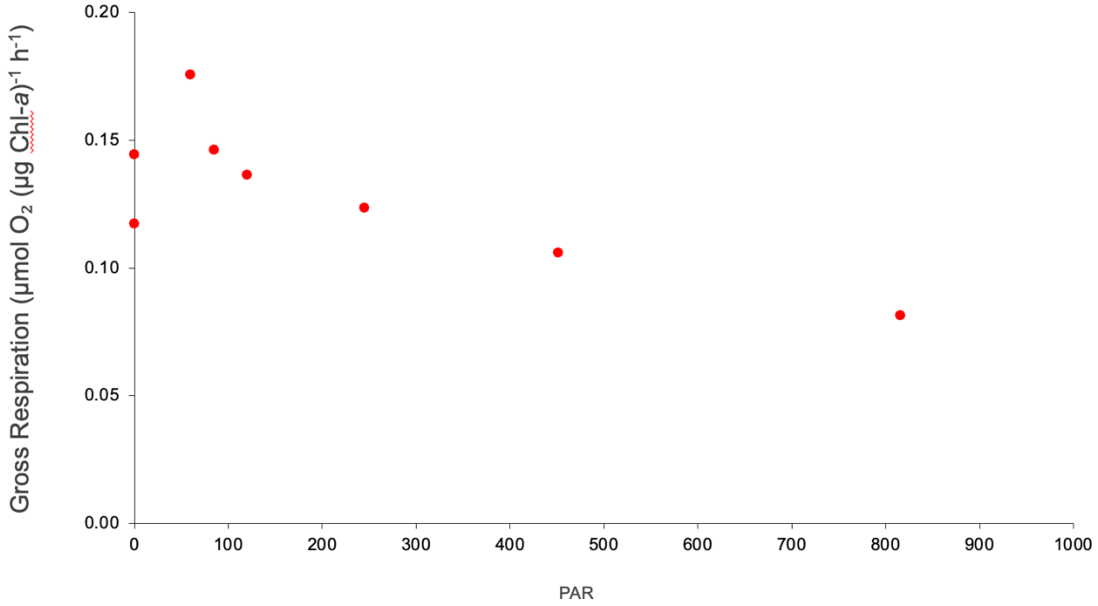

Supplementary Figure 1 Gross Respiration (µmol O_2 (µg Chl-*a*)$^{-1}$ h^{-1}) as a function of light (PAR, PAR, µmol photons m^{-2} s^{-1}) measured in surface waters following Hurricane Idalia.

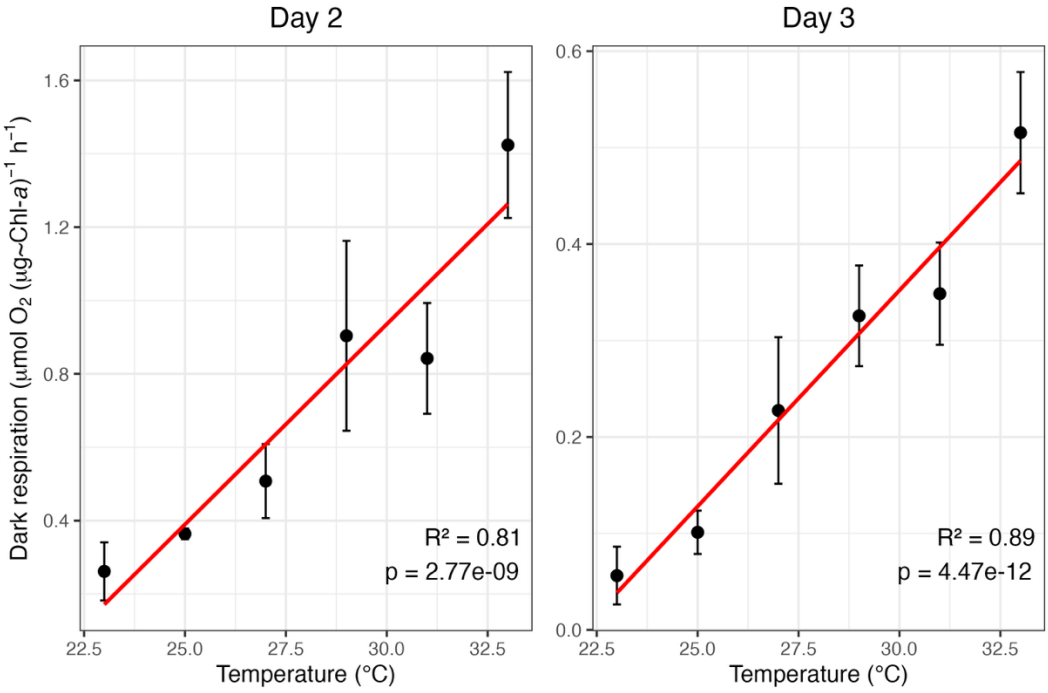

Supplementary Figure 2 Dark respiration (µmol O_2 (µg Chl-*a*)$^{-1}$ h^{-1}) across a temperature gradient (23 to 33˚C) in New Pass at Day 2 and Day 3.

Chapter 5: Influence of warming and nitrogen enrichment on photosynthesis and respiration rates during *Karenia brevis* blooms

Abstract

Warming and nutrient inputs may alter the metabolic balance of phytoplankton community and influence oxygen dynamics in coastal ecosystems. This study investigated how temperature and nitrogen form affect metabolic rates and photophysiological responses in natural phytoplankton assemblages containing *Karenia brevis* collected on the West Florida Shelf (WFS). Short-term incubations were conducted manipulating temperature and nitrogen source (NO_3^- and NH_4^+). Primary production and respiration were quantified using the $H_2{}^{18}O$ membrane-inlet mass spectrometry (MIMS) technique, while photophysiological responses were assessed using pulse-amplitude-modulation (PAM) fluorometry. Additions of NO_3^- significantly increased primary production, whereas NH_4^+-enrichment did not significantly influence those rates. In contrast, warming significantly increased respiration rates. Photophysiological measurements showed declines in electron transport rates (ETRmax) and light utilization capacity (Ek) at higher temperatures, indicating thermal stress on the photosynthetic apparatus. However, under NH_4^+-enrichment, photosynthetic parameters were higher. Together, these results demonstrate that nutrient form and temperature regulate phytoplankton metabolism. In coastal systems such as the WFS, where episodic nutrient inputs and warming waters frequently co-occur, these interactions may influence bloom persistence, metabolic balance, and the potential development of hypoxia.

Introduction

Warming and nutrient enrichment are among the major drivers of change in coastal aquatic ecosystems. The impacts of ongoing climate change on ocean systems are increasingly evident, including the global expansion of harmful algal blooms (HABs) and the intensification of coastal hypoxia (Ershadifar et al., 2020; Gobler, 2020; Glibert and Li, 2023; Brenckman et al., 2025). Elevated temperatures enhance water column stratification and, when coupled with increased inputs of inorganic and organic nutrients, can alter phytoplankton community composition and stimulate the development and persistence of HABs (Glibert et al., 2022). Occurrences of HABs have frequently been associated with oxygen depletion in coastal waters. Oxygen consumption during bloom senescence and biomass decomposition is well documented (e.g., Brush et al., 2020; Anderson et al., 2021; Oh et al., 2023). However, the direct contribution of bloom-associated respiration to deoxygenation has not been fully quantified.

Hypoxic conditions have been reported during intense *Karenia brevis* blooms (Smith, 1975; Heyl et al., 1978; Milbrandt et al., 2021; Turley et al., 2022). Toxigenic *K. brevis* is the most recurrent bloom-forming species on the West Florida Shelf (WFS), where blooms occur nearly annually and can persist for extended periods (Heil and Muni-Morgan, 2021). Despite extensive research on bloom ecology and dynamic, comparatively little attention has been given to how environmental drivers regulate the balance between photosynthetic production and respiratory oxygen consumption during *K. brevis* blooms. In particular, the combined influence of temperature, nutrient availability, and light on metabolic processes is not well established.

Both photosynthesis and respiration are sensitive to temperature because enzymatic reactions controlling carbon fixation, electron transport, and respiratory pathways are thermally regulated (Raven and Geider, 1988). While growth and photosynthetic rates may increase with

warming up to a thermal optimum, respiration typically exhibits a stronger temperature dependence. As a result, elevated temperature can shift community metabolic balance by increasing respiration disproportionately relative to gross primary production (Barton et al., 2020 and references therein). This metabolic shift has important consequences for oxygen balance in marine system, particularly in regions such as the West Florida Shelf (WFS) where seasonal hypoxia is already present.

Light availability further regulates phytoplankton metabolism. Photosynthetic responses to irradiance are classically described by the photosynthesis–irradiance (PI or PE) relationship (Platt and Jassby, 1976), characterized by a linear increase at low light, saturation at intermediate irradiance, and potential photoinhibition at high light exposure (Sakshaug et al., 1997; Behrenfeld et al., 2004; Glibert, 2024). In contrast, respiration has historically been treated as light-independent and estimated from parallel dark incubations (Jassby and Platt, 1976). However, this assumption does not account for light-dependent respiratory processes that operate concurrently with photosynthesis. Multiple pathways, including cyclic electron flow, the Mehler reaction, and photorespiration, consume oxygen in the light (Kana, 1990; Kramer and Evans, 2011). These mechanisms play critical roles in maintaining cellular redox balance and preventing photoinhibition under excess irradiance or metabolic constraint. Because these pathways divert energy away from carbon fixation, increased light-dependent respiration can reduce net production efficiency (Halsey and Jones, 2015). Despite their physiological significance, such processes remain poorly measured. Measurements of respiration in *K. brevis* have been limited largely to dark respiration (Hitchcock et al., 2010), and comparisons of how light-respiration rates respond to interacting stressors such as temperature shifts and nutrient enrichment are needed, particularly for *K. brevis*. Given that dense blooms have been associated with oxygen

depletion, understating how photosynthesis and respiratory pathways respond to environmental change is essential for understanding bloom maintenance, decline, and ecosystem oxygen dynamics.

The overarching hypothesis of this study is that climate-related changes will alter the metabolic balance of *K. brevis* in multiple ways. Elevated temperature may cause physiological stress and reduce photosynthetic performance above the species' thermal optimum, while simultaneously enhancing respiration. Increased runoff may further modify metabolic responses by supplying inorganic and organic nutrients. Interactions between nutrient availability and temperature may therefore alter the effective thermal niche of both photosynthesis and respiration, potentially facilitating persistence under warmer conditions when nutrient limitation is alleviated. In addition, different nutrient forms may differentially influence thermal responses due to distinct metabolic pathways required for assimilation.

To evaluate these hypotheses, natural assemblages collected during a *K. brevis* bloom on the WFS were exposed to short-term manipulations of temperature and nitrogen form. Primary production and respiration were quantified using two complementary approaches: oxygen-based measurements employing the $H_2{}^{18}O$–MIMS technique and photophysiological assessments using Pulse-Amplitude-Modulation (PAM) fluorometry. By integrating metabolic flux measurements with photochemical indicators, this study provides a mechanistic assessment of how warming and nutrient form influence the metabolic balance of *K. brevis* blooms and their potential contribution to hypoxia.

Methods

Sampling and environmental parameters

Samples were collected from coastal WFS waters, specifically in New Pass (Longboat Key) and in waters just off Fort Myers, in November 2024 and February 2025 respectively. After returning to the laboratory, samples were immediately filtered through GF/F and filtrates and filters were stored frozen. Chlorophyll-*a* was analyzed using high-performance liquid chromatography (HPLC, Agilent HPL) at the Horn Point Analytical Services Laboratory according to Van Heukelum and Thomas (2001). Abundance of *K. brevis* were performed in a Sedgewick-Rafter chamber (1 mL) after fixation with Lugol's solution (5%) using a Zeiss Axio Vert.A1 inverted microscope.

Experimental plan

Two types of experiments measuring primary production rates were undertaken in this study but using different approaches (Table 5.1). First type of experiments measured rates of primary production and light-dependent respiration (i.e., GR), in the natural waters across ambient and manipulated temperatures (+ 3–5˚C) and nutrient enrichment applying the $H_2{}^{18}O$ method using Membrane Inlet Mass Spectrometry (MIMS). In the second type of experiment, rates of photosynthesis were determined using Pulse-Amplitude-Modulation (PAM) across a gradient of temperature (ambient and manipulated temperatures up to + 6˚C) and nutrient enrichment.

Table 5.1 Summary of sampling efforts including the stations where water was collected and the experiments conducted for each sampling date.

Sampling date	Sampling site	Experiments
November 2024	New Pass	• Primary Production and Gross Respiration Rates + NO_3^- enrichment vs. temperature • Primary Production and Gross Respiration Rates as a function of light (PE curves) + NO_3^- vs. temperature • Rates of photosynthesis (PE curves) under a gradient of temperature
February 2025	Fort Myers	• Primary Production and Gross Respiration Rates + NH_4^+ enrichment vs. temperature • Primary Production and Gross Respiration Rates as a function of light (PE curves) + NH_4^+ and NO_3^- enrichment vs. temperature • Rates of photosynthesis (PE curves) under a gradient of temperature and NH_4^+ enrichment

Primary production and respiration rates measurements

Water samples were first screened through a 100-micron nylon mesh and enriched with approximately 1% of $H_2{}^{18}O$. To test the influence of nutrients and temperature on primary production and respiration rates, aliquots (30 – 60 mL) were enriched with 0, 1, 5, 10 μM of

NO_3^- or NH_4^+. Samples were then carefully dispensed into 3 mL screw-capped vials with Viton septa containing glass beads. The vials were incubated in custom-made "Coronatrons" (Bay Instruments LLC; Sobrinho et al. in review) under constant light and at constant temperatures (ambient temperature, +3 and +5˚C). For experiments testing the combined effects of light, temperature, and nutrients, aliquots (30 – 60 mL) were enriched with 0 or 10 μM of NO_3^- or NH_4^+ and incubated using a "Photosynthetron" (MacIntyre et al., 1996). These incubations were conducted across ten light intensities, ranging from limited to saturated intensities (up to ~1000 μmol photons m^{-2} s^{-1}) at constant temperature (ambient temperature and +3˚C).

Prior to incubation of all experiments, triplicate samples from each experiment were immediately fixed with mercuric chloride ($HgCl_2$, ~1% v/v), representing a time zero value. At the end of the incubation period, samples were removed from the incubators, fixed with $HgCl_2$ (~1% v/v), placed completely underwater in jars at room temperature until analysis (within days). Samples were analyzed by Membrane Inlet Mass Spectrometry (MIMS), and data were recorded using the software Quickdata (Bay Instruments LLC, Easton, Maryland). The GPP, NPP, and GR rates were calculated as described below according to Kana (1990), Kana et al. (1994, 2006), and Ferrón et al. (2016) and normalized by the chlorophyll-*a* (Chl-*a*) concentration of each sample.

Rates of GPP were calculated based on the change in the isotope ratio of dissolved O_2 over the incubation time (mass 34/40) (Equation 1).

$$GPP = \left(\frac{\left(\Delta[\frac{34}{40}] \times [Ar] \right)}{2 * ({}^{18}O(H_2O) + 0.002) * t} \right) \quad \textit{(Equation 1)}$$

where $\Delta 34/40$, represents the change in the isotope to Ar ratio over time, [Ar] is the solubility of Argon at the incubation temperature, $^{18}O(H_2{}^{18}O)$ is the isotope ratio of the incubation water, which is calculated based on the amount of $^{18}O(H_2{}^{18}O)$ added in the total volume of the incubation flask and the percent enrichment (98-99%) of stock ^{18}O water; 0.002 represents the natural abundance of ^{18}O; and *t* represents the incubation time. This equation provides ^{18}O-GPP in μmol O_2 h^{-1}.

Rates of NPP were determined from the net change in O_2/Ar (mass 32/40) (Equation 2).

$$NPP = \frac{\Delta 32/40 \times [Ar]}{t} \qquad \textit{(Equation 2)}$$

where $\Delta 32/40$ represents the change in the O_2/Ar over time, [Ar] is the solubility of Ar at a certain temperature, and *t* represents the incubation time. This equation provides ^{18}O-NPP in μmol O_2 h^{-1}. Then, gross O_2 uptake was determined from the difference between GPP and NPP.

Finally, GPP, NPP, and GR ratios obtained were normalized by the chlorophyll-*a* (Chl-*a)* concentration of each sample, providing μmol O_2 (μg Chl-*a*) $^{-1}$ h^{-1}.

Fluorescence Measurements

Water samples were carefully dispensed in 50 mL tubes and placed in a custom-made temperature control block with cool water circulating at one end and warm water at another, yielding a gradient of five values ranging from -5˚C to +5˚C relative to ambient temperature. Photosynthetic parameters were measured using with Phyto-PAM-II fluorometer (Heinz Walz GmbH), and the data were exported from the PhytoWin-3 Software (Heinz Walz GmbH, Effeltrich, Germany). The measurements were made at the beginning of the experiment (T0),

after approximately 22 hours (T1), and 44 hours (T2) following dark acclimation of the samples for 20 min to open the PSII reaction centers. Then, maximum quantum yield of PSII (Fv/Fm) was calculated (Equation 3).

$$F_v/F_m = \frac{F_m - F_o}{F_m} \qquad \textit{(Equation 3)}$$

where F_m is the maximal fluorescence yield and F_o the minimal fluorescence yield after dark adaptation.

Rapid light curves were fitted to the models of Platt and Jassby (1976) to calculate the initial slope of the ETR versus irradiance relationship (α), the light saturation coefficient (E_k; μmol photons m^{-2} s^{-1}), and the maximum electron transport rate (ETR_{max}; μmol electrons m^{-2} s^{-1}). All parameters were calculated and exported from the PhytoWin-3 Software (Heinz Walz GmbH, Effeltrich, Germany).

Statistical analysis

To evaluate the effects of nutrient concentrations (control, 1μM, 5μM, and 10μM; four levels), temperature (ambient temperature, +3 and +5˚C; three levels), and their interaction on primary production and respiration rates (GPP, NPP, and GR), three-way analyses of variance (ANOVA) with permutation tests were conducted using the *lmPerm* package in R (Wheeler, 2016). When significant differences among treatments were detected, post-hoc pairwise comparisons were performed using Šidák-adjusted p-values to identify specific group differences. All results were evaluated at a significance level of 0.05, and statistical analyses were conducted in R version 4.4.2 (R Core Team, 2024).

Results

November 2024

Environmental conditions

In November 2024, surface water temperature was 25˚C at New Pass. Concentrations of *K. brevis* varied from 70,000 to 90,000 cells L^{-1}. Nutrient concentrations were 0.77 µM NO_3^-, 13.35 µM NH_4^+, and 0.63 µM PO_4^{3-}.

Effects of NO_3^- addition and temperature on primary production and respiration

Primary production and respiration rates (GPP, NPP, and GR) were significantly affected by both NO_3^-enrichment and temperature (p-values < 0.001 for all parameters), but there was no significant interaction between NO_3^- concentration and temperature (Table 5.2). Rates of GPP increased with NO_3^- enrichment, with the highest rates observed at 10 µM NO_3^-, while the control exhibited lower values (Figure 5.1A). Temperature also influenced GPP, with similar rates observed at 25˚C and 28˚C, whereas significantly lower values were measured at 33˚C (Figure 5.1D). Similarly, NPP rates increased with even the smallest addition of NO_3^-, with all enriched treatments showing higher rates compared to the control (Figure 5.1B). The lowest addition of NO_3^- was sufficient to stimulate NPP, and no significant differences were observed among the enriched concentrations. Temperature had a strong effect on NPP, with the highest values observed at 25˚C and a pronounced decline at 33˚C (Figure 5.1E). Rates of GR was highest in the control treatment and decreased with NO_3^-enrichment (Figure 5.1C). In contrast, GR increased with temperature, with the highest rates observed at 33˚C (Figure 5.1F).

Table 5. 2 Three-way permutation ANOVA results, testing the effect of NO_3^- concentration (control, 1µM, 5µM, and 10µM; four levels), temperature (ambient temperature, +3 and +5˚C; three levels), and their interaction on primary production and respiration rates (GPP, NPP, and GR). df: degrees of freedom, SS: sum of squares. Bold values represent $p < 0.05$.

	df	SS	F	p-value
GPP				
Treatment	3	0.02	8.30	**0.00**
Temperature	2	0.15	68.96	**0.00**
Treatment:Temperature	6	0.00	0.32	0.91
NPP				
Treatment	3	0.47	32.49	**0.00**
Temperature	2	3.46	354.38	**0.00**
Treatment:Temperature	6	0.05	1.86	0.12
GR				
Treatment	3	0.33	26.35	**0.00**
Temperature	2	2.18	259.68	**0.00**
Treatment:Temperature	6	0.04	1.72	0.16

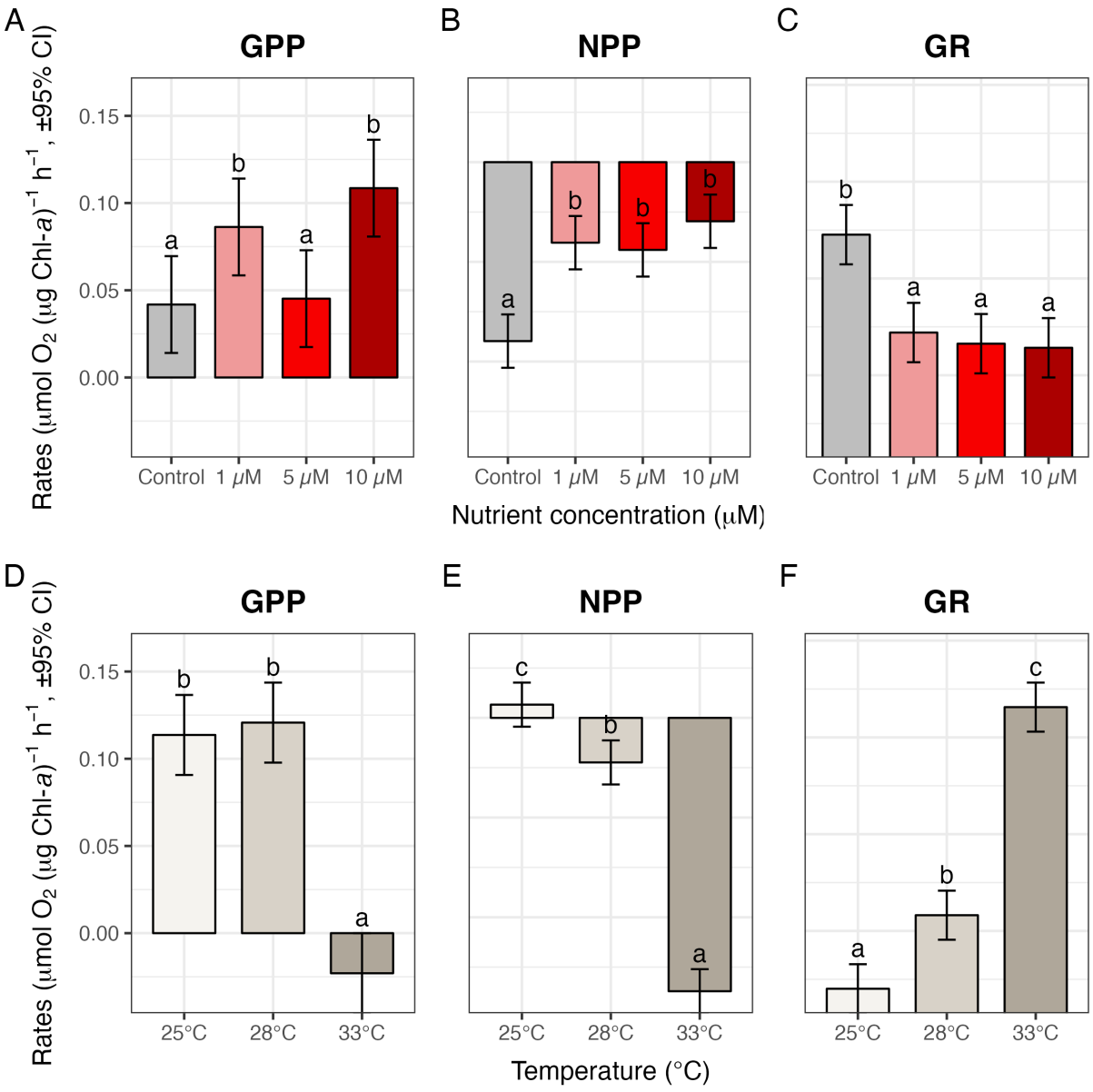

Figure 5.1 Mean gross primary production (GPP) (A, D), net primary production (NPP) (B, E), and gross respiration (GR) (C, F) of natural *Karenia brevis* exposed to short-term NO_3^- enrichment across three temperatures (25˚C, 28˚C, and 33˚C). Bars represent estimated marginal means (EMMs), corresponding to model-adjusted mean rates of GPP, NPP, and GR across replicates for each experimental treatment, ± 95% confidence intervals, derived from a three-way permutational analysis of variance (ANOVA). Different letters above the bars indicate statistically significant differences between the nutrient treatments within each specific concentration, temperature, and time point, based on Tukey-adjusted pairwise comparisons.

Photosynthesis-irradiance, nutrient and temperature response curve

Primary production and respiration rates varied across light intensity, temperature, and nutrient treatments (Figure 5.2). In the control treatment at 22˚C, GR was generally higher than NPP across most irradiance levels (Figure 5.2A). When NO_3^- was added, GR decreased relative to the control, while GPP increased with irradiance and reached higher values compared to the control treatment (Figure 5.2B). At the higher temperature (27˚C), GR exceeded both NPP and and GPP across much of the light gradient (Figure 5.2C, D).

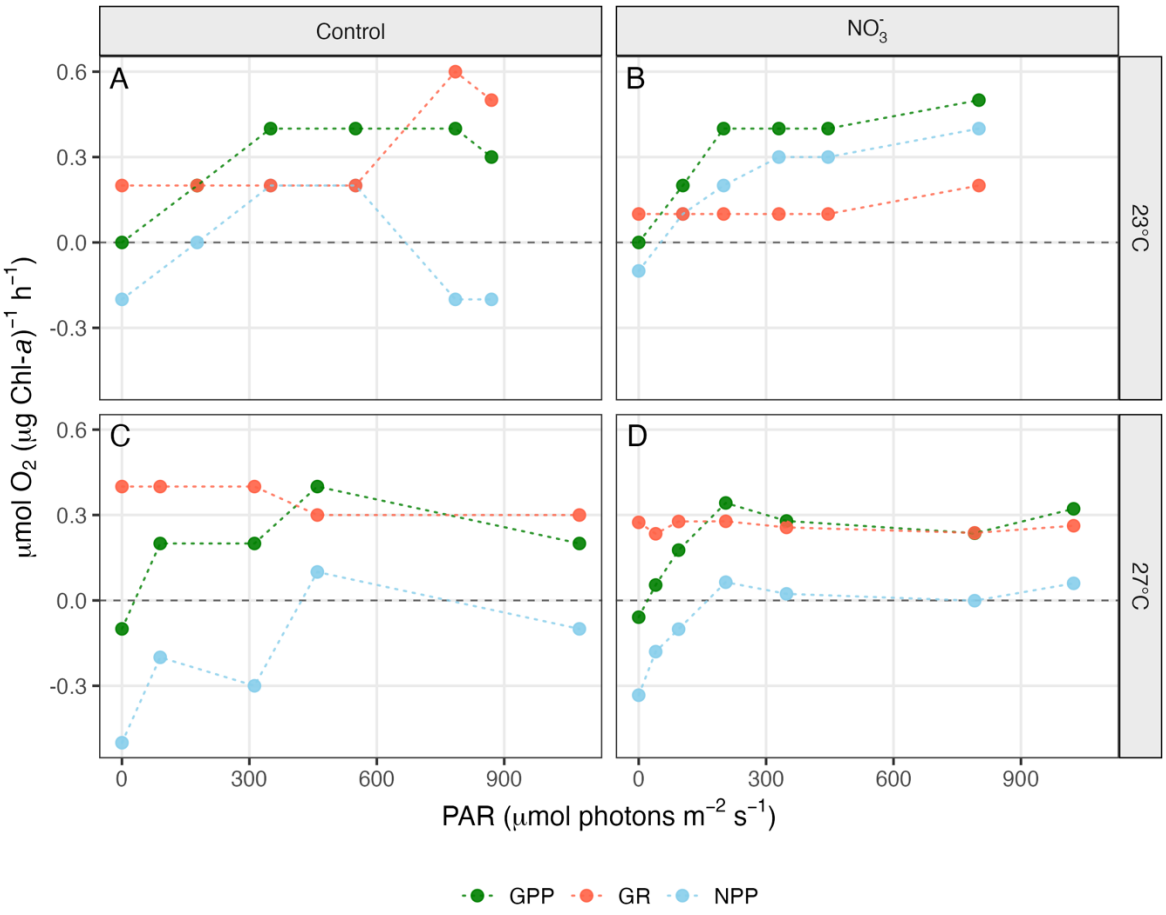

Figure 5.2 Photosynthesis-Irradiance curves of gross primary production (GPP), net primary production (NPP), and gross respiration (GR) measured under control conditions (A, C) and with NO_3^-enrichment (B, D) at two temperatures (23˚C and 27˚C).

Effects of temperature on photosynthetic parameter

Maximum quantum yield (Fv/Fm) varied discretely across temperatures and time sampling (Figure 5.3A). The initial slope of (α) slightly increased with temperature and it was higher at 47h in comparison with 22.5h (Figure 5.3B). The light saturation parameter (Ek) decreased with increasing temperature across treatments (Figure 5. 3C). Highest Ek values were observed at 20 – 22˚C, particularly for 22.5h. Maximum electron transport rates (ETRmax) was higher at intermediate temperatures (22–25˚C) (Fig. 5.3D), especially at 22.5h. At temperature higher than 28˚C, ETRmax declined across treatments (Figure 5.3D).

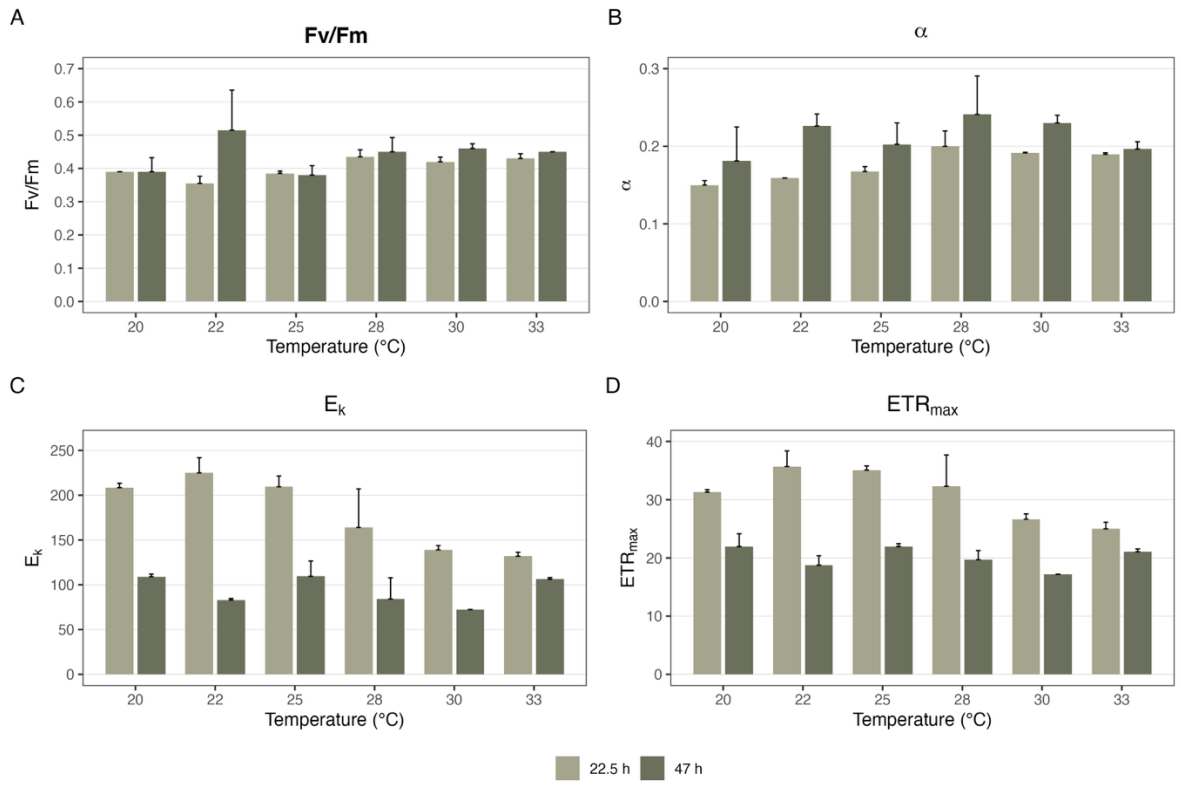

Figure 5.3 Photophysiological responses of natural water with *Karenia brevis* across a temperature gradient (20–33˚C) measured at three times (T0, T22.5h, and T47h) in November 2024 at New Pass. Panels show (A) maximum quantum yield of PSII (Fv/Fm), (B) initial slope of the photosynthesis–irradiance curve (α), (C) light saturation parameter (Ek), and (D) maximum electron transport rate (ETRmax). Bars represent mean ± SD.

February 2025

Environmental conditions

In February 2025, surface water temperature was 21˚C at Fort Myers. *K. brevis* was present at concentrations around 100,000 cells L^{-1}. Nutrient concentrations were 1.29 µM NO_3^-, 3.55 µM NH_4^+, and 1.21 µM PO_4^{3-}.

Effects of NH_4^+ addition and temperature on primary production and respiration

Primary production and respiration rates (GPP, NPP, and GR) were not significantly affected by NH_4^+ enrichment, temperature, or their interaction (Table 5.3). For GPP, neither NH_4^+concentration (p-value = 0.12) nor temperature (p-value = 0.30) showed significant effects, and no interaction between these factors was detected (p-value = 0.73). Rates of GPP remained relatively similar across all NH_4^+ treatments, with no statistically significant differences among concentrations or temperatures (Figure 5.4A,D). Although some variability was observed, GPP showed a slight initial increase following NH_4^+ addition.

Similarly, NPP did not vary significantly across NH_4^+ treatments (p-value = 0.64), temperature levels (p-value = 0.94), or their interaction (p-value = 0.70). Rates of NPP exhibited substantial variability among replicates but did not show consistent trends across nutrient concentrations or temperature treatments (Figure 5.4B,E). Rates of GR also remained statistically similar across NH_4^+ concentrations (p-value = 0.73) and temperature treatments (p-value = 0.88), with no significant interaction between factors (p-value = 0.52). The values observed for GR

were statistically similar among NH_4^+ treatments and across temperatures (Figure 5.4C,F), although rates tended to be lower under NH_4^+ enrichment.

Table 5.3 Three-way permutation ANOVA results, testing the effect of NH_4^+ concentration (control, 1μM, 5μM, and 10μM; four levels), temperature (ambient temperature, +3 and +5˚C; three levels), and their interaction on primary production and respiration rates (GPP, NPP, and GR). df: degrees of freedom, SS: sum of squares. Bold values represent $p < 0.05$.

	df	SS	F	p-value
GPP				
Treatment	3	0.01	1.97	0.12
Temperature	2	0.00	1.29	0.30
Treatment:Temperature	6	0.01	0.60	0.73
NPP				
Treatment	3	0.10	0.57	0.64
Temperature	2	0.00	0.05	0.94
Treatment:Temperature	6	0.23	0.64	0.70
GR				
Treatment	3	0.05	0.43	0.73
Temperature	2	0.00	0.11	0.88
Treatment:Temperature	6	0.21	0.90	0.52

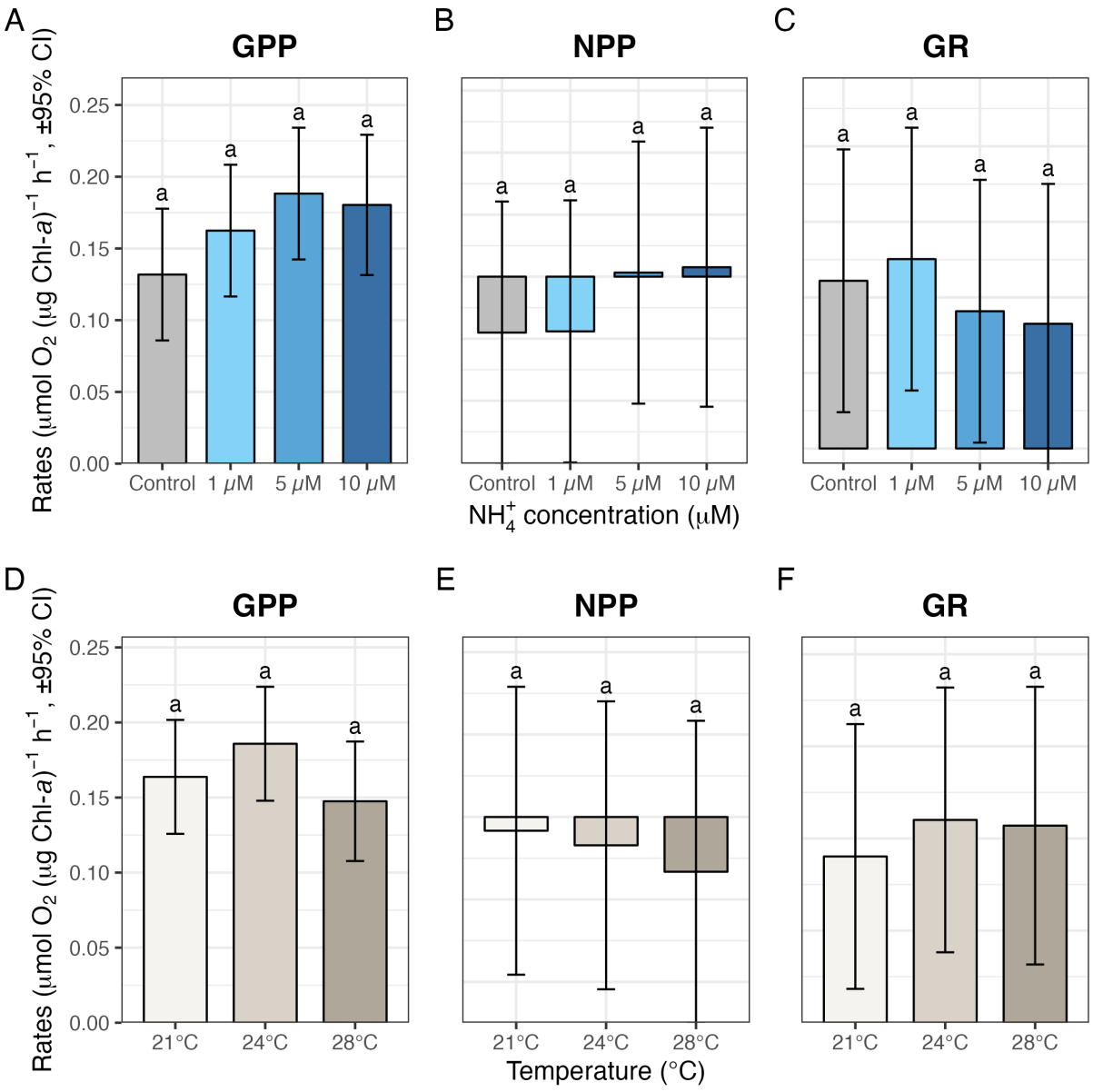

Figure 5.4 Gross primary production (GPP), net primary production (NPP), and gross respiration (GR) of natural *Karenia brevis* exposed to short-term nitrate enrichment across three temperatures (21˚C, 24˚C, and 28˚C). Bars represent estimated marginal means (EMMs), corresponding to model-adjusted mean rates of GPP, NPP, and GR across replicates for each experimental treatment, ± 95% confidence intervals, derived from a three-way permutational analysis of variance (ANOVA). Different letters above the bars indicate statistically significant differences between the nutrient treatments within each specific concentration, temperature, and time point, based on Tukey-adjusted pairwise comparisons.

Photosynthesis-irradiance, nutrient and temperature response curve

Primary production and respiration rates varied across irradiance levels and nutrient treatments (Figure 5.5). In the control treatment, GR increased with irradiance and remained higher than both GPP and NPP across most light levels. GPP increased moderately with light, while NPP remained negative throughout the irradiance range (Figure 5.5A). In the NH_4^+ treatment, both GPP and GR increased with irradiance. GR remained higher than GPP at most light levels, and NPP decreased at higher irradiances (Figure 5.5B). In the NO_3^- treatment, GPP and GR also increased with light. NPP was generally negative but slightly higher at intermediate irradiances (Figure 5.5C). Both NH_4^+ and NO_3^- additions reduced respiration rates relative to the control treatment.

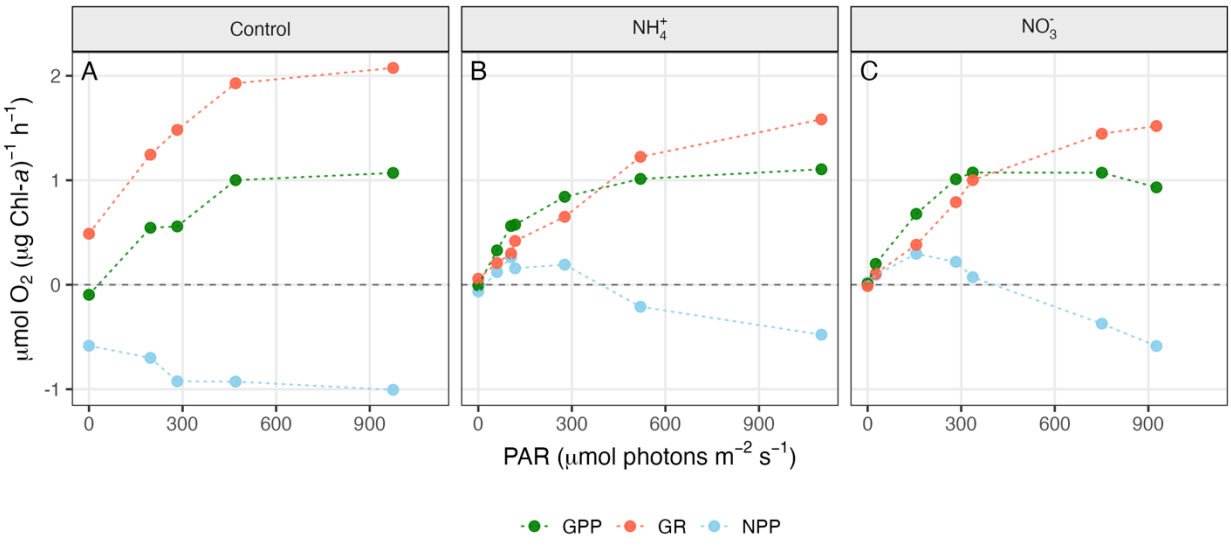

Figure 5. 5 Photosynthesis-Irradiance curves of gross primary production (GPP), net primary production (NPP), and gross respiration (GR) measured under control conditions (A) and with NH_4^+ (B) and NO_3^- (C) enrichment at ambient temperature (21˚C) during sampling in February, 2025. Points represent measured values and lines indicate fitted LOESS curves.

Effects of temperature and NH_4^+ on photosynthetic parameter

The Fv/Fm values increased from 28˚C to 33.5˚C under the control treatment at 24 h. At 48 h, values were generally lower than at 24 h across temperatures. Under NH_4^+, Fv/Fm values were generally higher at 24 h compared to the control at most temperatures (Figure 5.6A).

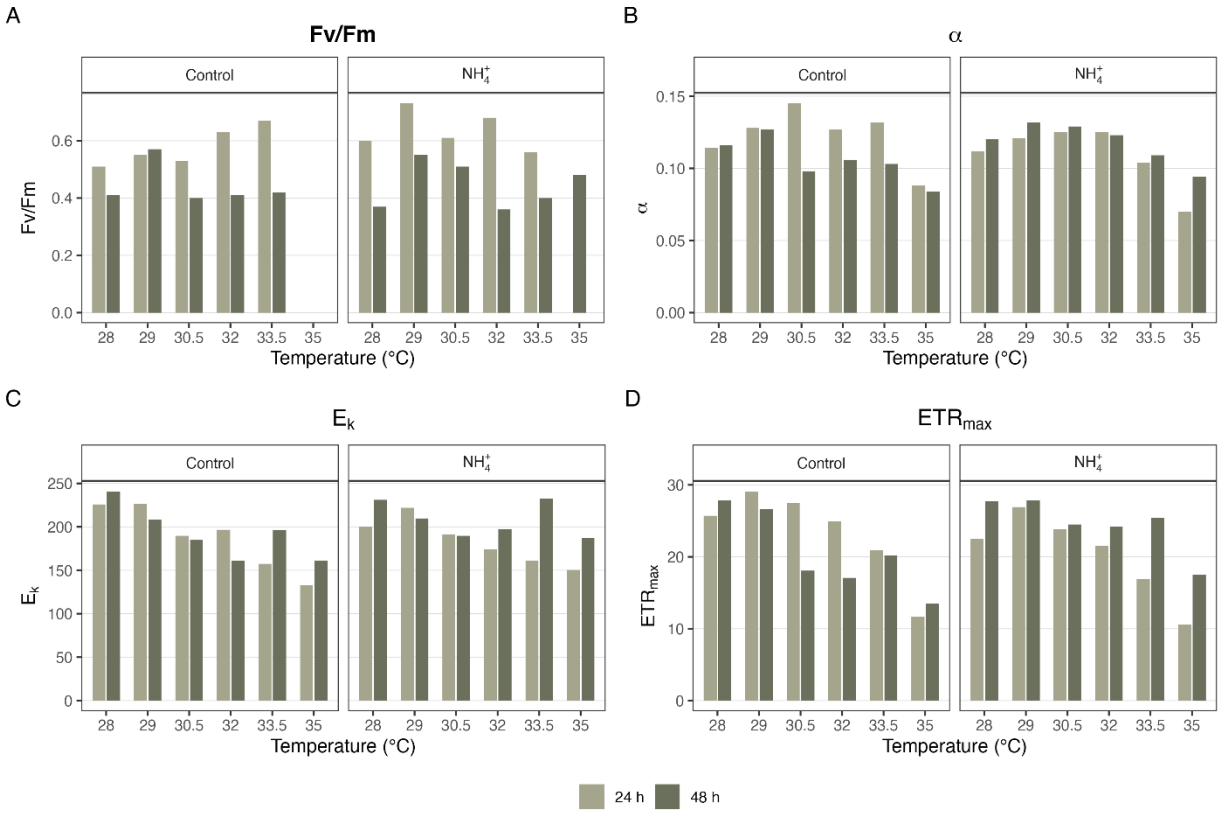

Figure 5.6 Photophysiological responses of natural water with *Karenia brevis* exposed to increasing temperature (28–35˚C) under control and NH_4^+-enrichment conditions. Panels show (A) maximum quantum yield of PSII (Fv/Fm), (B) initial slope of the photosynthesis–irradiance curve (α), (C) light saturation parameter (Ek), and (D) maximum electron transport rate (ETRmax). Bars represent measurements after 24 h and 48 h incubations.

The initial slope (α) showed moderate variability with temperature. In the control treatment, α increased from 28˚C to 30.5˚C at 24 h and declined at 35˚C. Under NH_4^+, α

remained relatively stable across 28–33.5˚C at 24 h, with a decline observed at 35˚C. At 48 h, α values were generally reduced at higher temperatures in both treatments (Figure 5.6B). Values of Ek decreased progressively with increasing temperature in the control treatment, particularly at 48 h. Under NH_4^+enrichment, Ek values were higher than in the control, especially at 33.5˚C and 35˚C at 48h (Figure 5.6C). The ETRmax declined with increasing temperature in both treatments. In the control, ETRmax was highest at 28–29˚C and decreased substantially at 35˚C. Under NH_4^+, ETRmax was generally higher than in the control across temperatures, especially at 48 h (Figure 5.6D).

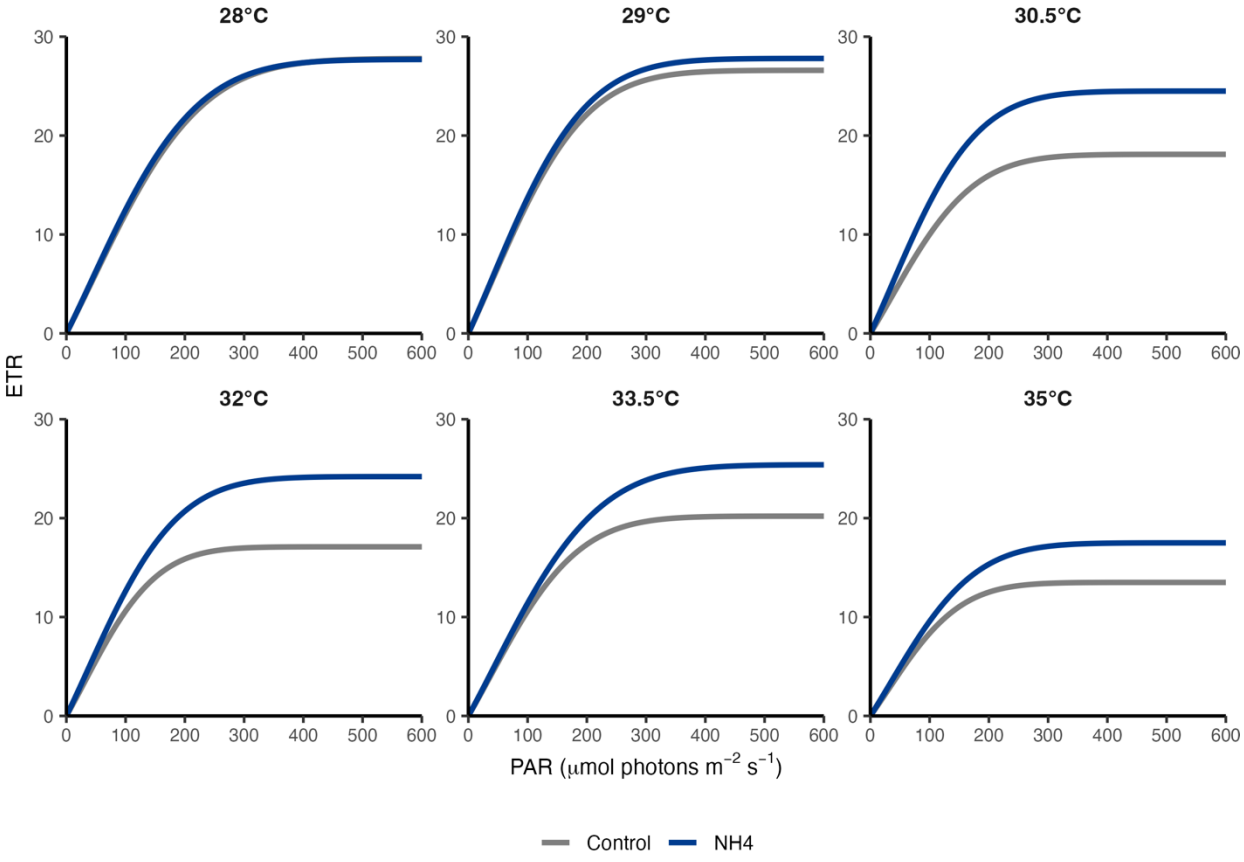

Figure 5.7 Idealized photosynthesis–irradiance (PE) curves derived from fitted photophysiological parameters across temperatures (28–35˚C) under control (grey) and NH_4^+ (blue) conditions at 48 h.

Consistent with these patterns, PE curves showed a clear decline in photosynthetic performance with increasing temperature. However, NH_4^+ enrichment partially mitigated these negative effects, allowing cells to maintain higher ETR rates and overall photosynthetic performance under thermal stress conditions (Figure 5.7).

Discussion

This study evaluated how temperature and nutrient enrichment influence metabolic rates and photophysiological responses in natural phytoplankton communities containing *K. brevis* using different approaches. Results indicated that NO_3^--enrichment significantly enhanced primary production and decreased GR, while warming increased respiration relative to production. In contrast, NH_4^+-enrichment did not significantly alter metabolic rates under the experimental conditions tested, despite minor and variable responses, including a slight initial increase in GPP and a tendency toward lower GR rates. Photophysiological parameters indicated that temperature exerted an important influence on photosynthetic performance, with declines in several metrics observed at the highest temperatures. Together, these results suggest that nutrient form and temperature play an important role in regulating plankton metabolism through distinct physiological pathways.

Nutrient effects on primary production and respiration

Additions of NO_3^- significantly increased both GPP and NPP in the natural plankton assemblages containing *K. brevis*. The P-E curves provided additional insight into how nutrients regulate metabolic balance. In the control treatment, respiration rates were generally higher than NPP across most irradiance levels, suggesting that respiration represented a substantial metabolic

loss under nutrient-limited conditions. When NO_3^- was added, GR decreased relative to the control while NPP increased, indicating that nutrient enrichment enhanced photosynthetic performance and improved the balance between production and respiration.

Nutrient availability and nutrient form are well known to influence phytoplankton production and community composition in coastal systems. Previous studies have shown that episodic inputs of NO_3^- to the WFS, such as those associated with upwelling of deeper waters, can stimulate rapid phytoplankton responses in this typically N-limited region. Intrusions of cooler, NO_3^--rich water onto the WFS have been linked to increases in Chl-*a* and phytoplankton productivity (Walsh et al., 2003). Field observations from the southwest Florida inner shelf further highlight the importance of nutrient inputs in regulating phytoplankton dynamics. Another study reported that seasonal increases in freshwater discharge from the Everglades enhance nutrient delivery to coastal waters and initiate diatom blooms during the wet season, between spring and early summer. Their results also indicated that N often represents the primary limiting nutrient for phytoplankton growth in this region (Jurado et al., 2007).

Successional patterns following large nutrient inputs have also been documented. Using a coupled hydrodynamic–biogeochemical model, Chen et al. (2023) examined phytoplankton responses to a major nutrient release in Tampa Bay. Their results showed that the rapid input of dissolved nitrogen initially stimulated rapid blooms of fast-growing phytoplankton, particularly diatoms. As nutrient concentrations declined due to rapid uptake, the system shifted toward conditions dominated by regenerated N sources such as NH_4^+ and DON. Under these conditions, slower-growing dinoflagellates, including *K. brevis*, increased in relative abundance, highlighting how changes in nutrient availability and form can drive shifts in phytoplankton community composition.

In contrast to the significantly response observed with NO_3^- additions, NH_4^+-enrichment did not significantly affect metabolic rates, with GPP, NPP, and GR remaining statistically similar across NH_4^+ concentrations and temperature treatments in this study. However, the P–E curves indicated that nutrient additions, including both NH_4^+ and NO_3^-, decreased respiration rates relative to the control treatment, suggesting that nutrient availability may alleviate metabolic stress. Field studies have shown that phytoplankton dynamics are influenced not only by nutrient availability but also by nutrient form. Moschonas et al. (2017) demonstrated that seasonal shifts in phytoplankton community composition were strongly associated with changes in nitrogen form, with different assemblages dominating under conditions characterized by higher availability of regenerated nitrogen. These findings highlight the importance of considering both inorganic and organic nitrogen pools when evaluating controls on phytoplankton productivity and community structure.

In nearshore waters of the southwest Florida shelf, Heil et al. (2007) reported low concentrations of inorganic N but elevated levels of DON in nearshore waters of the southwest Florida shelf, suggesting an important role for organic nutrient sources in supporting phytoplankton growth. Further, that study showed that phytoplankton composition shifted from dinoflagellate- and cyanobacteria-dominated communities to diatom-dominated assemblages where NO_3^- availability increased (Heil et al., 2007). These findings highlight how differences in nutrient form and availability can strongly influence phytoplankton community composition and physiological status in coastal ecosystems.

In this study, GR rates decreased with NO_3^--enrichment. Despite many studies have measured high rates of photorespiration in dinoflagellates (e.g., Hochachka and Teal, 1964; Burris, 1977; Prézelin et al., 1977; Heil, 2005; Schaeffer et al., 2007; Hitchcock et al., 2010;

Schmoker et al., 2011; López-Sandoval et al., 2014; Hansen et al., 2016; Bercel and Kranz, 2019), there are no measurements comparing photorespiration (or other respiratory pathways) under varying temperature or nutrient-enriched conditions, especially in *K. brevis*.

Most previous studies have measured community respiration, which represents respiration occurring in the dark. In coastal planktonic systems, community respiration is often closely linked to phytoplankton biomass and nutrient availability. For example, Jensen et al. (1990) reported that plankton community respiration increased along a nutrient gradient in a shallow Danish estuary and was strongly correlated with Chl-*a* concentration. Their results suggest that nutrient enrichment can stimulate both primary production and heterotrophic metabolism, as increased phytoplankton production provides organic substrates that fuel microbial respiration. In contrast, the decrease in GR observed in the present study suggests that nutrient additions may reduce respiratory processes under certain conditions, potentially reflecting reduced metabolic stress when nutrients become more available.

Temperature effects on primary production and respiration

Temperature also significantly influenced metabolic rates. While GPP and NPP declined at the highest temperature tested (33˚C), respiration increased, shifting the metabolic balance toward greater respiratory losses. This pattern is consistent with the general response of plankton communities to warming, where respiration tends to increase more rapidly than photosynthesis (Barton et al., 2020). Similar metabolic dynamics have been observed in Florida estuaries, where gross primary production and ecosystem respiration are often of similar magnitude, resulting in relatively small net production and systems operating near metabolic balance (Arriola et al.,

2025). Under these conditions, relatively small environmental changes such as light availability, nutrient supply, or organic matter inputs can shift the balance toward autotrophy or heterotrophy. Since respiration is generally more temperature-sensitive than photosynthesis, continued ocean warming may enhance respiratory processes and increase the likelihood of hypoxia development in coastal systems such as the Gulf of Mexico.

However, the response of phytoplankton metabolism to warming can also depend on nutrient availability. For example, Marañón et al. (2018) used continuous cultures of three common phytoplankton species (*Synechococcus* sp., *Skeletonema costatum*, and *Emiliania huxleyi)* to examine temperature dependence (activation energy, Ea) of metabolism under different degrees of N-limitation. They found that both CO_2 fixation and respiration increased with nitrogen availability but showed little response to temperature under N-limited conditions. This is reflected in the low activation energies for photosynthesis (Ea = 0.11 ± 0.06 eV) and respiration (Ea = 0.04 ± 0.17 eV). In contrast, under nutrient-replete conditions, growth was much more sensitive to temperature (Ea = 0.77 ± 0.06 eV). Overall, this suggests that the effect of temperature on phytoplankton metabolism depends strongly on nutrient availability, becoming more important when nutrients are not limiting. This is consistent with our results, while NO_3^- addition increased primary production, NH_4^+ did not significantly change production rates, but NH_4^+-enrichment improved photophysiological performance, with higher ETRmax and Ek under warming, suggesting that cells were better able to cope with thermal stress.

Temperature and NH_4^+ effects on photophysiological parameters

Temperature also influenced several photophysiological parameters derived from fluorescence measurements. The ETRmax was highest at intermediate temperatures and declined

substantially above 28˚C. Similarly, Ek decreased with increasing temperature, indicating a reduced capacity of the photosynthetic apparatus to utilize higher irradiance under warmer conditions. Additions of NH_4^+ appeared to partially mitigate these effects at intermediate temperatures. Under NH_4^+ treatments, Ek and ETRmax were generally higher than in the control at some temperatures, particularly after longer incubation periods. This response suggests that nutrient availability may help sustain photochemical performance under moderate warming. Similar responses have been reported for *K. brevis*, where photophysiological parameters adjust dynamically in response to combined temperature and nutrient conditions (Sobrinho et al., 2025, in review). Since NH_4^+ can be directly assimilated without the energetic cost of reduction, it may provide a readily available N source to support photosynthetic processes under elevated metabolic demand (Raven et al., 1992). However, the photophysiological response of *Karenia mikimotoi,* a species closely related to *K. brevis,* to temperature and N form can vary depending on prior thermal history (Ahn & Glibert, 2021).

Implications for plankton metabolism and bloom dynamics

Together, these results highlight the complex interactions between temperature and nutrient availability in regulating plankton metabolism. Addition of NO_3^- enhanced primary production, while warming increased respiration rates. At higher temperatures, increased respiration combined with declines in photochemical performance suggests that thermal stress may reduce the efficiency of carbon fixation in plankton communities. For coastal systems such as the WFS, where *K. brevis* blooms frequently occur, these metabolic shifts may have important ecological consequences. Episodic nutrient inputs may stimulate photosynthetic activity, while increasing temperatures associated with climate change may enhance respiratory processes and

alter the balance between autotrophy and heterotrophy. Understanding how these factors interact to regulate phytoplankton metabolism is therefore critical for predicting how coastal ecosystems may be shaped in a changing ocean.

The trends observed in these experiments suggest that even modest increases in temperature may shift plankton communities toward a more heterotrophic state, particularly when combined with storm-driven inputs of organic matter. In the experiments herein, respiration frequently exceeded production, indicating that warming may increase the likelihood of hypoxia development on the WFS. Hypoxic conditions have previously been associated with *K. brevis* blooms in this region (Smith, 1975; Heyl et al., 1978; Milbrandt et al., 2021; Turley et al., 2022). Although *K. brevis* blooms typically occur from late summer to early spring (Heil and Muni-Morgan, 2021), they can occasionally persist into summer even when temperatures exceed their optimal growth range (22–28 ˚C). This persistence suggests that temperatures above 30˚C do not necessarily suppress blooms, as *K. brevis* can acclimate to thermal conditions and adjust its physiological responses depending on environmental history and N availability (Ahn and Glibert, 2021; Ahn et al., 2023).

Despite the ecological importance of these processes, studies examining respiration in the light under interacting environmental stressors remain limited. Comparisons of how light-dependent respiration responds to combined drivers such as warming and nutrient enrichment are essential, particularly for bloom-forming species such as *K. brevis*. In that dense blooms have been associated with oxygen depletion, understanding how photosynthetic and respiratory pathways respond to environmental change is essential for predicting bloom persistence, decline, and broader ecosystem oxygen dynamics.

Conclusion

This study demonstrated that nutrient form and temperature play distinct roles in regulating metabolic and photophysiological responses in natural phytoplankton communities containing *K. brevis*. Addition of NO_3^- stimulated primary production and decreased respiration rates, while NH_4^+ enrichment did not significantly alter metabolic rates under the experimental conditions tested. In contrast, warming increased respiration relative to production and reduced photochemical performance at higher temperatures, indicating that thermal stress can shift plankton metabolism toward greater respiratory losses. These findings highlight the importance of investigating both nutrient form and temperature on phytoplankton metabolism. In regions such as the WFS, where episodic nutrient inputs and warming waters frequently occur, these environmental drivers may alter the balance between autotrophy and heterotrophy, with potential consequences for bloom dynamics and development of hypoxia conditions. As respiration in the light remains poorly understood, further studies examining how metabolic pathways respond to interacting stressors such as warming and nutrient enrichment will be critical for improving predictions of harmful algal bloom persistence and ecosystem oxygen dynamics in a changing ocean.

References

Ahn, S. H., & Glibert, P. M. (2021). Shining light on photosynthesis in the harmful dinoflagellate *Karenia mikimotoi*: Responses to short-term changes in temperature, nitrogen form, and availability. *Phycology, 2*(1), 30–44. https://doi.org/10.3390/phycology2010002

Ahn, S. H., Glibert, P. M., & Heil, C. A. (2023). In hot water: Interactions of temperature, nitrogen form and availability and photosynthetic and nitrogen uptake responses in natural

Karenia brevis populations. *Harmful Algae, 129*, 102519. https://doi.org/10.1016/j.hal.2023.102519

Anderson, D. M., Fensin, E., Gobler, C. J., Hoeglund, A. E., Hubbard, K. A., Kulis, D. M., et al. (2021). Marine harmful algal blooms (HABs) in the United States: History, current status and future trends. *Harmful Algae, 102*, 101975. https://doi.org/10.1016/j.hal.2021.101975

Arriola, J. M., Najjar, R. G., Briceño, H., Hu, C., Herrmann, M., & Beck, M. W. (2025). Ecosystem metabolic rates estimated from diel oxygen measurements in two subtropical estuaries. *Estuaries and Coasts, 48*(6), 155. https://doi.org/10.1007/s12237-025-01597-y

Barton, S., Jenkins, J., Buckling, A., Schaum, C. E., Smirnoff, N., Raven, J. A., & Yvon-Durocher, G. (2020). Evolutionary temperature compensation of carbon fixation in marine phytoplankton. *Ecology Letters, 23*(4), 722–733. https://doi.org/10.1111/ele.13469

Behrenfeld, M. J., Prasil, O., Babin, M., & Bruyant, F. (2004). In search of a physiological basis for covariations in light-limited and light-saturated photosynthesis. *Journal of Phycology, 40*(1), 4–25. https://doi.org/10.1046/j.1529-8817.2004.03083.x

Bercel, T. L., & Kranz, S. A. (2019). Insights into carbon acquisition and photosynthesis in *Karenia brevis* under a range of CO_2 concentrations. *Progress in Oceanography, 172*, 65–76. https://doi.org/10.1016/j.pocean.2019.01.011

Brenckman, C. M., Parameswarappa Jayalakshmamma, M., Pennock, W. H., Ashraf, F., & Borgaonkar, A. D. (2025). A review of harmful algal blooms: Causes, effects, monitoring, and prevention methods. *Water, 17*(13), 1980. https://doi.org/10.3390/w17131980

Brush, M. J., Giani, M., Totti, C., Testa, J. M., Faganeli, J., Ogrinc, N., et al. (2020). Eutrophication, harmful algae, oxygen depletion, and acidification. In *Coastal ecosystems in transition: A comparative analysis of the northern Adriatic and Chesapeake Bay* (pp. 75–104).

Burris, J. E. (1977). Photosynthesis, photorespiration, and dark respiration in eight species of algae. *Marine Biology, 39*, 371–379. https://doi.org/10.1007/BF00391940

Chen, Y., Li, M., Glibert, P. M., & Heil, C. A. (2023). Mu*r*Ky waters: Modeling the succession from *r* to K strategists (diatoms to dinoflagellates) following a nutrient release from a mining facility in Florida. *Limnology and Oceanography, 68*, 2288–2304. https://doi.org/10.1002/lno.12420

Ershadifar, H., Koochaknejad, E., Ghazilou, A., Kor, K., Negarestan, H., & Baskaleh, G. (2020). Response of phytoplankton assemblages to variations in environmental parameters in a subtropical bay (Chabahar Bay, Iran): Harmful algal blooms and coastal hypoxia. *Regional Studies in Marine Science, 39*, 101421. https://doi.org/10.1016/j.rsma.2020.101421

Glibert, P. M. (2024). *Phytoplankton whispering: An introduction to the physiology and ecology of microalgae*. Springer Nature. 758 pp.

Glibert, P. M., Cai, W.-J., Hall, E. R., Li, M., Main, K. L., Rose, K. A., Testa, J. M., & Vidyarathna, N. K. (2022). Stressing over the complexities of multiple stressors in marine and estuarine systems. *Ocean-Land-Atmosphere Research*, *2022*, 9787258. https://doi.org/10.34133/2022/9787258

Glibert, P. M., & Li, M. (2023). Warming, wheezing, blooming waters: Hypoxia and harmful algae. In D. Baird (Ed.), *Treatise on estuarine and coastal science* (2nd ed., pp. 401–444). Elsevier. https://doi.org/10.1016/B978-0-323-90798-9.00066-4

Gobler, C. J. (2020). Climate change and harmful algal blooms: Insights and perspective. *Harmful Algae, 91*, 101731. https://doi.org/10.1016/j.hal.2019.101731

Halsey, K. H., & Jones, B. M. (2015). Phytoplankton strategies for photosynthetic energy allocation. *Annual Review of Marine Science, 7*, 265–297. https://doi.org/10.1146/annurev-marine-010814-015813

Hansen, P. J., Ojamäe, K., Berge, T., Trampe, E. C., Nielsen, L. T., Lips, I., & Kühl, M. (2016). Photoregulation in a kleptochloroplastidic dinoflagellate, *Dinophysis acuta*. *Frontiers in Microbiology, 7*, 785. https://doi.org/10.3389/fmicb.2016.00785

Heil, C. A. (2005). Influence of humic, fulvic and hydrophilic acids on the growth, photosynthesis and respiration of the dinoflagellate *Prorocentrum minimum* (Pavillard) Schiller. *Harmful Algae, 4*(3), 603–618. https://doi.org/10.1016/j.hal.2004.08.010

Heil, C. A., & Muni-Morgan, A. L. (2021). Florida's harmful algal bloom (HAB) problem: Escalating risks to human, environmental and economic health with climate change. *Frontiers in Ecology and Evolution, 9*, 646080. https://doi.org/10.3389/fevo.2021.646080

Heil, C. A., Revilla, M., Glibert, P. M., & Murasko, S. (2007). Nutrient quality drives differential phytoplankton community composition on the southwest Florida shelf. *Limnology and Oceanography, 52*(3), 1067–1078. https://doi.org/10.4319/lo.2007.52.3.1067

Heyl, M. G., Freeberg, L. R., & Dickinson, K. D. (1978). Dissolved oxygen during *Gymnodinium breve* blooms along the Florida west coast, 1976–1978. *Journal of Environmental Science & Health, Part A, 13*(10), 725–731. https://doi.org/10.1080/10934527809374851

Hitchcock, G. L., Kirkpatrick, G., Minnett, P., & Palubok, V. (2010). Net community production and dark community respiration in a *Karenia brevis* (Davis) bloom in West Florida coastal waters, USA. *Harmful Algae, 9*(4), 351–358. https://doi.org/10.1016/j.hal.2010.01.002

Hochachka, P. W., & Teal, J. M. (1964). Respiratory metabolism in a marine dinoflagellate. *The Biological Bulletin, 126*(2), 274–281. https://doi.org/10.2307/1539525

Jensen, L. M., Sand-Jensen, K., Marcher, S., & Hansen, M. (1990). Plankton community respiration along a nutrient gradient in a shallow Danish estuary. *Marine Ecology Progress Series, 61*, 75–85.

Jurado, J. L., Hitchcock, G. L., & Ortner, P. B. (2007). Seasonal variability in nutrient and phytoplankton distributions on the southwest Florida inner shelf. *Bulletin of Marine Science, 80*(1), 21–43.

Kana, T. M. (1990). Light-dependent oxygen cycling measured by an oxygen-18 isotope dilution technique. *Marine Ecology Progress Series, 64*, 293–300. https://doi.org/10.3354/meps064293

Kramer, D. M., & Evans, J. R. (2011). The importance of energy balance in improving photosynthetic productivity. *Plant Physiology, 155*(1), 70–78. https://doi.org/10.1104/pp.110.166652

López-Sandoval, D. C., Rodríguez-Ramos, T., Cermeño, P., Sobrino, C., & Marañón, E. (2014). Photosynthesis and respiration in marine phytoplankton: Relationship with cell size, taxonomic affiliation, and growth phase. *Journal of Experimental Marine Biology and Ecology, 457*, 151–159. https://doi.org/10.1016/j.jembe.2014.04.013

MacIntyre, H. L., Geider, R. J., & McKay, R. M. (1996). Photosynthesis and regulation of Rubisco activity in net phytoplankton from Delaware Bay. *Journal of Phycology, 32*(5), 718–731. https://doi.org/10.1111/j.0022-3646.1996.00718.x

Marañón, E., Lorenzo, M. P., Cermeño, P., & Mouriño-Carballido, B. (2018). Nutrient limitation suppresses the temperature dependence of phytoplankton metabolic rates. *The ISME Journal, 12*(7), 1836–1845. https://doi.org/10.1038/s41396-018-0105-1

Milbrandt, E. C., Martignette, A. J., Thompson, M. A., Bartleson, R. D., Phlips, E. J., Badylak, S., & Nelson, N. G. (2021). Geospatial distribution of hypoxia associated with a *Karenia brevis* bloom. *Estuarine, Coastal and Shelf Science, 259*, 107446. https://doi.org/10.1016/j.ecss.2021.107446

Moschonas, G., Gowen, R. J., Paterson, R. F., Mitchell, E., Stewart, B. M., McNeill, S., ... & Davidson, K. (2017). Nitrogen dynamics and phytoplankton community structure: The role of organic nutrients. *Biogeochemistry, 134*(1), 125–145. https://doi.org/10.1007/s10533-017-0351-8

Oh, J. W., Pushparaj, S. S. C., Muthu, M., & Gopal, J. (2023). Review of harmful algal blooms (HABs) causing marine fish kills: Toxicity and mitigation. *Plants, 12*(23), 3936. https://doi.org/10.3390/plants12233936

Platt, T., & Jassby, A. D. (1976). The relationship between photosynthesis and light for natural assemblages of coastal marine phytoplankton. *Journal of Phycology, 12*(4), 421–430. https://doi.org/10.1111/j.1529-8817.1976.tb02866.x

Prézelin, B. B., Meeson, B. W., & Sweeney, B. M. (1977). Characterization of photosynthetic rhythms in marine dinoflagellates: I. Pigmentation, photosynthetic capacity and respiration. *Plant Physiology, 60*(3), 384–387. https://doi.org/10.1104/pp.60.3.384

Raven, J. A., & Geider, R. J. (1988). Temperature and algal growth. *New Phytologist, 110*(4), 441–461. https://doi.org/10.1111/j.1469-8137.1988.tb00282.x

Raven, J. A., Wollenweber, B., & Handley, L. L. (1992). A comparison of ammonium and nitrate as nitrogen sources for photolithotrophs. *New Phytologist, 121*(1), 19–32. https://doi.org/10.1111/j.1469-8137.1992.tb01088.x

Sakshaug, E., Bricaud, A., Dandonneau, Y., Falkowski, P. G., Kiefer, D. A., Legendre, L., & Takahashi, M. (1997). Parameters of photosynthesis: Definitions, theory and interpretation of results. *Journal of Plankton Research, 19*(11), 1637–1670. https://doi.org/10.1093/plankt/19.11.1637

Schaeffer, B. A., Kamykowski, D., McKay, L., Sinclair, G., & Milligan, E. J. (2007). A comparison of photoresponse among ten different *Karenia brevis* (Dinophyceae) isolates. *Journal of Phycology, 43*(4), 702–714. https://doi.org/10.1111/j.1529-8817.2007.00377.x

Schmoker, C., Thor, P., Hernández-León, S., & Hansen, B. W. (2011). Feeding, growth and metabolism of the marine heterotrophic dinoflagellate *Gyrodinium dominans*. *Aquatic Microbial Ecology, 65*(1), 65–73. https://doi.org/10.3354/ame01533

Smith, G. B. (1975). The 1971 red tide and its impact on certain reef communities in the mid-eastern Gulf of Mexico. *Environmental Letters, 9*(2), 141–152. https://doi.org/10.1080/00139307509435843

Sobrinho, B. F., Vidyarathna, N., Kana, T. M., & Glibert, P. M. Improved primary production and gross respiration measurements using the $H_2{}^{18}O$ technique with membrane inlet mass spectrometry and introduction of a small volume–uniform irradiance incubation chamber. *Manuscript submitted for publication.*

Sobrinho, B. F., Pinheiro-Silva, L., & Glibert, P. M. Interactive effects of temperature, nitrogen form, and humic substances on photosynthetic performance of the toxigenic dinoflagellate, *Karenia brevis*. *Manuscript submitted for publication.*

Turley, B. D., Karnauskas, M., Campbell, M. D., Hanisko, D. S., & Kelble, C. R. (2022). Relationships between blooms of *Karenia brevis* and hypoxia across the West Florida Shelf. *Harmful Algae, 114*, 102223. https://doi.org/10.1016/j.hal.2022.102223

Van Heukelem, L., & Thomas, C. S. (2001). Computer-assisted high-performance liquid chromatography method development with applications to the isolation and analysis of phytoplankton pigments. *Journal of Chromatography A, 910*(1), 31–49. https://doi.org/10.1016/S0378-4347(00)00603-4

Walsh, J. J., Weisberg, R. H., Dieterle, D. A., He, R., Darrow, B. P., Jolliff, J. K., ... & Muller-Karger, F. E. (2003). Phytoplankton response to intrusions of slope water on the West Florida Shelf: Models and observations. *Journal of Geophysical Research: Oceans, 108*(C6). https://doi.org/10.1029/2002JC001406

Wheeler, R. E., & Torchiano, M. (2016). Permutation tests for linear models in R. *The Comprehensive R Archive Network*.

Chapter 6: Interactive effects of temperature, nitrogen form, and humic substances on photosynthetic performance of the toxigenic dinoflagellate, *Karenia brevis*[4]

Abstract

Blooms of *Karenia brevis* are frequent on the West Florida Shelf (WFS) and have increased in duration and severity in recent years with changes in climate, including temperature and with changes in land based nutrient input associated with altered river flow and precipitation. A key question is how rapid changes in temperature and nutrient availability may alter photosynthetic performance of this bloom taxa, as might be experienced following a weather or storm event. This study tested the hypothesis that *K. brevis* photosynthetic efficiency can exceed its thermal optimum when nutrient limitation is alleviated, and that photosynthetic responses differ according to the type of nutrient supplied. Experiments were conducted with exponentially growing cultures adapted to 27˚C exposed to three temperatures (24, 27, and 30˚C) and five levels of enrichments: nitrate (NO_3^-), ammonium (NH_4^+), and humic acids (HA) exposed for up to 10 hrs. The photosynthetic response (Fv/Fm, α, Ek, and ETRmax) was evaluated using PAM fluorometry. Strong interactive effects were observed among temperature, nutrient type, and exposure time. Both NO_3^- and HA supported stable photosynthetic performance at the two lower temperatures for the full time course, while NH_4^+ initially enhanced photosynthetic efficiency but led to declines in Fv/Fm and ETRmax with increased exposure time. These findings demonstrate that *K. brevis* exhibits physiological plasticity that possibly contributes to bloom persistence under variable environmental conditions.

[4] **Sobrinho, B. F.**; Pinheiro-Silva, L; Glibert, P.M. Interactive effects of temperature, nitrogen form, and humic substances on photosynthetic performance of the toxigenic dinoflagellate, *Karenia brevis. Submitted to Harmful Algae*.

Introduction

The toxigenic dinoflagellate *Karenia brevis* is the most frequent and most studied bloom-forming species found on the Western Florida Shelf (WFS). Their blooms generally originate offshore (up to 65 km) in oligotrophic waters, and then the cells are transported nearshore to nutrient-enriched waters (Steidinger, 1975; Heil et al., 2014; Weisberg et al., 2016; O'Neil et al., 2024). Once near the coast, river discharge and its associated nutrient delivery can play an important role in *K. brevis* blooms (Dixon and Steidinger, 2002; Brand and Compton, 2007; Medina et al., 2020, 2022; Li et al., 2021; Glibert et al., 2025). Generally, the blooms initiate in early fall (August- September) and terminate in early spring (February-April) as the cells are dispersed offshore (Heil et al., 2022). However, blooms can occasionally persist during summer, even when temperatures exceed the optimum range for growth of 22 – 28˚C (Vargo, 2009; Ahn and Glibert, 2021), indicating that values above 30˚C do not necessarily inhibit their development. A recent study conducted during an unusual, prolonged bloom in 2020 – 2021 compared photosynthetic rates between a summer *K. brevis* bloom and a more typical overwintering bloom under varying temperature and nutrient conditions, demonstrating that photosynthetic performance is influenced by thermal history, which can shift the optimal temperature window for photosynthesis (Ahn et al., 2023). We thus hypothesized that *K. brevis* photosynthetic efficiency can be maintained even when the thermal optimum for growth is exceeded if a secondary stress, i.e., nutrient limitation, is alleviated. However, different nutrient types (inorganic or organic compounds like humic acids) may influence the temperature response differently due to different physiology associated with metabolizing different nutrient forms.

Karenia brevis can use a wide array of inorganic and organic nutrients from different sources, including ingestion of prey (Glibert et al., 2009; Heil et al., 2014; Ahn et al., 2023,

2025; Ahn and Glibert, 2024). Higher nitrogen (N) affinity and uptake rates have been shown for *K. brevis* with chemically reduced inorganic N forms, such as NH_4^+, in comparison to other N forms (e.g., NO_3^-) (Vargo, 2009; Bronk et al., 2014, Killberg-Thoreson et al., 2014; Ahn et al., 2023). One of the main sources of nutrients supporting these blooms in coastal and estuarine areas comes from river flow, including the Caloosahatchee River, Peace River and Tampa Bay, (e.g., Brand and Compton, 2007; Vargo et al., 2008; Tomasko et al., 2024; Glibert et al., 2025). In addition to the inorganic nutrients delivered by runoff, organic substances such as humic acids have terrestrial origin and can be an important source of N for *K. brev*is (Vargo et al., 2008; Killberg-Thoreson et al., 2014). However, only a few studies have investigated the influence of humic compounds in this species (Heil, 2005, See et al., 2006). During a nearshore *K. brevis* bloom, Mendoza et al. (2012) detected humic-like components on the fluorescent fraction of DOM (FDOM), suggesting that the contributions of terrestrial organic matter may sustain blooms. Moreover, stormwater inputs provide labile DOM predominantly in the form of allochthonous humic substances and dissolved organic nitrogen (DON) supporting *K. brevis* growth (Muni-Morgan et al., 2024).

Quantifying photosynthetic rates under varying conditions is therefore critical to understanding *K. brevis* physiological adaptations during blooms on the WFS. Evaluating short-term changes in these rates provides valuable insights into how blooms can develop and persist under extreme conditions, such as temperatures above the species' growth optimum during summer. To test this, the photosynthetic performance in *K. brevis* was analyzed in response to short-term exposures (~10 h) to different combinations of temperature, N forms, and HA enrichment, simulating how cells may respond to environmental variability during summer

blooms and/or following pulses of organic matter and nutrient inputs associated with hurricane-driven runoff.

Materials and Methods

Algal culture and cell count

Non-axenic cultures of *K. brevis*, originally isolated from New Pass, Sarasota, Florida, USA (CCMP2228), was obtained from Mote Marine Laboratory (Sarasota, FL, USA), were grown in semi-batch cultures using L1 medium without the addition of silicate (Guillard, 1975). The culture medium was prepared with low nutrient offshore water collected from the WFS. This water was filtered through Whatman GF/F glass microfiber filters (0.7 µm pore size) and sterilized by autoclaving. Cultures were maintained under a 12 h light:12 h dark cycle at ~120 µmol photons m^{-2} s^{-1}, salinity 33, and 27 ˚C.

Experiments were conducted with exponentially growing cultures. To determine this growth phase, changes in cell abundance over time were monitored by counting cells in a Sedgewick-Rafter chamber (1 mL) after fixation with Lugol's solution (5%) using a Zeiss Axio Vert.A1 inverted microscope. The specific growth rate (µ) was calculated according to:

$$\mu = \frac{\ln X_2 - ln\, X_1}{t_2 - t_1} \qquad \textit{(Equation 1)}$$

where X_1 and X_2 represent the cell numbers at time t1 and t2, respectively.

Experimental Setup

Aliquots of the culture were separated and enriched with the following concentrations of NO_3^- and NH_4^+: 10, 20, 40, and 60 µM; and humic acids: 6, 12, 24, and 48 mg L^{-1}. Nutrient additions were intended to mimic the nutrient concentrations that can be delivered with storm or other freshwater runoff events. The humic acid used in these experiments was originally collected and isolated from the Shark River, Florida, several years prior to this study according to extraction protocols detailed in Heil (2004).

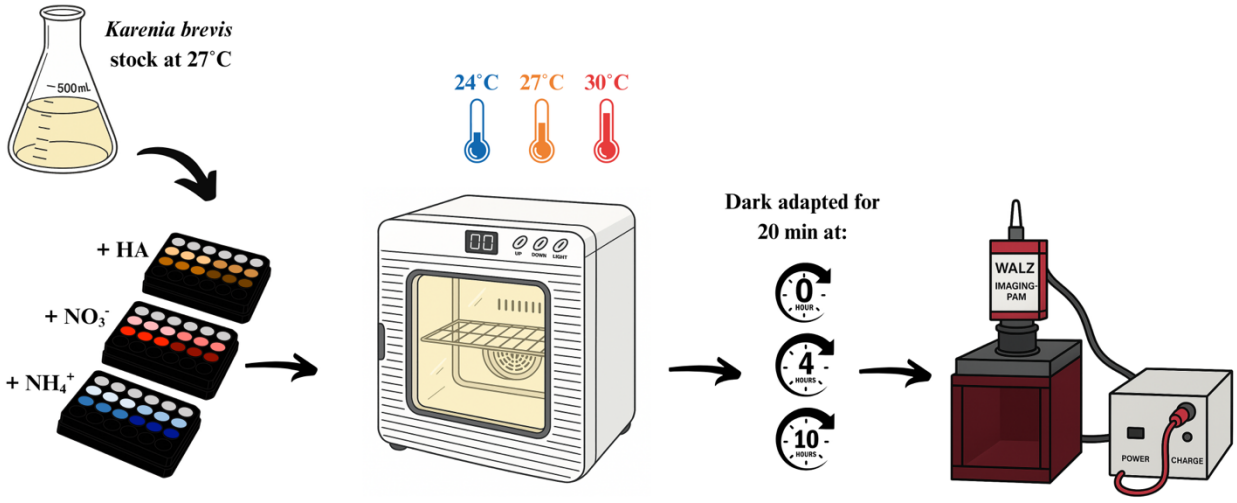

Figure 6.1 Experimental design to measure photosynthesis-irradiance (PE) response of *K. brevis* under different temperatures and nutrient forms and concentrations using a MAXI-Imaging PAM. Individual culture aliquots were held in black well plates.

Subsequently, individual wells of black multiwell plates (24 wells each) were filled with the nutrient enriched *K. brevis* cultures, and with non-enriched *K. brevis* culture as the control

condition. The plates were transferred to mini-incubators with controlled temperature (24, 27, and 30˚C) and continuous light (~120 µmol photons m^{-2} s^{-1}) for approximately 10 hours (Figure 6.1). In total, four experiments were conducted for each nutrient, two experiments comparing the responses at 24˚C and 27˚C, and two experiments comparing 27˚C and 30˚C, with three replicates for each combination of temperature and nutrient in each experiment.

Fluorescence Measurements

Measurements were made at the beginning of the experiment (T0), after approximately 4 hours (T1), and 10 hours (T2) following the dark acclimation of the black multiwell plates for 20 min to open the PSII reaction centers. Pulse-amplitude-modulated (PAM) fluorescence emission from PSII was measured using with a MAXI-Imaging PAM M-Series, and the data were exported from the ImagingWin Software (Heinz Walz GmbH, Effeltrich, Germany).

The maximum quantum yield of PSII (Fv/Fm) was quantified after a saturation pulse and calculated as:

$$F_v/F_m = \frac{F_m - F_o}{F_m} \qquad \textit{(Equation 2)}$$

where F_m is the maximal fluorescence yield and F_o the minimal fluorescence yield after dark adaptation.

Rapid light curves were run to monitor the fluorescence parameters as a function of rapid changes in irradiance (12 steps for 20s at each step: 0, 3, 23, 58, 113, 188, 283, 338, 398, 463, 533, 613, and 703 µmol photons m^{-2} s^{-1}). The electron transfer rate (ETR, µmol electrons m^{-2} s^{-1}) was calculated as:

$$ETR = YII \times PAR \times 0.5 \times 0.84 \quad \textit{(Equation 3)}$$

where YII is the quantum yield of PSII at a certain irradiance (PAR, photosynthetically active radiation) adjusted by a factor of 0.5, which considers that the absorbed light is equally distributed between the two photosystems, and the factor 0.84, which is the presumed PAR absorptivity (Genty et al. 1992). The photosynthesis-irradiance curves were fitted using the Jassby and Platt (1976) model. Using the same model, the initial slope of the ETR versus irradiance relationship (α), the light saturation coefficient (E_k; µmol photons m^{-2} s^{-1}), and the maximum electron transport rate (ETRmax; µmol electrons m^{-2} $s^{-}1$) were calculated. The models were fit using the R package 'phytotools' (Silsbe and Malkin, 2015).

Statistical analysis

To evaluate the effects of nutrient concentrations (HA, NO_3^-, NH_4^+; 15 levels–three nutrients at five concentration levels each), temperature (initial condition ± 3˚C; three levels), and their interaction on photosynthetic responses (Fv/Fm, α, E_k, ETR_{max}), multiple four-way analyses of variance (ANOVA) with permutation tests were conducted using the *lmPerm* package in R (Wheeler, 2016). A permutational ANOVA was selected since it does not rely on assumptions about underlying distributions. In this approach, the dataset is repeatedly randomized while preserving its overall structure, generating a distribution of all possible permutations of the experimental values. The resulting distribution is then compared with the original dataset to obtain the *p*-values and to determine whether the treatment effects differ from what would be expected by chance. When significant differences among groups were detected,

Tukey's HSD post-hoc tests were applied for multiple pairwise comparisons. All results were evaluated at a significance level of 0.05, and statistical analyses were conducted in R version 4.4.2 (R Core Team, 2024).

Results

Initial Cell

The specific growth rates of the initial cultures at the time of the experiment were 0.20 – 0.26 day^{-1}.

Fluorescence parameters

The maximum quantum yield of photosystem II: Fv/Fm

The maximum quantum yield of photosystem II (Fv/Fm) was significantly affected by the interaction among nutrient enrichment, nutrient concentration, and sampling time (pseudo-F = 2.25, $p = 0.004$; Table 6.1). Similarly, the interaction among temperature, nutrient enrichment, and sampling time was also significant (pseudo-F = 5.03, $p < 0.001$; Table 6.1). Overall, Fv/Fm values ranged between 0.29 and 0.48.

Table 6.1 Two-way permutation ANOVA results, testing the effect of nutrient enrichment (humic acid, NH_4^+ and NO_3^-) and their different concentrations, temperatures (24˚C, 27˚C, and 30˚C), time (T0, T1, and T2), and their interaction on Fv/Fm df: degrees of freedom, SS: sum of squares. Bold values represent $p< 0.05$.

	df	SS	F	p-value
Nutrient	2	0.07	58.05	**0.00**
Temperature	2	0.01	6.22	**0.00**
Time	2	0.40	332.09	**0.00**
Nutrient concentration	4	0.08	31.61	**0.00**
Nutrient:Temperature	4	0.01	5.56	**0.00**
Nutrient:Time	4	0.05	20.99	**0.00**
Temperature:Time	4	0.07	30.43	**0.00**
Nutrient:Nutrient concentration	8	0.03	6.46	**0.00**
Temperature:Nutrient concentration	8	0.00	0.64	0.74
Time:Nutrient concentration	8	0.01	1.50	0.15
Nutrient:Temperature:Time	8	0.02	5.03	**0.00**
Nutrient:Temperature:Nutrient Concentration	16	0.01	0.56	0.92
Nutrient:Time:Nutrient concentration	16	0.02	2.25	**0.00**
Temperature:Time:Nutrient concentration	16	0.01	0.57	0.91
Nutrient:Temperature:Time:Nutrient concentration	32	0.01	0.49	0.99
Residuals	1055	0.63		

At the beginning of the experiment (T0), no significant differences were observed among treatments (Figure 6.2a,d,g). By T1, differences among nutrient types became more apparent, particularly at 27˚C, where NH_4^+ treatments exhibited significantly lower Fv/Fm (Figure 6.2e) than the humic acid and NO_3^- treatments (Figure 6.2b,h). A similar pattern occurred at 30 ˚C, with NH_4^+-enriched cultures showing lower Fv/Fm (Figure 6.2e). By T2, the variability among treatments increased. The NO_3^- treatments consistently maintained the highest Fv/Fm (Figure 6.2i), while NH_4^+ treatment showed the lowest, especially at higher concentrations and higher temperatures (Figure 6.2f).

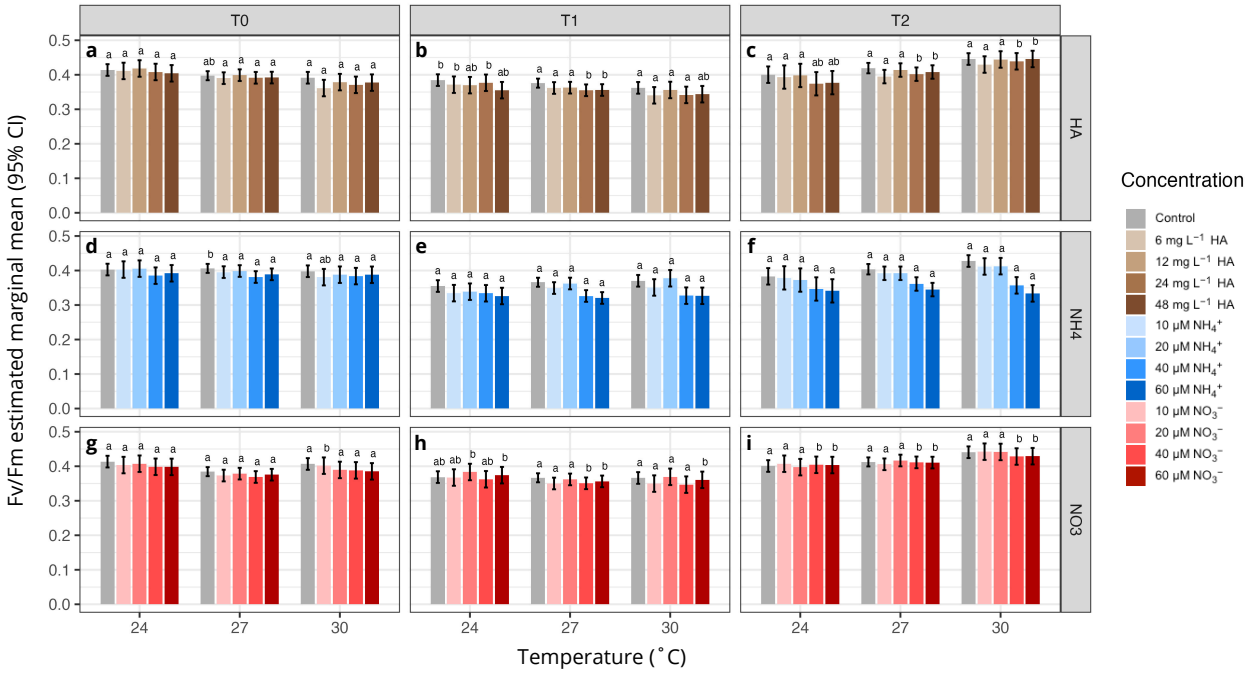

Figure 6.2 Maximum quantum yield of photosystem II (Fv/Fm) in *K. brevis* cultures grown at 27˚C and enriched with different substrates (humic acids (HA), NH_4^+, and NO_3^-), and incubated at three temperatures (24˚C, 27˚C, and 30˚C). Panels a-c represent cultures enriched with humic acids; panels d-f, cultures enriched with NH_4^+, and panels g-i, cultures enriched with NO_3^-. The gradation of color within each panel indicates enrichment concentration. Measurements were taken at the start of the experiment (T0), after ~4 h (T1), and after ~10 h (T2). Bars represent estimated marginal means (EMMs) ± 95% confidence intervals derived from a four-way permutational analysis of variance (ANOVA). Different letters above the bars indicate statistically significant differences between the nutrient treatments within each specific concentration, temperature, and time point, based on Tukey-adjusted pairwise comparisons.

Photosynthetic efficiency (α)

The photosynthetic efficiency (α) was significantly affected by the interaction among nutrient enrichment, temperature, and time (pseudo-F = 5.56, $p < 0.001$; Table 6.2), as well as by the interaction between nutrient concentration and the sampling time (pseudo-F = 2.49; $p = 0.01$; Table 6.2). Across treatments, α values ranged between 0.05 and 0.12.

Table 6.2 Two-way permutation ANOVA results, testing the effect of nutrient enrichment (humic acids, NH_4^+, and NO_3^-) and their different concentrations, temperatures (24˚C, 27˚C, and 30˚C), time (T0, T1, and T2), and their interaction on the initial slope (α). df: degrees of freedom, SS: sum of squares. Bold values represent $p < 0.05$.

	df	SS	F	p-value
Nutrient	2	0.14	297.28	**0.00**
Temperature	2	0.04	93.08	**0.00**
Time	2	0.02	34.20	**0.00**
Nutrient concentration	4	0.01	13.11	**0.00**
Nutrient:Temperature	4	0.13	139.80	**0.00**
Nutrient:Time	4	0.03	32.78	**0.00**
Temperature:Time	4	0.00	0.95	0.44
Nutrient:Nutrient concentration	8	0.01	4.79	**0.00**
Temperature:Nutrient concentration	8	0.00	1.21	0.29
Time:Nutrient concentration	8	0.00	2.49	**0.01**
Nutrient:Temperature:Time	8	0.01	5.56	**0.00**
Nutrient:Temperature:Nutrient Concentration	16	0.00	0.69	0.80
Nutrient:Time:Nutrient concentration	16	0.01	1.48	0.10
Temperature:Time:Nutrient concentration	16	0.00	0.67	0.83
Nutrient:Temperature:Time:Nutrient concentration	32	0.00	0.44	1.00
Residuals	1217	0.29		

At T0, α values were relatively similar among the control, humic acids, and NO_3^- treatments, indicating little immediate response to enrichment. In contrast, NH_4^+ treatments exhibited significantly higher α values, particularly at 27˚C and 30˚C (Figure 6.3d). By T1, differences among nutrient types began to emerge, particularly at 27˚C, where NH_4^+-enriched cultures showed significantly higher α values than the humic acid and NO_3^- treatments (Figure 6.3b,e,h). This effect became more pronounced at 30˚C, with NH_4^+ maintaining higher α values across most concentrations, while humic acid and NO_3^- remained similar to controls. At T2, the contrasts among nutrients were further accentuated. At 27˚C, NH_4^+ treatments significantly reached the highest α values (Figure 6.3f), exceeding humic acid and NO_3^- at all concentrations, which maintained lower and statistically similar means (Figure 6.3c,i). The same trend was

observed at 30˚C, where NH_4^+ sustained higher α values across all concentrations, while humic acid consistently exhibited the lowest α values. However, within the NH_4^+ treatments, α significantly declined as NH_4^+ concentrations increased (Figure 6.3f).

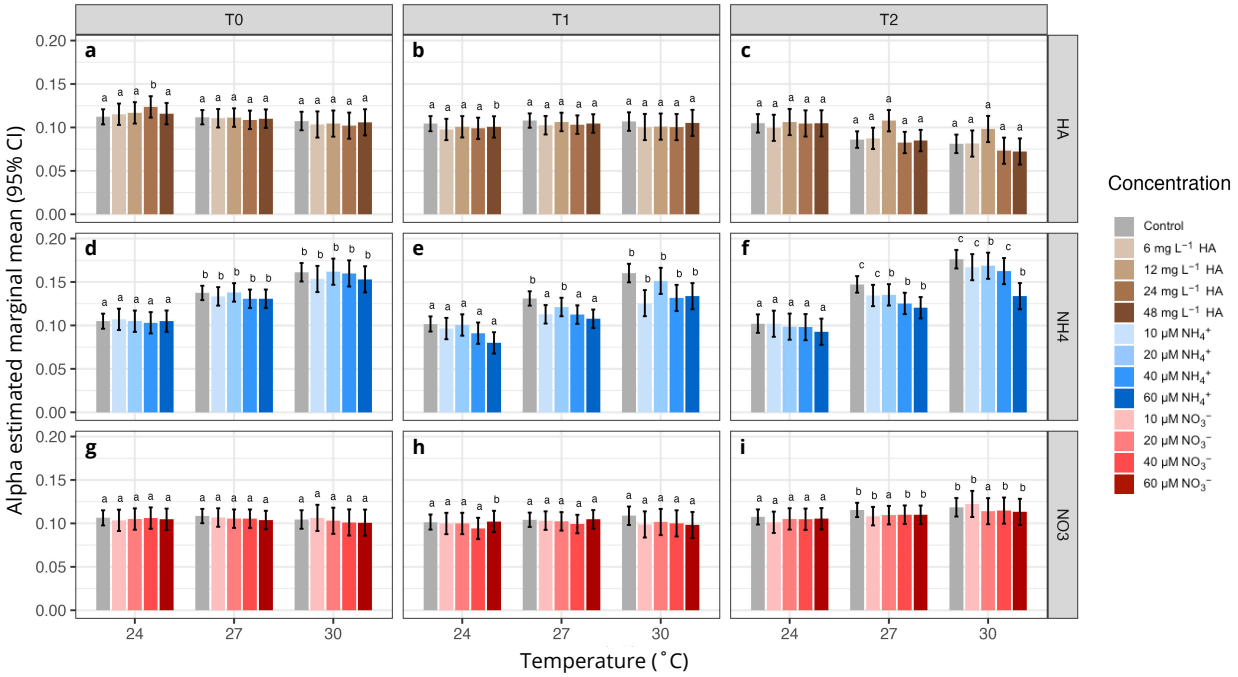

Figure 6.3 Initial slope of the photosynthesis-irradiance curve (α) in *K. brevis* cultures grown at 27˚C and enriched with humic acids (HA), ammonium (NH_4^+), and nitrate (NO_3^-) at different concentrations and incubated at three temperatures (24, 27, and 30˚C). Panels a-c represent cultures enriched with humic acids; panels d-f, cultures enriched with NH_4^+, and panels g-i, cultures enriched with NO_3^-. The gradation of color within each panel indicates enrichment concentration. Measurements were taken at the start of the experiment (T0), after ~4 h (T1), and after ~10 h (T2). Bars represent estimated marginal means (EMMs) ± 95% confidence intervals derived from a four-way permutational analysis of variance (ANOVA). Different letters above the bars indicate statistically significant differences between the nutrient treatments within each specific concentration, temperature, and time point, based on Tukey-adjusted pairwise comparisons.

Light saturation (E_k)

The light saturation values (E_k) were significantly affected by the interaction among temperature, nutrient concentration, and time (pseudo-F = 3.41, $p < 0.001$; Table 6.3), as well as by nutrient enrichment, nutrient concentration, and temperature (pseudo-F =1.70, $p = 0.04$; Table 6.3). The values ranged between ~40 and 80 µmol photons m^{-2} s^{-1} (Figure 6.4).

Table 6.3 Two-way permutation ANOVA results, testing the effect of nutrient enrichment (humic acid, NH_4^+, and NO_3^-) and their different concentrations, temperatures (24˚C, 27˚C, and 30˚C), time (T0, T1, and T2), and their interaction on the light saturation values (E_k). df: degrees of freedom, SS: sum of squares. Bold values represent p< 0.05.

	df	SS	F	p-value
Nutrient	2	38068	121.91	**0.00**
Temperature	2	9859	31.57	**0.00**
Time	2	107224	343.36	**0.00**
Nutrient concentration	4	4050	6.48	**0.00**
Nutrient:Temperature	4	7378	11.81	**0.00**
Nutrient:Time	4	4233	6.78	**0.00**
Temperature:Time	4	5885	9.42	**0.00**
Nutrient:Nutrient concentration	8	4491	3.60	**0.00**
Temperature:Nutrient concentration	8	5494	4.40	**0.00**
Time:Nutrient concentration	8	1996	1.60	0.12
Nutrient:Temperature:Time	8	6046	4.84	**0.00**
Nutrient:Temperature:Nutrient Concentration	16	4245	1.70	**0.04**
Nutrient:Time:Nutrient concentration	16	3907	1.56	0.07
Temperature:Time:Nutrient concentration	16	8510	3.41	**0.00**
Nutrient:Temperature:Time:Nutrient concentration	32	7048	1.41	0.06
Residuals	1217	190022		

At T0, E_k values were relatively similar among treatments, with no significant differences relative to the control. By T1, E_k tended to increase with rising concentrations of humic acid, particularly at 24˚C, where humic acid-enriched cultures showed significantly higher values than

NO_3^- and NH_4^+ treatments (Figure 6.4b,e,h). A similar, though less pronounced, pattern was observed under NO_3^- enrichments, whereas NH_4^+ enrichment values remained statistically comparable to control.

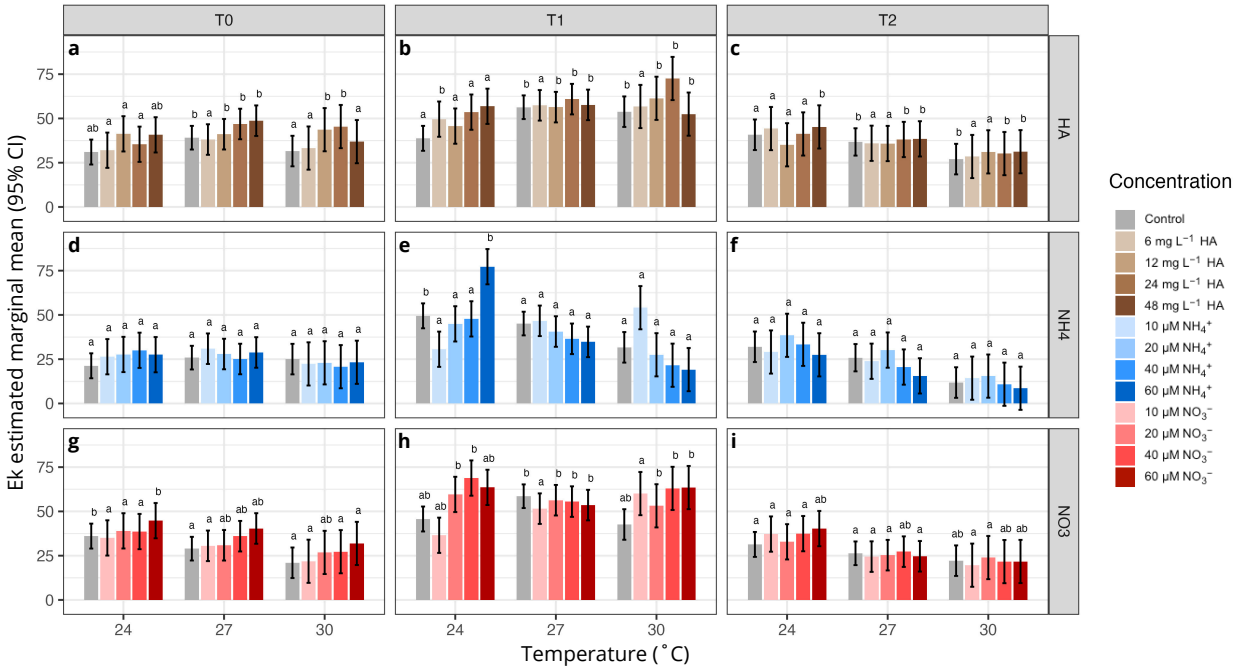

Figure 6.4 Light saturation (E_k) of *K. brevis* cultures grown at 27˚C and enriched with humic acids (HA), ammonium (NH_4^+), and nitrate (NO_3^-) at different concentrations and incubated at three temperatures (24, 27, and 30˚C). Panels a-c represent cultures enriched with humic acids; panels d-f, cultures enriched with NH_4^+, and panels g-i, cultures enriched with NO_3^-. The gradation of color within each panel indicates enrichment concentration. Measurements were taken at the start of the experiment (T0), after ~4 h (T1), and after ~10 h (T2). Bars represent estimated marginal means (EMMs) ± 95% confidence intervals derived from a four-way permutational analysis of variance (ANOVA). Different letters above the bars indicate statistically significant differences between the nutrient treatments within each specific concentration, temperature, and time point, based on Tukey-adjusted pairwise comparisons.

At 27˚C, humic acid treatments continued to exhibit slightly higher E_k values than the other nutrient treatments (Figure 6.4b), while at 30˚C, NO_3^- enrichment produced the highest E_k values, significantly exceeding those of NH_4^+ at most concentrations (Figure 6.4e,h). At T2, E_k values declined across all treatments, suggesting reduced light utilization capacity after

prolonged exposure. However, nutrient-specific patterns persisted: at 27 ˚C, humic acid treatments maintained significantly higher E_k values than the NO_3^- and NH_4^+ treatments (Figure 6.4c,f,i), while at 30˚C, NH_4^+ treatments exhibited the lowest E_k values across all concentrations (Figure 6.4f).

ETRmax

The interactions among nutrient, temperature, and time (pseudo-F = 5.35, $p < 0.001$), as well as among temperature, time, and nutrient concentration (pseudo-F = 2.67, $p < 0.001$), were significant, indicating that the combined effects of nutrient form, temperature, and time strongly influenced ETRmax responses (Table 6.4).

Table 6.4 Two-way permutation ANOVA results, testing the effect of nutrient enrichment (humic acid, NH_4^+, and NO_3^-) and their different concentrations, temperatures (24 ˚C, 27 ˚C, and 30 ˚C), time (T0, T1, and T2), and their interaction on ETRmax. df: degrees of freedom, SS: sum of squares. Bold values represent p< 0.05.

	df	SS	F	p-value
Nutrient	2	170.2	48.65	**0.00**
Temperature	2	44.3	12.66	**0.00**
Time	2	1040.0	297.28	**0.00**
Nutrient concentration	4	14.7	2.11	0.08
Nutrient:Temperature	4	20.6	2.95	**0.02**
Nutrient:Time	4	47.7	6.83	**0.00**
Temperature:Time	4	105.9	15.14	**0.00**
Nutrient:Nutrient concentration	8	95.3	6.81	**0.00**
Temperature:Nutrient concentration	8	63.6	4.55	**0.00**
Time:Nutrient concentration	8	28.0	2.00	0.04
Nutrient:Temperature:Time	8	74.8	5.35	**0.00**
Nutrient:Temperature:Nutrient Concentration	16	35.8	1.28	0.20
Nutrient:Time:Nutrient concentration	16	42.8	1.53	0.08
Temperature:Time:Nutrient concentration	16	74.6	2.67	**0.00**
Nutrient:Temperature:Time:Nutrient concentration	32	61.6	1.10	0.33
Residuals	1217	2128.8		

At T0, higher ETRmax values were observed in NO_3^- and humic-enriched cultures at 24˚C, with significant differences compared to NH_4^+ treatments. Similar trends occurred at 27˚C and 30˚C, where the NO_3^- and humic acid treatments generally supported higher ETRmax than the NH_4^+ treatments, particularly at intermediate concentrations (Figure 6.5a,d,g).

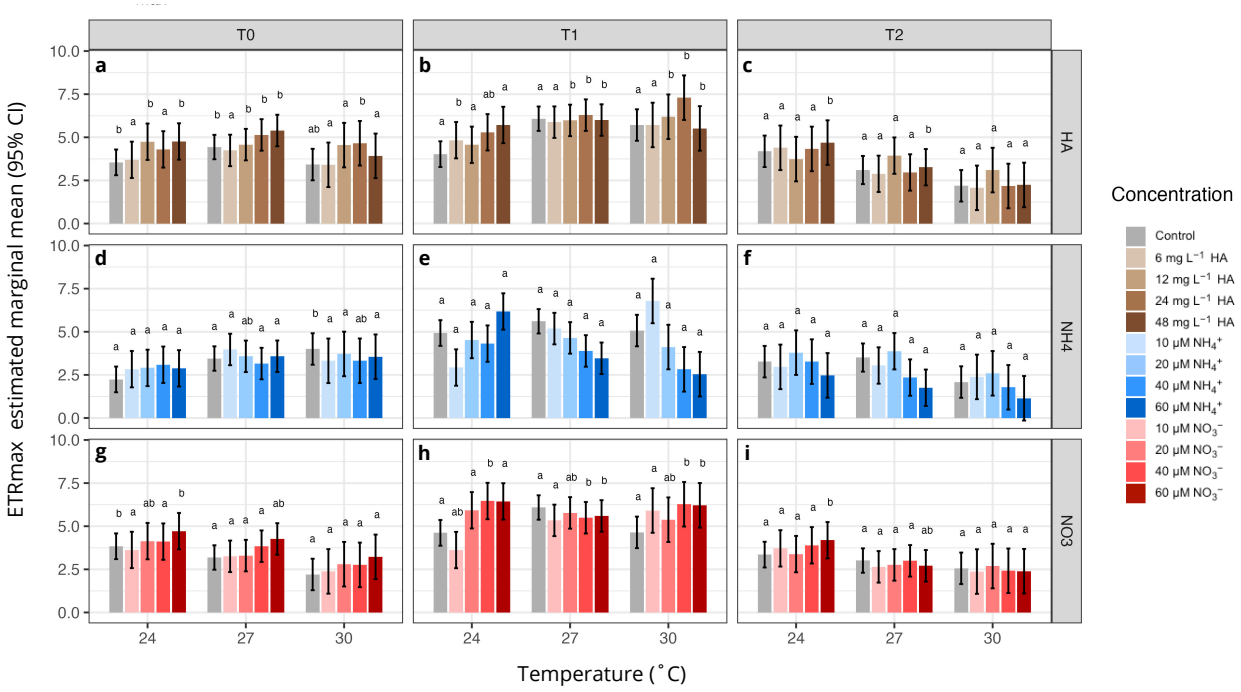

Figure 6.5 Maximum relative electron transport rate (ETRmax) of *K. brevis* cultures grown at 27˚C and enriched with humic acids (HA), ammonium (NH_4^+), and nitrate (NO_3^-) at different concentrations and incubated at three temperatures (24, 27, and 30 ˚C). Panels a-c represent cultures enriched with humic acids; panels d-f, cultures enriched with NH_4^+, and panels g-i, cultures enriched with NO_3^-. The gradation of color within each panel indicates enrichment concentration. Measurements were taken at the start of the experiment (T0), after ~4 h (T1), and after ~10 h (T2). Bars represent estimated marginal means (EMMs) ± 95% confidence intervals derived from a four-way permutational analysis of variance (ANOVA). Different letters above the bars indicate statistically significant differences between the nutrient treatments within each specific concentration, temperature, and time point, based on Tukey-adjusted pairwise comparisons.

By T1, ETRmax increased across all nutrient treatments, most notably at 24˚C, where NO_3^- enrichment produced the highest values (Figure 6.5h), followed by humic acid and NH_4^+

(Figure 6.5b,e). At 27˚C and 30˚C, humic acid and NO_3^- treatments maintained comparable and significantly higher ETRmax values than NH_4^+. Under NH_4^+ enrichment, ETRmax began to decline slightly, with higher NH_4^+ concentrations leading to reductions at both 27˚C and 30˚C (Figure 6.5e). At T2, ETRmax declined across all treatments, most notably at 30˚C, indicating reduced photosynthetic capacity after prolonged exposure. Under these conditions, NH_4^+ consistently produced the lowest ETRmax values, while NO_3^- maintained higher electron transport rates across most concentrations (Figure 6.5f,i). The humic acid treatments exhibited intermediate responses, with slight decreases at 27˚C and 30˚C relative to earlier time points (Figure 6.5c).

Idealized PE curves

The results observed in this study highlight the complexity of the interaction between temperature, nutrient type, and concentration. To better illustrate these patterns, idealized PE curves using experimental data herein were generated using the fitted photophysiological parameters across the three temperatures tested (Figure 6.6). Overall, increasing temperature reduced photosynthetic performance, as shown by lower ETRmax at 30˚C. Nutrient form clearly modulated these responses. At lower temperature (24˚C), both NO_3^- and humic acid increased ETRmax, α, and Ek compared to the control. At intermediate temperature (27˚C), these treatments still enhanced α and Ek, although differences in ETRmax were less pronounced. At higher temperature (30˚C), NO_3^- and low NH_4^+ maintained higher ETRmax relative to the control, suggesting improved performance under thermal stress. In contrast, high NH_4^+ concentrations consistently reduced photosynthetic parameters across temperatures. Together,

these results show that both nutrient form and concentration play a key role in shaping phytoplankton responses to warming.

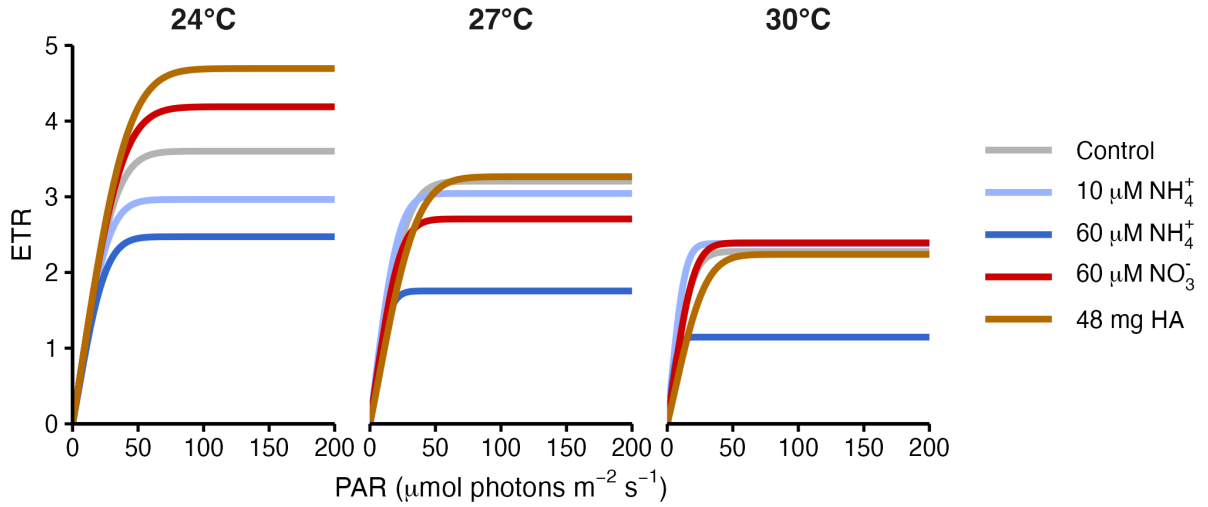

Figure 6.6 Idealized photosynthesis–irradiance (PE) curves derived from fitted photophysiological parameters at three temperatures (24, 27, and 30˚C). Curves represent control conditions (grey), low and high NH_4^+ enrichment (light and dark blue), NO_3^- enrichment (red), and humic acids (HA; brown).

Discussion

The results of this study support the hypothesis that *K. brevis* photosynthetic efficiency can exceed its expected thermal optimum when nutrients are not limited. The interactive effects observed across Fv/Fm, α, E_k, and ETRmax reveal how *K. brevis* adjusts different components of its photosynthetic machinery in response to combined temperature and nutrient stresses. Each parameter reflects a distinct aspect of the photosynthetic process and together, their responses provide an integrated view of how *K. brevis* maintains photophysiological performance under short-term environmental variability.

Overall, the maximum efficiency of PSII in the dark-adapted state (Fv/Fm) remained relatively stable across treatments, except in the NH_4^+-enriched cultures, which exhibited significant declines in photochemical efficiency under prolonged exposure and elevated temperature. In contrast, NO_3^- enrichments maintained higher and more stable Fv/Fm values. These results suggest that high concentrations of NH_4^+ may exacerbate stress on photosystem II under warmer conditions, whereas NO_3^- appears to alleviate it. Different responses were observed in a laboratory experiment with *K. mikimotoi* acclimated to 20˚C, where Fv/Fm increased with both NO_3^- and NH_4^+additions at lower temperatures (Ahn and Glibert, 2021). In that study, when exposed to 30˚C, NO_3^--enriched cultures showed the strongest stress (Fv/Fm = 0.07), whereas cells treated with urea exhibited higher photochemical efficiency (Fv/Fm = 0.17), suggesting that urea may induce a photoprotective mechanism (Ahn and Glibert, 2021). In this study, *K. brevis* cultures had been maintained at 27˚C, and when exposed to 30˚C, Fv/Fm was not as strongly affected. This highlights the importance of the species' thermal history in shaping its capacity to tolerate elevated temperatures.

The photosynthetic efficiency (α) increased with NH_4^+ enrichment under warmer and prolonged exposure conditions, suggesting that NH_4^+ supported more efficient light-harvesting in *K. brevis*. As the most chemically reduced form, NH_4^+ can be directly incorporated without the energetic cost of reduction, providing a more readily available N source to support protein synthesis and photosynthetic enzyme activity (Raven et al., 1992) which likely allowed cells to maintain higher photosynthetic efficiency even under thermal stress, when metabolic energy demands are elevated. However, in this study within the NH_4^+ treatments, α significantly declined as NH_4^+ concentration increased. Toxicity associated with elevated NH_4^+ concentrations is well recognized; it can suppress growth, and the cells might not easily recover from this

condition (e.g., Britto and Kronzucker, 2002). Further, NH_4^+ may affect oxidation and reduction of the chloroplastidic metabolic pathways, leading to enhanced photorespiration or increased reactive oxygen species (ROS) (Glibert, 2024).

Patterns in E_k provided additional insights into photoacclimation. Higher E_k under humic acid and NO_3^- enrichment at moderate temperatures (24 and 27˚C) suggest that these conditions promoted tolerance to higher irradiance. At higher temperatures, however, E_k declined sharply under NH_4^+ enrichment, consistent with photophysiological stress and reduced light utilization capacity. This indicates that *K. brevis* can maintain higher light saturation values when supplied with NO_3^- or humic substances, but experiences light limitation under excessive NH_4^+ and heat exposure. Similarly, NO_3^- enrichment consistently sustained higher ETRmax values across temperatures, while NH_4^+ enrichment resulted in reduced ETRmax at elevated temperatures. The intermediate responses in the humic treatments suggest that humic acid compounds may support photosynthesis moderately. Humic acids may also release NH_4^+ which is the largest fraction of N in these compounds and often loosely bound and released via photooxidation (Bushaw et al., 1996) and/or as salinity increases, as might occur with seawater inundation (Cochlan and Bronk, 2001). Despite some evidence, there are still questions remained about the influence of humic acids as another source of nutrients sustaining blooms of this species on WFS.

These findings highlight the complexity of environmental effects on *K. brevis* photosynthesis, indicating that the influence of individual factors cannot be easily isolated. Instead, these findings demonstrate that photosynthetic responses are driven by the interactions among temperature, nutrient form and concentration, and exposure time, with several significant interaction terms detected in the analyses. Temperature and nutrient supply are key

environmental drivers controlling phytoplankton growth and productivity and their effects on those rates are often interactive (Cross et al., 2015; Van de Waal and Litchman, 2020).

Temperature modulates resource allocation into light-harvesting complexes, due to the different temperature sensitivity of the light and dark reactions of photosynthesis. For example, increasing Chl-*a* content under warmer temperatures allows cells to balance between the temperature-dependent dark reactions and the largely temperature-independent light reactions that supply the energy and reducing power needed for carbon fixation (Fernández-Gonzáles et al., 2022 and references therein). Consequently, photosynthesis rates generally increase as temperature increases, and they often rise until an optimal limit (Baly, 1935), but this optimal temperature for maximum photosynthesis can shift depending on acclimation history and nutrient availability (Hikosaka et al., 2006). For example, *K. brevis* acclimated to winter (~20˚C) and summer (>30˚C) temperatures showed that photosynthetic performance at the same temperature depended on the thermal history of the cells, demonstrating this species' capacity for thermal acclimation (Ahn et al., 2023). However, even though the summer populations were photosynthetically and nutritionally stressed, cells from the Ahn et al. (2023) study treated with urea exhibited higher uptake rates and greater total C and N per cell than those treated with other N substrates, highlighting differential thermal responses depending on N form.

The interaction between temperature and the pathways for metabolizing different N sources also interact in complex ways. The enzyme involved in NH_4^+ assimilation, glutamine synthetase-glutamate synthase (GS-GOGAT), typically has a positive relationship to temperature, while the enzyme involved in NO_3^- reduction, NO_3^- reductase (NR), has a negative relationship with temperature (Glibert et al., 2016 and references therein). Consequently, NH_4^+ metabolism is expected to increase at higher temperature, while NO_3^- metabolism is more

efficient at cooler temperatures (Glibert et al., 2016; Ahn et al., 2023). Temperature also indirectly influences nutrient dynamics by affecting the production of humic substances. Since the decomposition of these substances is mediated by bacterial activity, and microbial growth rates are strongly temperature-dependent, higher temperatures can enhance the formation and accumulation of humic acids in surface waters (Lipczynska-Kochany, 2018 and references therein).

The significant interactions among temperature, nutrient forms, and concentration observed in this study reflect these biochemical and ecological complexities, highlighting that temperature may influence *K. brevis* physiology both directly, by modulating photosynthetic processes, and indirectly, by altering nutrient acquisition and metabolism. While each factor alone contributed to variation in photosynthetic parameters, their combined effects often amplified or moderated responses in ways that would not be predicted from single drivers. New dominant species, including HABs may emerge as a result of multiple stressor interactions (Glibert et al., 2022). This complexity is ecologically relevant, as *K. brevis* cells in the natural environment are continuously exposed to abrupt shifts in temperature, light, and nutrient availability due to vertical migration and episodic pulses of inorganic and organic nutrients, especially after hurricane-driven runoff. Taken together, these results emphasize the importance of considering multiple environmental drivers simultaneously to better understand the dynamics and persistence of *K. brevis* blooms under variable coastal conditions on the WFS.

Ecological implications

Extreme weather events, including storms, heatwaves, and droughts, are becoming more intense and frequent (Glibert and Li, 2023). The greater occurrence of hurricanes and increased riverine runoff associated with climate change are altering nutrient supplies in coastal waters. Florida is more frequently affected by hurricanes than any other U.S. state, with major events occurring approximately every two years (Malmstadt et al., 2009). Several studies have shown that hurricanes can play an important role in *K. brevis* blooms. Hu et al. (2006) demonstrated that the unusual number of hurricanes in 2004 resulted in high runoff and stronger-than-normal submarine groundwater discharge along the west Florida coast in 2005, supporting the initiation and fueling of the persistent *K. brevis* bloom that year. Similarly, the 2018 bloom was related to intense flooding and runoff that followed Hurricane Irma in 2017 (Fritz, 2018). More recently, the model by Chen and Li (2025) showed that the strong winds and heavy rainfall associated with Hurricane Ian created favorable conditions for the development of large phytoplankton blooms on the WFS, beginning with a short diatom bloom that transitioned into a prolonged *K. brevis* bloom.

Blooms of *K. brevis*, particularly in years with prolonged extreme events, represent a complex ecological, environmental, and socioeconomic challenge on the WFS. The severity of these blooms has increased over time according to the Bloom Severity Index (BSI) developed by Stumpf et al. (2022), which integrates cell concentration data across 0.2˚ latitude intervals (~25 km) along the southwest Florida coast to represent both spatial and temporal bloom intensity. Glibert et al. (2025) examined the relationship between BSI values and environmental parameters and found that the combined stresses of warmer temperatures and high N loads,

largely influenced by the Caloosahatchee River, lead to more severe and longer-lasting blooms. Furthermore, as coastal waters continue to warm, nutrient regeneration and the mixotrophic nutrition of *K. brevis* may help sustain blooms through the summer months. By maintaining access to alternative nutrient sources that alleviate nutrient limitation, *K. brevis* cells may be better able to tolerate thermal stress that would otherwise limit their survival during midsummer (Glibert et al., 2025).

The photophysiological responses described in this study further highlight the plasticity of *K. brevis* in modulating photosynthesis according to the available N form and thermal conditions. The availability of NO_3^- and humic-derived N appeared to support photosynthetic performance across moderate temperature ranges, while NH_4^+ initially promoted an increase in photosynthetic efficiency followed by stress-induced declines under prolonged or high-temperature exposure. These findings suggests that the ability of *K. brevis* to shift among nutrient strategies likely contributes to the persistence of blooms in dynamic coastal systems, particularly during summers when both temperature and terrestrial nutrient inputs are elevated. The influx of humic acid following heavy rainfall, storm surges, and hurricane-driven runoff may provide an additional N source that sustains photosynthetic activity and helps cells overcome nutrient limitation under thermally stressful conditions.

Conclusion

This study demonstrated that *K. brevis* can maintain high photosynthetic efficiency even when the thermal optimum for growth is exceeded when nutrient limitation is alleviated. The results showed that nutrient form, temperature, and exposure time interact in complex ways to

shape photosynthetic performance. Moreover, the increasing occurrence of hurricanes and heavy rainfall events is expected to intensify terrestrial nutrient inputs, including humic acids. Such inputs can alleviate nutrient limitation and potentially sustain photosynthesis even under elevated temperatures, favoring bloom development and persistence during summer months. Altogether, these findings provide new insight into the interactive effects of temperature and nutrient form on *K. brevis* physiology and highlight the need to incorporate both inorganic and organic nutrient sources into future models of bloom dynamics. Understanding these interactions is essential for predicting how this species will respond to a warming and increasingly nutrient-enriched coastal ocean.

References

Ahn, S.H., & Glibert, P.M. (2021). Shining light on photosynthesis in the harmful dinoflagellate *Karenia mikimotoi* – responses to short-term changes in temperature, nitrogen form, and availability. *Phycology*, 2(1), 30–44. https://doi.org/10.3390/phycology2010002

Ahn, S.H., & Glibert, P.M. (2024). Temperature-dependent mixotrophy in natural populations of the toxic dinoflagellate *Karenia brevis*. *Water*, 16, 1555. https://doi.org/10.3390/w16111555

Ahn, S.H., Glibert, P.M., & Heil, C.A. (2023). In hot water: interactions of temperature, nitrogen form and availability and photosynthetic and nitrogen uptake responses in natural *Karenia brevis* populations. *Harmful Algae*, 129, 102519. https://doi.org/10.1016/j.hal.2023.102519

Ahn, S.H., Mayali, X., Weber, P.K., & Glibert, P.M. (2025). Impact of nutritional history, prey quality, and quantity on grazing and photophysiological responses in the mixoplanktonic dinoflagellate *Karenia brevis*. *Limnology and Oceanography*. https://doi.org/10.1002/lno.70158

Baly, E.C.C. (1935). The kinetics of photosynthesis. *Proceedings of the Royal Society of London. Series B – Biological Sciences*, 117(804), 218–239. https://doi.org/10.1098/rspb.1935.0026

Brand, L.E., & Compton, A. (2007). Long-term increase in *Karenia brevis* abundance along the Southwest Florida Coast. *Harmful Algae*, 6(2), 232–252. https://doi.org/10.1016/j.hal.2006.08.005

Britto, D.T., & Kronzucker, H.J. (2002). NH_4^+ toxicity in higher plants: a critical review. *Journal of Plant Physiology*, 159(6), 567–584. https://doi.org/10.1078/0176-1617-0774

Bronk, D.A., Killberg-Thoreson, L., Sipler, R.E., Mulholland, M.R., Roberts, Q.N., Bernhardt, P.W., Garrett, M., O'Neil, J.M., & Heil, C.A. (2014). Nitrogen uptake and regeneration (ammonium regeneration, nitrification and photoproduction) in waters of the West Florida Shelf prone to blooms of *Karenia brevis*. *Harmful Algae*, 38, 50–62. https://doi.org/10.1016/j.hal.2014.04.007

Bushaw, K.L., Zepp, R.G., Tarr, M.A., Schulz-Jander, D., Bourbonniere, R.A., Hodson, R.E., Moran, M.A. (1996). Photochemical release of biologically available nitrogen from aquatic dissolved organic matter. *Nature*, 381, 404–407. https://doi.org/10.1038/381404a0

Chen, Y., & Li, M. (2025). Impact of Hurricane Ian (2022) on *Karenia brevis* bloom on the West Florida Shelf. *Geophysical Research Letters*, 52(6), e2024GL113500. https://doi.org/10.1029/2024GL113500

Cochlan, W. P., & Bronk, D. A. (2001). Nitrogen uptake kinetics in the Ross Sea, Antarctica. *Deep Sea Research Part II: Topical Studies in Oceanography*, 48(19-20), 4127-4153. https://doi.org/10.1016/S0967-0645(01)00083-

Cross, W.F., Hood, J.M., Benstead, J.P., Huryn, A.D., & Nelson, D. (2015). Interactions between temperature and nutrients across levels of ecological organization. *Global Change Biology*, 21(3), 1025–1040. 178. https://doi.org/10.1111/gcb.12809

Dixon, L.K., & Steidinger, K.A. (2002). Correlation of *Karenia brevis* presence in the eastern Gulf of Mexico with rainfall and riverine flow. *Marine Ecology Progress Series*, 636, 29–32.

Fernández-González, C., Tarran, G.A., Schuback, N., Woodward, E.M.S., Arístegui, J., & Marañón, E. (2022). Phytoplankton responses to changing temperature and nutrient availability are consistent across the tropical and subtropical Atlantic. *Communications Biology*, 5, 1035. https://doi.org/10.1038/s42003-022-03971-z

Fritz, A. (2018). How climate change is making 'Red Tide' algal blooms worse. *The Washington Post*. https://www.washingtonpost.com/news/capital-weather-gang/wp/2018/08/14/how-climate-change-is-making-red-tide-algal-blooms-even-worse/ Accessed on November 10, 2025.

Genty, B., Briantais, J., Baker, N.R. (1989) The relationship between the quantum yield of photosynthetic electron transport and quenching of chlorophyll fluorescence. *Biochim. Biophys. Acta* 990:87-92.

Glibert, P.M. (2024). *Phytoplankton Whispering: An Introduction to the Physiology and Ecology of Microalgae*. Springer Nature. Cham, Switzerland, 758 pp.

Glibert, P.M. and M. Li. 2023. Warming, wheezing, blooming waters: hypoxia and harmful algae. In: D. Baird (ed), Treatise on estuarine and coastal science, 2nd edition. Elsevier, pp. 401-444. https://doi.org/10.1016/b978-0-323-90798-9.00066-4

Glibert, P.M., Burkholder, J.A.M., Kana, T.M., Alexander, J., Skelton, H., & Shilling, C. (2009). Grazing by *Karenia brevis* on *Synechococcus* enhances its growth rate and may help to sustain blooms. *Aquatic Microbial Ecology*, 55(1), 17–30. https://doi.org/10.3354/ame01279

Glibert, P.M., Cai, W.-J., Hall, E.R., Li, M., Main, K.L., Rose, K.A., Testa, J.M., & Vidyarathna, N.K. (2022). Stressing over the complexities of multiple stressors in marine and estuarine systems. *Ocean–Land–Atmosphere Research*, 2022, 9787258. https://doi.org/10.34133/2022/9787258

Glibert, P.M., Heil, C.A., & Li, M. (2025). More sustained, more severe blooms and shifting monthly patterns of the toxigenic dinoflagellate *Karenia brevis* on the West Florida Shelf. *Harmful Algae*, 139, 102967. https://doi.org/10.1016/j.hal.2025.102967

Glibert, P.M., Wilkerson, F.P., Dugdale, R.C., Raven, J.A., Dupont, C.L., Leavitt, P.R., Parker, A.E., Burkholder, J.M., & Kana, T.M. (2016). Pluses and minuses of ammonium and nitrate uptake and assimilation by phytoplankton and implications for productivity and community composition. *Limnology and Oceanography*, 61(1), 165–197. https://doi.org/10.1002/lno.10203

Guillard, R.R. (1975) Culture of phytoplankton for feeding marine invertebrates. In: Smith, W.L., Chanley, M.H., (eds.) *Culture of Marine Invertebrate Animals*, Plenum Press: New York, NY, USA, pp.29–60.

Heil, C.A. (2005). Influence of humic, fulvic and hydrophilic acids on the growth, photosynthesis and respiration of the dinoflagellate *Prorocentrum minimum*. *Harmful Algae*, 4(3), 603–618. https://doi.org/10.1016/j.hal.2004.08.010

Heil, C.A., Dixon, L.K., Hall, E., Garrett, M., Lenes, J.M., O'Neil, J.M., Walsh, B.M., Bronk, D.A., Killberg-Thoreson, L., & Weisberg, R.H. (2014). Blooms of *Karenia brevis* on the West Florida Shelf: nutrient sources and potential management strategies based on a multi-year regional study. *Harmful Algae*, 38, 127–140. https://doi.org/10.1016/j.hal.2014.07.016

Heil, C.A., Amin, S.A., Glibert, P.M., Hubbard, K.A., Li, M., Martínez Martínez, J., Weisberg, R., Liu, Y., & Sun, Y. (2022). Termination patterns of *Karenia brevis* blooms in the eastern Gulf of Mexico. In: Band-Schmidt, C., Rodríguez-Gómez, C.F. (Eds.), *Proceedings of the International Harmful Algal Bloom Conference*. https://doi.org/10.5281/zenodo.7034923

Hikosaka, K., Ishikawa, K., Borjigidai, A., Muller, O., & Onoda, Y. (2006). Temperature acclimation of photosynthesis: mechanisms involved in the changes in temperature dependence of photosynthetic rate. *Journal of Experimental Botany*, 57(2), 291–302. https://doi.org/10.1093/jxb/erj049

Hu, C., Muller-Karger, F. E., & Swarzenski, P. W. (2006). Hurricanes, submarine groundwater discharge, and Florida's red tides. *Geophysical Research Letters*, 33(11), L11601. https://doi.org/10.1029/2005GL025449

Jassby, A. D., & Platt, T. (1976). Mathematical formulation of the relationship between photosynthesis and light for phytoplankton. *Limnology and Oceanography*, 21(4), 540-547. https://doi.org/10.4319/lo.1976.21.4.0540

Killberg-Thoreson, L., Mulholland, M. R., Heil, C. A., Sanderson, M. P., O'Neil, J. M., & Bronk, D. A. (2014). Nitrogen uptake kinetics in field populations and cultured strains of *Karenia brevis*. *Harmful Algae*, 38, 73-85. https://doi.org/10.1016/j.hal.2014.04.008

Li, M.F., Glibert, P.M., & Lyubchich, V. (2021). Machine learning classification algorithms for predicting *Karenia brevis* blooms on the West Florida Shelf. *Journal of Marine Science and Engineering*, 9(9), 999. https://doi.org/10.3390/jmse9090999

Lipczynska-Kochany, E. (2018). Effect of climate change on humic substances and associated impacts on the quality of surface water and groundwater. *Science of the Total Environment*, 640, 1548–1565. https://doi.org/10.1016/j.scitotenv.2018.05.376

Malmstadt, J., Scheitlin, K., & Elsner, J. (2009). Florida hurricanes and damage costs. *Southeastern Geographer*, 49, 108–131. https://doi.org/10.1353/sgo.0.0045

Medina, M., Huffaker, R., Jawitz, J.W., & Muñoz-Carpena, R. (2020). Seasonal dynamics of terrestrially sourced nitrogen influence *Karenia brevis* blooms of Florida's southern Gulf Coast. *Harmful Algae*, 98, 101900. https://doi.org/10.1016/j.hal.2020.101900

Medina, M., Kaplan, D., Milbrandt, E., Tomasko, D., Huffaker, R., & Angelini, C. (2022). Nitrogen-enriched discharges from a highly managed watershed intensify *Karenia brevis* blooms in southwest Florida. *Science of the Total Environment*, 827, 154149. https://doi.org/10.1016/j.scitotenv.2022.154149

Mendoza, W.G., Kang, Y., & Zika, R.G. (2012). Resolving DOM fluorescence fractions during a *Karenia brevis* bloom patch on the Southwest Florida Shelf. *Continental Shelf Research*, 32, 121–129. https://doi.org/10.1016/j.csr.2011.11.001

Muni-Morgan, A.L., Lusk, M.G., & Heil, C.A. (2024). *Karenia brevis* and *Pyrodinium bahamense* utilization of dissolved organic matter in urban stormwater runoff and rainfall entering Tampa Bay, Florida. *Water*, 16(10), 1448. https://doi.org/10.3390/w16101448

O'Neil, J.M., Heil, C.A., Glibert, P.M., Solomon, C.M., Greenwood, J., & Greenwood, J.G. (2024). Plankton community changes and nutrient dynamics associated with blooms of *Trichodesmium* in the Gulf of Mexico and Great Barrier Reef. *Water*, 16, 1663. https://doi.org/10.3390/w16121663

Raven, J. A., Wollenweber, B., & Handley, L. L. (1992). A comparison of ammonium and nitrate as nitrogen sources for photolithotrophs. *New Phytologist*, 121(1), 19-32. https://doi.org/10.1111/j.1469-8137.1992.tb01088.x

See, J. H., Bronk, D. A., & Lewitus, A. J. (2006). Uptake of Spartina-derived humic nitrogen by estuarine phytoplankton in nonaxenic and axenic culture. *Limnology and Oceanography*, 51(5), 2290-2299. https://doi.org/10.4319/lo.2006.51.5.2290

Steidinger, K.A. (1975). Implications of dinoflagellate life cycles on initiation of *Gymnodinium breve* red tides. *Environmental Letters*, 9(2), 129–139. https://doi.org/10.1080/00139307509435842

Stumpf, R.P., Li, Y., Kirkpatrick, B., Litaker, R.W., Hubbard, K.A., Currier, R.D., & Tomlinson, M.C. (2022). Quantifying *Karenia brevis* bloom severity and respiratory irritation impact along the shoreline of Southwest Florida. *PLoS ONE*, 17(1), e0260755. https://doi.org/10.1371/journal.pone.0260755

Tomasko, D., Landau, L., Suau, S., Medina, M., & Hecker, J. (2024). An evaluation of the relationships between the duration of red tide (*Karenia brevis*) blooms and watershed nitrogen loads in southwest Florida. *Florida Scientist*, 87(2), 61–72. http://dx.doi.org/10.2139/ssrn.4592652

Van de Waal, D.B., & Litchman, E. (2020). Multiple global change stressor effects on phytoplankton nutrient acquisition in a future ocean. *Philosophical Transactions of the Royal Society B*, 375(1798), 20190706. https://doi.org/10.1098/rstb.2019.0706

Vargo, G.A. (2009). A brief summary of the physiology and ecology of *Karenia brevis* red tides on the West Florida Shelf. *Harmful Algae*, 8, 573–584. https://doi.org/10.1016/j.hal.2008.11.002

Vargo, G.A., Heil, C.A., Fanning, K.A., Dixon, L.K., Neely, M.B., Lester, K., Bell, S., & Weisberg, R.H. (2008). Nutrient availability in support of *Karenia brevis* blooms on the central West Florida Shelf. *Continental Shelf Research*, 28(1), 73–98. https://doi.org/10.1016/j.csr.2007.04.008

Weisberg, R.H., Zheng, L., Liu, Y., Corcoran, A.A., Lembke, C., Hu, C., Lenes, J.M., & Walsh, J.J. (2016). *Karenia brevis* blooms on the West Florida Shelf: A comparative study of the robust 2012 bloom and the nearly null 2013 event. *Continental Shelf Research*, 120, 106–121. https://doi.org/10.1016/j.csr.2016.03.011

Wheeler, R. E., & Torchiano, M. (2016). Permutation tests for linear models in R. The Comprehensive R Archive Network, 1(2), 1-36.

Chapter 7: Summary and conclusions

This study investigated how the interaction of multiple environmental stressors influences both primary production and respiration, including light-dependent and dark respiration, in the phytoplankton community, with particular emphasis on the dinoflagellate *Karenia brevis*. The initial hypothesis that climate change conditions would alter habitat suitability for *K. brevis* in multiple ways was supported throughout the chapters presented here. Although it was not possible to conduct experiments during massive *K. brevis* blooms, due either to their absence during the field period or to logistical limitations associated with sampling, this work integrated multiple complementary approaches. These included time-series analyses, methodological development, opportunistic experiments conducted following hurricane events, field experiments with natural samples when *K. brevis* was both present and absent, and controlled laboratory experiments using *K. brevis* cultures.

One of the specific hypotheses of this study was that interannual variability in *K. brevis* abundance is, at least in part, driven by climatic variability, including ENSO and storm frequency. In Florida, El Niño is generally associated with cooler and wetter conditions, whereas La Niña tends to bring warmer and drier weather. However, mild La Niña phases and ENSO transition periods are often linked to increased hurricane activity affecting the region. To investigate the relationship between *K. brevis* blooms and environmental conditions on the West Florida Shelf (WFS), a time-series analysis was conducted using long-term data from 1998 to 2020 (*Chapter 2*). Excluding the 2020–2021 bloom that was not analyzed here, the highest *K. brevis* abundances were observed during the 2004–2005 and 2017–2018 bloom events, both of which followed drought periods and coincided with hurricane activity. Correlations between cell

concentrations, Peace River discharge, and the ENSO index suggested that freshwater inflow and large-scale climate oscillations play both direct and indirect roles in regulating bloom dynamics on the WFS.

To better understand how environmental factors associated with climate change influence primary production and respiration, both dark and light-dependent, the first necessary step was to improve the methodology and develop incubation devices capable of addressing these questions. In collaboration with Bay Instruments, LLC (Easton, MD), methodological improvements were implemented to optimize the use of Membrane Inlet Mass Spectrometry (MIMS) for quantifying primary production (GPP and NPP) and gross respiration (GR; light-dependent respiration) using the $H_2{}^{18}O$ method (*Chapter 3*). This study advances the application of the $H_2{}^{18}O$–MIMS approach by demonstrating its effectiveness in simultaneously quantifying GPP, NPP, and GR in natural phytoplankton communities using small-volume incubations (3 mL). Compared to traditional techniques, this method provides a simpler, more cost-effective, and rapid alternative, thereby expanding its potential applicability. Development of an incubation device, termed a Coronatron, that provided constant irradiance to incubation tubes allowed nutrient manipulations to be done under consistent conditions. With broader application, this approach may enable the development of comparative datasets describing respiration–irradiance (R–E or R–I) relationships analogous to traditional photosynthesis–irradiance (P–E or P–I) curves.

The overarching hypothesis of this dissertation is that climate change conditions will alter habitat suitability for *K. brevis* in multiple ways. Warmer waters, such as those expected during summer, may impose physiological stress on *K. brevis*, reducing photosynthetic rates while simultaneously increasing respiration rates. In addition, enhanced runoff associated with storms and hurricanes may stimulate both primary production and respiration by increasing nutrient and

organic matter inputs to coastal systems. Opportunistic post-hurricane sampling following Hurricanes Debby, Milton, and Helene provided the chance to examine how elevated temperature and humic acid enrichment influence the metabolic rates of natural phytoplankton communities including *K. brevis* (*Chapter 4*). Rates of GPP, NPP, GR, and dark respiration were quantified using MIMS. Across stations, increasing temperature consistently reduced GPP (Figure 7.1), with even stronger reductions observed in colored, DOM-rich waters following Hurricane Debby. Temperature increases shifted NPP toward negative values and enhanced both dark and light-dependent respiration. In many experiments, GR exceeded NPP and occasionally even GPP, indicating that the system was often net heterotrophic and highlighting the substantial, and often under-quantified, contribution of light-dependent respiration to total oxygen consumption. The downward transport of these oxygen-depleted surface waters (e.g., through mixing or advection) may further contribute to the intensification of bottom-water hypoxia. Together, these findings demonstrate how warming and hurricane-driven brownification interact to amplify respiratory metabolism, underscoring the vulnerability of subtropical coastal systems to hypoxia development under future climate scenarios.

To further examine how environmental drivers regulate primary production and respiration rates, the effects of temperature and nitrogen form on metabolic and photophysiological responses of natural phytoplankton communities including *Karenia brevis* on the WFS (*Chapter 5*). The results showed that NO_3^--enrichment significantly enhanced primary production, whereas NH_4^+ response was not clear as a consistent increase or decrease in the rates was not observed with increasing substrate or temperature (Figure 7.1). In some cases, GPP showed an initial increase following NH_4^+ addition, but overall variability was higher and patterns were less consistent compared to NO_3^- treatments. Although some differences were

observed, primary production and respiration rates were not significantly affected by NH_4^+ likely due to high variability and limited replication in that experiment. Warming, however, consistently increased respiration relative to production and reduced photosynthesis performance at higher temperatures (Figure 7.1), suggesting that temperature and nutrient form regulate plankton metabolism through distinct physiological pathways.

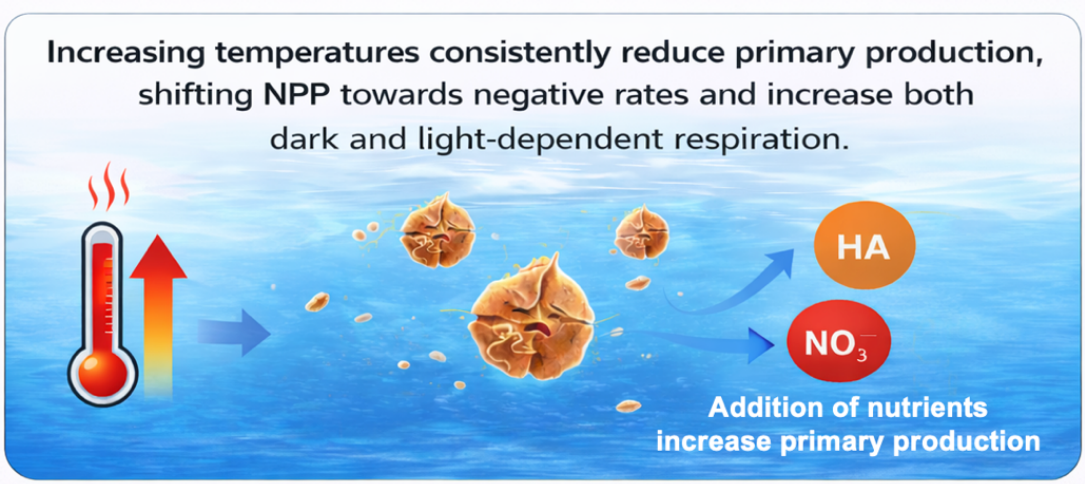

	Primary production		*Respiration*	
	GPP	NPP	Light (GR)	Dark (CR)
Temperature	↓	↓	↑	↑
HA Lab addition	↑	↑	↓	—
NO_3^-	↑	↑	↓	—
NH_4^+	—	—	—	—

Figure 7.1 Summary of temperature and nutrient effects on primary production (GPP and NPP) and respiration, both light (GR) and dark (CR) rates. Figure was created with ChatGPT.

Another hypothesis tested in this study was that *K. brevis* photosynthetic efficiency can exceed its thermal optimum when nutrient limitation is alleviated, and that photosynthetic responses vary depending on the form of nutrient supplied, reflecting physiological differences in nutrient assimilation pathways. To test this hypothesis, exponentially growing cultures acclimated to 27˚C were exposed to three temperatures (24, 27, and 30˚C) and to five levels of nutrient enrichment (NO_3^-, NH_4^+, and humic acids). Photosynthetic performance (Fv/Fm, α, Ek, and ETRmax) was assessed using PAM fluorometry (*Chapter 6*). The results demonstrated that nutrient form, temperature, and exposure time interact in complex ways to regulate photosynthetic performance. Both NO_3^- and humic acids supported relatively stable photosynthetic responses at the two lower temperatures, whereas NH_4^+ initially enhanced photosynthetic efficiency but resulted in declines in Fv/Fm and ETRmax with prolonged exposure. These findings indicate that *K. brevis* exhibits considerable physiological plasticity, which may contribute to bloom persistence under fluctuating environmental conditions.

Results from Chapters 5 and 6 showed that nutrient additions can mitigate the thermal stress caused by temperature changes in both natural phytoplankton communities containing *K. brevis* and in *K. brevis* cultures. However, the nutrient form modulated how distinct photosynthetic parameters responded (Figure 7.3). For example, NO_3^-enrichment supported more stable photosynthetic responses across temperatures and exposure times both experiments. While response to NH_4^+ enrichment was more complex. In natural communities (*Chapter 5*), NH_4^+ enrichment generally supported higher values of several photosynthetic parameters (Fv/Fm, Ek, and ETRmax) compared to the control at moderate temperatures. However, laboratory experiments with cultured *K. brevis* (Chapter 6) showed that although NH_4^+ initially enhanced photosynthetic efficiency, prolonged exposure and elevated concentration resulted in declines in

Fv/Fm and ETRmax. The differences between experiments conducted with natural samples and laboratory cultures are likely related to the NH_4^+ concentrations used. In the culture experiments, cells were exposed to higher stress conditions (Figure 7.2), and as mentioned earlier, highly elevated NH_4^+ concentrations can be toxic for the cell. In addition, differences in phytoplankton community composition and the temperature ranges tested may also influence physiological responses to nutrient enrichment.

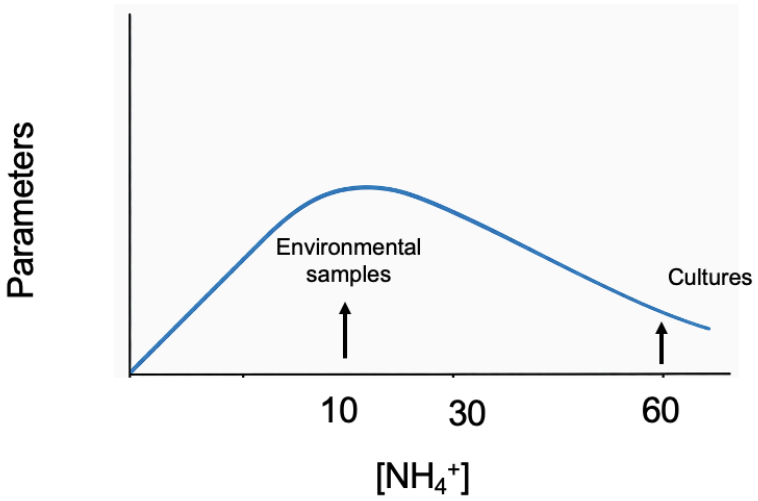

Figure 7.2. Conceptual relationship between NH_4^+concentration and photophysiological parameters. At low to moderate concentrations, NH_4^+ can enhance photosynthetic performance, as observed in environmental samples. However, at higher concentrations, performance declines, likely due to ammonium toxicity, as observed in laboratory cultures.

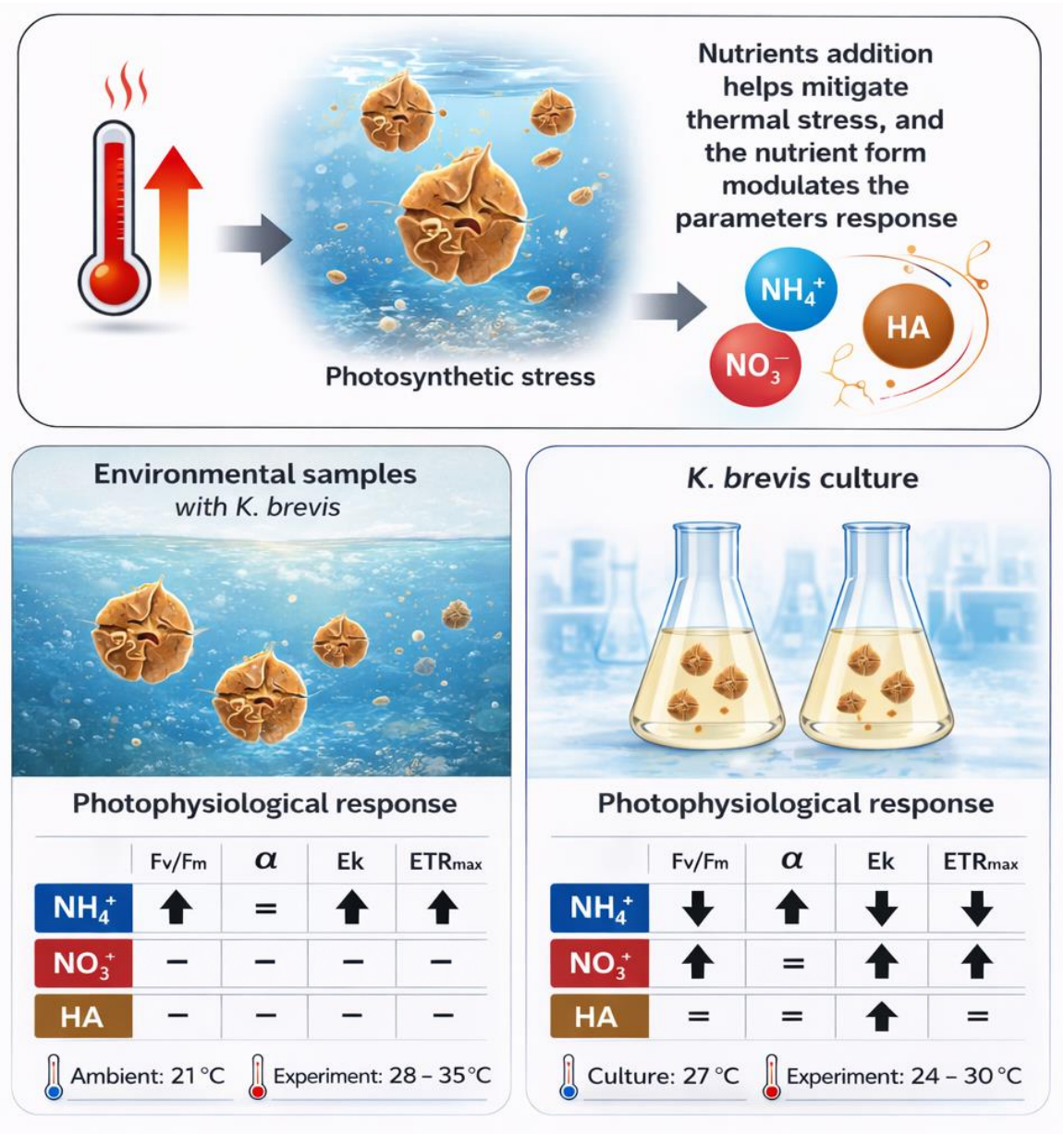

Figure 7.3. Conceptual summary of the effects of temperature and nutrient form on the photophysiological responses of *Karenia brevis* in natural phytoplankton communities and laboratory cultures. Figure was created with ChatGPT.

This dissertation has demonstrated that increasing temperature alters the metabolic balance of *K. brevis* and associated phytoplankton communities in multiple and interacting ways. Warming consistently reduced primary production while enhancing both dark and light-

dependent respiration, shifting the system toward greater net heterotrophy. Further, the photosynthetic performance (Fv/Fm, α, Ek, and ETRmax) responds dynamically to the interaction between temperature and nutrient form, demonstrating that *K. brevis* can exhibit physiological plasticity under changing environmental conditions. While elevated temperatures may impact photosynthetic efficiency, the alleviation of nutrient limitation can partially mitigate these effects, allowing bloom persistence. At the same time, climate-driven changes in storm frequency and freshwater discharge were shown to influence bloom dynamics at interannual scales, reinforcing the importance of large-scale climatic oscillations in regulating *K. brevis* variability on the WFS.

The increasing frequency of hurricanes and extreme rainfall events is expected to intensify terrestrial nutrient and organic matter inputs, including humic acids. Such inputs may alleviate nutrient limitation and sustain photosynthetic performance, even under elevated temperatures, thereby promoting bloom persistence during warmer months. At the same time, enhanced nutrient and organic matter availability is likely to stimulate both primary production and respiratory metabolism, potentially increasing overall oxygen demand and shifting the metabolic balance toward conditions that favor hypoxia development. Collectively, the findings of this study highlight that bloom development and persistence cannot be understood solely through nutrient supply or temperature in isolation, but rather by their combined effects on phytoplankton physiology. By integrating time-series analysis, methodological advancements, and controlled physiological experiments, this work provides new insight into how warming and shifting nutrient regimes interact to shape *K. brevis* physiology and bloom dynamics.

Future studies might consider:

a. Refining methodological approaches to improve measurement reliability in low-biomass samples, expanding the applicability of high-resolution estimates of primary production and both dark and light-dependent respiration across diverse aquatic systems. Broader application of the $H_2{}^{18}O$–MIMS approach across contrasting environments will enable comparative studies and support the development of more robust mechanistic and biogeochemical models of aquatic metabolism.
b. Expanding measurements of light-dependent respiration across varying environmental conditions and diverse aquatic environments. The limited quantification of light-dependent respiration may lead to an underestimation of its contribution to the overall metabolic balance of aquatic systems and its role in shaping the balance between production and respiration. Increasing measurements across environmental gradients is therefore critical not only for accurately characterizing ecosystem metabolism, but also for supporting the development of mechanistic and predictive models that incorporate these processes. Further, the development of conceptual and quantitative respiration–irradiance (R–E or R–I) models should be considered, as current models do not adequately capture the variability in respiratory responses to light.
c. Conducting further experimental studies on the physiological responses of *K. brevis* to humic acids. Such studies should quantify metabolic responses to humic acid enrichment and characterize the composition of these compounds entering

the system to better understand their effects on light availability, nutrient dynamics, and phytoplankton metabolism.

d. Improving experimental design and replication in future studies to strengthen statistical power and enable more robust analyses of relationships between predictor and response variables. Some experiments, particularly opportunistic post-hurricane studies and those restricted by equipment availability, were limited in replication, which constrained the ability to detect significant statistical relationships. Future studies would benefit from improved experimental design, increased replication, and more comprehensive sampling strategies to strengthen statistical inference and further support the mechanistic relationships identified here.

References

Ahn, S. H., & Glibert, P. M. (2021). Shining light on photosynthesis in the harmful dinoflagellate *Karenia mikimotoi* – Responses to short-term changes in temperature, nitrogen form, and availability. *Phycology*, 2(1), 30–44. https://doi.org/10.3390/phycology2010002

Ahn, S. H., Glibert, P. M., & Heil, C. A. (2023). In hot water: Interactions of temperature, nitrogen form and availability and photosynthetic and nitrogen uptake responses in natural *Karenia brevis* populations. *Harmful Algae*, 129, 102519. https://doi.org/10.1016/j.hal.2023.102519

Ahn, S. H., Mayali, X., Weber, P. K., & Glibert, P. M. (2025). Impact of nutritional history, prey quality, and quantity on grazing and photophysiological responses in the mixoplanktonic dinoflagellate *Karenia brevis*. *Limnology and Oceanography.* https://doi.org/10.1002/lno.70158

Ahn, S.H., & Glibert, P.M. (2024). Temperature-dependent mixotrophy in natural populations of the toxic dinoflagellate *Karenia brevis*. *Water*, 16, 1555. https://doi.org/10.3390/w16111555

Alam, M. A. (2023). Climate change and its impact on depletion of oxygen levels on coastal waters and shallow seas. In N. Jayaraju, G. Sreenivasulu, M. Madakka, & M. Manjulatha (Eds.), *Coasts, Estuaries and Lakes*. Springer, Cham. https://doi.org/10.1007/978-3-031-21644-2_20

Anderson, D. M., Burkholder, J. M., Cochlan, W. P., Glibert, P. M., Gobler, C. J., Heil, C. A., Kudela, R. M., Parsons, M. L., Rensel, J. E. J., Townsend, D. W., Trainer, V. L., & Vargo, G. A. (2008). Harmful algal blooms and eutrophication: Examining linkages from selected coastal regions of the United States. *Harmful Algae*, 8(1), 39–53. https://doi.org/10.1016/j.hal.2008.08.017

Anderson, D. M., Fensin, E., Gobler, C. J., Hoeglund, A. E., Hubbard, K. A., Kulis, D. M., et al. (2021). Marine harmful algal blooms (HABs) in the United States: History, current status and future trends. *Harmful Algae*, 102, 101975. https://doi.org/10.1016/j.hal.2021.101975

Arriola, J. M., Najjar, R. G., Briceño, H., Hu, C., Herrmann, M., & Beck, M. W. (2025). Ecosystem metabolic rates estimated from diel oxygen measurements in two subtropical estuaries. *Estuaries and Coasts*, 48(6), 155. https://doi.org/10.1007/s12237-025-01597-y

Baly, E.C.C. (1935). The kinetics of photosynthesis. Proceedings of the Royal Society of London. Series B – *Biological Sciences*, 117(804), 218–239. https://doi.org/10.1098/rspb.1935.0026

Barton, S., Jenkins, J., Buckling, A., Schaum, C. E., Smirnoff, N., Raven, J. A., & Yvon-Durocher, G. (2020). Evolutionary temperature compensation of carbon fixation in

marine phytoplankton. *Ecology Letters*, 23(4), 722–733. https://doi.org/10.1111/ele.13469

Behrenfeld, M. J., Prasil, O., Babin, M., & Bruyant, F. (2004). In search of a physiological basis for covariations in light-limited and light-saturated photosynthesis. *Journal of Phycology*, 40(1), 4–25. https://doi.org/10.1046/j.1529-8817.2004.03083.x

Bender, M., Grande, K., Johnson, K., Marra, J., Williams, P. J. L., Sieburth, J., & Heinemann, K. (1987). A comparison of four methods for determining planktonic community production. *Limnology and Oceanography*, 32(5), 1085–1098. https://doi.org/10.4319/lo.1987.32.5.1085

Benner, R. (2002). Chemical composition and reactivity. In D. A. Hansell & C. A. Carlson (Eds.), *Biogeochemistry of marine dissolved organic matter* (pp. 59–90). Academic Press. https://doi.org/10.1016/B978-012323841-2/50005-1

Bercel, T. L., & Kranz, S. A. (2019). Insights into carbon acquisition and photosynthesis in *Karenia brevis* under a range of CO_2 concentrations. *Progress in Oceanography*, 172, 65–76. https://doi.org/10.1016/j.pocean.2019.01.011

Bianucci, L., Balaguru, K., Smith, R. W., Leung, L. R., & Moriarty, J. M. (2018). Contribution of hurricane-induced sediment resuspension to coastal oxygen dynamics. *Scientific Reports*, 8(1), 15740. https://doi.org/10.1038/s41598-018-33640-3

Bijma, J., Pörtner, H. O., Yesson, C., & Rogers, A. D. (2013). Climate change and the oceans–What does the future hold? *Marine Pollution Bulletin*, 74(2), 495-505. https://doi.org/10.1016/j.marpolbul.2013.07.022

Blanchet, C. C., Arzel, C., Davranche, A., Kahilainen, K. K., Secondi, J., Taipale, S., Lindberg, H., Loehr, J., Manninen-Johansen, S., Sundell, J., Maanan, M., & Nummi, P. (2022). Ecology and extent of freshwater browning – What we know and what should be studied next in the context of global change. *Science of the Total Environment*, 812, 152420. https://doi.org/10.1016/j.scitotenv.2021.152420

Boyer, J. N., Dailey, S. K., Gibson, P. J., Rogers, M. T., & Mir-Gonzalez, D. (2006). The role of dissolved organic matter bioavailability in promoting phytoplankton blooms in Florida Bay. *Hydrobiologia*, 569(1), 71–85. https://doi.org/10.1007/s10750-006-0123-2

Brand, L.E., & Compton, A. (2007). Long-term increase in *Karenia brevis* abundance along the Southwest Florida Coast. *Harmful Algae*, 6(2), 232–252. https://doi.org/10.1016/j.hal.2006.08.005

Breitburg, D., Levin, L. A., Oschlies, A., Grégoire, M., Chavez, F. P., Conley, D. J., Garçon, V., Gilbert, D., Gutiérrez, D., Isensee, K., Jacinto, G. S., Limburg, K. E., Montes, I., Naqvi, S. W. A., Pitcher, G. C., Rabalais, N. N., Roman, M. R., Rose, K. A., Seibel, B. A., Telszewski, M., Yasuhara, M., & Zhang, J. (2018). Declining oxygen in the global ocean

and coastal waters. *Science*, 359(6371), eaam7240. https://doi.org/10.1126/science.aam7240

Brenckman, C. M., Parameswarappa Jayalakshmamma, M., Pennock, W. H., Ashraf, F., & Borgaonkar, A. D. (2025). A review of harmful algal blooms: Causes, effects, monitoring, and prevention methods. *Water*, 17(13), 1980. https://doi.org/10.3390/w17131980

Britto, D.T., & Kronzucker, H.J. (2002). NH_4^+ toxicity in higher plants: a critical review. *Journal of Plant Physiology*, 159(6), 567–584. https://doi.org/10.1078/0176-1617-0774

Bronk, D. A., Glibert, P. M., & Ward, B. B. (1994). Nitrogen uptake, dissolved organic nitrogen release, and new production. *Science*, 265(5180), 1843–1846. https://doi.org/10.1126/science.265.5180.1843

Bronk, D. A., Roberts, Q. N., Sanderson, M. P., Canuel, E. A., Hatcher, P. G., Mesfioui, R., Filippino, K. C., Mulholland, M. R., & Love, N. G. (2010). Effluent organic nitrogen (EON): bioavailability and photochemical and salinity-mediated release. *Environmental Science & Technology,* 44(15), 5830-5835. https://doi.org/10.1021/es101115g

Bronk, D.A., Killberg-Thoreson, L., Sipler, R.E., Mulholland, M.R., Roberts, Q.N., Bernhardt, P.W., Garrett, M., O'Neil, J.M., & Heil, C.A. (2014). Nitrogen uptake and regeneration (ammonium regeneration, nitrification and photoproduction) in waters of the West Florida Shelf prone to blooms of *Karenia brevis*. *Harmful Algae*, 38, 50–62. https://doi.org/10.1016/j.hal.2014.04.007

Brush, M. J., Giani, M., Totti, C., Testa, J. M., Faganeli, J., Ogrinc, N., et al. (2020). Eutrophication, harmful algae, oxygen depletion, and acidification. In Coastal ecosystems in transition: A comparative analysis of the northern Adriatic and Chesapeake Bay (pp. 75–104).

Burris, J. E. (1977). Photosynthesis, photorespiration, and dark respiration in eight species of algae. *Marine Biology*, 39, 371–379. https://doi.org/10.1007/BF00391940

Bushaw, K. L., Zepp, R. G., Tarr, M. A., Schulz-Jander, D., Bourbonniere, R. A., Hodson, R. E., Miller, W. L., Bronk, D. A., & Moran, M. A. (1996). Photochemical release of biologically available nitrogen from aquatic dissolved organic matter. *Nature*, 381(6581), 404–407. https://doi.org/10.1038/381404a0

Bushaw-Newton, K. L., & Moran, M. A. (1999). Photochemical formation of biologically available nitrogen from dissolved humic substances in coastal marine systems. *Aquatic Microbial Ecology*, 18(3), 285-292. https://doi.org/10.3354/ame018285

Campbell, A. M., Fleisher, J., Sinigalliano, C., White, J. R., & Lopez, J. V. (2015). Dynamics of marine bacterial community diversity of the coastal waters of the reefs, inlets, and

wastewater outfalls of southeast Florida. *Microbiology Open*, 4(2), 1–19. https://doi.org/10.1002/mbo3.245

Chen, S., Lu, Y., Dash, P., Das, P., Li, J., Capps, K., Majidzadeh, H., & Elliott, M. (2019). Hurricane pulses: Small watershed exports of dissolved nutrients and organic matter during large storms in the Southeastern USA. *Science of the Total Environment*, 689, 232-244. https://doi.org/10.1016/j.scitotenv.2019.06.351

Chen, Y., & Li, M. (2025). Impact of Hurricane Ian (2022) on a Karenia brevis bloom on the West Florida Shelf. *Geophysical Research Letters,* 52(6), e2024GL113500. https://doi.org/10.1029/2024GL113500

Chen, Y., Li, M., Glibert, P. M., & Heil, C. A. (2023). MurKy waters: Modeling the succession from r to K strategists (diatoms to dinoflagellates) following a nutrient release from a mining facility in Florida. *Limnology and Oceanography*, 68, 2288–2304. https://doi.org/10.1002/lno.12420

Cloern, J. E., Abreu, P. C., Carstensen, J., Chauvaud, L., Elmgren, R., Grall, J., Greening, H., Johansson, J. O. R., Kahru, M., Sherwood, E. T., Xu, J., & Yin, K. (2016). Human activities and climate variability drive fast-paced change across the world's estuarine–coastal ecosystems. *Global Change Biology*, 22(2), 513-529. https://doi.org/10.1111/gcb.13059

Coates, J. D., Cole, K. A., Chakraborty, R., O'Connor, S. M., & Achenbach, L. A. (2002). Diversity and ubiquity of bacteria capable of utilizing humic substances as electron donors for anaerobic respiration. *Applied and Environmental Microbiology*, 68(5), 2445-2452. https://doi.org/10.1128/AEM.68.5.2445-2452.2002

Coble, P. G. (1996). Characterization of marine and terrestrial DOM in seawater using excitation-emission matrix spectroscopy. *Marine Chemistry*, 51(4), 325-346. https://doi.org/10.1016/0304-4203(95)00062-3

Cochlan, W. P., & Bronk, D. A. (2001). Nitrogen uptake kinetics in the Ross Sea, Antarctica. *Deep Sea Research Part II: Topical Studies in Oceanography,* 48(19-20), 4127-4153. https://doi.org/10.1016/S0967-0645(01)00083-

Conmy, R. N., Coble, P. G., Cannizzaro, J. P., & Heil, C. A. (2009). Influence of extreme storm events on West Florida Shelf CDOM distributions. *Journal of Geophysical Research: Biogeosciences*, 114(G4). https://doi.org/10.1029/2009JG000981

Cross, W.F., Hood, J.M., Benstead, J.P., Huryn, A.D., & Nelson, D. (2015). Interactions between temperature and nutrients across levels of ecological organization. *Global Change Biology*, 21(3), 1025–1040. 178. https://doi.org/10.1111/gcb.12809

Diaz, R. J., & Rosenberg, R. (2008). Spreading dead zones and consequences for marine ecosystems. *Science*, 321(5891), 926-929. https://doi.org/10.1126/science.1156401

Dixon, L. K., & Steidinger, K. A. (2004). Correlation of *Karenia brevis* presence in the eastern Gulf of Mexico with rainfall and riverine flow. *Marine Ecology Progress Series*, 636, 29–32.

Dixon, L. K., Kirkpatrick, G. J., Hall, E. R., & Nissanka, A. (2014). Nitrogen, phosphorus and silica on the West Florida Shelf: Patterns and relationships with *Karenia* spp. occurrence. *Harmful Algae*, 38, 8-19. https://doi.org/10.1016/j.hal.2014.07.001

Dixon, L.K., & Steidinger, K.A. (2002). Correlation of *Karenia brevis* presence in the eastern Gulf of Mexico with rainfall and riverine flow. *Marine Ecology Progress Series*, 636, 29– 32.

Eddy, T. D., Heneghan, R. F., Bryndum- Buchholz, A., Fulton, E. A., Harrison, C. S., Tittensor, D. P., et al. (2025). Global and regional marine ecosystem models reveal key uncertainties in climate change projections. *Earth's Future*, 13, e2024EF005537. https://doi.org/10.1029/2024EF005537

Eppley, R. W. (1972). Temperature and phytoplankton growth in the sea. *Fishery Bulletin*, 70(4), 1063–1085.

Ershadifar, H., Koochaknejad, E., Ghazilou, A., Kor, K., Negarestan, H., & Baskaleh, G. (2020). Response of phytoplankton assemblages to variations in environmental parameters in a subtropical bay (Chabahar Bay, Iran): Harmful algal blooms and coastal hypoxia. *Regional Studies in Marine Science*, 39, 101421. https://doi.org/10.1016/j.rsma.2020.101421

Falkowski, P. G., & Raven, J. A. (2013). Aquatic photosynthesis. Princeton University Press.

Fernández-González, C., Tarran, G.A., Schuback, N., Woodward, E.M.S., Arístegui, J., & Marañón, E. (2022). Phytoplankton responses to changing temperature and nutrient availability are consistent across the tropical and subtropical Atlantic. *Communications Biology*, 5, 1035. https://doi.org/10.1038/s42003-022-03971-z

Ferrón, S., del Valle, D. A., Björkman, K. M., Quay, P. D., Church, M. J., & Karl, D. M. (2016). Application of membrane inlet mass spectrometry to measure aquatic gross primary production by the 18O in vitro method. *Limnology and Oceanography: Methods,* 14(9), 610–622. https://doi.org/10.1002/lom3.10116

Florida State University Climate Center. (2024). Hurricane Helene summary report. https://climatecenter.fsu.edu/images/docs/Hurricane-Helene-Summary-Report.pdf. Accessed on February 21, 2026

Fritz, A. (2018). How climate change is making 'Red Tide' algal blooms worse. The Washington Post. https://www.washingtonpost.com/news/capital-weather-gang/wp/2018/08/14/how-

climate-change-is-making-red-tide-algal-blooms-even-worse/. Accessed on February 21, 2026

Gaarder, T., & Gran, H. H. (1927). Investigations of the production of plankton in the Oslo Fjord. *ICES Journal of Marine Science*. https://doi.org/10.17895/ices.pub.19272251

Genty, B., Briantais, J., Baker, N.R. (1989) The relationship between the quantum yield of photosynthetic electron transport and quenching of chlorophyll fluorescence. *Biochim. Biophys.* Acta 990:87-92.

Gilliam, F. S. (2021). Impacts of tropical cyclones on longleaf pine ecosystems of Florida: Tropical cyclogenesis, landfall frequencies, and climate change. *Frontiers in Ecology and Evolution*, 9, 595791. https://doi.org/10.3389/fevo.2021.595791

Glenn, E., Comarazamy, D., González, J. E., & Smith, T. (2015). Detection of recent regional sea surface temperature warming in the Caribbean and surrounding region. *Geophysical Research Letters*, 42(16), 6785–6792. https://doi.org/10.1002/2015GL065002

Glibert, P. M. (2020). Harmful algae at the complex nexus of eutrophication and climate change. *Harmful Algae*, 91, 101583. https://doi.org/10.1016/j.hal.2019.03.001

Glibert, P. M. (2024). Phytoplankton whispering: An introduction to the physiology and ecology of microalgae. Springer Nature. Cham, Switzerland, 758 pp.

Glibert, P. M., & Li, M. (2024). Warming, wheezing, blooming waters: Hypoxia and harmful algae. In D. Baird (Ed.), *Treatise on estuarine and coastal science* (2nd ed., pp. 401–444). Elsevier. https://doi.org/10.1016/B978-0-323-90798-9.00066-4

Glibert, P. M., Beusen, A. H. W., Bouwman, A. F., Burkholder, J. M., Flynn, K. J., Heil, C. A., Li, M., Lin, C.-H., Madden, C. J., Mitra, A., Nardin, W., Silsbe, G., Song, Y., & Zhang, F. (2020). Multifaceted climatic change and nutrient effects on harmful algae require multifaceted models. In L. M. Botana, M. C. Louzao, & N. Vilariño (Eds.), *Climate change and marine and freshwater toxins* (2nd ed., pp. 473–518). De Gruyter. https://doi.org/10.1515/9783110625738-012

Glibert, P. M., Burkholder, J. A. M., Kana, T. M., Alexander, J., Skelton, H., & Shilling, C. (2009). Grazing by *Karenia brevis* on *Synechococcus* enhances its growth rate and may help to sustain blooms. *Aquatic Microbial Ecology*, 55(1), 17–30. https://doi.org/10.3354/ame01279

Glibert, P. M., Cai, W.-J., Hall, E. R., Li, M., Main, K. L., Rose, K. A., Testa, J. M., & Vidyarathna, N. K. (2022). Stressing over the complexities of multiple stressors in marine and estuarine systems. *Ocean-Land-Atmosphere Research*, 2022, 9787258. https://doi.org/10.34133/2022/9787258

Glibert, P. M., Heil, C. A., & Li, M. (2025). More sustained, more severe blooms and shifting monthly patterns of the toxigenic dinoflagellate *Karenia brevis* on the West Florida Shelf. *Harmful Algae*, 139, 102967. https://doi.org/10.1016/j.hal.2025.102967

Glibert, P. M., Heil, C. A., Madden, C. J., & Kelly, S. P. (2023). Dissolved organic nutrients at the interface of fresh and marine waters: flow regime changes, biogeochemical cascades and picocyanobacterial blooms—the example of Florida Bay, USA. *Biogeochemistry*, 164(1), 229-255. https://doi.org/10.1007/s10533-021-00760-4

Glibert, P. M., Middelburg, J. J., McClelland, J. W., & Jake Vander Zanden, M. (2019). Stable isotope tracers: Enriching our perspectives and questions on sources, fates, rates, and pathways of major elements in aquatic systems. *Limnology and Oceanography*, 64(3), 950–981. https://doi.org/10.1002/lno.11087

Glibert, P. M., Wilkerson, F. P., Dugdale, R. C., Raven, J. A., Dupont, C. L., Leavitt, P. R., Parker, A. E., Burkholder, J. M., & Kana, T. M. (2016). Pluses and minuses of ammonium and nitrate uptake and assimilation by phytoplankton and implications for productivity and community composition, with emphasis on nitrogen-enriched conditions. *Limnology and Oceanography*, 61(1), 165–197. https://doi.org/10.1002/lno.10203

Glibert, P.M., A.H.W. Beusen, A.F. Bouwman, J.M. Burkholder, K.J. Flynn, C.A. Heil, M. Li, C.-H. Lin, C.J. Madden, A. Mitra, W. Nardin, G. Silsbe, Y. Song and F. Zhang. (2021). Multifacteted climate change and nutrient effects on harmful algae require multifaceted models. In: L.M. Botana, M. C. Louzao and. N. Vilariño. *Climate change and marine and freshwater toxins*, 2nd edition. De Gruyter GmbH, Berlin. pp. 473-518.

Gobler, C. J. (2020). Climate change and harmful algal blooms: Insights and perspective. *Harmful Algae*, 91, 101731. https://doi.org/10.1016/j.hal.2019.101731

Gobler, C. J., Doherty, O. M., Hattenrath-Lehmann, T. K., Griffith, A. W., Kang, Y., & Litaker, R. W. (2017). Ocean warming since 1982 has expanded the niche of toxic algal blooms in the North Atlantic and North Pacific oceans. *Proceedings of the National Academy of Sciences*, 114(19), 201619575. https://doi.org/10.1073/pnas.1619575114

Gomez, F.A., Lee, SK., Hernandez, F.J. et al. ENSO-induced co-variability of salinity, plankton biomass and coastal currents in the northern Gulf of Mexico. (2019) *Sci Rep* 9, 178. https://doi.org/10.1038/s41598-018-36655-y

Goñi, M. A., Juranek, L. W., Sipler, R. E., & Welch, K. A. (2021). Particulate organic matter distributions in the water column of the Chukchi Sea during late summer. *Journal of Geophysical Research: Oceans*, 126(9), e2021JC017664. https://doi.org/10.1029/2021JC017664

Granéli, E., Carlsson, P., & Legrand, C. (1999). The role of C, N and P in dissolved and particulate organic matter as a nutrient source for phytoplankton growth, including toxic species. *Aquatic Ecology*, 33(1), 17–27. https://doi.org/10.1023/A:1009925515059

Griffith, A. W., & Gobler, C. J. (2020). Harmful algal blooms: A climate change co-stressor in marine and freshwater ecosystems. *Harmful Algae*, 91, 101590. https://doi.org/10.1016/j.hal.2019.03.008

Grégoire, M., Garçon, V., Garcia, H., Breitburg, D., Isensee, K., Oschlies, A., et al. (2021). A global ocean oxygen database and atlas for assessing and predicting deoxygenation and ocean health in the open and coastal ocean. *Frontiers in Marine Science*, 8, 724913. https://doi.org/10.3389/fmars.2021.724913

Guild, R., Wang, X., & Quijón, P. A. (2025). Climate change impacts on coastal ecosystems. *Environmental Research: Climate*, 3(4), 042006. https://doi.org/10.1088/2752-5295/ad9f90

Guillard, R.R. (1975) Culture of phytoplankton for feeding marine invertebrates. In: Smith, W.L., Chanley, M.H., (eds.) *Culture of Marine Invertebrate Animals,* Plenum Press: New York, NY, USA, pp.29–60.

Hallegraeff, G. M. (2010). Ocean climate change, phytoplankton community responses, and harmful algal blooms: A formidable predictive challenge. *Journal of Phycology*, 46(2), 220–235. https://doi.org/10.1111/j.1529-8817.2010.00815.x

Halsey, K. H., & Jones, B. M. (2015). Phytoplankton strategies for photosynthetic energy allocation. *Annual Review of Marine Science*, 7, 265–297. https://doi.org/10.1146/annurev-marine-010814-015813

Hansen, G., Moestrup, Ø., & Roberts, K. R. (2000). Light and electron microscopical observations on the type species of *Gymnodinium, G. fuscum* (Dinophyceae). *Phycologia,* 39(5), 365–376. https://doi.org/10.2216/i0031-8884-39-5-365.1

Hansen, P. J., Ojamäe, K., Berge, T., Trampe, E. C., Nielsen, L. T., Lips, I., & Kühl, M. (2016). Photoregulation in a kleptochloroplastidic dinoflagellate, *Dinophysis acuta. Frontiers in Microbiology*, 7, 785. https://doi.org/10.3389/fmicb.2016.00785

Harris, N. A., Sorensen, J. P. R., Marchant, B., Old, G. H., Naden, P. S., Bowes, M. J., Scarlett, P. M., Nicholls, D. J. E., Armstrong, L. K., Wickham, H. D., Read, D. S., Lapworth, D., Bond, T., & Pond, K. (2024). Temporal drivers of tryptophan-like fluorescent dissolved organic matter along a river continuum. *Science of the Total Environment*, 928, 172285. https://doi.org/https://doi.org/10.1016/j.scitotenv.2024.172285

Heil, C. A. (2005). Influence of humic, fulvic and hydrophilic acids on the growth, photosynthesis and respiration of the dinoflagellate *Prorocentrum minimum* (Pavillard) Schiller. *Harmful Algae*, 4(3), 603–618. https://doi.org/10.1016/j.hal.2004.08.010

Heil, C. A., & Muni-Morgan, A. L. (2021). Florida's harmful algal bloom (HAB) problem: Escalating risks to human, environmental and economic health with climate change. *Frontiers in Ecology and Evolution*, 9, 646080. https://doi.org/10.3389/fevo.2021.646080

Heil, C. A., Dixon, L. K., Hall, E., Garrett, M., Lenes, J. M., O'Neil, J. M., Walsh, B. M., Bronk, D. A., Killberg-Thoreson, L., & Weisberg, R. H. (2014). Blooms of *Karenia brevis* on the West Florida Shelf: Nutrient sources and potential management strategies based on a multi-year regional study. *Harmful Algae*, 38, 127–140. https://doi.org/10.1016/j.hal.2014.07.016

Heil, C. A., Revilla, M., Glibert, P. M., & Murasko, S. (2007). Nutrient quality drives differential phytoplankton community composition on the southwest Florida shelf. *Limnology and Oceanography*, 52(3), 1067–1078. https://doi.org/10.4319/lo.2007.52.3.1067

Heil, C.A., Amin, S.A., Glibert, P.M., Hubbard, K.A., Li, M., Martínez Martínez, J., Weisberg, R., Liu, Y., & Sun, Y. (2022). Termination patterns of *Karenia brevis* blooms in the eastern Gulf of Mexico. In: Band-Schmidt, C., Rodríguez-Gómez, C.F. (Eds.), *Proceedings of the International Harmful Algal Bloom Conference*. https://doi.org/10.5281/zenodo.7034923

Heyl, M. G., Freeberg, L. R., & Dickinson, K. D. (1978). Dissolved oxygen during *Gymnodinium breve* blooms along the Florida west coast, 1976–1978. *Journal of Environmental Science & Health, Part A*, 13(10), 725–731. https://doi.org/10.1080/10934527809374851

Hikosaka, K., Ishikawa, K., Borjigidai, A., Muller, O., & Onoda, Y. (2006). Temperature acclimation of photosynthesis: mechanisms involved in the changes in temperature dependence of photosynthetic rate. *Journal of Experimental Botany*, 57(2), 291–302. https://doi.org/10.1093/jxb/erj049

Hitchcock, G. L., Kirkpatrick, G., Minnett, P., & Palubok, V. (2010). Net community production and dark community respiration in a *Karenia brevis* (Davis) bloom in West Florida coastal waters, USA. *Harmful Algae*, 9(4), 351–358. https://doi.org/10.1016/j.hal.2010.01.002

Hitchcock, G. L., Vargo, G. A., & Dickson, M. L. (2000). Plankton community composition, production, and respiration in relation to dissolved inorganic carbon on the West Florida Shelf, April 1996. *Journal of Geophysical Research: Oceans*, 105(C3), 6579-6589. https://doi.org/10.1029/1998JC000293

Hoch, G., & Kok, B. (1963). A mass spectrometer inlet system for sampling gases dissolved in liquid phases. *Archives of Biochemistry and Biophysics*, 101(1), 160–170. https://doi.org/10.1016/0003-9861(63)90546-0

Hochachka, P. W., & Teal, J. M. (1964). Respiratory metabolism in a marine dinoflagellate. *The Biological Bulletin,* 126(2), 274–281. https://doi.org/10.2307/1539525

Hounshell, A.G., Fegley, S.R., Hall, N.S. et al. (2022). Riverine discharge and phytoplankton biomass control dissolved and particulate organic matter dynamics over spatial and temporal scales in the Neuse River Estuary, North Carolina. *Estuaries and Coasts*, 45, 96–113. https://doi.org/10.1007/s12237-021-00955-w

Hu, C., Muller-Karger, F. E., & Swarzenski, P. W. (2006). Hurricanes, submarine groundwater discharge, and Florida's red tides. *Geophysical Research Letters*, 33(11), L11601. https://doi.org/10.1029/2005GL025449

Huguet, A., Vacher, L., Relexans, S., Saubusse, S., Froidefond, J. M., & Parlanti, E. (2009). Properties of fluorescent dissolved organic matter in the Gironde Estuary. *Organic Geochemistry*, 40(6), 706-719. https://doi.org/10.1016/j.orggeochem.2009.03.002

Jassby, A. D., & Platt, T. (1976). Mathematical formulation of the relationship between photosynthesis and light for phytoplankton. *Limnology and Oceanography*, 21(4), 540–547. https://doi.org/10.4319/lo.1976.21.4.0540

Jensen, L. M., Sand-Jensen, K., Marcher, S., & Hansen, M. (1990). Plankton community respiration along a nutrient gradient in a shallow Danish estuary. *Marine Ecology Progress Series*, 61, 75–85.

Jurado, J. L., Hitchcock, G. L., & Ortner, P. B. (2007). Seasonal variability in nutrient and phytoplankton distributions on the southwest Florida inner shelf. *Bulletin of Marine Science,* 80(1), 21–43.

Kana, T. M. (1990). Light-dependent oxygen cycling measured by an oxygen-18 isotope dilution technique. *Marine Ecology Progress Series*, 64, 293-300. https://doi.org/10.3354/meps064293

Kana, T. M. (1992). Relationship between photosynthetic oxygen cycling and carbon assimilation in *Synechococcus*WH7803 (Cyanophyta). *Journal of Phycology*, 28(3), 304–308. https://doi.org/10.1111/j.0022-3646.1992.00304.x

Kana, T. M. (1993). Rapid oxygen cycling in *Trichodesmium thiebautii*. *Limnology and Oceanography*, 38(1), 18–24. https://doi.org/10.4319/lo.1993.38.1.0018

Kana, T. M., Cornwell, J. C., & Zhong, L. (2006). Determination of denitrification in the Chesapeake Bay from measurements of N2 accumulation in bottom water. *Estuaries and Coasts*, 29, 222-231. https://doi.org/10.1007/BF02781991

Kana, T. M., Darkangelo, C., Hunt, M. D., Oldham, J. B., Bennett, G. E., & Cornwell, J. C. (1994). Membrane inlet mass spectrometer for rapid high-precision determination of N2, O2, and Ar in environmental water samples. *Analytical Chemistry*, 66(23), 4166–4170. https://doi.org/10.1021/ac00095a009

Kaushal, S. S., & Belt, K. T. (2012). The urban watershed continuum: evolving spatial and temporal dimensions. *Urban Ecosystems*, 15(2), 409-435. https://doi.org/10.1007/s11252-012-0226-7

Killberg-Thoreson, L., Mulholland, M. R., Heil, C. A., Sanderson, M. P., O'Neil, J. M., & Bronk, D. A. (2014). Nitrogen uptake kinetics in field populations and cultured strains of *Karenia brevis*. *Harmful Algae*, 38, 73-85. https://doi.org/10.1016/j.hal.2014.04.008

Klotzbach, P. J. (2011). El Niño–Southern Oscillation's impact on Atlantic basin hurricanes and U.S. landfalls. *Journal of Climate*, 24(4), 1252–1263. https://doi.org/10.1175/2010JCLI3799.1

Kramer, D. M., & Evans, J. R. (2011). The importance of energy balance in improving photosynthetic productivity. *Plant Physiology*, 155(1), 70– 78. https://doi.org/10.1104/pp.110.166652

Leenheer, J. A. (1981). Comprehensive approach to preparative isolation and fractionation of dissolved organic carbon from natural waters and wastewaters. *Environmental Science & Technology*, 15(5), 578-587. https://doi.org/10.1021/es00087a010

Lenes, J. M., & Heil, C. A. (2010). A historical analysis of the potential nutrient supply from the N2-fixing marine cyanobacterium *Trichodesmium* spp. to *Karenia brevis* blooms in the eastern Gulf of Mexico. *Journal of Plankton Research*, 32(10), 1421–1431. https://doi.org/10.1093/plankt/fbq061

Lewitus, A. J., & Kana, T. M. (1995). Light respiration in six estuarine phytoplankton species: Contrasts under photoautotrophic and mixotrophic growth conditions. *Journal of Phycology*, 31(5), 754–761. https://doi.org/10.1111/j.0022-3646.1995.00754.x

Li, G., Wang, Z., & Wang, B. (2022). Multidecade trends of sea surface temperature, chlorophyll-a concentration, and ocean eddies in the Gulf of Mexico. *Remote Sensing*, 14(15), 3754. https://doi.org/10.3390/rs14153754

Li, M. F., Glibert, P. M., & Lyubchich, V. (2021). Machine learning classification algorithms for predicting *Karenia brevis* blooms on the West Florida Shelf. *Journal of Marine Science and Engineering,* 9(9), 999. https://doi.org/10.3390/jmse9090999

Lipczynska-Kochany, E. (2018). Effect of climate change on humic substances and associated impacts on the quality of surface water and groundwater. *Science of the Total Environment,* 640, 1548–1565. https://doi.org/10.1016/j.scitotenv.2018.05.376

Liu, Y., Weisberg, R. H., & He, R. (2006). Sea surface temperature patterns on the West Florida Shelf using growing hierarchical self-organizing maps. *Journal of Atmospheric and Oceanic Technology*, 23(2), 325-338. https://doi.org/10.1175/JTECH1848.1

Liu, Y., Weisberg, R. H., Lenes, J. M., Zheng, L., Hubbard, K., & Walsh, J. J. (2016). Offshore forcing on the "pressure point" of the West Florida Shelf: Anomalous upwelling and its influence on harmful algal blooms. *Journal of Geophysical Research: Oceans*, 121, 10.1002/2016JC011938.

Lomas, M. W., Baer, S. E., Mouginot, C., Terpis, K. X., Lomas, D. A., Altabet, M. A., & Martiny, A. C. (2021). Varying influence of phytoplankton biodiversity and stoichiometric plasticity on bulk particulate stoichiometry across ocean basins. *Communications Earth & Environment*, 2(1), 143. https://doi.org/10.1038/s43247-021-00212-9

López-Sandoval, D. C., Rodríguez-Ramos, T., Cermeño, P., Sobrino, C., & Marañón, E. (2014). Photosynthesis and respiration in marine phytoplankton: Relationship with cell size, taxonomic affiliation, and growth phase. *Journal of Experimental Marine Biology and Ecology*, 457, 151–159. https://doi.org/10.1016/j.jembe.2014.04.013

Lønborg, C., Carreira, C., Jickells, T., & Álvarez-Salgado, X. A. (2020). Impacts of global change on ocean dissolved organic carbon (DOC) cycling. *Frontiers in Marine Science*, 7, 466. https://doi.org/10.3389/fmars.2020.00466

MacIntyre, H. L., Geider, R. J., & McKay, R. M. (1996). Photosynthesis and regulation of Rubisco activity in net phytoplankton from Delaware Bay. *Journal of Phycology*, 32(5), 718–731. https://doi.org/10.1111/j.0022-3646.1996.00718.x

Makino, A., Miyake, C., & Yokota, A. (2002). Physiological functions of the water–water cycle (Mehler reaction) and the cyclic electron flow around PSI in rice leaves. *Plant and Cell Physiology*, 43(9), 1017–1026. https://doi.org/10.1093/pcp/pcf124

Malmstadt, J., Scheitlin, K., & Elsner, J. (2009). Florida hurricanes and damage costs. *Southeastern Geographer*, 49, 108–131. https://doi.org/10.1353/sgo.0.0045

Malmstadt, J.C., Elsner, J.B., Jagger, T.H. (2010). Frequency and Intensity of Hurricanes Within Florida's Threat Zone. In: Elsner, J., Hodges, R., Malmstadt, J., Scheitlin, K. (eds) *Hurricanes and Climate Change*. Springer, Dordrecht. https://doi.org/10.1007/978-90-481-9510-7_11

Marañón, E., Lorenzo, M. P., Cermeño, P., & Mouriño-Carballido, B. (2018). Nutrient limitation suppresses the temperature dependence of phytoplankton metabolic rates. *The ISME Journal,* 12(7), 1836–1845. https://doi.org/10.1038/s41396-018-0105-1

Martínez, A., Méndez, Si., Fabre, A., & Ortega, L. (2017). Intensificación de floraciones de dinoflagelados marinos en Uruguay. *INNOTEC*, 13(13), 19–25. https://doi.org/10.26461/13.02

Medina, M., Huffaker, R., Jawitz, J. W., & Muñoz-Carpena, R. (2020). Seasonal dynamics of terrestrially sourced nitrogen influenced *Karenia brevis* blooms off Florida's southern Gulf Coast. *Harmful Algae*, 98, 101900. https://doi.org/10.1016/j.hal.2020.101900

Medina, M., Kaplan, D., Milbrandt, E., Tomasko, D., Huffaker, R., & Angelini, C. (2022). Nitrogen-enriched discharges from a highly managed watershed intensify *Karenia brevis* blooms in southwest Florida. *Science of the Total Environment*, 827, 154149. https://doi.org/10.1016/j.scitotenv.2022.154149

Mehler, A. H., & Brown, A. H. (1952). Studies on reactions of illuminated chloroplasts. III. Simultaneous photoproduction and consumption of oxygen studied with oxygen isotopes. *Archives of Biochemistry and Biophysics*, 38(1), 365–370. https://doi.org/10.1016/0003-9861(52)90042-8

Mendoza, W. G., & Zika, R. G. (2014). On the temporal variation of DOM fluorescence on the southwest Florida continental shelf. *Progress in Oceanography*, 120, 189-204. https://doi.org/10.1016/j.pocean.2013.08.010

Mendoza, W.G., Kang, Y., & Zika, R.G. (2012). Resolving DOM fluorescence fractions during a Karenia brevis bloom patch on the Southwest Florida Shelf. *Continental Shelf Research*, 32, 121–129. https://doi.org/10.1016/j.csr.2011.11.001

Milbrandt, E. C., Martignette, A. J., Thompson, M. A., Bartleson, R. D., Phlips, E. J., Badylak, S., & Nelson, N. G. (2021). Geospatial distribution of hypoxia associated with a *Karenia brevis* bloom. *Estuarine, Coastal and Shelf Science*, 259, 107446. https://doi.org/10.1016/j.ecss.2021.107446

Miles, T., Glenn, S. M., & Schofield, O. (2013). Temporal and spatial variability in fall storm induced sediment resuspension on the Mid-Atlantic Bight. *Continental Shelf Research*, 63, S36-S49. https://doi.org/10.1016/j.csr.2012.08.006

Miller, C. B., & Wheeler, P. A. (2012). Biological oceanography. John Wiley & Sons.

Moran, M. A., & Hodson, R. E. (1994). Dissolved humic substances of vascular plant origin in a coastal marine environment. *Limnology and Oceanography*, 39(4), 762–771. https://doi.org/10.4319/lo.1994.39.4.0762

Moschonas, G., Gowen, R. J., Paterson, R. F., Mitchell, E., Stewart, B. M., McNeill, S., ... & Davidson, K. (2017). Nitrogen dynamics and phytoplankton community structure: The role of organic nutrients. *Biogeochemistry*, 134(1), 125–145. https://doi.org/10.1007/s10533-017-0351-8

Muni-Morgan, A. L., Lusk, M. G., & Heil, C. A. (2024). *Karenia brevis* and *Pyrodinium bahamense* utilization of dissolved organic matter in urban stormwater runoff and rainfall entering Tampa Bay, Florida. *Water*, 16(10), 1448. https://doi.org/10.3390/w16101448

Muni-Morgan, A., Lusk, M. G., Heil, C., Goeckner, A. H., Chen, H., McKenna, A. M., & Holland, P. S. (2023). Molecular characterization of dissolved organic matter in urban stormwater pond and municipal wastewater discharges transformed by the Florida red tide dinoflagellate *Karenia brevis*. *Science of the Total Environment*, 904, 166291. https://doi.org/10.1016/j.scitotenv.2023.166291

Murphy, K. R., Stedmon, C. A., Wenig, P., & Bro, R. (2014). OpenFluor–an online spectral library of auto-fluorescence by organic compounds in the environment. *Analytical Methods,* 6(3), 658-661. https://doi.org/10.1039/C3AY41935E

Musani, L., Valenta, P., Nürnberg, H. W., Konrad, Z., & Branica, M. (1980). On the chelation of toxic trace metals by humic acid of marine origin. *Estuarine and Coastal Marine Science*, 11(6), 639-649. https://doi.org/10.1016/S0302-3524(80)80015-6

National Hurricane Center. (2024). Tropical cyclone report: Hurricane Milton (AL142024). National Oceanic and Atmospheric Administration. https://www.nhc.noaa.gov/data/tcr/AL142024_Milton.pdf. Accessed on February 21, 2026

National Weather Service. (2024). Post tropical cyclone report. National Oceanic and Atmospheric Administration. https://www.weather.gov/media/tbw/TropicalEventSummary/PSHTBW_2024AL04_Debby_Summary.pdf. Accessed on February 21, 2026

Nickerson, A. K., Weisberg, R. H., Zheng, L., & Liu, Y. (2023). Sea surface temperature trends for Tampa Bay, West Florida Shelf and the deep Gulf of Mexico. D*eep Sea Research Part II: Topical Studies in Oceanography*, 211, 105321. https://doi.org/10.1016/j.dsr2.2023.105321

Odum, H. T. (1956). Primary production in flowing waters. *Limnology and Oceanography*, 1(2), 102–117. https://doi.org/10.4319/lo.1956.1.2.0102

Oh, J. W., Pushparaj, S. S. C., Muthu, M., & Gopal, J. (2023). Review of harmful algal blooms (HABs) causing marine fish kills: Toxicity and mitigation. *Plants*, 12(23), 3936. https://doi.org/10.3390/plants12233936

Ohno, T. (2002). Fluorescence inner-filtering correction for determining the humification index of dissolved organic matter. *Environmental Science & Technology*, 36(4), 742-746. https://doi.org/10.1021/es0155276

Opsahl, S., & Benner, R. Distribution and cycling of terrigenous dissolved organic matter in the ocean. *Nature*, 386, 480–482 (1997). https://doi.org/10.1038/386480a0

O'Neil, J.M., Heil, C.A., Glibert, P.M., Solomon, C.M., Greenwood, J., & Greenwood, J.G. (2024). Plankton community changes and nutrient dynamics associated with blooms of

Trichodesmium in the Gulf of Mexico and Great Barrier Reef. *Water,* 16, 1663. https://doi.org/10.3390/w16121663

Pace, M. L., Buelo, C. D., & Carpenter, S. R. (2021). Phytoplankton biomass, dissolved organic matter, and temperature drive respiration in whole lake nutrient additions. *Limnology and Oceanography,* 66(6), 2174-2186. https://doi.org/10.1002/lno.11738

Phlips, E. J., Badylak, S., Nelson, N. G., & Havens, K. E. (2020). Hurricanes, El Niño and harmful algal blooms in two sub-tropical Florida estuaries: Direct and indirect impacts. *Scientific Reports*, 10(1), 1910. https://doi.org/10.1038/s41598-020-58771-4

Pilla, R. M., Williamson, C. E., Zhang, J., Smyth, R. L., Lenters, J. D., Brentrup, J. A., Knoll, L. B., & Fisher, T. J. (2018). Browning-related decreases in water transparency lead to long-term increases in surface water temperature and thermal stratification in two small lakes. *Journal of Geophysical Research: Biogeosciences*, 123(5), 1651-1665. https://doi.org/10.1029/2017JG004321

Platt, T., & Jassby, A. D. (1976). The relationship between photosynthesis and light for natural assemblages of coastal marine phytoplankton. *Journal of Phycology*, 12(4), 421–430. https://doi.org/10.1111/j.1529-8817.1976.tb02866.x

Pontius, J., & McIntosh, A. (2024). Gulf of Mexico dead zone. In *Environmental Problem Solving in an Age of Climate Change: Volume One: Basic Tools and Techniques* (pp. 45-56). Cham: Springer International Publishing. https://doi.org/10.1007/978-3-031-48762-0_5

Pringault, O., Tassas, V., & Rochelle-Newall, E. (2007). Consequences of respiration in the light on the determination of production in pelagic systems. *Biogeosciences*, 4(1), 105–114. https://doi.org/10.5194/bg-4-105-2007

Prézelin, B. B., Meeson, B. W., & Sweeney, B. M. (1977). Characterization of photosynthetic rhythms in marine dinoflagellates: I. Pigmentation, photosynthetic capacity and respiration. *Plant Physiology*, 60(3), 384–387. https://doi.org/10.1104/pp.60.3.384

R Core Team. A Language and Environment for Statistical Computing. (2021). Available online: https://www.R-project.org/

Rabalais, N. N., & Turner, R. E. (2019). Gulf of Mexico hypoxia: Past, present, and future. *Limnology and Oceanography Bulletin*, 28(4), 117-124. https://doi.org/10.1002/lob.10351

Raven, J. A., & Geider, R. J. (1988). Temperature and algal growth. *New Phytologist*, 110(4), 441–461. https://doi.org/10.1111/j.1469-8137.1988.tb00282.x

Raven, J. A., Wollenweber, B., & Handley, L. L. (1992). A comparison of ammonium and nitrate as nitrogen sources for photolithotrophs. *New Phytologist*, 121(1), 19–32. https://doi.org/10.1111/j.1469-8137.1992.tb01088.x

Sakshaug, E., Bricaud, A., Dandonneau, Y., Falkowski, P. G., Kiefer, D. A., Legendre, L., & Takahashi, M. (1997). Parameters of photosynthesis: Definitions, theory and interpretation of results. *Journal of Plankton Research*, 19(11), 1637–1670. https://doi.org/10.1093/plankt/19.11.1637

Saunders, M. A., & Lea, A. S. (2008). Large contribution of sea surface warming to recent increase in Atlantic hurricane activity. *Nature*, 451(7178), 557–560. https://doi.org/10.1038/nature06422

Schaeffer, B. A., Kamykowski, D., McKay, L., Sinclair, G., & Milligan, E. J. (2007). A comparison of photoresponse among ten different *Karenia brevis* (Dinophyceae) isolates. *Journal of Phycology*, 43(4), 702–714. https://doi.org/10.1111/j.1529-8817.2007.00377.x

Schmidt, N., Lipp, E. K., Rose, J. B., & Luther, M. E. (2001). ENSO influences on seasonal rainfall and river discharge in Florida. *Journal of Climate*, 14(4), 615–628. https://doi.org/10.1175/1520-0442(2001)014<0615:EIOSRA>2.0.CO;2

Schmidtko, S., Stramma, L., & Visbeck, M. (2017). Decline in global oceanic oxygen content during the past five decades. *Nature*, 542(7641), 335-339. https://doi.org/10.1038/nature21399

Schmoker, C., Thor, P., Hernández-León, S., & Hansen, B. W. (2011). Feeding, growth and metabolism of the marine heterotrophic dinoflagellate *Gyrodinium dominans*. *Aquatic Microbial Ecology*, 65(1), 65–73. https://doi.org/10.3354/ame01533

See, J. H., Bronk, D. A., & Lewitus, A. J. (2006). Uptake of Spartina-derived humic nitrogen by estuarine phytoplankton in nonaxenic and axenic culture. *Limnology and Oceanography*, 51(5), 2290–2299. https://doi.org/10.4319/lo.2006.51.5.2290

Silsbe, G. M., & Malkin, S. Y. (2015). Package 'phytotools'.

Smith, G. B. (1975). The 1971 red tide and its impact on certain reef communities in the mid-eastern Gulf of Mexico. *Environmental Letters*, 9(2), 141-152. https://doi.org/10.1080/00139307509435843

Sobrinho, B. F., Pinheiro-Silva, L., & Glibert, P. M. Interactive effects of temperature, nitrogen form, and humic substances on photosynthetic performance of the toxigenic dinoflagellate, *Karenia brevis*. Manuscript submitted for publication.

Sobrinho, B. F., Vidyarathna, N., Kana, T. M., & Glibert, P. M. Improved primary production and gross respiration measurements using the $H_{218}O$ technique with membrane inlet mass

spectrometry and introduction of a small volume–uniform irradiance incubation chamber. Manuscript submitted for publication.

Sorinas, L., Weisberg, R. H., Liu, Y., & Law, J. (2023). Ocean-atmosphere heat exchange seasonal cycle on the West Florida Shelf derived from long term moored data. *Deep Sea Research Part II: Topical Studies in Oceanography*, 212, 105341. https://doi.org/10.1016/j.dsr2.2023.105341

Stedmon, C. A., & Bro, R. (2008). Characterizing dissolved organic matter fluorescence with parallel factor analysis: a tutorial. *Limnology and Oceanography: Methods*, 6(11), 572-579. https://doi.org/10.4319/lom.2008.6.572

Stedmon, C. A., & Markager, S. (2005). Resolving the variability in dissolved organic matter fluorescence in a temperate estuary and its catchment using PARAFAC analysis. *Limnology and Oceanography*, 50(2), 686-697. https://doi.org/10.4319/lo.2005.50.2.0686

Steidinger, K. A. (1975). Implications of dinoflagellate life cycles on initiation of *Gymnodinium breve* red tides. *Environmental Letters*, 9(2), 129–139. https://doi.org/10.1080/00139307509435842

Steidinger, K. A. (2009). Historical perspective on *Karenia brevis* red tide research in the Gulf of Mexico. *Harmful Algae*, 8(4), 549–561. https://doi.org/10.1016/j.hal.2008.11.009

Stepanauskas, R., Jørgensen, N. O., Eigaard, O. R., Žvikas, A., Tranvik, L. J., & Leonardson, L. (2002). Summer inputs of riverine nutrients to the Baltic Sea: Bioavailability and eutrophication relevance. *Ecological Monographs*, 72(4), 579-597. https://doi.org/10.1890/0012-9615(2002)072[0579:SIORNT]2.0.CO;2

Stumpf, R.P., Li, Y., Kirkpatrick, B., Litaker, R.W., Hubbard, K.A., Currier, R.D., & Tomlinson, M.C. (2022). Quantifying *Karenia brevis* bloom severity and respiratory irritation impact along the shoreline of Southwest Florida. *PLoS ONE*, 17(1), e0260755. https://doi.org/10.1371/journal.pone.0260755

Suggett, D. J., MacIntyre, H. L., Kana, T. M., & Geider, R. J. (2009). Comparing electron transport with gas exchange: Parameterizing exchange rates between alternative photosynthetic currencies for eukaryotic phytoplankton. *Aquatic Microbial Ecology*, 56(2), 147–162. https://doi.org/10.3354/ame01303

Thurman, E. M. (1985). Transport, origin and source of dissolved organic carbon. In E. M. Thurman (Ed.), *Organic Geochemistry of Natural Waters* (pp. 67–85). Dordrecht: Springer Netherlands. https://doi.org/10.1007/978-94-009-5095-5_3

Tomasko, D., Landau, L., Suau, S., Medina, M., & Hecker, J. (2024). An evaluation of the relationships between the duration of red tide (*Karenia brevis*) blooms and watershed nitrogen loads in southwest Florida. *Florida Scientist*, 87(2), 61–72. http://dx.doi.org/10.2139/ssrn.4592652

Turley, B. D., Karnauskas, M., Campbell, M. D., Hanisko, D. S., & Kelble, C. R. (2022). Relationships between blooms of *Karenia brevis* and hypoxia across the West Florida Shelf. *Harmful Algae*, 114, 102223. https://doi.org/10.1016/j.hal.2022.102223

Urrutia-Cordero, P., Ekvall, M. K., Ratcovich, J., Soares, M., Wilken, S., Zhang, H., & Hansson, L. A. (2017). Phytoplankton diversity loss along a gradient of future warming and brownification in freshwater mesocosms. *Freshwater Biology*, 62(11), 1869–1878. https://doi.org/10.1111/fwb.13027

Van de Waal, D.B., & Litchman, E. (2020). Multiple global change stressor effects on phytoplankton nutrient acquisition in a future ocean. *Philosophical Transactions of the Royal Society B*, 375(1798), 20190706. https://doi.org/10.1098/rstb.2019.0706

Van Heukelem, L., & Thomas, C. S. (2001). Computer-assisted high-performance liquid chromatography method development with applications to the isolation and analysis of phytoplankton pigments. *Journal of Chromatography A,* 910(1), 31–49. https://doi.org/10.1016/S0378-4347(00)00603-4

Vargo, G. A. (2009). A brief summary of the physiology and ecology of *Karenia brevis* Davis (G. Hansen and Moestrup comb. nov.) red tides on the West Florida Shelf and of hypotheses posed for their initiation, growth, maintenance, and termination. *Harmful Algae*, 8(4), 573–584. https://doi.org/10.1016/j.hal.2008.11.002

Vargo, G.A., Heil, C.A., Fanning, K.A., Dixon, L.K., Neely, M.B., Lester, K., Bell, S., & Weisberg, R.H. (2008). Nutrient availability in support of *Karenia brevis* blooms on the central West Florida Shelf. *Continental Shelf Research*, 28(1), 73–98. https://doi.org/10.1016/j.csr.2007.04.008

Walsh, J. J., & Steidinger, K. A. (2001). Saharan dust and Florida red tides: The cyanophyte connection. *Journal of Geophysical Research: Oceans*, 106(C6), 11597–11612. https://doi.org/10.1029/1999JC000123

Walsh, J. J., Weisberg, R. H., Dieterle, D. A., He, R., Darrow, B. P., Jolliff, J. K., ... & Muller-Karger, F. E. (2003). Phytoplankton response to intrusions of slope water on the West Florida Shelf: Models and observations. *Journal of Geophysical Research: Oceans*, 108(C6). https://doi.org/10.1029/2002JC001406

Wang, Z., Boyer, T., Reagan, J., & Hogan, P. (2023). Upper-oceanic warming in the Gulf of Mexico between 1950 and 2020. *Journal of Climate*, 36(8), 2721–2734. https://doi.org/10.1175/JCLI-D-22-0409.1

Weisberg, R. H., Liu, Y., Lembke, C., Hu, C., Hubbard, K., & Garrett, M. (2019). The coastal ocean circulation influence on the 2018 West Florida Shelf *K. brevis* red tide bloom. *Journal of Geophysical Research: Oceans*, 124(4), 2501–2512. https://doi.org/10.1029/2018JC014887

Weisberg, R. H., Zheng, L., Liu, Y., Corcoran, A. A., Lembke, C., Hu, C., Lenes, J. M., & Walsh, J. J. (2016). *Karenia brevis* blooms on the West Florida Shelf: A comparative study of the robust 2012 bloom and the nearly null 2013 event. *Continental Shelf Research*, 120, 106–121. https://doi.org/10.1016/j.csr.2016.03.011

Weisberg, R. H., Zheng, L., Liu, Y., Lembke, C., Lenes, J. M., & Walsh, J. J. (2014). Why no red tide was observed on the West Florida Continental Shelf in 2010. *Harmful Algae*, 38, 119–126. https://doi.org/10.1016/j.hal.2014.04.010

Weiss, R. F. (1970). The solubility of nitrogen, oxygen and argon in water and seawater. *Deep-Sea Research and Oceanographic Abstracts*, 17(4), 721–735. https://doi.org/10.1016/0011-7471(70)90037-9

Wheeler, R. E., & Torchiano, M. (2016). Permutation tests for linear models in R. *The Comprehensive R Archive Network,* 1(2), 1-36.

Wiegner, T. N., Seitzinger, S. P., Glibert, P. M., & Bronk, D. A. (2006). Bioavailability of dissolved organic nitrogen and carbon from nine rivers in the eastern United States. *Aquatic Microbial Ecology*, 43(3), 277-287. https://doi.org/10.3354/ame043277

Wikner, J., Vikström, K., & Verma, A. (2023). Regulation of marine plankton respiration: A test of models. *Frontiers in Marine Science*, 10, 1134699. https://doi.org/10.3389/fmars.2023.1134699

Williamson, C. E., Overholt, E. P., Pilla, R. M., Leach, T. H., Brentrup, J. A., Knoll, L. B., Mette, E. M., & Moeller, R. E. (2015). Ecological consequences of long-term browning in lakes. *Scientific Reports*, 5(1), 18666. https://doi.org/10.1038/srep18666

Yin, H., Huang, T., Wang, B., Zhang, Y., Hu, J., Zhu, L., & Chen, K. (2025). Dissolved organic matter sources in urban outfall water before and during rainfall, indicated via its fluorescence fingerprinting. *Applied Geochemistry*, 106447. https://doi.org/10.1016/j.apgeochem.2025.106447

Zhang, H., Zeng, C., Zhang, X., Wang, X., & Li, K. (2025). Differential responses and adaptive mechanisms of diatoms and dinoflagellates to changes in dissolved organic nitrogen components. *Harmful Algae*, 150, 103005. https://doi.org/10.1016/j.hal.2025.103005